Members of the Examination Committee:

Prof. dr. ir. Jules van Lier
Faculty of Civil Engineering and Geosciences, Delft University of Technology, The Netherlands

Prof. dr. ir. Ingmar Nopens
Faculty of Bioscience Engineering, Ghent University, Belgium

Prof. dr. ir. Isabella Wierinck
Biogas Consulting & Support (BCS), OWS, Belgium

Prof. dr. ir. Korneel Rabaey
Faculty of Bioscience Engineering, Ghent University, Belgium

Prof. dr. ir. Jo Dewulf
Faculty of Bioscience Engineering, Ghent University, Belgium

Prof. dr. ir. Henri Spanjers
Faculty of Civil Engineering and Geosciences, Delft University of Technology, The Netherlands

Prof. dr. ir. Filip Tack (Chairman)
Faculty of Bioscience Engineering, Ghent University, Belgium

Promoters:
Prof. dr. ir. Jo Dewulf
Department of Sustainable Organic Chemistry and Technology
Faculty of Bioscience Engineering, Ghent University

Prof. dr. ir. Henri Spanjers
Department of Water Management
Faculty of Civil Engineering and Geosciences, Delft University of Technology

Prof. dr. ir. Osvaldo Romero Romero
Study Center of Energy and Industrial Processes
Sancti Spiritus University

Prof. dr. ir. Elena Rosa
Chemical Engineering Department
Faculty of Chemical and Pharmacy, Central University of Las Villas

Dean Prof. dr. ir. Guido Van Huylenbroeck
Rector Prof. dr. Anne De Paepe

Faculty of Bioscience Engineering

Ir. Ernesto Luis Barrera Cardoso

Anaerobic digestion of a very high strength and sulfate-rich vinasse: from experiments to modeling and sustainability assessment

Thesis submitted in fulfillment of the requirements for the degree of Doctor (PhD) in Applied Biological Sciences

Cover design by Ernesto Luis Barrera Cardoso based on the graphical abastract of the Manuscript Submitted to Water Research (Chapter 3 of this dissertation).

To refer this thesis:

Barrera Cardoso E.L. 2014. Anaerobic digestion of a very high strength and sulfate-rich vinasse: from experiments to modeling and sustainability assessment

ISBN: 978-90-5989-742-7

WORD OF THANKS

From the very beginning, during, at the very end, and for sure, after a PhD work, there are always great people giving their hands and their support. To them, these words of thanks, even when I know that it is impossible to express in words all my gratitude and feelings.

I will never forget when Osvaldo Romero Romero (one of my Cuban supervisors) told me: "I have a proposal for your PhD work". To be honest it sounded distant and strange to me. Osvaldo has always been supporting my work from the very beginning: He was one of the supervisors of my "Diploma Thesis", "Master Thesis" and "PhD Thesis". I am really grateful to you Osvaldo; thanks for trusting me, thanks for this opportunity and let's keep in touch for future researches.

Some years later, I met two great Professors, Prof. dr. ir. Jo Dewulf and Prof. dr. ir. Henri Spanjers; I have, for them both, a very special respect. Thanks Professors for your guidance, for your expertise, thanks for showing me another way of thinking in terms of science, thanks for helping me to understand and appreciate your culture, and thanks for entrusting me this PhD project.

Thanks also to all my colleagues in my department, the Study Center of Energy and Industrial Processes, University of Sancti Spiritus, Cuba. Thanks for providing me with the time to do this research, for covering my job (in many cases) and for your professional advice. Thanks especially to you Yenima, for your effort and devotion with the English corrections regardless of time or day. Thanks also to my colleagues in the Central University of Las Villas (Villa Clara, Cuba); thanks to my supervisor there, Elena Rosa; thanks to all my Professors who formed me as a Chemical Engineer (1996-2001). Thanks to Steven, Wouter, Thomas, Rodrigo, Diego, Sam, Emilie and all my colleagues at EnVOC department, Gent University, for being friendly and helpful; "when one is abroad people like you become a family".

A great number of friends supported this project in different ways, friends from Cuba, from Ecuador, from Chile, from Venezuela, from Italy and from Belgium. I really appreciate their friendship, their positive suggestions and their encouragement. I don't have to mention you here, "My Friend"; a real friend knows when his friend is talking about him.

My family…I really love my family; it is like a compact block always together even when life becomes tough. Thanks to my parents for guiding me all throughout my life, thanks for being my friends, and thanks for supporting my studies from the very beginning. Thanks also to you and my sisters for understanding that I cannot be always there. Thanks to you and my parents-in-law for taking care of my son and my wife when I was here in Belgium; I will never forget that!!! Thanks to my wife. Thanks a lot Vivian, I really appreciate your support and effort during these four years; thanks for understanding that this was a project of our little family, and be sure, that this project will enhance our life and will be seen as an example for our son. And you boys, I have been always thinking on you both, Ernestico (my son) and Dieguito (my nephew); you are the reason for my inspiration and effort; thanks for making me happy and for all your love.

This is a message for you all!!! "This PhD research cannot be done without you!!!" Thanks a lot and let's stay always together!!!

LIST OF CONTENT

ABBREVIATION INDEX

aSRB	Acetate sulfate reducing bacteria
ADM1	Anaerobic Digestion Model No. 1
BP	Biogas production
bSRB	Butyrate sulfate reducing bacteria
COD	Chemical oxygen demand
CHP	Combined heat and power
CI	Confidence interval
COV	Covariance matrix
FIM	Fisher information matrix
EA	Exergy analysis
EDTA	Ethylenediaminetetraacetic acid
EG	Energy generation
FP	Ferti-irrigation pumping
hMA	Hydrogenotrophic methanogenic archea
HRT	Hydraulic retention time
IDA	Iminodiacetic acid
M	Methanogens
n	Charge of the organic ligand
L	Organic ligand
LCA	Life Cycle Assessment
LCFA	Long chain fatty acids
LCI	Life cycle inventory
LCIA	Life cycle impact assessment
LHV	Lower heating value
LS	Lagoons

ODE	Ordinary differential equation
OLR	Organic loading rate
pSRB	Propionate sulfate reducing bacteria
SCOD	Soluble COD
SD	Sludge drying
SLR	Sulfate loading rate
SR	Sulfide removal
SRB	Sulfate reducing bacteria
SWW	Sugar wastewater
TSC	Traditional supply chain
UASB	Upflow anaerobic sludge bed reactor
XCOD	Particulate COD

LIST OF SYMBOLS

C_i	Carbon content of the component i (kmol C· kg COD^{-1})
c_p	Heat capacity of the substance (kJ· kg^{-1} ·K^{-1})
COD	Chemical oxygen demand concentration (g COD· L^{-1})
COD	COD flow for Eqs. 1.18 & 4.7 (kg COD· d^{-1})
$COD\_\Delta SO_4^{2-}$	COD of reduced SO_4^{2-} used for COD mass balances (g COD· d^{-1})
COD_CH_{4gas}	COD of gas CH_4 used for COD mass balances (g COD· d^{-1})
$COD_{removed}$	Removed COD (kg COD· d^{-1})
eff_COD	COD flow in the reactor effluent (used for COD mass balances in chapter 2) (g COD· d^{-1})
eff_COD	COD concentration in the reactor effluent (used in chapter 3) (kg COD· m^{-3})
eff_COD	COD concentration in the lagoon effluent (used in chapter 4) (g COD· m^{-3})
$eff\_SO_4^{2-}$	Effluent SO_4^{2-} used for sulfur mass balances (mg S· d^{-1})
Ex_{ch}	Chemical exergy (kJ_{ex})
Ex_e	Electrical exergy (kJ_{ex})
Ex_S	Solar exergy (kJ_{ex})
Ex_{ph}	Physical exergy (kJ_{ex})
Ex_{tot}	Total exergy of a product or process (kJ_{ex})
VFAs	Volatile fatty acids (mg· L^{-1})
H	Enthalpy of the substance (kJ)
H_2S_{aq}	Concentration of total aqueous H_2S (mg S· L^{-1})
HS^-	Concentration of ionized H_2S (mg S· L^{-1})
$[H_2S]_{free}$	Concentration of free H_2S (mg S· L^{-1})
H_2S_{gas}	Concentration of H_2S in biogas (mg S· L^{-1})
inf_COD	Influent COD (as g COD· d^{-1} for mass balances consistency in chapter 2) (g COD· L^{-1})
inf_COD	Influent COD concentration (used in chapter 4 as g COD· m^{-3})

$I_{1\text{-}4}$	Inhibition functions
$I_{h2s,j}$	Sulfide inhibition function for process j
$I_{pH,j}$	pH inhibition function for process j
$inf\_SO_4^{2-}$	Influent SO_4^{2-} concentration (as mg S· d^{-1} for sulfur mass balance consistency) (g SO_4^{2-}· L^{-1})
k_{20}	COD removal rate coefficient for lagoons at 20°C (d^{-1})
$k_{dec,j}$	First order decay rate for process j (d^{-1})
k_La	Gas-liquid transfer coefficient (d^{-1})
$k_{m,j}$	Monod maximum specific uptake rate for process j (kg COD_S_i· kg $COD\_X_i^{-1}$· d^{-1})
K_{100}	Concentration of H_2S or pH at which the uptake rate is decreased 100 times (kmol· m^{-3})
K_2	Concentration of H_2S or pH at which the uptake rate is decreased twice (kmol· m^{-3})
$K_{a,\,i}$	Acid-base equilibrium coefficient for component i (kmol· m^{-3})
$K_{A/B,i}$	Acid-base kinetic parameter for component i (m^3· $kmol^{-1}$· d^{-1})
$K_{H,i}$	Henry's law coefficient for component i (kmol· m^{-3}· bar^{-1})
$K_{I,h2s,\,j}$	50% inhibitory concentration of free H_2S on the process j (kmol· m^{-3})
$K_{S,j}$	Half saturation coefficient of component i on process j (for SO_4^{2-} units are in kmol· m^{-3}) (kg COD_S_i· m^{-3})
k_T	First-order COD removal rate coefficient (d^{-1})
L^{n-}	Organic ligand L with its charge n
m	Mass of the substance (kg)
N_i	Nitrogen content of the component i (kmol N· kg COD^{-1})
OLR	Organic loading rate (g COD· L_R^{-1}· d^{-1})
$P_{gas,i}$	Pressure of gas component i (bar)
pH_{LL}	Lower pH limits where the groups of microorganism are 50% inhibited
pH_{UL}	Upper pH limits where the groups of microorganism are 50% inhibited
Q_{gas}	Gas flow rate (m^3· d^{-1})
R_{CH4}	Methane production rate (L·m^{-2} d^{-1})

S	Entropy of the substance (kJ· K^{-1})
$S_{gas,i}$	Gas phase concentration of the component i (expressed as fraction for CH_4 and CO_2 in Figure 3.2 & 3.3) (kmol· m^{-3})
$S\_H_2S_{gas}$	H_2S in biogas used for sulfur mass balances (mg S· d^{-1})
S_HS^-	Ionized H_2S in the effluent used for sulfur mass balances (mg S· d^{-1})
$S\_[H_2S]_{free}$	Free H_2S in the effluent used for sulfur mass balances (mg S· d^{-1})
S_i	Concentration of the soluble components i (for hydrogen ions, sulfates, sulfides and its ionized forms units are in kmol· m^{-3}) (kg COD_S_I· m^{-3})
SLR	Sulfate loading rate (g SO_4^{2-}· L_R^{-1}· d^{-1})
T	Temperature (°C or K)
$TCOD$	Total COD concentration (kg COD· m^{-3})
TKN	Total kjeldahl nitrogen concentration (mol N· L^{-1})
TOC	Total organic carbon concentration (mol C· L^{-1})
TP	Total phosphorous concentration (mol P· L^{-1})
$t_{\alpha,df}$	t-values obtained from the Student-t distribution
Vup	Liquid upflow velocity (m· h^{-1})
X_i	Particulate component (kg COD_X_i^{-1}· m^{-3})
Y_i	Yield of biomass on the substrate (kg COD_X_i^{-1}· kg COD_S_i^{-1})

Greek letter

α_{LL}- α_{UL}	Positive values which affect the steepness of the curve
$\eta_{ex,1\text{-}3}$	Exergy efficiencies (%)
Θ_h	Mean hydraulic retention time (d)
ρ_j	Kinetic rate of process j (kg COD_S_i · m^{-3} d^{-1}) (for acid-base and gas-liquid equations units are in kmol· m^{-3}· d^{-1})
$\rho_{uptake,j}$	Kinetic rate of substrate uptake for process j (kg COD_S_i · m^{-3}· d^{-1})
$\rho_{growth,j}$	Kinetic rate of bacterial growth for process j (kg COD_X_i · m^{-3}· d^{-1})
$\rho_{decay,j}$	Kinetic rate of bacterial decay for process j (kg COD_X_i · m^{-3}· d^{-1})
$\mu_{max,j}$	Maximum specific growth rate of microorganisms for process j (d^{-1})

$\Gamma_{n,m}$	Sensitivity value of the n^{th} process variable (y) with respect to the m^{th} model parameter (θ)
τ	Temperature correction factor
$v_{i,j}$	Biochemical rate (or liquid phase yield) coefficient for component i on process j
δ	Perturbation factor (Fraction)
σ	Standard deviations (Vary with θ)
α	Significance level (%)

Subscript

bac	Pertaining to bacteria
dec	Pertaining to decay processes
df	Degree of freedom
free	Undissociated form of the species
gas	Pertaining to the gas phase
i	Pertaining to soluble or particulate component
I	Pertaining to the inert fraction
j	Pertaining to processes
lag	Pertaining to the lagoon
0	Pertaining to the reference environment
air	Pertaining to the air

ACKNOWLEDGEMENTS

This research has been supported financially by the VLIR Program, Project ZEIN2009PR362 (Biogas production from waste from local food, wood and sugar cane industries for increasing self-sufficiency of energy in Sancti Spiritus, Cuba). The research was conducted at two research groups:

Research Group of Environmental Organic Chemistry and Technology (EnVOC), Faculty of Bioscience Engineering, Ghent University, Coupure Links 653, 9000 Ghent, URL: http://www.envoc.ugent.be/.

Study Center of Energy and Industrial Processes, Sancti Spiritus University. Ave de los Mártires 360, 60100 Sancti Spiritus, Cuba, URL: http://www.uniss.edu.cu/.

CHAPTER 1. General introduction

Redrafted from:

Barrera, E.L., Spanjers, H., Dewulf, J., Romero, O. and Rosa, E., 2013. The sulfur chain in biogas production from sulfate-rich liquid substrates: a review on dynamic modeling with vinasse as model substrate. Journal of Chemical Technology and Biotechnology 88, 1405–1420.

The last sections of the original article are related to the modeling of sulfide removal processes. Since they were used for mass balance calculations in Chapter 4 only, they were placed in Appendix A for a proper balance of Chapter 1.

1.1 Introduction

The global energetic panorama based on fossil fuels is characterized by a continuous growth of energy demand, causing scarcity of resources and environmental pollution. To ensure future sustainability, the use of renewable technologies has been increasing over the world. One of the main renewable technologies is based on the anaerobic digestion of biodegradable wastes to produce biogas, a versatile gas fuel that can replace fossil fuels in power and heat production plants. The energetic value of biogas and its potential to achieve negative carbon emissions (Budzianowski, 2011) together with the additional compost production and chemical oxygen demand (COD) removal are the principal benefits of anaerobic digestion (Contreras et al., 2009; Nandy et al., 2002).

Vinasse is a liquid waste that is very suitable for anaerobic digestion. Vinasse, also termed as distillery wastewater, stillage, distillery slops, distillery spent wash and thin stillage, is an aqueous by-product obtained after the distillation of fermented molasses to produce ethanol. For example, Cuban vinasse is produced from the distillation of fermented cane molasses and it possesses a high chemical oxygen demand (> 40 kg m^{-3}) that can serve as organic matter source in anaerobic treatment.

However, during the fermentation of cane molasses in the ethanol production process in Cuba, sulfuric acid is added to reduce pH to the range of 4.2 to 4.5. Although nitric and phosphoric acids can be used as alternatives to sulfuric acid, they are considered expensive and rarely used for the ethanol production process (see also Chapter 5) (Rojas-Sariol et al., 2011). Besides, ammonium sulfate is added as a nutrient to provide the nitrogen required by yeast. These additions (sulfuric acid and ammonium sulfate) provoke a high sulfate content in Cuban vinasse (up to 15.8 kg m^{-3}), what makes it a sulfate-rich liquid substrate for anaerobic digestion. From these high sulfate and organic matter contents of Cuban vinasse, sulfate reducing bacteria (SRB) can grow to produce H_2S, which is distributed between H_2S_{aq} ($[H_2S]_{free}$, HS^- and S^{2-}), insoluble metallic sulfides and H_2S_{gas}. The H_2S_{gas} is corrosive to energy conversion systems and its removal is a necessity for any utilization of biogas (Abatzoglou and Boivin, 2009) while H_2S_{aq} and $[H_2S]_{free}$ are inhibitory for the anaerobic digestion and should be controlled to ensure process performance.

The production and characteristics of vinasse are variable and dependent on the feed stocks and the ethanol production process. The variations in the COD and SO_4^{2-} concentrations of

the influent vinasse may cause dynamical responses in the sulfate reduction process during the anaerobic treatment, influencing the biogas quality as well as the process performance. Therefore, sulfate reduction in the anaerobic digestion of cane-molasses vinasse should be studied to assist the energetic use of the biogas and the process performance by predicting hydrogen sulfide concentrations in the gas and liquid phases, respectively.

Modeling and simulation are useful tools to predict the behavior and collect data of process steps. Anaerobic Digestion Model No. 1 (ADM1) is the global consensus in anaerobic digestion modeling (Batstone et al., 2002) but the sulfate reduction process was not included. Some extensions of ADM1 have been proposed to model sulfate reduction. The simple approach of Batstone (2006) is based on the oxidation of the available hydrogen only. This has been used to model the anaerobic digestion of vinasse under dynamic conditions without success (Hinken et al., 2013). The approach of Fedorovich et al. (2003) has been considered as complex because of the inclusion of valerate/butyrate, propionate, acetate and hydrogen in the sulfate degradation reactions (Batstone, 2006). In addition, this extension did not report the agreement between model and experimental values for the concentrations of total aqueous sulfide, free sulfides and gas phase sulfides. Likely because of these limitations, the extension of Fedorovich et al. (2003) is not commonly used (Lauwers et al., 2013). Consequently, an extension of ADM1 with sulfate reduction to model the anaerobic digestion of a very high strength and sulfate rich vinasse is needed to overcome the existing limitations of models (see also Chapter 3).

Although the anaerobic digestion of vinasse is widely accepted as the first treatment step in distilleries, most of Cuban vinasses (≈99%) are treated in lagoons where methane, carbon dioxide and hydrogen sulfide emissions have been reported as a result of uncontrolled anaerobic decomposition of the organic matter (Safley and Westerman, 1988; Toprak, 1995). As methane is an important greenhouse gas that has a global warming potential of 34 CO_2-equivalents over a 100 year time horizon (IPCC, 2013), the principal environmental damage reported for lagooning is the methane emission (Chen et al., 2013). If it is assumed that 1 m^3 of vinasse produces 24 to 27 m^3 of biogas (60% methane) (Nandy et al., 2002; Salomon and Silva, 2009), and 1 m^3 of methane produces 6.25 to 10 kWh of electricity and heat (Salomon and Silva, 2009), then the emissions of 1.3 million cubic meters of vinasse reported by the Cuban Ministry of the Cane Sugar Industry in 2009 could supply 117 to 211 GWh per year

of renewable energy (electricity and heat). Thus, the use of vinasse to produce renewable energy in anaerobic digestion power plants as alternative for lagooning can be advantageous in the Cuban context from the environmental and energetic point of view. In order to compare the environmental impacts and the process inefficiencies of alternatives, the methodology of Life Cycle Assessment (LCA) and the exergy analysis (EA), respectively, have been applied (Casas et al., 2011; Contreras et al., 2009; De Meester et al., 2012; Gil et al., 2013).

Therefore, modeling sulfate reduction process in the anaerobic digestion of cane-molasses vinasse can help to predict how the concentration of relevant sulfur compounds (in the gas and liquid phases) change when the composition of the substrate and the process conditions vary, assisting the energetic use of the biogas and the process performance, whereas LCA and EA can quantify the environmental impacts and the process inefficiencies, respectively, of anaerobic digestion power plants as alternative for lagooning Cuban vinasse.

1.2 Vinasse generation in the sugar sector: an overview

In order to illustrate the generation of vinasse, an overview of the process steps in the sugar and ethanol factories is given within this section (Figure 1.1). The sugarcane is milled during 100 days (because sugarcane is only available for that period) to produce juice (70%) and bagasse (30%) in the sugar factory (Casas, 2012; Romero Romero, 2005). During this period, bagasse is traditionally incinerated to supply the heat and electricity demand of the sugar and ethanol factories and the surplus of electricity (0-0.14 kWh/t_{cane}) is delivered to the national grid (Casas, 2012; Romero Romero, 2005). Sugar wastewaters (0.40 t/t_{cane}) and filter cake (0.03 t/t_{cane}) are wasted during the juice clarification step, whereas sugar (0.14 t/t_{cane}) and molasses (0.04 t/t_{cane}) are obtained as product and by-product, respectively, after concentration, crystallization and centrifugation (Casas, 2012).

The molasses obtained from the sugar factory are used as feedstock for the ethanol production process. Typically, sulfuric acid and ammonium sulfate are added during fermentation (Rojas-Sariol et al., 2011). An amount of 2.4 HL of alcohol per ton of molasses (Casas, 2012) and 13L of vinasse per 1L of ethanol can be obtained during distillation (Salomon and Silva, 2009). Molasses from the nearby sugar factories are stored to guarantee

the 300 operation days of the ethanol factory. The electricity and heat demanded during the remaining 200 days in which the sugar factory is out of operation, are produced from fuel oil.

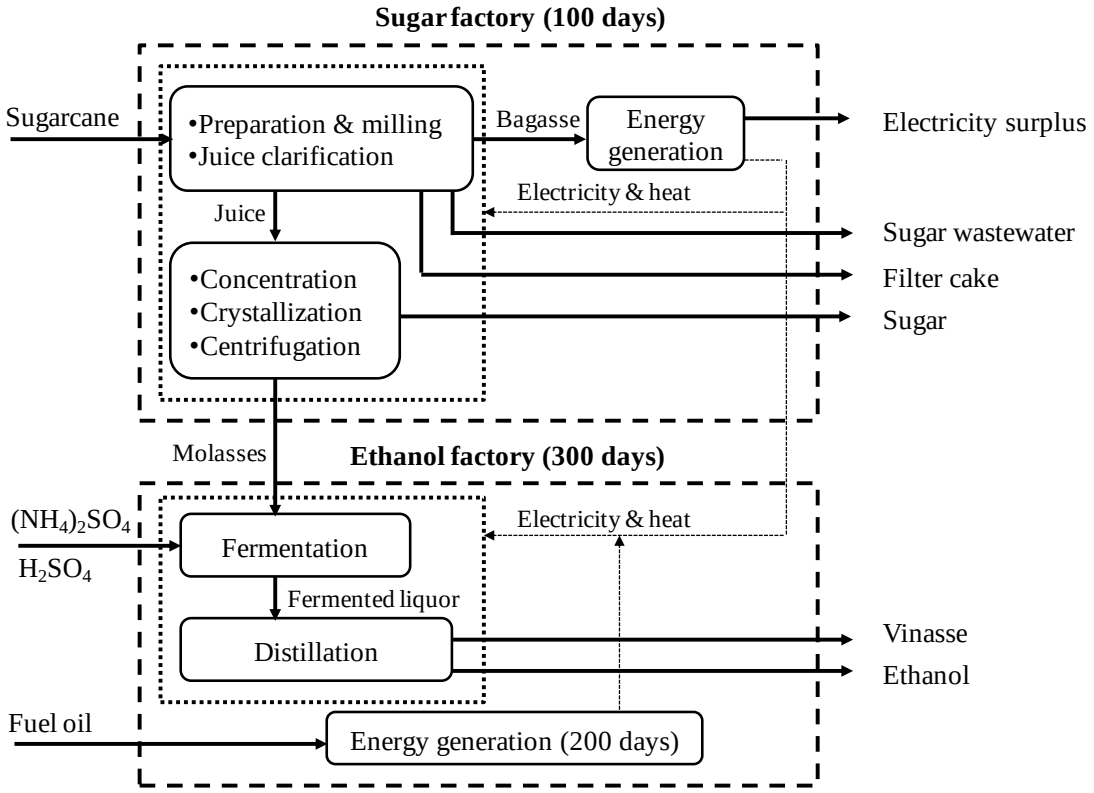

Figure 1.1. Overview of the process steps in sugar and ethanol factories

Therefore the anaerobic digestion of vinasse seems to be a good alternative for vinasse treatment and renewable energy production in distilleries. The characteristics of vinasse as a substrate for anaerobic digestion are discussed in the following section.

1.3 Anaerobic digestion of sulfate-rich liquid substrates: vinasse

1.3.1 Vinasse as a substrate

Most of the distillery wastewaters are highly polluted and considered to be medium–high strength wastewaters (Ince et al., 2005). Vinasses are dark brown in color, with an acid nature; they leave the ethanol distillation tower at high temperature (> 50 °C) and have a chemical oxygen demand of typically above 60 kg COD m^{-3}. The anaerobic digestion of vinasse can convert a significant portion of its COD into biogas (>50%), which can be used

as an implant fuel in alcohol factories, reducing at the same time its detrimental impact on the receiving environment (Pant and Adholeya, 2007).

Despite this, some factors can strongly inhibit the anaerobic digestion of vinasse, including COD values over 100 kg m^{-3} (Wilkie et al., 2000), and high levels of light metals (Na^+ and Ca^{2+} over 8 kg m^{-3}, and K^+ over 12 kg m^{-3}) (Chen et al., 2008; Parkin and Owen, 1986). The heavy metals (Fe^{2+}) have been found non-toxic up to several hundreds of g m^{-3} (Chen et al., 2008). Direct inhibition by sulfates (SO_4^{2-}) has hardly been reported. The decrease of the maximum activity of aceticlastic methanogens at concentrations exceeding 5 kg SO_4^{2-} m^{-3}, has been attributed to the presence of Na^+ because of the use of Na_2SO_4 (Rinzema and Lettinga, 1988). Regarding the sulfate concentrations, the anaerobic digestion inhibition is particularly determined by the ratio SO_4^{2-}/COD in the substrate and the production of hydrogen sulfide in the reactor bulk, which is discussed in the next section.

Characteristics of vinasses obtained from the distillation of sugar cane molasses in different regions are shown in Table 1.1. Column A shows the maximum, minimum and average values of 25 vinasses grouped by Wilkie et. al. (2000), whereas columns B, C and D show vinasses from India, Brazil and Cuba respectively (Nandy et al., 2002; Obaya et al., 2004; Salomon and Silva, 2009). The parameters depicted are: chemical oxygen demand (COD), sulfate (SO_4^{2-}), pH, temperature (T), volatile matter (VM), volatile fatty acids (VFAs), total nitrogen (N), total organic carbon (TOC), heavy and light metals (Fe^{2+}, Ca^{2+}, K^+ & Na^+), sulfides and chlorides (Cl^-).

The use of vinasse as a substrate in anaerobic digestion is questionable if the concentration of at least one parameter is above its corresponding inhibition concentration. For example, based on the COD values, vinasses from India, Brazil and Cuba are good substrates for anaerobic digestion (Table 1.1), whereas seven COD values in column A are above 100 kg m^{-3} and may cause inhibition of the anaerobic digestion. The content of volatile material (VM) between 38.7 and 60 kg m^{-3} indicates that vinasses possess the organic material to be anaerobically degraded. Temperatures are between 71-100 °C and the pH is in the range of 3.5 to 5.5 (given the acid nature of vinasse), which lead to consider cooling and neutralization pretreatment, respectively, before the anaerobic digestion (Table 1.1).

Vinasse alkalinity is not reported as inorganic carbon because of its low pH, where the alkalinity is due to the volatile fatty acids. Banerjee and Biswas (2004) and Parnaudeau et. al.

(2008) found that inorganic carbon in vinasse was negligible in comparison with the organic carbon content (fixed carbon).

Table 1.1. Characteristics of vinasses obtained from distillation of sugar cane molasses in different regions

Parameter	A	B	C	D	Inhibition conc.
Countries	Miscellaneous[a]	India	Brazil	Cub	-
COD (kg m^{-3})	22.5-130 (84.9)[b]	92-100	65	71.2	100
SO_4^{2-} (kg m^{-3})	0.067-9.5 (4.2)[b]	2.1-2.3	6.4	15.8	-
pH	3.5-5.5 (4.46)[b]	4.2-4.3	4.2-5	4.47	-
T (°C)	-	71-81	80-100	-	-
VM (kg m^{-3})	-	-	60	38.7	-
VFA (kg COD m^{-3})	-	2.3-2.4	-	-	-
N (kg m^{-3})	0.2-2.5 (1.23)[b]	1.6-1.8[c]	0.45–1.6	0.21	-
C (kg m^{-3})	-	-	11.2–22.9	-	-
Iron (Fe) (kg m^{-3})	-	15.5-18.0	-	-	-
K (kg m^{-3} K_2O)	1.2-10.3 (5.12)[b]	8.7-9.7	3.74–7.83	-	12
Na (kg m^{-3})	-	0.4-0.5	-	-	8
Ca (kg m^{-3})	-	0.75-0.82	-	0.55	8
Sulfides (kg m^{-3})	-	0.6-0.7	-	-	-
Cl^- (kg m^{-3})	-	5.8-7.6	-	-	-
References	(1)	(2)	(3)	(4)	(1) (5) (6)

[a] Groups of 25 vinasses from different countries reviewed by Wilkie et. al., (2000) [b] Average values reported. [c] Kjeldahl nitrogen. (1) (Wilkie et al., 2000); (2) (Nandy et al., 2002); (3) (Salomon and Silva, 2009); (4) (Obaya et al., 2004) (5) (Chen et al., 2008) (6) (Chen et al., 2008; Parkin and Owen, 1986)

Iron concentrations between 15.5 and 18.0 kg m^{-3} have been reported in Indian vinasse, which is much higher than the several hundreds of g m^{-3} considered as inhibitory. Even being below those levels, the presence of iron in vinasse could affect the sulfate reduction process by the precipitation of iron sulfides (particularly FeS and Fe_2S_3) when S^{2-} ions are present in the bulk solution (Batstone et al., 2002).

Sulfate concentrations are above (5 kg SO_4^{2-} m^{-3}) in three vinasses of column A, in column C and D, being in the case of Cuba (column D) 1.66 times higher than the second highest value reported (9.5 kg SO_4^{2-} m^{-3}). In the anaerobic digestion processes, those sulfates can be reduced to hydrogen sulfide by SRB using a carbon source and hydrogen, what affects methane production.

In general, vinasse can serve as a substrate in anaerobic digestion processes. However, the existence of high COD and SO_4^{2-} concentrations makes vinasse a very high strength and sulfate rich liquid substrate for anaerobic digestion, being relevant the study of the sulfate reduction process.

1.3.2 Sulfate reduction in vinasse

In the anaerobic treatment of sulfate-rich liquid substrates, as vinasse, sulfate is converted into sulfide, which is distributed among H_2S, HS^- and S^{2-} in solution, insoluble metallic sulfides and H_2S in the gas phase. However, at the neutral pH required for anaerobic treatment (pH between 6.5-8), dissolved sulfides occur in the form of H_2S and HS^- (Rinzema and Lettinga, 1988), what makes the formation of metal sulfide precipitates less important.

Only the free form H_2S in solution is considered to be toxic for microorganisms because it can penetrate through the cell membrane (Annachhatre and Suktrakoolvait, 2001), causing inhibition of the anaerobic systems in the 0.05 to 0.43 kg S m^{-3} range (Parkin et al., 1990). Hydrogen sulfide in the gas phase causes operational problems when the biogas is used as an energy source. Hence, sulfate reduction processes in the anaerobic digestion of vinasse should be focused on the estimation of both forms of hydrogen sulfide.

The inhibition by the free form of hydrogen sulfide is related to the ratio SO_4^{2-}/ COD in the fed substrate, being not severely below 0.1 (Rinzema and Lettinga, 1988). Even when high sulfate concentration exists, if the ratio SO_4^{2-}/COD is below 0.1, severe inhibition is not found because of the existence of high COD values, which lead to higher biogas production rates and a rapid removal of sulfide as it is formed (Wilkie et al., 2000).

The ratios SO_4^{2-}/COD of vinasse in Table 1.1 are equal or below 0.1 for the references of the columns A, B and C, being 0.04 (calculated from average values in column A), 0.023 (calculated from maximum values in column B) and 0.1, respectively. These ratios ensure no severe inhibition by the presence of hydrogen sulfide. However, for the case of Cuban vinasse (column D, Table 1.1) the ratio SO_4^{2-}/COD was 0.22, which is above 0.1 where inhibition problems due to free H_2S concentrations above 0.2 kg S m^{-3} can be found (Rinzema and Lettinga, 1988). Hence, vinasse must be anaerobically treated with precautions even when acceptable treatment capacities can be achieved (Rinzema and Lettinga, 1988).

By using synthetic wastewater or a mixture of sulfate-containing wastewater and carbon-containing wastewater as substrates, several authors (Alphenaar et al., 1993; Annachhatre and Suktrakoolvait, 2001; Harada et al., 1994; Isa et al., 1986; Omil et al., 1997a; Omil et al., 1996) have studied the interactions between sulfate reducing processes and methanogenesis. However, no studies have been published for sulfate reduction processes in vinasse with similar simultaneous high levels of COD and SO_4^{2-} and lack of experimental data exists (e.g., Harada et. al. (1996)) to study its dynamical behavior in the SO_4^{2-}/COD ratios reported.

1.4 Modeling sulfate reduction processes in the anaerobic digestion

Modeling approaches (based on sulfur conversion and transfer processes), usefulness and limitations of sulfate reduction models for the prediction of anaerobic digestion of sulfate-rich liquid substrates as vinasse are discussed in this section.

1.4.1 Process and reactions involved

Sulfate reduction is an important process that has to be modeled for operational and technical solutions in anaerobic digestion plants (Batstone, 2006). A simple method to model sulfate reduction is the oxidation of available hydrogen only (Batstone et al., 2002). However in systems with high sulfate concentrations all the reactions involving volatile fatty acids (butyric, propionic and acetic) have to be included as electron donor (Batstone, 2006).

Several authors have been modeling the process following different pathways and approaches. A generalized scheme of sulfate reduction processes in the anaerobic digestion illustrating substrate competition between sulfate reducing bacteria, acetogenic bacteria and methanogenic archea is shown in Figure 1.2. Sulfate reduction from sugars and amino acids (monomers) are not depicted in the scheme because these processes play unimportant roles (Batstone, 2006) and for that reason they are not considered in most models (Kalyuzhnyi et al., 1998; Kalyuzhnyi and Fedorovich, 1998).

In general, substrate competition in anaerobic systems has been modeled in most cases on three levels (I, II and III) (Figure 1.2) (Kalyuzhnyi et al., 1998; Kalyuzhnyi and Fedorovich, 1998; Ristow et al., 2002). Starting from the volatile fatty acids, butyrate and propionate sulfate reducing bacteria (bSRB and pSRB respectively) compete with acetogenic bacteria (AB) to form hydrogen sulfide, carbon dioxide, water and acetic acid (level I). From acetic

acid, acetotrophic sulfate reducing bacteria (aSRB) compete with acetotrophic methanogenic archea (aMA) to produce only hydrogen sulfide, water and carbon dioxide (level II). Hydrogenotrophic sulfate reducing bacteria (hSRB) compete with hydrogenotrophic methanogenic archea (hMA) for hydrogen to produce hydrogen sulfide and water (level III) (Kalyuzhnyi et al., 1998).

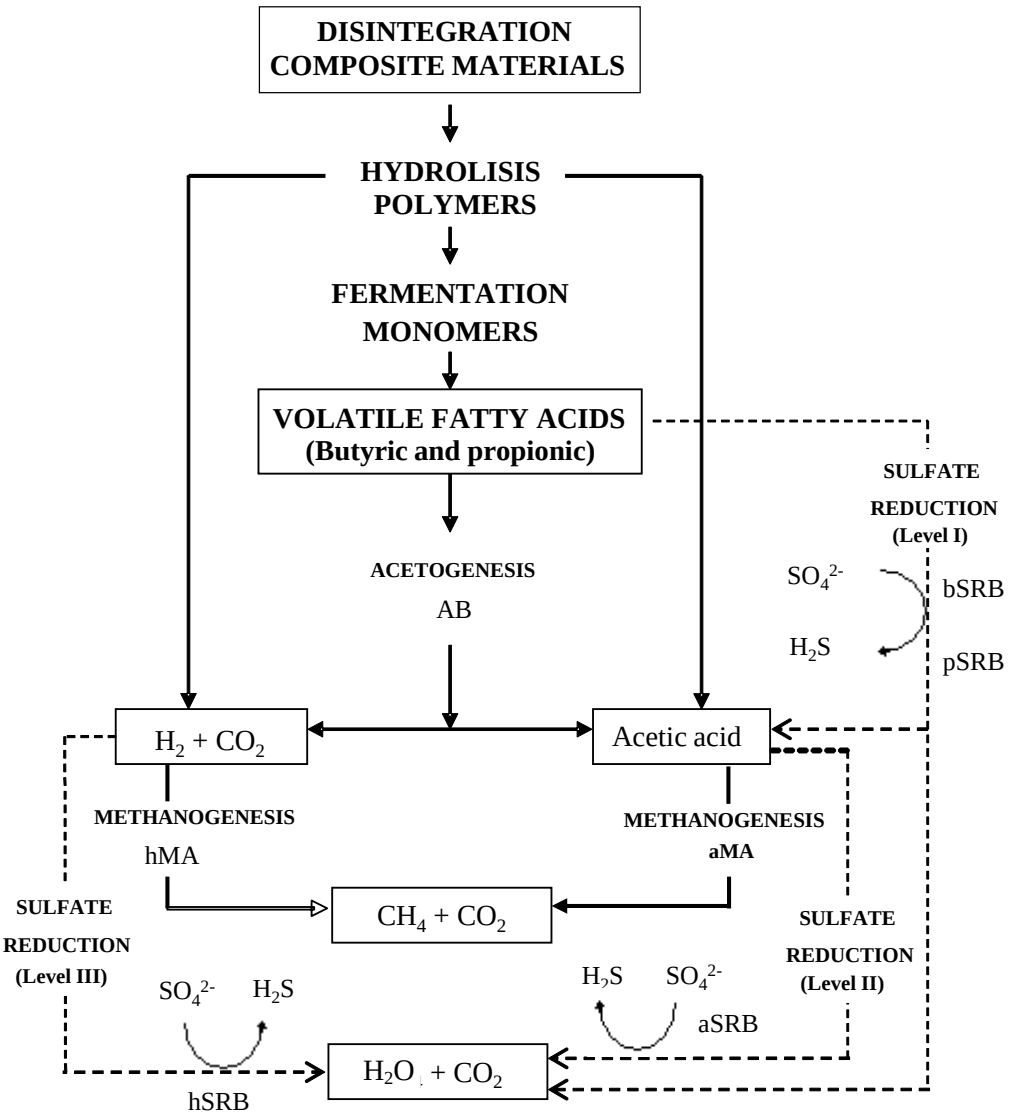

Figure 1.2. Scheme of the substrate competition between sulfate reducing bacteria, acetogenic bacteria and methanogenic archea

A summary of sulfate degradation reactions is shown in Table 1.2. The same reactions have been represented by authors in a dissociated and undissociated form, inclusive and exclusive of water production. Reactions 1.1-1.2 and 2.1-2.2 have been found to end up in acetate (incomplete) or in carbon dioxide and sulfide (complete) (1.3 and 2.3) (Visser, 1995), but it has not been modeled to reduce the number of reaction pathways and to avoid model complexities (Kalyuzhnyi and Fedorovich, 1998). Reactions selected by each model define the kinetic equations.

Table 1.2. Sulfate degradation reactions in the anaerobic digestion process

Sulfate degradation reactions	**References**
1. Butyrate SRB	
1.1 $C_3H_7COOH + 0.5\ H_2SO_4 \rightarrow 2CH_3COOH + 0.5H_2S$	(1),(2),(3)
1.2 $C_3H_7COO^- + 0.5\ SO_4^{2-} \rightarrow 2CH_3COO^- + 0.5HS^- + 0.5H^+$	(4)
1.3 $C_3H_7COO^- + 2.5\ SO_4^{2-} + 0.25H_2O \rightarrow 4HCO_3^- + 2.5HS^- + 0.75H^+ + 0.25OH^-$	(4)
2. Propionate SRB	
2.1 $C_2H_5COOH + 0.75\ H_2SO_4 \rightarrow CH_3COOH + CO_2 + H_2O + 0.75H_2S$	(1),(2),(3),(5),(6)
2.2 $C_2H_5COO^- + 0.75\ SO_4^{2-} \rightarrow CH_3COO^- + HCO_3^- + 0.75HS^- + 0.25H^+$	(4)
2.3 $C_2H_5COO^- + 1.75\ SO_4^{2-} + 0.25H_2O \rightarrow 3HCO_3^- + 1.75HS^- + 0.5H^+ + 0.25OH^-$	(4), (5), (6)
3. Acetate SRB	
3.1 $CH_3COOH + H_2SO_4 \rightarrow 2CO_2 + 2H_2O + H_2S$	(1),(2),(5),(6)
3.2 $CH_3COO^- + SO_4^{2-} \rightarrow 2HCO_3^- + HS^-$	(4)
4. Hydrogenotrophic SRB	
4.1 $4H_2 + H_2SO_4 \rightarrow 4H_2O + H_2S$	(1),(2),(5),(6)
4.2 $4H_2 + SO_4^{2-} + H^+ \rightarrow HS^- + 4H_2O$	(4)

(1) (Fedorovich et al., 2003); (2) (Knobel and Lewis, 2002); (3) (Kalyuzhnyi et al., 1998); (4) (Visser, 1995); (5) (Kalyuzhnyi and Fedorovich, 1998); (6) (Poinapen and Ekama, 2010)

As no studies have been published for sulfate reduction processes in vinasse with similar simultaneous high levels of COD and SO_4^{2-}, where variations in the concentration of the influent vinasse may cause dynamical responses during the anaerobic digestion process

involving organic matter (butyric, propionic and acetic) and hydrogen degradation, the sulfate degradation reactions 1, 2, 3 and 4 (Table 1.2) should be considered as a general approach.

1.4.2 Kinetics of SRB: growth, inhibition and endogenous processes

Kinetics of sulfate reduction processes have been considered in different ways. A dual term Monod type kinetic is commonly used (Eq. (1.1)) to represent the bacterial growth rate ($\rho_{growth,j}$) (Fedorovich et al., 2003; Kalyuzhnyi et al., 1998; Kalyuzhnyi and Fedorovich, 1998; Knobel and Lewis, 2002; Poinapen and Ekama, 2010; Ristow et al., 2002), with both concentrations: sulfate (S_{SO4}) as electron acceptor and the electron donor (S_i) (hydrogen or organic matter) following the equations of Table 1.2. The expression is generally written in the form of substrate uptake ($\rho_{uptake,j}$) by dividing the maximum specific growth rate (μ_{max}) by the yield of biomass on the substrate ($\mu_{max}/Y = k_m$) to obtain Eq. (1.1'). Where, $K_{S,j}$ and $K_{S,SO4j}$ are the half saturation coefficient of the component i and sulfates respectively.

$$\rho_{growth,j} = \mu_{max,j} \frac{S_i}{(K_{S,j}+S_i)} \cdot \frac{S_{SO4}}{(K_{S,SO4j}+S_{SO4})} \cdot X_i \qquad (1.1)$$

$$\rho_{uptake,j} = k_{m,j} \frac{S_i}{(K_{S,j}+S_i)} \cdot \frac{S_{SO4}}{(K_{S,SO4j}+S_{SO4})} \cdot X_i \qquad (1.1')$$

However, some inhibitor compounds affect the growth rate of microorganisms and the uptake of substrates, transforming Eq. (1.1') in (1.1'') by means of the inclusion of pH ($I_{pH,j}$) and sulfide ($I_{h2s,j}$) inhibition functions.

$$\rho_{uptake,j} = k_{m,j} \frac{S_i}{(K_{S,j}+S_i)} \cdot \frac{S_{SO4}}{(K_{S,SO4j}+S_{SO4})} \cdot X_i \cdot I_{pH,j} \cdot I_{h2s,j} \qquad (1.1'')$$

Undissociated H_2S ($S_{h2s,free}$) inhibition has been considered by Kalyuzhnyi and Fedorovich (1998) according to first order inhibition kinetics (Eq. (1.2)), in agreement with some other works (Fedorovich et al., 2003; Ristow et al., 2002). Where, $K_{I,h2s,j}$ is 50% inhibitory concentration of undissociated H_2S.

$$I_{h2s,j} = 1 - [S_{h2s,free}/K_{I,h2s,j}] \qquad (1.2)$$

A noncompetitive inhibition function (Eq. (1.3)) has been used by Knobel and Lewis (2002) whereas Kalyuzhnyi et al. (1998) used the inhibition terms in the form of the so-called 2x2

constants (Eq. (1.4)), which is a modification of noncompetitive functions (K_2 and K_{100} are the concentration of H_2S at which the uptake rate is decreased twice or 100 times, respectively).

$$I_{h2s,j} = 1/[1 + (S_{h2s,free}/K_{I,h2s,j})] \quad (1.3)$$

$$I_{h2s,j} = F(S_{h2s,free}, K_2, K_{100}) = 1/[1+(S_{h2s,free}/K_2)^{\ln 99/(K_{100}/K_2)}] \quad (1.4)$$

Poinapen and Ekama (2010) assessed the first order inhibition function, finding inconsistencies (negative values and instability of the inhibition function) when H_2S concentration ($S_{h2s,free}$) was above the $K_{I,h2s,j}$ value (see Eq. (1.2)). They proposed a more stable function which approaches zero more gradually (Eq. (1.5)) with the increment of the H_2S concentration. The use of this inhibition function seems to be more reasonable when high H_2S concentrations are found.

$$I_{h2s,j} = \exp\left[-\left(S_{h2s,free}/0.60056 \cdot K_{I,h2s,j}\right)^2\right] \quad (1.5)$$

In addition to sulfide inhibition, inhibition effects of pH must be considered in the overall rate equations (see Eq. (1.1'')). It has been included in the form of 2x2 constants (Eq. (1.6) where, K_2 and K_{100} are the pH values at which the uptake rate is decreased twice or 100 times, respectively) and as a function of lower (pH_{LL}) and upper (pH_{UL}) pH inhibition values (Eqs. (1.7) and (1.8)).

$$I_{pH,j} = F(pH, K_2, K_{100}) = 1/(1+(pH/K_2)^{\ln 99/(K_{100}/K_2)}) \quad (1.6)$$

$$I_{pH,j} = (1 + \exp(-\alpha_{LL}(pH - pH_{LL})))^{-1} \cdot (1 + \exp(-\alpha_{UL}(pH - pH_{UL})))^{-1} \quad (1.7)$$

$$I_{pH,j} = \left[1 + 2 \cdot 10^{0.5(pH_{UL}-pH_{LL})}\right]/\left[1 + 10^{(pH-pH_{UL})} + 10^{(pH_{LL}-pH)}\right] \quad (1.8)$$

Some of the models have not considered pH inhibition in order to reduce complexity (Kalyuzhnyi and Fedorovich, 1998; Ristow et al., 2002), while others like Kalyuzhnyi et al., (1998); Knobel and Lewis (2002) and Fedorovich et al. (2003) have used Eqs. (1.6), (1.7) and (1.8), respectively, without consensus. Poinapen and Ekama (2010) considered the pH effect by means of the multiplication of the appropriate half saturation values (K_S) by the undissociated species to total species concentration ratio (this ratio changes as a function of pH), considering this more appropriate and eliminating I_{pH} function from Eq. (1.1''). This

could be used to reduce complexity in pH inhibition modeling. However, pH inhibition also occurs by the disruption of homeostasis affecting all organisms in some degree (Batstone et al., 2002), depending on pH_{LL} and pH_{UL} values of each microbial group. Therefore, pH inhibition is better modeled by using the I_{pH} function of Eq. (1.7) or (1.8) in Eq. (1.1'').

Table 1.3. Kinetic coefficients used in the modeling of sulfate reduction processes in the anaerobic digestion

SRB	Constants	Unit	A	B	C	D
			References			
			(1),(2)	(3), (4)	(3)	(5)
bSRB	$\mu_{max,j}$	d^{-1}	-	-	0.22	0.45
	$k_{m,j}$	kg COD_S_i· kg COD_X_i $^{-1}$· d^{-}			7.33	13.7
	$K_{S,j}$	10^{-3} kg COD_S_i · m^{-3}	-	-	9	100
	$K_{S,SO4,j}$	10^{-3} kmol· m^{-3}	-	-	0.104	0.21
	Y_i	kg COD_X_i · kg COD_S_i^{-1}	-	-	0.03	0.0329
	$K_{I,h2s,j}$	10^{-3} kmol· m^{-3}	-	-	12.5	8.13
	$k_{dec,j}$	d^{-1}			0.035	0.01
pSRB	$\mu_{max,j}$	d^{-1}	0.81	0.583	0.29	0.414
	$k_{m,j}$	kg COD_S_i· kg COD_X_i $^{-1}$· d^{-}	23.1	21.5	9.6	12.6
	$K_{S,j}$	10^{-3} kg COD_S_i · m^{-3}	295	295	15	110
	$K_{S,SO4,j}$	10^{-3} kmol· m^{-3}	0.077	0.077	0.19	0.20
	Y_i	kg COD_X_i · kg COD_S_i^{-1}	0.035	0.027	0.03	0.0329
	$K_{I,h2s,j}$	10^{-3} kmol· m^{-3}	8.90	5.78	6.80	8.13
	$k_{dec,j}$	d^{-1}	0.018	0.0185	0.035	0.01
aSRB	$\mu_{max,j}$	d^{-1}	0.51	0.612	0.151	0.243
	$k_{m,j}$	kg COD_S_i· kg COD_X_i^{-1}· d^{-1}	12.4	18.5	4.19	7.1
	$K_{S,j}$	10^{-3} kg COD_S_i · m^{-3}	24	24	25	220
	$K_{S,SO4,j}$	10^{-3} kmol· m^{-3}	0.20	0.20	0.20	0.10
	Y_i	kg COD_X_i · kg COD_S_i^{-1}	0.041	0.033	0.036	0.0342
	$K_{I,h2s,j}$	10^{-3} kmol· m^{-3}	8.90	5.13	18.75	7.81
	$k_{dec,j}$	d^{-1}	0.025	0.0275	0.044	0.015
hSRB	$\mu_{max,j}$	d^{-1}	5	2.8	-	0.977
	$k_{m,j}$	kg COD_S_i· kg COD_X_i $^{-1}$· d^{-}	64.9	56		26.7
	$K_{S,j}$	10^{-3} kg COD_S_i · m^{-3}	0.05	0.07	-	0.1
	$K_{S,SO4,j}$	10^{-3} kmol· m^{-3}	0.009	0.20	-	0.104
	Y_i	kg COD_X_i · kg COD_S_i^{-1}	0.077	0.05	-	0.0366
	$K_{I,h2s,j}$	10^{-3} kmol· m^{-3}	17.1	17.1	-	7.8
	$k_{dec,j}$	d^{-1}	0.03	0.0600		0.01

(1) (Kalyuzhnyi and Fedorovich, 1998); (2) (Ristow et al., 2002) (3) (Kalyuzhnyi et al., 1998); (4) (Poinapen and Ekama, 2010); (5) (Fedorovich et al., 2003)

The endogenous processes are described as decay of SRB. It has been modeled following Eq. (1.9) for all bacteria groups, describing the rate of death (endogenous mass loss, $\rho_{decay,j}$) as a function of the specific endogenous mass loss rate ($k_{dec,j}$) and the particulate component concentration (X_i) (Fedorovich et al., 2003; Kalyuzhnyi et al., 1998; Kalyuzhnyi and Fedorovich, 1998; Knobel and Lewis, 2002; Poinapen and Ekama, 2010).

$$\rho_{decay,j} = k_{dec,j} \cdot X_i \qquad (1.9)$$

Calibration of models has to be done for any implementation depending on the kind of substrate, component concentrations and bacterial behavior. A summary of the kinetic coefficients used by different authors is shown in Table 1.3. These coefficients have shown values in the same order of magnitude for the bacteria yield coefficient for all SRB, demonstrating its low growing capacity in anaerobic environments. The fact that only the sulfate reduction process using hydrogen as electron donor is modeled in low sulfate containing substrates can be explained by the Monod parameter values (μ_{max} and K_S) shown in Table 1.3. In this table, μ_{max} for hSRB was higher (more than 4.5 times) in column A and B (in which bSRB were not considered) than for aSRB and pSRB. However when all SRB were considered, μ_{max} was distributed almost equally (column D); being for hSRB even the double of the others (bSRB, pSRB and aSRB). At the same time, the half saturation coefficient (K_S) reported for hSRB was lower than for the rest (bSRB, pSRB and aSRB) in columns A, B, C and D, expecting faster bacterial growth and higher uptake rate of substrate by hSRB. Hence, sulfate reduction process by hSRB can outcompete bSRB, pSRB and aSRB when hydrogen is available as electron donor.

1.4.3 Acid-base equilibrium and gas-liquid transfer equation

The inclusion of sulfate reduction processes leads to a proper description of H_2S/HS^- acid base equilibrium, H_2S_{gas} stripping, and the impact of SO_4^{2-} on the charge balance (Batstone, 2006).

Kalyuzhnyi and Fedorovich (1998) included in the charge balance the effect of the ionized compounds [SO_4^{2-}], [HS^-] and [S^{2-}], based on the acid-base Eqs. (1.11), (1.12) and (1.13). However, [S^{2-}] is produced in small amounts at neutral pH and is negligible (Rinzema and Lettinga, 1988). Fedorovich et al. (2003) proposed the inclusion of acid base equations, in the

same form as Batstone et al. (2002) without information of included equations. In agreement with Batstone (2006) the model of Poinapen and Ekama (2010) only adds Eqs (1.11) and (1.12) to describe the acid-base equilibrium of the sulfate reduction process in the anaerobic digestion. This approach is because sulfuric acid (Eq. (1.10), pKa < - 2) is a strong acid and can be considered completely dissociated into HSO_4^- to follow Eq. (1.11); while sulfide ions [S^{2-}] from Eq. (1.13) (pK_a ≈14) exist in small amounts in the liquid phase of anaerobic reactors where pH between 6 and 8 is required. The Van 't Hoff equation is used to describe the temperature-dependent variation in the acid-base equilibrium.

Sulfuric acid (pK_a and K_a at 25 °C)

$H_2SO_4 \leftrightarrows H^+ + HSO_4^-$	$pK_{a1} < -2$	$K_{a1} > 100$ (strong)	(1.10)
$HSO_4^- \leftrightarrows H^+ + SO_4^{2-}$	$pK_{a2} = 1.99$	$K_{a2} = 1.02\ 10^{-2}$	(1.11)

Hydrogen sulfide (pK_a and K_a at 25 °C)

$H_2S \leftrightarrows H^+ + HS^-$	$pK_{a1} = 7.01$	$K_{a1} = 9.6\ 10^{-8}$	(1.12)
$HS^- \leftrightarrows H^+ + S^{2-}$	$pK_{a2} = 13.88$	$K_{a2} = 1.3\ 10^{-14}$	(1.13)

The concentration of the dissociated species has been calculated starting from the acid-base constant in the form of Eq. (1.14) for the equilibrium of Eq. (1.12). This Eq. (1.14), which is written in the form recommended by Rosen and Jeppsson (2006), represents the change in the HS^- concentration (S_{hs-}) due to changes in hydrogen sulfide total form ($S_{h2s,total}$) and pH (S_{H+}) in the liquid media. Values of the acid-base kinetic parameters ($K_{A/B}$) have been usually adjusted from 10^8 m^3 $kmol^{-1}$ d^{-1} and can be optimized for each acid-base reaction.

$$\rho_j = K_{A/B,h2s}(S_{hs-} \cdot (S_{H+} + K_{a,h2s}) - K_{a,h2s} \cdot S_{h2s,total}) \quad (1.14)$$

The stripping of the produced hydrogen sulfide has been modeled following Eq. (1.15) (Fedorovich et al., 2003; Kalyuzhnyi et al., 1998; Kalyuzhnyi and Fedorovich, 1998; Knobel and Lewis, 2002; Poinapen and Ekama, 2010), which is based on Henry's law (where, $P_{gas,h2s}$ is the partial pressure of H_2S in the gas phase). Henry's temperature-dependent coefficient has been modeled using van 't Hoff equation with values of $K_{H(25°C),h2s} = 0.105$ kmol m^{-3} bar^{-1} as in Batstone (2006) and $K_{H(30°C),h2s} = 0.09$ kmol m^{-3} bar^{-1} as in Kalyuzhnyi and Fedorovich (1998). The most common limitation of the mass transfer modeling is the

assumption of a unique mass transfer coefficient (k_La) for all biogas components, because of their similar diffusivities in water as is recommended by Batstone et al. (2002).

$$\rho_j = k_La \cdot \left(S_{h2s,free} - K_{H,h2s} \cdot P_{gas,h2s}\right) \quad (1.15)$$

Batstone et al. (2002) proposed the use of k_La calculated from a relationship between O_2 diffusivity in aerobic systems and gas diffusivities in water. Nevertheless, an appropriate value of the mass transfer coefficient must be used to properly describe the inhibition effects of undissociated hydrogen sulfide over microbial groups (Knobel and Lewis, 2002) and its concentrations in the biogas streams.

1.5 Sulfate reduction models as alternatives or extension to Anaerobic Digestion Model No. 1 (ADM1): usefulness and limitations

Anaerobic digestion is a series of complex biochemical processes that are not easy to understand and predict. Scientists have developed a number of models with the purpose of better understanding the anaerobic digestion process, but because of the wide range of existing models, a generalized simple model was proposed by the International Water Association (IWA). This model, the Anaerobic Digestion Model No. 1 (ADM1) (Batstone et al., 2002), was developed to increase its applicability in full-scale design, the operation and optimization for direct implementation, the creation of common basis for further modeling and validation studies, as well as to assist a technology transfer from research to industry.

The model uses substrate uptake Monod type kinetics for intracellular biochemical reactions (i.e., acidogenesis including fermentation of monomers, acetogenesis and methanogenesis) and first order extracellular disintegration and hydrolysis. Besides, ADM1 includes physical and chemical processes including the acid-base equilibrium and gas-liquid rate transfer.

However, some disadvantages have been observed in the original ADM1 as reported by Fuentes et al., (2008). Its shortcomings to model the anaerobic digestion of vinasse are the omission of processes related to sulfate reduction and the associated sulfide inhibition, and prediction of H_2S in the biogas.

Some studies have been carried out to include sulfate reduction in anaerobic digestion modeling as was discussed. All these models (Fedorovich et al., 2003; Kalyuzhnyi et al., 1998; Kalyuzhnyi and Fedorovich, 1998; Knobel and Lewis, 2002; Poinapen and Ekama,

2010; Ristow et al., 2002) have been developed and calibrated for specific purposes and substrates (see section 1.5.1), and for the prediction of a number of variables. The usefulness and limitations of these models are discussed in the next section, classified as ¨alternatives to ADM1¨ -model that follow a different principle in its conception with respect to ADM1 to model sulfate reduction processes (e.g., conception of processes rate equations, stoichiometry and units)- or ¨extension of ADM1¨ -model that follow the same concepts as the ADM1 to model sulfate reduction processes.

1.5.1 Sulfate reduction models ¨alternatives to ADM1¨

As an alternative to ADM1, Kalyuzhnyi and Fedorovich (1998) used the results of Alphenaar (1993) obtained from a synthetic high sulfate containing wastewater treated in a UASB reactor, to evaluate the competition between SRB and methanogens (M). The model agreed well with the experimental data, giving special attention to the competition for acetate, because the consumption of propionate and hydrogen by methanogens was negligible in comparison with SRB (propionate and hydrogen were 100 % converted by SRB). The modeling results were obtained under variations of hydraulic retention time (HRT), SO_4^{2-} /COD ratio, initial proportion of SRB/M, efficiency of retention of SRB, and sludge quality. However, the influence of these variables in the hydrogen sulfide concentrations of the biogas as well as the substrate uptake in the sulfate degradation reaction of bSRB, were not simulated.

Based on similar considerations, Kalyuzhnyi et al. (1998) developed a dispersed plug flow model of a sulfate fed UASB reactor and assessed the competition between methanogens and SRB specifically for the UASB reactor configuration. Data to calibrate the model was taken from Alphenaar (1993) and Omil et al. (1997a; 1996). Good agreement was also demonstrated between observation and model simulation, and special emphasis was put on the acetate competition. The model was able to predict system performance with regard to variations in the liquid upward velocity as an important control parameter, and in the butyrate and propionate influent concentrations. However, when pH changes occurred the results were not correctly predicted.

Moreover, the model of Knobel and Lewis (2002) was calibrated for a number of reactor configurations (packed bed, UASB and fed gas lift reactor) under steady state and dynamic

conditions in three simulation tests. The first two simulation tests (fed gas lift reactor is beyond the scope of this review) using molasses (carbon source) and acid mine drainage (sulfate containing wastewater) were able to predict COD and sulfate concentrations in the effluent, but the prediction of the biogas composition was not reported although the mass transfer equations and mass transfer coefficient of the gas components were discussed.

Ristow et al. (2002) used AQUASIM software to simulate the anaerobic digestion process including sulfate reduction in a recycling sludge bed reactor (RSBR) for acid mine drainage (sulfate containing wastewater) and primary sludge (carbon source). The model calculations agreed well with experimental data obtained from the pilot plant, showing influences of various operational variables (sludge recycle ratio, SO_4^{2-}/COD ratio and HRT) on the sulfate reduction process. This and the other models have a common limitation: the biogas composition and its variation as a function of operational parameters were not predicted.

Poinapen and Ekama (2010) used a kinetic model with the inclusion of sulfate reduction processes. The kinetic model, calibrated with experimental data starting from different SO_4^{2-}/COD ratios (Poinapen et al., 2009b; Poinapen et al., 2009c), shows good agreements with respect to the simulated results in the effluent variables of the liquid phase (COD and sulfate concentrations, ratio H_2S/HS^-, pH and alkalinities) when a carbon deficient influent was fed into the reactor. To predict the gas phase compositions, only hydrogen sulfide gas-liquid equilibrium equation was included. Carbon dioxide concentration was negligible due to the use of a carbon deficient substrate and methane was considered to be produced directly to the gas phase because of its low solubility. However, the hydrogen sulfide concentrations in the gas phase were set to zero in the model results to fit with the experimental data, because in those experiments, H_2S was completely removed by bubbling the biogas through a ferric solution to close the sulfur mass balance. That is why the real hydrogen sulfide concentration in the gas phase with respect to the variation of the SO_4^{2-}/COD ratios in the experimental data was not predicted by the kinetic model.

Hence, models "alternatives to ADM1" have been calibrated to predict the influence of operational parameters and influent concentrations (efficiency of retention of SRB, HRT, SO_4^{2-}/COD and SRB/M ratio, and liquid upward velocity) on the uptake of substrates (butyrate, propionate, acetate) and removal efficiencies (COD, SO_4^{2-}). Nevertheless, hydrogen sulfide concentrations in the gas phase have not been correctly predicted.

1.5.2 Sulfate reduction model as an extension of ADM1

Fedorovich et al. (2003) described sulfate reduction processes as an extension of ADM1. The model was calibrated against experimental data from literature (Omil et al., 1997a; Omil et al., 1996) and it was able to predict sulfate removal in the anaerobic digestion process and concentrations of butyrate, propionate and acetate, as well as methane and biomass production. Although the model of Fedorovich et al. (2003) is reported today as the most appropriate extension of ADM1 when sulfate removal efficiencies are of primary interest, it was not calibrated to predict the concentrations of total aqueous sulfide (S_{h2s}), free sulfides ($S_{h2s,free}$) and gas phase sulfides ($S_{gas,h2s}$).

Process rate

$$\rho_{uptake,j} = k_{m,j}\frac{S_i}{(K_{S,j}+S_i)}\cdot\frac{S_{SO4}}{(K_{S,SO4,j}+S_{SO4})}\cdot X_i \cdot I_{pH,j}\cdot I_{h2s,j}$$

Decay rate

$$\rho_{decay,j} = k_{dec,j}\cdot X_i$$

Acid-based rates

$$\rho_j = K_{A/B,h2s}(S_{hs^-}\cdot(S_{H^+}+K_{a,h2s})-K_{a,h2s}\cdot S_{h2s,total})$$

$$\rho_j = K_{A/B,so4}(S_{so4,total}\cdot S_{H^+}-S_{HSO_4^-}\cdot(K_{a,so4}+S_{H^+})$$

Gas transfer rates

$$\rho_j = k_L a\cdot\left(S_{h2s,free}-K_{H,h2s}\cdot P_{gas,h2s}\right)$$

Process inhibition

- Sulfides

$$I_{h2s,j} = \exp\left[-\left(S_{h2s,free}/0.60056K_{I,h2s,j}\right)^2\right]$$

$$I_{h2s,j} = 1/[1+(S_{h2s,free}/K_{I,h2s,j})]$$

$$I_{h2s,j} = F\left(S_{h2s,free},K_2,K_{100}\right) = 1/[1+(S_{h2s,free}/K_2)^{\ln 99/(K_{100}/K_2)}]$$

- pH

$$I_{pH,j} = F(pH,K_2,K_{100}) = 1/(1+(pH/K_2)^{\ln 99/(K_{100}/K_2)})$$

$$I_{pH,j} = (1+\exp(-\alpha_{LL}(pH-pH_{LL})))^{-1}\cdot(1+\exp(-\alpha_{UL}(pH-pH_{UL})))^{-1}$$

$$I_{pH,j} = \left[1+2\cdot 10^{0.5(pH_{UL}-pH_{LL})}\right]/\left[1+10^{(pH-pH_{UL})}+10^{(pH_{LL}-pH)}\right]$$

Figure 1.3. Summary of the equations used to model sulfate reduction processes in the anaerobic digestion of sulfate-rich liquid substrates

A summary of equations to model the sulfate reduction processes in the anaerobic digestion of sulfate-rich liquid substrates, as vinasse, is provided in Figure 1.3. As simultaneous degradation of organic matter and hydrogen by SRB ought to occur during the anaerobic digestion of vinasse, the most complete approach to model sulfate reduction could correspond to Fedorovich et al. (2003) which involves organic matter (butyric, propionic and acetic) and hydrogen degradation reactions. However, it should be noted that a more stable sulfide inhibition function (see section 1.4.2) following Poinapen and Ekama (2010) could be used instead of the first order inhibition function (Figure 1.3).

Therefore it can be concluded that:

- Vinasse has been reported over the world as a typical sulfate-rich liquid substrate for anaerobic digestion with SO_4/COD ratios in the range of 0.04 to 0.22.
- Further studies are needed to investigate the sulfate reduction processes in vinasses with similar simultaneous high levels of COD and SO_4^{2-}, thereby generating experimental data to support the modeling of the dynamic behavior of sulfur compounds.
- The most comprehensive approach to model sulfate reduction in the anaerobic digestion is the ADM1 extension reported by Fedorovich et al. (2003).
- Although the model equations are available in literature no results have been shown (as an extension of ADM1) to predict the concentrations of total aqueous sulfide (S_{h2s}), free sulfides ($S_{h2s,free}$) and gas phase sulfides ($S_{gas,h2s}$).
- Kinetic coefficients to model sulfate reduction in the anaerobic digestion of vinasse have not been reported in literature and this fact is limiting the prediction of the sulfides in the gas and liquid phases to assist the energetic use of the biogas and the process performance.

1.6 Environmental assessment tools

The concept of sustainability is conceived in three dimensions: social, economic and environmental (Prosuite, 2013). The social sustainable development aims at maintaining the stability of social and cultural systems, the economic sustainability considers the attaining of the maximum incomes whereas the environmental sustainability refers to preserving the ability of 'natural' to adapt. In order to assess the impact of resources and emissions on the

natural environment for alternative technologies or products, the environmental sustainability concept is commonly applied by using life cycle assessment and exergy analysis tools (Contreras, 2007; Contreras et al., 2013; De Meester et al., 2012; Nzila et al., 2012). This approach was assumed as sustainability assessment in the present work.

1.6.1 Environmental Life Cycle Assessment

Life cycle assessment (LCA) has been used in the academic world and industry to evaluate the overall impact on the environment of the whole life cycle of processes and products (Azapagic, 1999). It can assist the identification of opportunities to improve the environmental profiles of products and services at several stages of their life cycle, informing decision-makers in industry, governmental or non-governmental organizations (e.g. for the purpose of strategic planning, priority setting, product or process design or redesign) (ISO14040; ISO14044). Consequently, its application to the treatment of cane molasses vinasse can generate useful information about the environmental profiles of different scenarios for the Cuban context.

The LCA methodology contains four phases (Figure 1.4) which are subsequently discussed in detail:

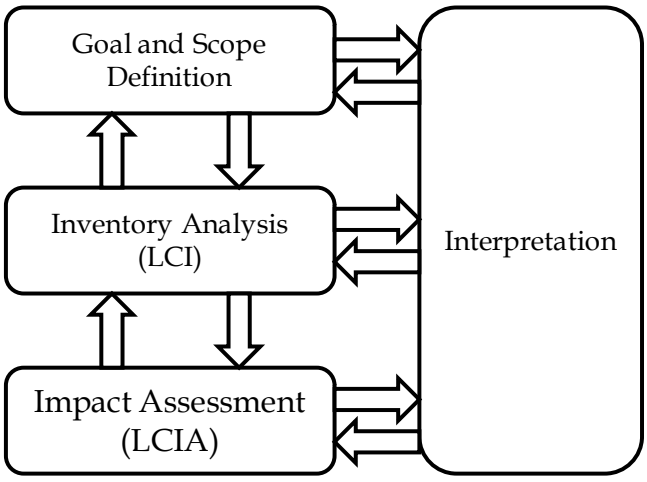

Figure 1.4 Phases of Life Cycle Assessment Methodology (LCA) (Guinee et al., 2002)

1.Goal and scope definition: As a first step of an LCA study, it is recommended to give a clear definition of the goal and scope, being consistent with the intended application

(ISO14044). In defining the goal of an LCA, the following items should be stated: the intended application; the reasons for carrying out the study; the intended stakeholders (i.e. to whom the results of the study are intended to be communicated) and whether the results are intended to be used in comparative assertions intended to be disclosed to the public (ISO14040; ISO14044). Further, in defining the scope of an LCA, the following aspects are considered and clearly described: the product system to be studied; the functions of the product system or, in the case of comparative studies, the systems; the functional unit; the system boundary; allocation procedures; Life Cycle Impact Assessment (LCIA) methodology and types of impacts; interpretation to be used; data requirements; assumptions; value choices and optional elements; limitations; data quality requirements; type of critical review, if any; type and format of the report required for the study (ISO14040; ISO14044).

2. Life cycle inventory (LCI): The definition of the goal and scope of a study provides the initial plan for conducting the life cycle inventory phase of an LCA. Inventory analysis involves data collection and calculation procedures to quantify relevant inputs and outputs of a product system (including modeling to generate data). The process of conducting an inventory analysis is iterative. As data are collected and more is learned about the system, new data requirements or limitations may be identified that require a change in the data collection procedures so that the goals of the study will still be met (ISO14040).

3. Life cycle impact assessment (LCIA): The impact assessment phase is aimed to the evaluation of the significance of potential environmental impacts using the LCI results. In general, this process involves associating inventory data with specific environmental impact categories and category indicators, thereby attempting to understand these impacts. The LCIA phase also provides information for the life cycle interpretation phase and should include selection of impact categories, category indicators and characterization models; assignment of LCI results to the selected impact categories (classification); and calculation of category indicator results (characterization) (ISO14040; ISO14044).

The Centrum Milieukunde Leiden (CML) and the Eco-indicator guides are widely accepted as the LCIA methodologies (Goedkoop et al., 2008). The first one (CML-guide) is based on the midpoint approach, while the second one (Eco-indicator) focus on the interpretation of the results and uses the endpoint approach (European-Commission, 2010b; Goedkoop et al., 2008). In order to harmonize the midpoint and endpoint approach in a consistent framework,

the methodology "ReCiPe" was developed (European-Commission, 2010b; Goedkoop et al., 2008). Therefore, ReCiPe follows up CML and Eco-indicator methodologies, allowing the determination of the contribution of the midpoint impact categories to the endpoint impact categories (European-Commission, 2010b; Goedkoop et al., 2008).

4. Life cycle interpretation: During the interpretation step the finding of either inventory analysis or the impact assessment, or both, are analyzed in relation to the defined goal and scope in order to deliver conclusions, limitations and recommendations to decision-makers. The interpretation should reflect the fact that the LCIA results are based on a relative approach, that they indicate potential environmental effects, and that they do not predict actual impacts on category endpoints, the exceeding of thresholds or safety margins or risks (ISO14040; ISO14044).

Some works have been addressing, in a life cycle perspective, the environmental impact assessment of the biogas production for different scenarios (Afrane and Ntiamoah, 2011; Aye and Widjaya, 2006; Contreras et al., 2009; Rocha et al., 2010). Aye and Widjaya (2006) assessed options for traditional market waste disposal in Indonesia, showing the best environmental benefits for biogas production alternatives. Contreras et al., (2009) studied four scenarios for the Cuban sugar factories, showing the highest benefits when biodegradable wastes were used for biogas production. In the same way, Afrane and Ntiamoah (2011) compared the environmental impacts of three different cooking fuels used in Ghana, namely, charcoal, biogas, and liquefied petroleum gas. They found that biogas had the lowest environmental impact in five of the seven categories investigated. Also with environmental benefits for anaerobic digestion, Rocha et al. (2010) studied disposal alternatives for the treatment of ethanol vinasse in Brazil, such as: conventional fertirrigation, vinasse biodigestion and biogas used as fuel in factory boilers, vinasse dewatering up to 65% and its direct combustion in boilers; and vinasse dewatering up to 40% before fertirrigation in order to reduce transport costs. Despite all of these studies, no reports were found about the environmental impact of anaerobic digestion power plants as alternative for lagooning Cuban vinasse.

1.6.2 Exergy analysis

The results from the LCA can be complemented with exergy analysis to obtain more solid conclusions on the environmental performance of the process (Contreras et al., 2013). Exergy analysis (EA) is based on the second law of thermodynamics, which states that all macroscopic processes are irreversible. Exergy is defined as the maximum amount of work that can be delivered by a system, or a flow of matter or energy as it comes to equilibrium with a reference environment (Kotas, 1995; Rosen et al., 2008; Szargut et al., 1988). The exergy can be consumed or destroyed, due to the irreversibility of any real process. The irreversible process involves a non-recoverable loss of exergy, expressed as the product of the ambient temperature and the entropy generated. Therefore exergy is a measure for quality of energy.

In exergy analysis, the characteristics of the reference environment must be specified. By defining a reference temperature, pressure and chemical composition of the natural environment, it is possible to define universal exergy content for every substance (fuels and non-fuels) and subsequently for all streams. The most common reference environment is the one defined by Szargut et al. (1988) with a reference temperature of 298.15 K and a reference pressure of 1 atm. The exergy of the reference environment is zero and the stream or system exergy is zero when it is in equilibrium with the reference environment.

The exergy content in a material stream can be calculated as the sum of four components: physical exergy, chemical exergy, potential exergy and kinetic exergy (see equations in section 4.2.4, Chapter 4). However, kinetic and potential exergy are often considered negligible in comparison with physical and chemical exergy (Wall, 1990). For this reason generally they are not considered in the determination of the exergy contained in a stream.

Exergy efficiencies: The exergy efficiency of the process is a sustainability parameter and focuses on the conversion of exergy in the process itself. Since exergy rather than any other resource is the ultimate limiting factor to production activities, a process is most sustainable when it uses the exergy of its ingoing resources most efficiently. The ratio of exergy output to exergy input for a control region has been considered as the global exergy efficiency η_{ex} (Figure 1.5) (Wall, 2010).

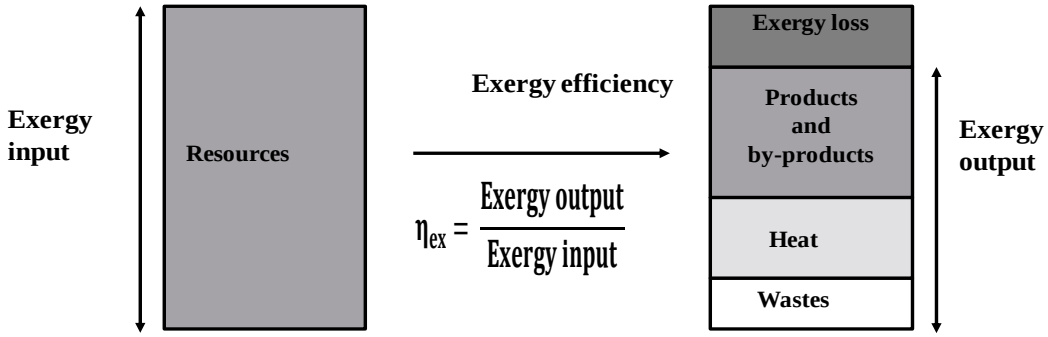

Figure 1.5. Second law analysis of a real process: adapted from Dewulf et al. (2008)

Where Exergy output and Exergy input are the sum (in the control region) of all the exergies making up at the output and input streams, respectively. This efficiency does not always provide an adequate characterization of the thermodynamic efficiency of processes. Often, there exists a part of the output exergy that is unused, i.e. an exergy wasted to the environment (Wall, 2010). The difference between exergy output and exergy waste is called the exergy of the products (Wall, 2010). At the gate-to-gate level, several exergy efficiencies can be calculated to account for the influence of the different products in the exergy efficiency of processes (see Chapter 4). The percentage of exergy destroyed and lost (irreversibility) can be calculated from the difference between 100% and the actual value of the global exergy efficiency (expressed as percent).

The exergy analysis has been applied in scenarios of the cane sugar industry to complement LCA results (Contreras et al., 2013). Although they (LCA and EA) may differ, the results of both methodologies agreed between Contreras et al. (2009) and Contreras et al. (2013), giving the best scores for the alternative considering anaerobic digestion of biodegradables wastes to produce biogas. Multicriterial techniques have been used to compare alternatives with different results in the LCA and EA (Nzila et al., 2012).

The use of vinasse biogas as fuel for combined cycles (gas and steam turbines) has been studied in order to evaluate energy and exergy efficiencies, and to identify the main irreversibilities of the cycle (Constantino and Higa, 2011). An exergy destruction around 60% for gas and steam turbines has been reported (Constantino and Higa, 2011). Although the exergy concept has been also applied to the anaerobic digestion of biomass as a valorization technology (De Meester et al., 2012), little research has been done to determine

the process inefficiencies of anaerobic digestion power plants (including biogas production, sulfide removal and energy generation) and lagooning of Cuban vinasse by means of exergy analysis.

1.7 Outline and objectives

In order to mitigate the emissions of greenhouse gases and the fossil fuel consumption, the use of renewable technologies has been increasing over the world. The anaerobic digestion of biodegradable wastes to produce biogas is an example of renewable technology. The energetic value of the biogas and its potential to reduce carbon emissions together with the additional compost production and chemical oxygen demand (COD) removal are the principal benefits of anaerobic digestion.

In Cuba, the emissions of more than 1.3 million of cubic meters of vinasse are reported every year by Cuban Ministry of the Cane Sugar Industry. Although 99% of Cuban vinasses are treated in lagoons, its anaerobic digestion is widely accepted as the first treatment step. However, vinasse is considered as a very high strength and sulfate rich liquid substrate that causes sulfate reduction activity during its anaerobic digestion, leading to the production of H_2S in the liquid and gas phases, which affects the biogas quality and the process performance.

Modeling the sulfate reduction process in the anaerobic digestion of vinasse can help to predict how the concentration of the sulfur compounds changes when the composition of the substrates and the conditions of the process vary, assisting the energetic use of the biogas and the process performance in anaerobic digestion power plants, which can produce environmental and energetic benefits in the Cuban context.

The present study focuses on the sulfate reduction process in the anaerobic digestion of a very high strength and sulfate rich vinasse, looking for the prediction of the sulfur compounds (in the gas and liquid phases) to assist the energetic use of the biogas and the process performance as well as for the impacts of anaerobic digestion power plants as alternative for lagooning Cuban vinasse. In order to fulfill the present research four specific objectives are developed. These are:

1. To characterize the sulfate reduction process in the anaerobic digestion of a very high strength and sulfate rich vinasse by means of giving COD and SO_4^{2-} pulses at different SO_4^{2-}/COD ratios to obtain dynamical responses.
2. To model the anaerobic digestion of cane-molasses vinasse by extending ADM1 with sulfate reduction for a very high strength and sulfate-rich complex wastewater, including organic matter and hydrogen degradation reactions, hereby also aiming at the accurate prediction of H_2S in the gas and liquid phases.
3. To assess the environmental impacts of anaerobic digestion power plants as alternative for lagooning Cuban vinasse, making a comparative study from a life cycle perspective (LCA).
4. To determine the process inefficiencies of anaerobic digestion power plants and lagooning of Cuban vinasse by means of exergy analysis (EA).

The present dissertation is structured in five chapters, which are briefly introduced below (Figure 1.6). **Chapter 1** provides an overview of the vinasse generation in the sugar sector, the sulfate reduction process in the anaerobic digestion of vinasse and its modeling considering process and reactions involved, kinetics (growth, inhibition and endogenous processes), acid–base equilibrium and gas–liquid transfer equation. In addition, the principal approaches to model sulfate reduction are discussed. Furthermore, the currently available environmental sustainability concepts of Life Cycle Assessment and exergy analysis are also discussed. In **Chapter 2**, the sulfate reduction process in the anaerobic digestion of vinasse is characterized, based on a set of dynamical data. In **Chapter 3**, an extension of ADM1 with sulfate reduction is proposed, calibrated and validated to describe the anaerobic digestion of vinasse, by using the dynamical data obtained in Chapter 2.

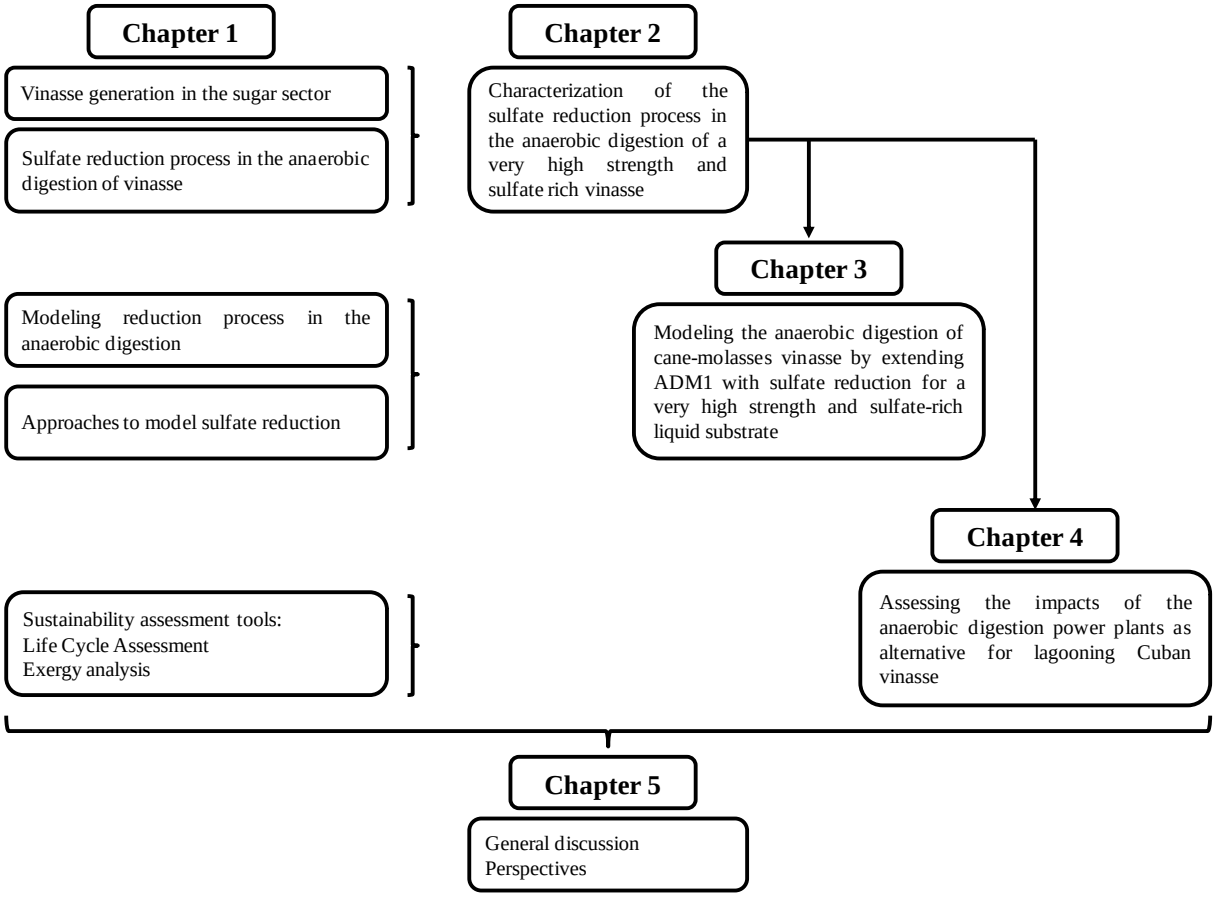

Figure 1.6. Overview and link between the different chapters in this dissertation

In **Chapter 4** (connected to Chapter 2 by using the experimental results of one experimental condition and the biogas production from raw vinasse as one of the subprocesses for the sustainability assessment), the impacts of the anaerobic digestion power plants as alternative for lagooning Cuban vinasse are assessed by using Life Cycle Assessment (LCA) and exergy analysis (EA). The comparative LCA is based on the endpoint impact categories "human health", "ecosystem quality" and "natural resources". The exergy efficiency was used to assess potential process improvement and irreversibilities in the subprocesses forming the anaerobic digestion power plants. **Chapter** 5 provides a general discussion of the results obtained specific to the research objectives. Conclusions are drawn and perspectives for future research are proposed.

CHAPTER 2

Characterization of the sulfate reduction process in the anaerobic digestion of a very high strength and sulfate rich vinasse

This Chapter characterizes the sulfate reduction process in the anaerobic digestion of a very high strength and sulfate rich vinasse, where chemical oxygen demand (COD) and sulfate (SO_4^{2-}) pulses were applied at different SO_4^{2-}/COD ratios to obtain dynamical responses. The results showed an increase in H_2S_{gas} of up to 33%, when influent COD (inf_COD) and influent SO_4^{2-} (inf_SO_4^{2-}) increased at a SO_4^{2-}/COD ratio of 0.05. A decrease of inf_COD together with an increase of inf_SO_4^{2-} caused propionic acid degradation (up to 90%), suggesting strong contribution of propionate degrading sulfate reducing bacteria at SO_4^{2-}/COD ratios $\leq$ 0.10, in contrast to literature results. The inf_COD and inf_SO_4^{2-} fluctuations at a SO_4^{2-}/COD ratio of 0.10 caused inhibition by H_2S_{aq}, $[H_2S]_{free}$ and propionic acid to sulfate reducing bacteria (SRB), methanogens or both. At a SO_4^{2-}/COD ratio of 0.20 this inhibition became severe for methanogens and SRB, leading to reactor failure. Mass balance calculations showed COD and sulfur recoveries from 90 to 98% in most cases. Increments of inf_COD within a constant SO_4^{2-}/COD ratio (0.05 or 0.10) accumulated as effluent COD rather than as COD_CH_{4gas}, showing deterioration of the anaerobic digestion, while the sulfur was displaced to the gas phase at a SO_4^{2-}/COD ratio of 0.05 or to the liquid phase at SO_4^{2-}/COD ratios $\geq$ 0.10. Based on the closed mass balances results, the data presented here are considered reliable for calibrating mathematical models, when sulfate reduction in the anaerobic digestion of a very high strength and sulfate rich vinasse is of primary interest.

Redrafted from:

Barrera, E.L., Spanjers, H., Romero, O., Rosa, E. and Dewulf, J., 2014. Characterization of the sulfate reduction process in the anaerobic digestion of a very high strength and sulfate rich vinasse. Chemical Engineering Journal 248, 383–393.

2.1 Introduction

Many industrial processes, especially in the food and fermentation industries, generate wastewaters with high levels of organic matter and sulfate (Zub et al., 2008). Vinasse obtained from ethanol distillation in the sugar cane industry is a typical example of a sulfate rich liquid substrate (Barrera et al., 2013). The anaerobic digestion of vinasse promotes the activity of sulfate reducing bacteria (SRB) producing H_2S, which is distributed among H_2S_{aq} ($[H_2S]_{free}$, HS^- and S^{2-}), insoluble metallic sulfides and H_2S_{gas}.

Sulfate reduction processes have been studied by many authors (Alphenaar et al., 1993; Annachhatre and Suktrakoolvait, 2001; Erdirencelebi et al., 2007; Harada et al., 1994; Isa et al., 1986; Omil et al., 1996; Omil et al., 1997b; Poinapen et al., 2009b; Poinapen et al., 2009c; Visser, 1995) by using synthetic wastewaters to feed upflow anaerobic sludge bed reactors (UASB). An overview of previous works is given in Table 2.1. These studies have mainly focused on the inhibitory effect of H_2S_{aq} and $[H_2S]_{free}$, the influence of operational parameters and the assessment of competition between SRB and methanogens, whereas the gas phase hydrogen sulfide produced from the sulfate reduction process has received less emphasis.

Typically, the ratio SO_4^{2-} to chemical oxygen demand (COD) in sugar cane vinasse (as g SO_4^{2-} g COD^{-1}) ranges from 0.05 to 0.10 (Wilkie et al., 2000) while maximum values of 0.22 have been reported (Obaya et al., 2004). Sulfate reduction at those SO_4^{2-}/COD ratios has been studied (Erdirencelebi et al., 2007; Harada et al., 1994; Isa et al., 1986; Visser, 1995) (Table 2.1). However, knowledge about sulfate reduction of substrates at very high COD concentration of vinasses (between 30 and 130 g COD L^{-1}, (Wilkie et al., 2000)) is needed. The dilution of wastewater streams may reduce the high COD content of vinasse, but in general this approach is considered undesirable because of the increase in the total volume of wastewater that must be treated (Chen et al., 2008). Successful treatment during the anaerobic digestion of very high strength and sulfate rich vinasse has been reported (Driessen et al., 1994; Espinosa et al., 1995; Riera et al., 1985). COD removal efficiencies up to 71% at COD concentrations between 36 and 100 g COD L^{-1} and organic loading rates between 5 and 24 g COD L^{-1} d^{-1} have been achieved (Driessen et al., 1994; Espinosa et al., 1995; Riera et al., 1985).

Table 2.1. Values of COD, SO_4^{2-} and SO_4^{2-}/COD ratios in synthetic wastewaters used to study sulfate reduction in UASB reactors

COD (g COD L^{-1})	**SO_4^{2-}** (g SO_4^{2-} L^{-1})	**SO_4^{2-}/COD** ratios (w/w)	**References**
5	0.3-30	0.06-6	(1)
2.5	5	2	(2)
0.5	0.03-0.6	0.06-1.2	(3)
1.5 - 4	0.75 - 8.3	0.1 - 2	(4)
0.53-2.54	1.2-4.55	1.78-2.5	(5)
0.1-3	0.45-1.8	0.6-4.5	(6)
5.14-6.8	0.28-1.36	0.05-0.2	(7)
1.87-2.63	1.5-1.8	0.57-0.8	(8)

(1) (Isa et al., 1986); (2) (Alphenaar et al., 1993); (3) (Harada et al., 1994); (4) (Visser, 1995); (5) (Omil et al., 1996); (6) (Annachhatre and Suktrakoolvait, 2001; Omil et al., 1997b) (7) (Erdirencelebi et al., 2007) (8) (Poinapen et al., 2009b; Poinapen et al., 2009c)

The production and characteristics of vinasse are variable and dependent on the feed stocks and the ethanol production process. Wash water used to clean the fermenters, cooling water blow down, and boiler water blow down may all be combined with the vinasse and contribute to its concentration variability (Wilkie et al., 2000). The variations in the COD and SO_4^{2-} concentrations of vinasse may cause dynamical responses in the sulfate reduction process during the anaerobic treatment, influencing the reactor performance as well as the biogas quality and the performance of the gas treatment processes. Although modeling and simulation are useful tools to predict these variations, dynamical data of the anaerobic digestion of very high strength and sulfate rich vinasse was not found in literature (Barrera et al., 2013). A low time consuming and appealing alternative to obtain this data is to evaluate the dynamical response of a continuous reactor after specific substrate pulses (Batstone et al., 2003).

Therefore, the research described in this Chapter characterizes the sulfate reduction process in the anaerobic digestion of a very high strength and sulfate rich vinasse by means of giving COD and SO_4^{2-} pulses at different SO_4^{2-}/COD ratios to obtain dynamical responses.

2.2 Materials and methods

2.2.1 Experimental setup

The 3.5 L working volume UASB reactor (as the sum of the sludge bed, the sludge blanket and the settler volumes) consisted of an acrylic transparent column with an internal diameter of 8 cm and a height of 70 cm. The sludge level in the reactor was set to 40% of the reactor working volume. Hot water was circulated through a jacket to ensure a temperature of 35±1 ºC during the UASB reactor operation. Sludge temperature and effluent pH were measured online and data stored with a data acquisition system. The influent vinasse supply tank was constantly stirred at 50 rpm. A schematic representation of the experimental setup used during the experiments is shown in Figure 2.1.

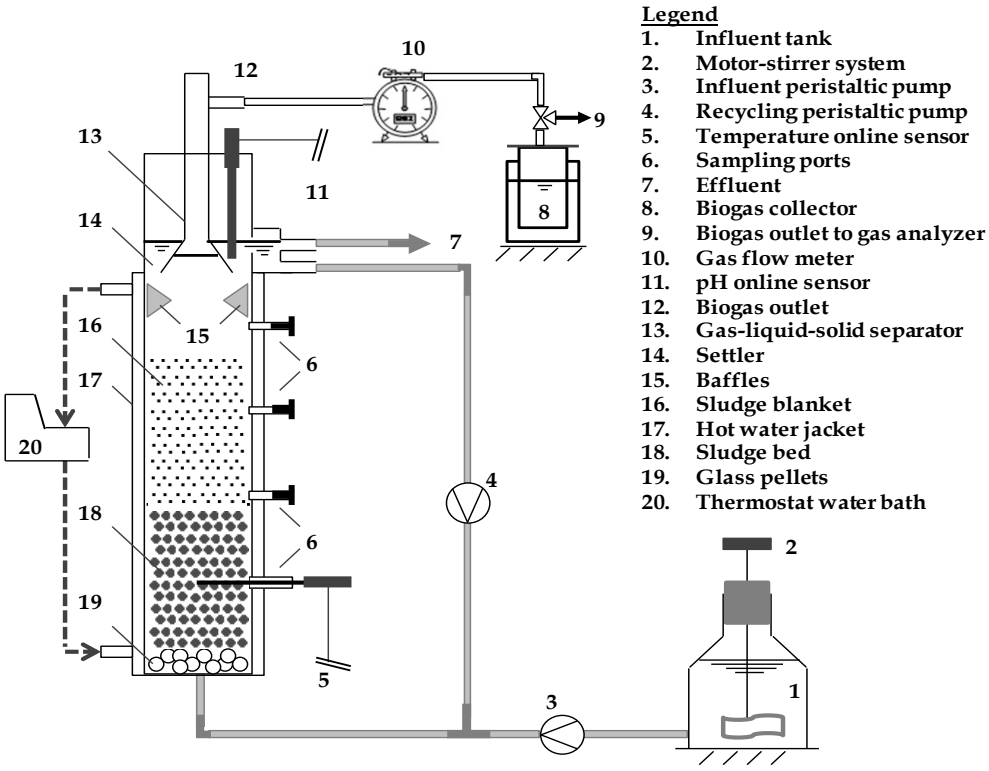

Figure 2.1. Schematic representation of the experimental setup

2.2.2 Seed sludge

Sludge was obtained from a 3600 m^3 UASB reactor treating vinasse (Heriberto Duquesne, Santa Clara, Cuba). After a 55 days startup and acclimatization period, granular sludge with the following characteristics was obtained: sludge volume index (16.7 ml g TSS^{-1}), average granular size (4 mm), settling velocity (47.2 m h^{-1}), volatile suspended solids (47.4 g VSS L^{-1}), and sulfidogenic (0.25 g COD_ΔSO_4 (COD of the reduced sulfates) g VSS^{-1} d^{-1}) and methanogenic (0.33 g COD-CH_4 g VSS^{-1} d^{-1}) activities (to vinasse) (Visser, 1995).

2.2.3 Substrate feed

A sample of 60 liter of sugar cane vinasse was obtained from a distillery plant in Sancti Spiritus, Cuba and immediately stored at -20 ºC to avoid excessive biodegradation. The COD concentration of vinasse was adjusted by adding tap water as required by the experiments. To increase the sulfate concentration of vinasse, Na_2SO_4 was used ensuring that sodium concentration (< 3.3 g L^{-1}) remained below the inhibition limit of 8 g L^{-1} (Chen et al., 2008). The characteristics of the raw vinasse are shown in Table 2.2.

Table 2.2. Characteristics of the raw vinasse (n=3)

Parameter	Units	Average	Parameter	Units	Average
COD	g COD L^{-1}	65.18 ± 0.66	Cations[f]		
TS	g L^{-1}	56.23 ± 0.93	Na^+	mol L^{-1}	$5.0 \cdot 10^{-3} \pm 2 \cdot 10^{-4}$
VS	g L^{-1}	43.33 ± 0.32	K^+	mol L^{-1}	$0.11 \pm 5 \cdot 10^{-4}$
TSS	g L^{-1}	3.24 ± 0.28	Ca^{2+}	mol L^{-1}	$0.04 \pm 2 \cdot 10^{-3}$
VSS	g L^{-1}	3.16 ± 0.17	Mg^{2+}	mol L^{-1}	$0.02 \pm 1 \cdot 10^{-3}$
TOC[a]	mol C L^{-1}	2.06 ± 0.10	Mn^{2+}	mol L^{-1}	$8.35 \cdot 10^{-5} \pm 4 \cdot 10^{-6}$
TKN[b]	mol N L^{-1}	$4.6 \cdot 10^{-2} \pm 3 \cdot 10^{-4}$	Zn^{2+}	mol L^{-1}	$2.28 \cdot 10^{-5} \pm 1 \cdot 10^{-6}$
NH_4^+ - N[c]	mol N L^{-1}	$3.1 \cdot 10^{-4} \pm 2 \cdot 10^{-5}$	Anions[b]		
TP[b]	mol P L^{-1}	$3.8 \cdot 10^{-3} \pm 2 \cdot 10^{-4}$	SO_4^{2-}	mol L^{-1}	$1.89 \cdot 10^{-2} \pm 4 \cdot 10^{-4}$
VFAs (HAc)	g COD L^{-1}	1.4 ± 0.07	NO_2^-	mol L^{-1}	$1.97 \cdot 10^{-5} \pm 3 \cdot 10^{-6}$
Sugars[d]	g COD L^{-1}	40.6± 0.83	NO_3^-	mol L^{-1}	$1.40 \cdot 10^{-4} \pm 1 \cdot 10^{-5}$
Proteins[e]	g COD L^{-1}	5.9 ± 3.10	PO_4^{3-}	mol L^{-1}	$8.72 \cdot 10^{-6} \pm 0.00$
Lipid[e]	g COD L^{-1}	$0.2 \pm 4 \cdot 10^{-3}$	Cl^-	mol L^{-1}	$5.28 \cdot 10^{-2} \pm 1 \cdot 10^{-3}$
pH	-	4.8 ± 0.06			

A sample of 2L was used to make three replicates in each assay. [a] (CMA/2/I/D.7); [b] (Clesceri et al., 1999); [c] (Bremner and Keeney, 1965); [d] (by difference between dry matter, lipids, proteins and VFAs); [e] (Egan et al., 1981) and [f] (CMA/2/I/B.1). The remaining parameters were determined as in section *2.2.5.1.*

2.2.4 Process operation

A set of experiments (from E-1 to E-9) were conducted using vinasse at different SO_4^{2-} and COD concentrations. From E-1 to E-3 and E-4 to E-6 the concentration of influent COD (inf_COD) and influent SO_4^{2-} (inf_SO_4^{2-}) were gradually increased while keeping the SO_4^{2-} /COD ratio constant. The inf_SO_4^{2-} and inf_COD in experiment E-7 were reduced to control toxicity. In E-8 and E-9, the inf_SO_4^{2-} was increased at a constant inf_COD to increase the SO_4^{2-}/COD ratio. A summary of the operating conditions is shown in detail in Table 2.3.

The hydrodynamic conditions were kept constant during the experiments at a hydraulic retention time (HRT) of 4.86 days (based on the reactor working volume), an influent flow of 0.72 L d^{-1}, an effluent recycling ratio of 15 (effluent flow/influent flow), and liquid upflow velocity (Vup) of 0.1 m h^{-1}. The buffering capacity of the recycled effluent was used to neutralize vinasse to a pH range of 7.0 - 7.5. Steady state conditions were characterized by a constant gas production rate (±5%) (Kaparaju et al., 2010).

Table 2.3. Operating conditions for each experiment

E	Duration (d)	SO_4^{2-}/COD (g SO_4^{2-} g COD^{-1}) (approximate)	inf_COD (g COD L^{-1}) (approximate)	inf_SO_4^{2-} (g SO_4^{2-} L^{-1}) (approximate)	OLR (g COD L_R^{-1} d^{-1}) (average)	SLR (g SO_4^{2-} L_R^{-1} d^{-1}) (average)
E-1	1-7	0.05	38	1.75	7.66	0.36
E-2	8-15	0.05	48	2.20	9.83	0.45
E-3	16-26	0.05	58	2.65[a]	12.00	0.53
E-4	27-36	0.10	38	3.65	7.90	0.76
E-5	37-45	0.10	48	4.60	9.89	0.95
E-6	46-49	0.10	56	5.50	10.79	1.12
E-7	50-58	0.10	48	4.60	9.94	0.97
E-8	59-68	0.15	38	5.65	7.72	1.15
E-9	69-75	0.20	38	7.50	7.98	1.57

[a] concentration applied at day 19. OLR: Organic loading rate. SLR: Sulfate loading rate. E: operating conditions

2.2.5 Chemical analysis

2.2.5.1 Chemical analysis of the liquid phase

A volume of 60 to 70 ml of sample was taken from the effluent and filtered to determine volatile suspended solids (VSS). Sulfates were determined by a turbidimetric method at 420 nm wavelength using a UV spectrophotometer (RAYLEIGH, UV-1601). For this purpose samples were incinerated and ashes were dissolved in HCl 1:1 in order to avoid color interferences. COD was determined using a close reflux titrimetric method (dichromate method). Effluent sulfide COD was subtracted from the total effluent COD. Dissolved sulfides were determined by the iodometric method. To avoid H_2S loss during sample filtration, pH was raised to 10 by adding a few drops of NaOH (6N) (Poinapen et al., 2009a). Interfering substances (thiosulfate, sulfite or organic matter) were removed by adding zinc acetate (2N) to precipitate sulfide as ZnS. Samples were filtered and the retentate was titrated. Free hydrogen sulfide concentrations in the liquid phase were calculated using the total dissolved sulfide concentrations, the pK_a values and the pH. Standard methods were followed in all cases (Clesceri et al., 1999). Volatile fatty acids (VFAs) were determined by gas chromatography (Thermo-scientific GC) with a FID, equipped with a 0.25 mm (i.d.) and 30 m length Stabilwax-DA column. Hydrogen gas was used as carrier gas at 0.8 ml min^{-1}. The average value of three replicates (at least) was used in all cases.

2.2.5.2 Chemical analysis of the gas phase

Methane and carbon dioxide percentages in the gas phase were measured by means of a Pronova (SSM 6000 Classic) gas analyzer equipped with the proper sensors. As gas phase hydrogen sulfide concentration was expected to be beyond the gas analyzer measuring range (5000 ppm), it was measured by bubbling the biogas in a zinc acetate solution (0.2 N) which was subsequently titrated using standard iodometric procedure (Clesceri et al., 1999). The average values of three replicates were used in all cases.

2.2.6 Mass balances

Mass balance calculations were done under the steady state conditions of experiments E-1 through E-9.

2.2.6.1 COD mass balance assumptions

In the COD mass balance, the COD dissolved as CH_4 was calculated as 45 mg COD L^{-1} at 35 ºC (Batstone, 2006) and was considered as negligible ($\leq$ 0.12%). An amount of COD is used to reduce sulfates, thus producing H_2S (as H_2S_{gas}, HS^- and $[H_2S]_{free}$). As H_2S can escape during sample filtration introducing possible errors in COD calculations, the COD consumed by SRB was calculated from the reduced SO_4^{2-} as in Harada et al. (1994). Hence, inf_COD leaves the reactor as the components:

(1) eff_COD (Effluent COD = Soluble COD + Suspended solid COD)

(2) COD_ ΔSO_4^{2-} (COD of reduced SO_4^{2-})

(3) COD_CH_{4gas} (COD converted to gas CH_4)

The fraction (expressed as %) of each component to the COD mass balances were calculated from the above items (1), (2) or (3) divided by inf_COD and the COD recovery as the sum of those fractions.

2.2.6.2 Sulfur mass balance assumptions

The sulfur mass balance considered negligible influent sulfides. At neutral pH (pH between 6.5-8) the formation of metal sulfide precipitates is also considered negligible (as S^{2-} is negligible) and sulfides occur in the form of $[H_2S]_{free}$ and HS^- (Rinzema and Lettinga, 1988). Then, the inf_SO_4^{2-} leaves the reactor as the components:

(1) eff_SO_4^{2-} (total effluent SO_4^{2-} as sulfur)

(2) S_H_2S_{gas} (H_2S in biogas as sulfur)

(3) S_HS^- (ionized H_2S in the effluent as sulfur)

(4) S_$[H_2S]_{free}$ (free H_2S in the effluent as sulfur)

The fraction (expressed as %) of each component to the sulfur mass balances were calculated from the above items (1), (2), (3) and (4) divided by inf_SO_4^{2-} and the sulfur recovery as the sum of those fractions.

2.3 Results and discussion

2.3.1 Dynamical behavior at low SO_4^{2-}/COD ratios

The dynamical behavior at low ratios (SO_4^{2-}/COD ratios of 0.05 and 0.10) for the experiments E-1, E-2, E-3, E-4, E-5 and E-6 is shown in Figure 2.2 (Although the SO_4^{2-}

/COD ratio for experiment E-7 was 0.10, it is not included here, see explanation in section 2.3.2). The dynamical response of the biogas production and H_2S_{aq} (Figure 2.2A), the H_2S_{gas} and $[H_2S]_{free}$ (Figure 2.2B), and the volatile fatty acids and pH (Figure 2.2C) following inf_COD and inf_SO_4^{2-} pulses (Figure 2.2D) are depicted.

2.3.1.1 SO_4^{2-}/COD ratio of 0.05

At a SO_4^{2-}/COD ratio of 0.05, the increase of inf_COD and inf_SO_4^{2-} (day 8) caused a gradual increase of biogas production and H_2S_{gas}, while H_2S_{aq} and $[H_2S]_{free}$ remained constant (Figure 2.2A, 2.2B and 2.2D). The stripping effect due to a higher biogas production keeps H_2S_{aq} and $[H_2S]_{free}$ constant despite inf_SO_4^{2-} was increased, as explained by Wilkie et al. (2000). At day 16th, the further increase of inf_COD provoked a gradual increase of the biogas production while sulfur species concentrations (H_2S_{aq}, $[H_2S]_{free}$ and H_2S_{gas}) remained constant. A stoichiometric amount of 1.49 g SO_4^{2-} is required to degrade 1 g COD (Poinapen et al., 2009c), therefore the experiments were performed under sulfate limiting conditions (see SO_4^{2-}/COD ratios in Table 2.3). For that reason, the constant concentration of the sulfur compounds from day 16th to 19th was attributed to sulfate limitations (constant inf_SO_4^{2-}). In addition, the results suggested that the stripping effect due to a higher biogas production is negligible when inf_SO_4^{2-} remains constant. A subsequent increase of inf_SO_4^{2-} (day 19) showed an instantaneous increase of H_2S_{gas}, keeping H_2S_{aq} constant. Therefore, an increase of H_2S_{gas} from 25 to 33% (reducing the biogas quality) is expected when both inf_COD and inf_SO_4^{2-} are increased from 21 to 26% at a constant SO_4^{2-}/COD ratio of 0.05. As the maximum concentrations of H_2S_{aq} and $[H_2S]_{free}$ were 200 and 75 mg S L^{-1} respectively (Figure 2.2A and 2.2B), no inhibition of methanogens and SRB was expected. H_2S_{aq} and $[H_2S]_{free}$ inhibitory limits (7.2 < pH < 7.4) have been reported above 564 mg S L^{-1} (Visser et al., 1996) and 150 mg S L^{-1} (Rinzema and Lettinga, 1988), respectively.

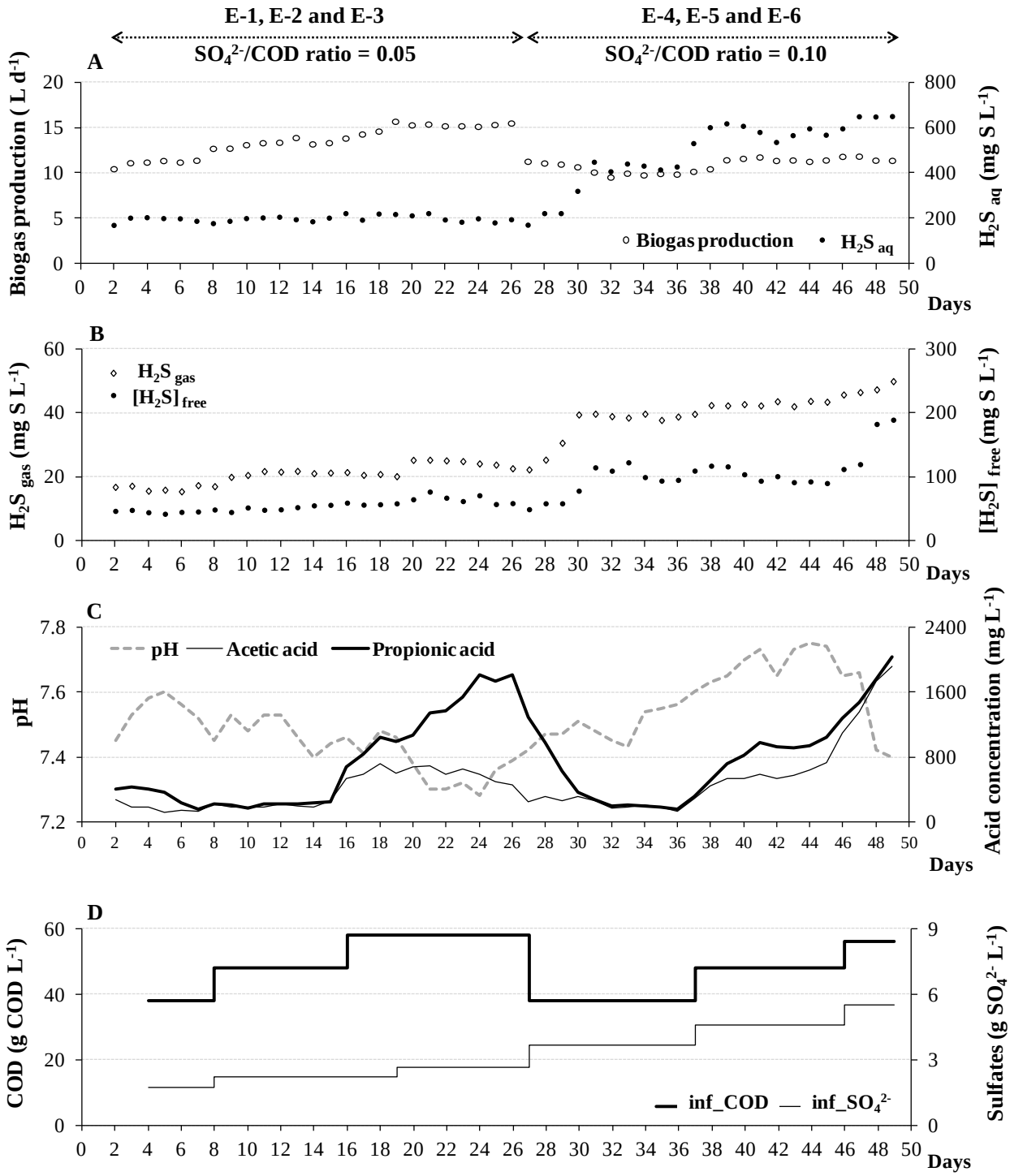

Figure 2.2. Dynamical behavior at low SO_4^{2-}/COD ratios. Experiments E-1, E-2, E-3 at the SO_4^{2-}/COD ratio of 0.05 and experiments E-4, E-5, and E-6 at the SO_4^{2-}/COD ratio of 0.10. (**A**) biogas production and H_2S_{aq}, (**B**) $[H_2S]_{free}$ and H_2S_{gas}, (**C**) pH, and propionic and acetic acids, and (**D**) inf_COD and inf_SO_4^{2-} pulses

An increase in the concentrations of propionic (1060 mg L^{-1}) and acetic (715 mg L^{-1}) acid was observed from days 16 to 18 as a result of the increase in inf_COD. However, the increase in the propionic acid concentration together with the slight decrease in acetic acid concentration, when the inf_SO_4^{2-} increased on day 19, suggested inhibition of propionate degrading bacteria (pDB) (Figure 2.2C). This inhibition might occur as a result of propionic acid concentrations above 900 mg L^{-1} (Demirel and Yenigün, 2002; Wang et al., 2009), and $[H_2S]_{free}$ concentrations above 70 mg S L^{-1} (Rinzema and Lettinga, 1988), due to the higher sulfide sensitivity of pDB in comparison to methanogens (Lens et al., 1998). Additionally, the increase of inf_COD could have caused hydrogen accumulation, decreasing the propionate degradation rate by pDB and accumulating propionic acid (Wiegant and de Man, 1986). Propionic acid accumulation in the anaerobic digestion of vinasse was attributed to hydrogen accumulation when the OLR was increased to 10 g COD L_R^{-1} d^{-1} in the experiments of Harada et al. (1996).

2.3.1.2 From a SO_4^{2-}/COD ratio of 0.05 to 0.10

At day 27, the SO_4^{2-}/COD ratio of 0.10 was applied (from E-3 to E-4). The double-pulse inf_COD decrease (- 34%) and inf_SO_4^{2-} increase (+ 38%) lowered the biogas production (- 25%), increased H_2S_{aq}, $[H_2S]_{free}$ and H_2S_{gas} (up to 400, 100 and 40 mg S L^{-1}, respectively), and reduced the propionic acid concentration with 90% after 3 days (Figure 2.2A, 2.2B, 2.2C and 2.2D). However, at SO_4^{2-}/COD ratios $\leq$ 0.10 the predominant route for propionate degradation has been reported as syntrophic oxidation of propionic acid by pDB coupled to sulfate reduction by hydrogenotrophic SRB (hSRB) using the generated hydrogen (Visser, 1995). The drastic reduction of the propionic acid concentration was attributed to increased propionate SRB (pSRB) activity. This assumption was based on several observations: (1) the inf_COD decrease could reduce the available hydrogen for hSRB increasing the available SO_4^{2-} for pSRB, (2) the increase of inf_SO_4^{2-} additionally increased the available SO_4^{2-} for pSRB, (3) propionate is consumed by pSRB (ΔG° = - 37.8 kJ mol^{-1}) rather than pDB (ΔG° = + 76.1 kJ mol^{-1}) if sulfates are available (Rinzema and Lettinga, 1988), and (4) in the anaerobic digestion of vinasse, a similar reduction in the OLR (- 34%) caused 70% reduction in the propionic acid concentration after 50 days when the inf_SO_4^{2-} was not increased (Harada et al., 1996).

A frequently reported undesirable phenomenon encountered during the anaerobic treatment of vinasse is the volatile fatty acid accumulation, principally propionic acid (Espinosa et al., 1995; Riera et al., 1985). Therefore, the double-pulse 'inf_COD decrease and inf_SO_4^{2-} increase' can be considered as an operational strategy to reduce propionic acid accumulation in the anaerobic treatment of vinasse. In that case, pSRB can contribute to the degradation of propionic acid at SO_4^{2-}/COD ratios ≤ 0.10 which is in contrast to literature reports (Batstone, 2006; Batstone et al., 2002; Visser, 1995), that have considered only hSRB activity at these ratios. Further application of modeling tools based on the kinetic coefficients, mass transfer properties and reactor configuration may support the above findings.

2.3.1.3 SO_4^{2-}/COD ratio of 0.10

At a SO_4^{2-}/COD ratio of 0.10 (E-4, E-5 and E-6), the increase of inf_COD and inf_SO_4^{2-} at day 37 (Figure 2.2D) doubled H_2S_{aq} (600 mg S L^{-1}) and slightly increased the biogas production (by 1.7 L d^{-1}). As the pH increased above 7.6, $[H_2S]_{free}$ remained constant below the inhibitory limits for methanogens and SRB, while H_2S_{gas} increased by 10% only. A small deterioration of the biogas quality (increasing by 10% H_2S_{gas}) was observed when inf_COD and inf_SO_4^{2-} were increased by 26%.

At the same time, a reduction of the methane yield from 336 to 306 ml CH_4 (g $COD_{removed}$)$^{-1}$ indicated inhibition of methanogens, likely because H_2S_{aq} concentrations exceeded 564 mg S L^{-1} (Visser et al., 1996). Carbon dioxide and acetic acid accumulation confirmed inhibition of both hydrogenotrophic and acetotrophic methanogenic archea (hMA and aMA) while the consistent hydrogen accumulation could cause pDB inhibition. The $[H_2S]_{free}$ remained around 100 mg S L^{-1} (> 70 mg S L^{-1}) and pDB were additionally inhibited by free sulfides leading to propionic acid accumulation (Figure 2.2C).

The theoretical (maximum) sulfur production (H_2S_{aq} and H_2S_{gas}) per unit of inf_SO_4^{2-} fed to the reactor, in the following denoted as "sulfur yield", is 333 mg S (g SO_4^{2-})$^{-1}$. However, lower sulfur yields can be found as a result of reactor efficiencies (depending on the fraction of inf_SO_4^{2-} released as eff_SO_4^{2-}), being, in turn, affected by variation of the inhibitor concentration ($[H_2S]_{free}$ and H_2S_{aq}). Therefore, although H_2S_{aq} concentrations around the inhibitory limits of 615 mg S L^{-1} for SRB (Visser et al., 1996) were found, they were not inhibited as the sulfur yield increased slightly from 262 to 273 mg S (g SO_4^{2-})$^{-1}$.

An increase of inf_COD and inf_SO_4^{2-} at day 46 caused reactor instability, as witnessed by the doubling of the propionic and acetic acid concentrations (both > 1600 mg L^{-1}), the decrease of the pH to 7.4 and the doubling of $[H_2S]_{free}$ (190 mg S L^{-1}), while H_2S_{aq} increased to 638 mg S L^{-1} (Figure 2.2A, 2.2B, 2.2C and 2.2D). A decrease of the methane yield to 268 ml CH_4 (g COD $_{removed}$)$^{-1}$ and the sulfur yield to 252 mg S (g SO_4^{2-})$^{-1}$ suggested inhibition by H_2S_{aq}, $[H_2S]_{free}$ and propionic acid for both methanogens and SRB. Acetic acid concentrations up to 2400 mg L^{-1} have not been inhibitory to methanogens (Wang et al., 2009). However, because sulfate reduction studies are mostly based on the use of substrates with SO_4^{2-}/COD ratios ≥ 1.5 (Alphenaar et al., 1993; Annachhatre and Suktrakoolvait, 2001; Isa et al., 1986; Omil et al., 1996; Omil et al., 1997b; Visser, 1995), volatile fatty acid accumulation is not reported, and for that reason little is known about inhibition of SRB by propionic and acetic acids.

2.3.2 Dynamical behavior at high SO_4^{2-}/COD ratios

The dynamical behavior at high ratios (SO_4^{2-}/COD ratios of 0.10, 0.15 and 0.20) for experiments E-7, E-8, and E-9 is shown in Figure 2.3. Despite the ratio 0.10 was already discussed in section 2.3.1.3, it was retaken as the starting point of this section to control toxicity from previous stage. The biogas production and H_2S_{aq} (Figure 2.3A), the H_2S_{gas} and $[H_2S]_{free}$ (Figure 2.3B), and the volatile fatty acids and pH (Figure 2.3C) following inf_COD and inf_SO_4^{2-} pulses (Figure 2.3D) were depicted.

2.3.2.1 SO_4^{2-}/COD ratio of 0.10 to control toxicity

On day 50, a decrease of inf_COD and inf_SO_4^{2-} was imposed to control toxicity at a SO_4^{2-}/COD ratio of 0.10 (E-7). A biogas production remaining in the same order of magnitude together with a decrease of H_2S_{aq} (576 mg S L^{-1}) and H_2S_{free} (130 mg S L^{-1}) below inhibitory limits were observed (Figure 2.3A and 2.3B). Both methane and sulfur yield increased to 317 ml CH_4 (g $COD_{removed}$)$^{-1}$ and 261 mg S (g SO_4^{2-})$^{-1}$, respectively, in spite of the persistent propionic acid concentrations around 2000 mg L^{-1} (Figure 2.3C). Then, propionic acid concentration remained stable and only sulfide toxicity was partially controlled by reducing both inf_COD and inf_SO_4^{2-} by 20%.

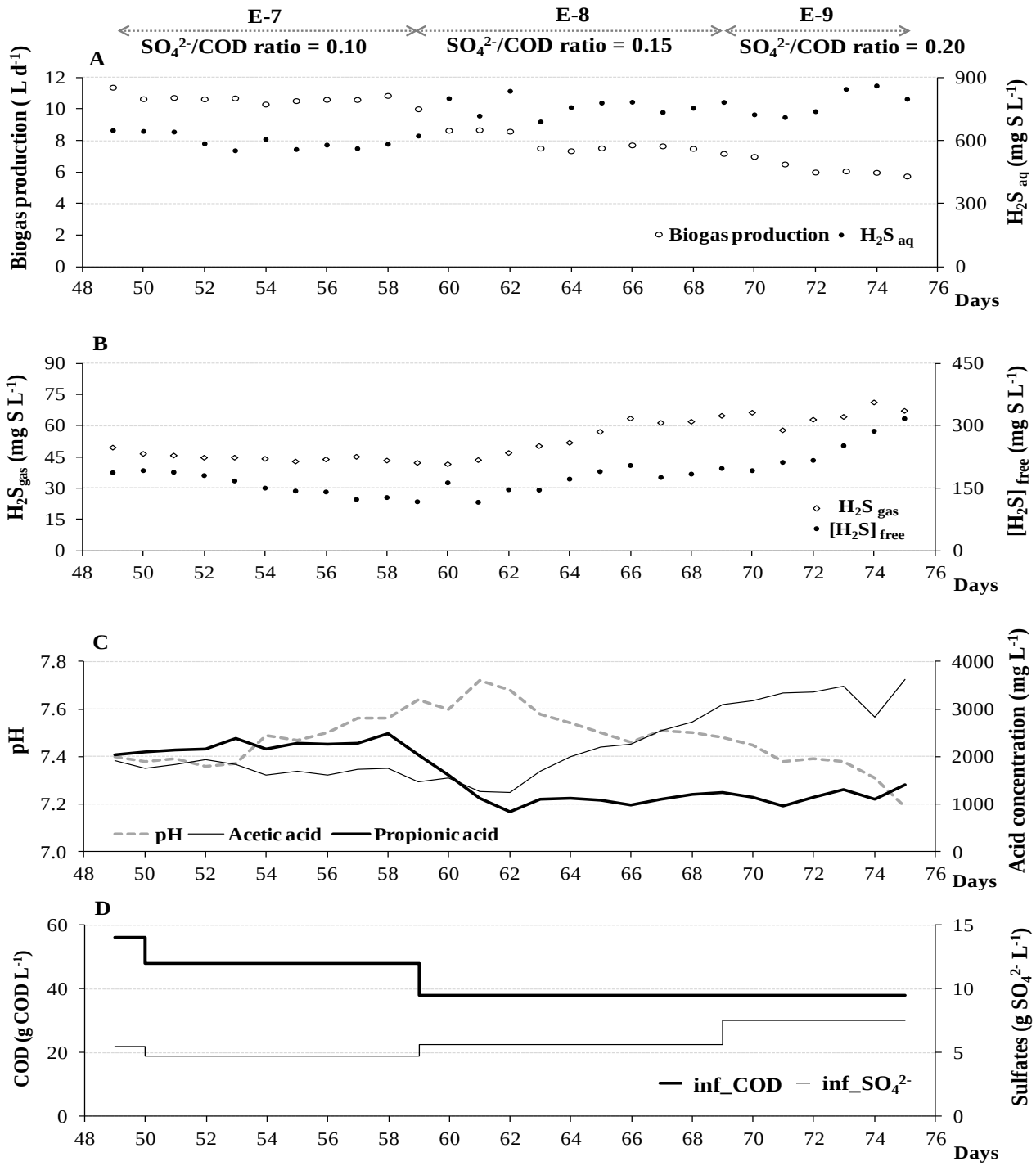

Figure 2.3. Dynamical behavior at high SO_4^{2-}/COD ratios. Experiments E-7, E-8 and E-9 at the SO_4^{2-}/COD ratio of 0.10, 0.15 and 0.20, respectively. (**A**) biogas production and H_2S_{aq}, (**B**) $[H_2S]_{free}$ and H_2S_{gas}, (**C**) pH and propionic and acetic acids, and (**D**) inf_COD and inf_SO_4^{2-} pulses

2.3.2.2 From a SO_4^{2-}/COD ratio of 0.10 to 0.15

On day 59, the SO_4^{2-}/COD ratio of 0.15 was imposed by a double-pulse inf_COD decrease (-20%) and inf_SO_4^{2-} increase (+ 22%) as in section 2.3.1.2 (Figure 2.3D). It caused a gradual reduction of the biogas production to 7.6 L d^{-1}, increasing H_2S_{aq}, $[H_2S]_{free}$ and H_2S_{gas} up to 750, 160 and 60 mg S L^{-1}, respectively, while propionic acid concentration was reduced by 55% after 3 days (Figure 2.3A, 2.3B and 2.3C). The acetic acid accumulation from day 63 suggested (1) incomplete oxidation of propionic acid by pSRB to acetate, and (2) inhibition of aMA by H_2S_{aq} and $[H_2S]_{free}$ with a decrease of the methane yield to 262 ml CH_4 (g COD $_{removed})^{-1}$.

Therefore, only the double-pulse 'inf_COD decrease and inf_SO_4^{2-} increase' contributed to the degradation of propionic acid, even at a SO_4^{2-}/COD ratio of 0.15. However, the acetic acid accumulation, the higher H_2S_{aq} and $[H_2S]_{free}$, and the lower methane yield suggested deterioration of the anaerobic digestion process.

2.3.2.3 From a SO_4^{2-}/COD ratio of 0.15 to 0.20

A subsequent increase of inf_SO_4^{2-} (E-9, day 69) (Figure 2.3D) caused an overall reactor failure. It was characterized by acetic acid accumulation (> 3000 mg L^{-1}), pH drop (7.2), and higher $[H_2S]_{free}$ (300 mg S L^{-1}). As a consequence, methane and sulfur yields continued to decrease to 238 ml CH_4 (g COD $_{removed})^{-1}$ and 178 mg S (g $SO_4^{2-})^{-1}$, respectively. Propionic acid concentration remained around 1100 mg L^{-1} until the end of the experiments. The reactor behavior at E-9 suggested incomplete degradation of propionic acid by pSRB as acetic acid concentration increased, as well as aggravation of the inhibition to methanogens and SRB as the methane and sulfur yields decreased.

2.3.3 Effect on the mass balances

Although the dynamical behavior of the sulfate reduction process in the anaerobic digestion was described in the previous sections, the effect of inf_COD and inf_SO_4^{2-} pulses on the COD and sulfur mass balances was not elucidated. Average values of each component during experiments E-1 through E-9 at steady state conditions were used for the mass balance calculations.

2.3.3.1 Effect on the COD mass balances

The effect of the inf_COD and inf_SO_4^{2-} pulses on the COD mass balances is shown in Figure 2.4 in terms of fractions of the components (eff_COD, COD_ΔSO_4^{2-} and COD_CH_{4gas}) with respect to inf_COD. COD recoveries between 94 and 98% during experiments E-1 through E-9 (except E-6) showed a closed mass balance. The lowest value of 87% at E-6 was attributed to reactor instability as discussed in section 2.3.1.3.

Although an increase of inf_COD from E-1 to E-3 showed an increase of the biogas production (Figure 2.2A), the fraction of the COD_CH_{4gas} decreased from 61 to 53%, while eff_COD fraction increased from 33 to 42%. From E-3 to E-4, an increase in the fraction of COD_ΔSO_4^{2-} by a factor of 2 was observed, while COD_CH_{4gas} and eff_COD fractions remained constant (≈53%) and decreased (to 39%), respectively. It confirmed that the double-pulse 'inf_COD decrease and inf_SO_4^{2-} increase' improved the anaerobic digestion process in terms of COD removal.

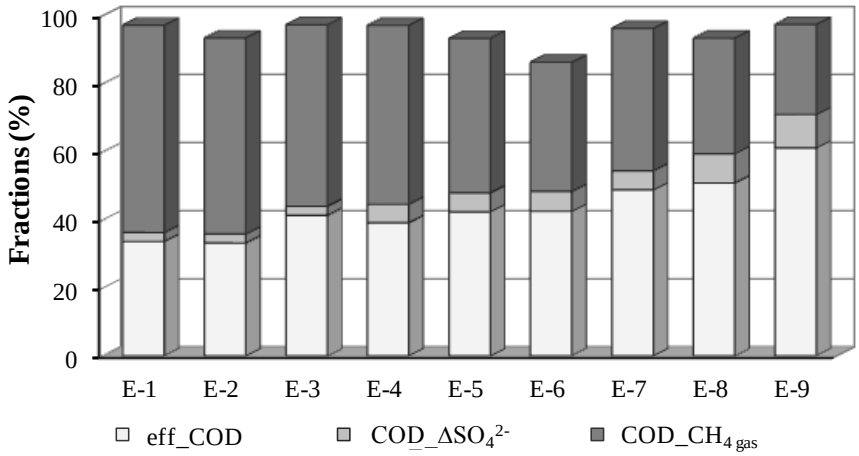

Figure 2.4. Fractions of eff_COD, COD_ΔSO_4^{2-} and COD_CH_{4gas} in the COD mass balances at experiments E-1 through E-9. Remaining fraction in the range reported in literature (Harada et al., 1994; Poinapen et al., 2009a; Poinapen et al., 2009c)

An increase of inf_COD from E-4 to E-6 showed a decrease in the COD_CH_{4gas} fraction while the eff_COD fraction increased from 39 to 42%. In general, an increase of inf_COD at a constant SO_4^{2-}/COD ratio (0.05 or 0.1) was accumulated in the reactor effluent as eff_COD rather than in the gas phase as COD_CH_{4gas}, indicating a deterioration of the anaerobic

process. From E-7 to E-9, a decrease of the COD_CH_{4gas} fraction until 27%, together with an increase of the eff_COD and the COD_ΔSO_4^{2-} fractions (up to 61 and 10%, respectively) aggravated the anaerobic digestion deterioration.

2.3.3.2 Effect on the sulfur mass balances

Figure 2.5 shows the effect of the inf_COD and inf_SO_4^{2-} pulses on the sulfur mass balances in terms of sulfur species fractions (eff_SO_4^{2-}, S_H_2S_{gas}, S_HS^- and S_$[H_2S]_{free}$). Sulfur recoveries between 90 and 94% during experiments E-1 through E-7 showed closed mass balances, while the sulfur recoveries were 82 and 86% at E-8 and E-9, respectively. These lower recoveries were attributed to the formation of sulfurous precipitates (not measured in this work) when inf_SO_4^{2-} increased (Annachhatre and Suktrakoolvait, 2001).

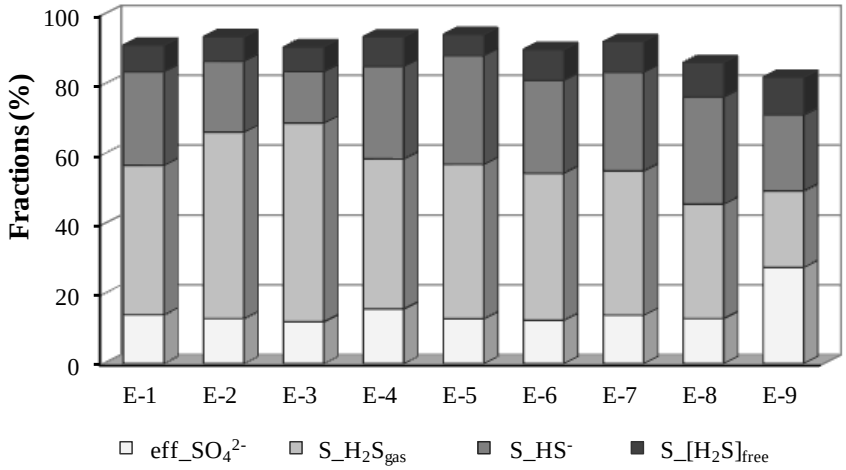

Figure 2.5. Fractions of eff_SO_4^{2-}, S_H_2S_{gas}, S_HS^- and S_$[H_2S]_{free}$ in the sulfur mass balances at experiments E-1 through E-9. Remaining fraction in the range reported in literature (Harada et al., 1994; Poinapen et al., 2009a; Poinapen et al., 2009c)

From E-1 to E-3 (SO_4^{2-}/COD ratio = 0.05) a remarkable increase in the S_H_2S_{gas} fraction was observed (from 43 to 57%). Then, the increase of the inf_COD and inf_SO_4^{2-} provoked sulfur accumulation in the gas phase (as S_H_2S_{gas}) rather than the liquid phase, causing deterioration of biogas quality. From E-3 to E-4, sulfur displacement to the liquid phase between acceptable inhibition limits was observed (as the fractions to the COD mass balances indicated improvement of the anaerobic digestion). Although those fractions

seemed stable during E-4, E-5, E-6 and E-7, a deterioration of the anaerobic digestion was observed from the COD mass balance fractions during E-5, E-6 and E-7 (Figure 2.4). The sulfur mass balance fractions could not explain this observation and it was attributed to the proximity of H_2S_{aq} and $[H_2S]_{free}$ to the inhibitory limits during E-5, E-6 and E-7 (Figure 2.2A, 2.2B, 2.3A and 2.3B).

During E-8, the increase of inf_SO_4^{2-} resulted in an increase in S_HS^- and S_$[H_2S]_{free}$, which suggested an increase of the sulfide toxicity (H_2S_{aq} and $[H_2S]_{free}$). From E-1 to E-8, the eff_SO_4^{2-} fraction remained constant and SRB were able to assimilate the gradual increase of inf_SO_4^{2-} (See Table 2.3). However, experiment E-9 showed a remarkable increase in the eff_SO_4^{2-} fraction (from 13 to 28%) while the COD_ΔSO_4^{2-} fraction remained constant (Figure 2.4), indicating failure of the sulfate reduction process. In general, a sulfur displacement to the gas phase was observed at the SO_4^{2-}/COD ratio of 0.05 or to the liquid phase at SO_4^{2-}/COD ratio $\geq$ 0.10; while sulfate accumulation during E-9 indicated a deterioration of the sulfate reduction process.

2.3.4 Usefulness, limitations and uncertainty sources

Additional information is required on the usefulness, limitations and uncertainty sources of the dynamical data for modeling purposes. The complete set of dynamical data for COD, sulfur and carbon is provided in Appendix B.

In terms of modeling, the ADM1 model (Batstone et al., 2002) has been considered as one of the most sophisticated and complex anaerobic digestion models (Dereli et al., 2010; Fezzani and Cheikh, 2008). It has been referenced in approximately 50% of the modeling papers published until 2013 (Batstone, 2013). In spite of that some limitations were found in the original ADM1, such as: absence of processes related to sulfur, phosphorous and nitrogen conversions (Batstone et al., 2002). Although some extensions have been proposed to overcome these limitations, consolidation of the existing extensions is still required (Batstone, 2013). As this study characterized the sulfate reduction process in the anaerobic digestion of a very high strength and sulfate rich vinasse, rendering closed COD and sulfur mass balances, the data presented here are considered useful to predict the anaerobic digestion of vinasse including the sulfate reduction processes.

As data were obtained while pH variations were in a narrow range during the whole experimental period (7.3 to 7.7, except for days 73, 74 and 75) (Figure 2.2C and 2.3C), the prediction of aqueous phase pH in the anaerobic treatment of vinasse was beyond the scope of this study. Species influencing the aqueous phase pH, such as phosphorous (P) and nitrogen (N) inorganic compounds were considered to be low in concentration and solely used for biomass cell growth, since the ratio COD: N: P in the fed vinasse (400:4:0.72) indicated limiting N and P nutrients (optimum 400:5:1, (Aiyuk et al., 2004; Thaveesri et al., 1995)). Our values agreed with the ratios COD: N: P reported in most of vinasse obtained from the distillation of fermented sugar cane molasses (Wilkie et al., 2000).

Dynamic data for carbon was also included in Appendix B, for completeness, and to reduce the degree of freedom when data is being used for modeling purposes. Although the carbon content of CH_4, CO_2, HCO_3^-, soluble inert and volatile fatty acids (HVa, HBu, HPr, HAc) were determined in the reactor effluents, a difference remained in the carbon balance (Appendix B, Carbon in vinasse - Total Carbon in the effluent). This difference was attributed to the existence of soluble compounds (mainly sugars and amino acids, See Table 2.2) in the effluent as a consequence of reactor inefficiencies and/or the carbon consumption for biomass cell growing, being a source of uncertainty in the present data set.

Therefore, the set of dynamic data that describe the COD, sulfur and carbon mass balances depicted in Appendix B can be considered an archive of data for modeling, when sulfate reduction in the anaerobic digestion of a very high strength and sulfate rich vinasse is of primary interest.

2.4 Conclusions

The highest variation of the biogas quality in terms of H_2S content is expected when inf_COD and inf_SO_4^{2-} increase at a SO_4^{2-}/COD ratio of 0.05. In addition, the double-pulse 'inf_COD decrease and inf_SO_4^{2-} increase' reduced the propionic acid accumulation up to 90%. In these cases, strong contribution of pSRB at SO_4^{2-}/COD ratios $\leq$ 0.10 was suggested, being in contrast to literature reports. This can be considered as an operational strategy to reduce propionic acid accumulation in the anaerobic treatment of vinasse. Influent COD and sulfate fluctuations at a SO_4^{2-}/COD ratio of 0.10 caused inhibition by $H_2S_{aq,}$ $[H_2S]_{free}$ and propionic acid to SRB, methanogens or both. At SO_4^{2-}/COD ratios of 0.20 this inhibition

became severe leading to reactor failure. Further application of modeling tools based on the kinetic coefficients, mass transfer properties and reactor configuration could support the above findings.

At steady state conditions, the mass balances showed COD and sulfur recoveries from 90 to 98% in most of the cases. The COD mass balances showed that an inf_COD increase at a constant SO_4^{2-}/COD ratio (0.05 or 0.1) resulted in an eff_COD increase rather than in a COD_CH_{4gas} increase, indicating a deterioration of the anaerobic digestion process. The sulfur mass balances indicated a sulfur displacement to the gas phase at a SO_4^{2-}/COD ratio of 0.05 or to the liquid phase at SO_4^{2-}/COD ratio $\geq$ 0.10 when influent COD and sulfate concentration increased; while sulfate accumulation in the effluent at the end of experiments indicated a deterioration of the sulfate reduction process. Based on the closed mass balances results, the data presented here are considered reliable for calibrating mathematical models, when sulfate reduction in the anaerobic digestion of a very high strength and sulfate rich vinasse is of primary interest.

CHAPTER 3

Modeling the anaerobic digestion of cane-molasses vinasse: extension of the Anaerobic Digestion Model No. 1 (ADM1) with sulfate reduction for very high strength and sulfate rich wastewater

This Chapter presents the modeling of the anaerobic digestion of cane-molasses vinasse, hereby extending the Anaerobic Digestion Model No. 1 with sulfate reduction for a very high strength and sulfate rich wastewater. Based on a sensitivity analysis, four parameters of the original ADM1 and all sulfate reduction parameters were calibrated. Although some deviations were observed between model predictions and experimental values, it was shown that sulfates, total aqueous sulfide, free sulfides, methane, carbon dioxide and sulfide in the gas phase, gas flow, propionic and acetic acids, chemical oxygen demand (COD), and pH were accurately predicted during model validation. The model showed high (±10%) to medium (10% - 30%) accuracy predictions with a mean absolute relative error ranging from 1% to 26%, and was able to predict failure of methanogenesis and sulfidogenesis when the sulfate loading rate increased. Therefore, the kinetic parameters and the model structure proposed in this work can be considered as valid for the sulfate reduction process in the anaerobic digestion of cane-molasses vinasse when sulfate and organic loading rates range from 0.36 to 1.57 kg SO_4^{2-} m^{-3} d^{-1} and from 7.66 to 12 kg COD m^{-3} d^{-1}, respectively.

Redrafted from:

Ernesto L. Barrera, Henri Spanjers, Kimberly Solon, Youri Amerlinck, Ingmar Nopens, Jo Dewulf. Modeling the anaerobic digestion of cane-molasses vinasse: extension of the Anaerobic Digestion Model No. 1 (ADM1) with sulfate reduction for very high strength and sulfate rich wastewater. Manuscript submitted to Water research.

3.1 Introduction

Many industrial processes, especially in food and fermentation industries, generate wastewaters with high levels of chemical oxygen demand (COD) and sulfate (Zub et al., 2008). Vinasse obtained from ethanol distillation in the sugar cane industry (cane-molasses vinasse) is a typical example of very high strength and sulfate rich liquid substrate (Barrera et al., 2013). Hence, the anaerobic digestion of vinasse promotes the activity of sulfate reducing bacteria (SRB) producing sulfide. The latter is distributed among aqueous sulfide (H_2S free, HS^- and S^{2-}), hydrogen sulfide in the biogas and insoluble metallic sulfides.

Modeling has proven to be an important tool for understanding, design and control of the sulfate reduction process (Batstone, 2006). A simple approach to model sulfate reduction is by considering the oxidation (by SRB) of the available hydrogen only (Batstone, 2006). However, in systems with high sulfate concentrations volatile fatty acids (butyric, propionic and acetic) have, to be included as electron donors in the sulfate degradation reactions in addition to hydrogen (Batstone, 2006). Barrera et al. (2014) provided a characterization of the sulfate reduction process in the anaerobic digestion of a very high strength and sulfate rich vinasse. The authors demonstrated that propionate sulfate reducing bacteria considerably contribute to propionic acid degradation at SO_4^{2-}/COD ratios ≤ 0.10 as a result of hydrogen limitation. This suggests that reactions involving volatile fatty acids need to be included to properly model sulfate reduction in the anaerobic digestion of such vinasses. The Anaerobic Digestion Model No. 1 (ADM1), developed by the IWA Task Group for Mathematical Modeling of Anaerobic Digestion Processes, is one of the most sophisticated and complex anaerobic digestion models, involving 19 biochemical processes and two types of physiochemical processes (Batstone et al., 2002). The simple approach of Batstone (2006) to model sulfate reduction as an extension of ADM1 has been used to model the anaerobic digestion of vinasse under dynamic conditions without success, exhibiting under prediction of H_2S and over prediction of volatile fatty acids (Hinken et al., 2013). In order to extend ADM1, Fedorovich et al. (2003) included the sulfate reduction process starting from previously reported work (Kalyuzhnyi et al., 1998; Kalyuzhnyi and Fedorovich, 1998; Knobel and Lewis, 2002; Ristow et al., 2002). The approach of Fedorovich et al. (2003) can be considered as complex because of the inclusion of valerate/butyrate, propionate, acetate and hydrogen in the sulfate degradation reactions (Batstone, 2006). This model (Fedorovich

et al., 2003) was calibrated for organic deficient (SO_4^{2-}/COD ratios ≥ 1.5) synthetic wastewaters (Omil et al., 1997a; Omil et al., 1996), hereby focusing on volatile fatty acids, sulfates and methane gas phase concentrations. Furthermore, the agreement between model and experimental values for the concentrations of total aqueous sulfide (S_{h2s}), free sulfides ($S_{h2s,free}$) and gas phase sulfides ($S_{gas,h2s}$) was not reported. Likely because of these limitations, the extension of Fedorovich et al. (2003) is not commonly used (Lauwers et al., 2013).

Consequently, an extension of ADM1 with sulfate reduction to model the anaerobic digestion of a very high strength and sulfate rich vinasse may overcome the current limitation of models by (1) describing the sulfate reduction process in the anaerobic digestion of vinasse, (2) predicting the sulfur compounds in both the gas and liquid phases, (3) increasing applicability of ADM1 to specific industrial wastewaters (vinasse), and (4) simplifying the existing approach to reduce complexity and to support further implementations.

Therefore, the work presented here attempts to model the anaerobic digestion of real cane-molasses vinasse by extending ADM1 with sulfate reduction for a very high strength and sulfate-rich complex wastewater, including volatile fatty acids (propionic and acetic acids) in the sulfate degradation reactions, hereby including an accurate prediction of S_{h2s}, $S_{h2s,free}$ and $S_{gas,h2s}$.

3.2. Materials and methods

3.2.1. Experimental data

Experimental observations from a characterization study of the sulfate reduction process in the anaerobic digestion of a very high strength and sulfate-rich vinasse (Barrera et al., 2014) were used for model calibration and validation (Chapter 2). During these experiments a 3.5 L UASB reactor was operated under dynamic conditions for a period of 75 days (following a 55 day start-up period). The experimental set-up, analytical methods and operating conditions are described in detail in Chapter 2. They can be briefly described as follows, where the E-codes indicate successive experiments conducted under different operating conditions:

- E-1 to E-3: the concentration of influent COD and SO_4^{2-} was gradually increased while keeping the SO_4^{2-}/COD ratio at 0.05.

- E-3 to E-4: the influent SO_4^{2-} was increased whereas the influent COD concentration was decreased to increase the SO_4^{2-}/COD ratio to 0.1.
- E-4 to E-6: the concentration of influent COD and SO_4^{2-} was increased while keeping the SO_4^{2-}/COD ratio at 0.1.
- E-7: the concentration of influent COD and SO_4^{2-} was reduced to control toxicity, keeping the SO_4^{2-}/COD ratio at 0.1.
- E-8 and E-9: the influent SO_4^{2-} was increased while keeping a constant influent COD concentration to increase the SO_4^{2-}/COD ratio to 0.15 and 0.20, respectively.

Operating conditions were grouped in data set D1 (operating conditions E-1, E-2, E-3 and E-4 in Chapter 2) for calibration and direct validation, and data set D2 (operating conditions E-5, E-6, E-7, E-8 and E-9 in Chapter 2) for cross validation.

3.2.2. Model description and implementation

The original ADM1 is described in a scientific and technical report prepared by an IWA Task Group (Batstone et al., 2002). This model takes into account seven bacterial groups. The biological degradation processes are described using Monod kinetics, while the extracellular processes (disintegration and hydrolysis) and the biomass decay are described using first-order kinetics.

The ADM1 extension with sulfate reduction for very high strength and sulfate rich wastewater was implemented in MatLab/Simulink 2008b (see the simulink architecture in Appendix C) following the original ADM1 (Batstone et al., 2002) and the approaches discussed in Chapter 1 (Barrera et al., 2013). The model was implemented as a set of ordinary differential equations using the ODE 15s as numerical solver (see the c-codes in Appendix D). Based on experimental observations previously discussed in Chapter 2 (Barrera et al., 2014), butyric acid was neglected as organic matter for SRB in the model structure (≤ 5% of the total volatile fatty acids concentration), whereas propionic (considered incompletely oxidized by propionate SRB) and acetic acids, as well as hydrogen, were considered as the electron donors for the sulfate reduction processes following the biochemical degradation reactions (3.1), (3.2) and (3.3) below:

$$C_2H_5COOH + 0.75H_2SO_4 \rightarrow CH_3COOH + CO_2 + H_2O + 0.75H_2S \quad (3.1)$$

$$CH_3COOH + H_2SO_4 \rightarrow 2CO_2 + 2H_2O + H_2S \quad (3.2)$$

$$4H_2 + H_2SO_4 \rightarrow H_2S + 4H_2O \quad (3.3)$$

Consequently, three SRB groups were considered to be active inside the reactor; i.e. propionate sulfate reducing bacteria (pSRB), acetate sulfate reducing bacteria (aSRB) and hydrogenotrophic sulfate reducing bacteria (hSRB). A dual term Monod type kinetics was used to describe the uptake rate of these substrates (Fedorovich et al., 2003). The biochemical rate coefficients ($\nu_{i,j}$) and kinetic rate equation (ρ_j) for soluble and particulate components are listed in Table 3.1. Similar to decay of other microbial species, first order kinetics was used to describe the decay of SRB. Additionally, rate coefficients and kinetic rate equations for acid-base reactions for sulfides and sulfates (in the form recommended by Rosen and Jeppsson (2006)) were considered (Table 3.2). Un-dissociated sulfuric acid (H_2SO_4) and sulfide ions (S^{2-}) were considered negligible and were not included in the acid-base reactions. As sulfuric acid is a strong acid (pKa < -2), it can considered completely dissociated, whereas sulfide ions S^{2-} exist in small amounts (pKa ≈14) in the liquid phase of anaerobic reactors in which a pH between 6.5 and 8 is required. The dissociation equations 3.4 and 3.5 were included in the model.

$$HSO_4^- \rightleftarrows H^+ + SO_4^{2-} \qquad pK_a = 1.99 \quad (3.4)$$

$$H_2S \rightleftarrows H^+ + HS^- \qquad pK_a = 7.01 \quad (3.5)$$

To model the stripping of H_2S, the liquid phase yield coefficient ($\nu_{i,j}$) and the rate equations (ρ_j) for liquid-gas transfer process were also included (Table 3.3). Nomenclature in Table 3.1, 3.2 and 3.3 was adopted from ADM1 (Batstone et al., 2002).

Despite the fact that S_{h2s} has been found to inhibit anaerobic digestion (Visser et al., 1996), for modeling purpose only $S_{h2s,free}$ was assumed to be inhibitory for modeling purposes (Kalyuzhnyi et al., 1998; Kalyuzhnyi and Fedorovich, 1998; Knobel and Lewis, 2002; Ristow et al., 2002). A non-competitive inhibition function for sulfides ($I_{h2s,j}$) was considered in all cases (Knobel and Lewis, 2002). The inhibition terms I_1 and I_2 were adopted from the original ADM1 for the uptake of sugars, amino acids and long chain fatty acids (processes not shown in Table 3.1).

Table 3.1. Biochemical rate coefficients ($\nu_{i,j}$) and kinetic rate equation (ρ_j) for soluble and particulate components added to ADM1 to model the sulfate reduction process in the anaerobic digestion of cane-molasses vinasse

	Component i →	**6**	**7**	**8**	**8a**	**9a**	**10**	**11**	**13**	**21a**	**22a**	**23a**	**Rate**
j	**Process ↓**	**S_{pro}**	**S_{ac}**	**S_{h2}**	**S_{so4}**	**S_{h2s}**	**S_{IC}**	**S_{IN}**	**X_c**	**X_{pSRB}**	**X_{aSRB}**	**X_{hSRB}**	**(ρ, kg COD m^{-3} d^{-1})**
10a	Uptake of Propionate by pSRB	-1	$(1\text{-}Y_{pSRB})0.57$		$-\frac{(1\text{-}Y_{pSRB})0.43}{64}$	$\frac{(1\text{-}Y_{pSRB})0.43}{64}$	$-\sum_{i=1\text{-}9a,\ i=11\text{-}24} C_i\nu_{i,10a}$	$-Y_{pSRB}\cdot N_{bac}$		Y_{pSRB}			$k_{m,pSRB}\cdot\frac{S_{pro}}{K_{S,pro}+S_{pro}}\cdot\frac{S_{so4}}{K_{S,so4,pSRB}+S_{so4}}\cdot X_{pSRB}\cdot I_4$
11a	Uptake of Acetate by aSRB		-1		$-\frac{(1\text{-}Y_{aSRB})}{64}$	$\frac{(1-Y_{aSRB})}{64}$	$-\sum_{i=1\text{-}9a,\ i=11\text{-}24} C_i\nu_{i,11a}$	$-Y_{aSRB}\cdot N_{bac}$			Y_{aSRB}		$k_{m,aSRB}\cdot\frac{S_{ac}}{K_{S,ac}+S_{ac}}\cdot\frac{S_{so4}}{K_{S,so4,aSRB}+S_{so4}}\cdot X_{aSRB}\cdot I_4$
12a	Uptake of Hydrogen by pSRB			-1	$-\frac{(1\text{-}Y_{hSRB})}{64}$	$\frac{(1\text{-}Y_{hSRB})}{64}$	$-\sum_{i=1\text{-}9a,\ i=11\text{-}24} C_i\nu_{i,12a}$	$-Y_{hSRB}\cdot N_{bac}$				Y_{hSRB}	$k_{m,hSRB}\cdot\frac{S_{h2}}{K_{S,h2}+S_{h2}}\cdot\frac{S_{so4}}{K_{S,so4,hSRB}+S_{so4}}\cdot X_{hSRB}\cdot I_4$
17a	Decay of X_{pSRB}						$-C_{bac}+C_{xc}$	$-N_{bac}+N_{xc}$	1	-1			$k_{dec,XpSRB}\cdot X_{pSRB}$
18a	Decay of X_{aSRB}						$-C_{bac}+C_{xc}$	$-N_{bac}+N_{xc}$	1		-1		$k_{dec,XaSRB}\cdot X_{aSRB}$
19a	Decay of X_{hSRB}						$-C_{bac}+C_{xc}$	$-N_{bac}+N_{xc}$	1			-1	$k_{dec,XhSRB}\cdot X_{hSRB}$
		Total propionate (kg COD m^{-3})	Total acetate (kg COD m^{-3})	Total hydrogen gas (kg COD m^{-3})	Total sulfates (kmol m^{-3})	Hydrogen sulfide gas (kmol m^{-3})	Inorganic carbon (k mol m^{-3})	Inorganic nitrogen (k mol m^{-3})	Composites (kg COD m^{-3})1	Propionate SRB (kg COD m^{-3})	Acetate SRB (kg COD m^{-3})	Hydrogenotrophic SRB (kg COD m^{-3})	Inhibition term for X_{c4} & X_{pro} (See I_2 in (Batstone et al., 2002)) $I_2\cdot I_{h2s,8-9}$ Inhibition term for X_{ac} (See I_3 in (Batstone et al., 2002)) $I_3\cdot I_{h2s,11}$ Inhibition term for X_{h2} (See I_1 in (Batstone et al., 2002)) $I_1\cdot I_{h2s,12}$ Inhibition term for pSRB, aSRB & hSRB $I_4 = I_{pH,(10a,11a,12a)}\cdot I_{h2s,(10a,11a,12a)}$

Table 3.2. Rate coefficients ($\nu_{i,j}$) and kinetic rate equation (ρ_j) for acid-base reactions in the differential equation implementation added to ADM1 to model the sulfate reduction process in the anaerobic digestion of cane-molasses vinasse

	Component → i	**8a.1**	**8a.2**	**9a.1**	**9a.2**	**Rate**
j	**Process ↓**	S_{hso4-}	$S_{so4}2-$	$S_{h2s,free}$	S_{hs-}	**(ρ, kmol m^{-3} d^{-1})**
A12	Sulfide acid - base			1	-1	$K_{A/B,h2s} \cdot (S_{hs-} \cdot (S_{H+} + K_{a,h2s}) - K_{a,h2s} \cdot S_{h2s,total})$
A13	Sulfate acid -base	1	-1			$K_{A/B,so4} \cdot (S_{so4,total} \cdot S_{H+} - (K_{a,so4} + S_{H+}))$

Table 3.3. Liquid phase yield coefficient ($\nu_{i,j}$) and rate equations (ρ_j) for the liquid-gas transfer process added to ADM1 to model the sulfate reduction process in the anaerobic digestion of cane-molasses vinasse

	Component i →	**9a**	**Rate**
j	**Process ↓**	$S_{h2s,free}$	**(ρ, kmol m^{-3} d^{-1})**
T9a	H_2S Transfer	-1	$k_L a \cdot (S_{h2s,free} - K_{H,h2s} \cdot P_{gas,h2s})$

However, the inhibition term for valerate, butyrate and propionate degraders (I_2 in Batstone et al. (2002)) as well as the inhibition term for acetotrophic methanogens (I_3 in Batstone et al. (2002)) and the inhibition term for hydrogenotrophic methanogens (I_1 in Batstone et al. (2002)) was multiplied by $I_{h2s,j}$ in order to include the free sulfide inhibition in this model extension. The inhibition term I_4 was added to account for pH inhibition ($I_{pH,j}$) and $I_{h2s,j}$ of pSRB, aSRB and hSRB (see inhibition terms in Table 3.1). All pH inhibitions were based on the Hill function as suggested in (Rosen and Jeppsson, 2006).

3.2.3. Model inputs and initial conditions

The influent characterization of cane-molasses vinasse is shown in Table 3.4. Sugar, protein and lipid contents were experimentally determined in the filtered and unfiltered vinasse and used to calculate the soluble sugars (S_{su}) and particulate carbohydrates (X_{ch}), the soluble amino acids

(S_{aa}) and particulate proteins (X_{pr}) as well as the long chain fatty acids (S_{fa}) and particulate lipids (X_{li}), respectively. The total cation concentration was determined as the sum of Na^{+}, K^{+}, Ca^{2+}, Mg^{2+}, Mn^{2+}, and Zn^{2+} species concentrations whereas NO_2^{-}, NO_3^{-}, PO_4^{3-}, and Cl^{-} concentrations were used to determine the total anion concentration of vinasse.

Table 3.4. Model based influent characterization of raw cane-molasses vinasse

Components	**Names**	**Units**	**Values**
Solubles			
S_{su}	Sugar concentration	kg COD m^{-3}	33.73
S_{aa}	Amino acid concentration	kg COD m^{-3}	5.82
S_{fa}	LCFA concentration	kg COD m^{-3}	0.09
S_{ac}	Acetic acid concentration	kg COD m^{-3}	1.36
S_{SI}	Inert concentration	kg COD m^{-3}	16.97
SCOD	Soluble COD concentration	kg COD m^{-3}	57.97
Particulates			
X_{ch}	Carbohydrate concentration	kg COD m^{-3}	6.91
X_{pr}	Protein concentration	kg COD m^{-3}	0.09
X_{li}	Lipid concentration	kg COD m^{-3}	0.14
X_I	Inert concentration	kg COD m^{-3}	0.00
X_c	Composite concentration	kg COD m^{-3}	0.00
XCOD	Particulate COD concentration	kg COD m^{-3}	7.15
TCOD	Total COD	kg COD m^{-3}	65.12
Total cation	Total cation concentration	kmol m^{-3}	0.315
Total anion	Total anion concentration	kmol m^{-3}	0.073

The difference between the soluble COD (SCOD) and the total COD of S_{su}, S_{aa}, S_{fa} and S_{ac} was assumed to be the soluble inert concentration of vinasse (S_I). Similarly, the difference between the COD concentration of the particulate matter (XCOD) and the total COD of X_{ch}, X_{pr} and X_{li}

was assumed to be the particulate inert concentration of vinasse (X_I) (See Table 3.4). The concentrations of these known input variables (S_{su}, S_{aa}, S_{fa}, S_{ac}, S_I, X_{ch}, X_{pr}, X_{li}, and X_I) under specific operating conditions (E-1 to E-9) were calculated from the total COD (TCOD) of the diluted vinasse at these operating conditions and the compositions of raw vinasse as given in Table 3.4. This is illustrated for sugars in Eq. 3.1.

$$S_{su\_operating\ conditions\ (E\text{-}1\ to\ E\text{-}9)} = \frac{TCOD\_diluted\_vinasse\_operating\ conditions\ (E\text{-}1\ to\ E\text{-}9)}{TCOD\_raw\_vinasse\_Table\ 3.4} \cdot S_{su\_raw\ vinasse\_Table\ 3.4} \quad (3.1)$$

ADM1 requires a large number of input variables. Reasonable assumptions were made for the concentration of the unknown input variables S_{h2}, S_{ch4}, X_{su}, X_{aa}, X_{fa}, X_{c4}, X_{pro}, X_{ac}, X_{h2}, X_{pSRB}, X_{aSRB} and X_{hSRB}. Their default concentrations in ADM1 were set for the operating condition E-1, whereas concentrations for the cases E-2 to E-9 were calculated similar to Eq. 3.1 (see all the input values in Appendix E).

The initial conditions for the dynamic simulation were estimated as recommended by Rieger et al. (2012). Steady state simulations were run and the values of the state variables at the end of this simulation period were used as initial conditions for the dynamic simulation. Since this procedure assumes that the reactor is operated in a typical way for an extended period prior to the dynamic simulation (similar to the experiments used for calibration and validation), this was considered sufficient to establish the initial conditions for this work (Rieger et al., 2012).

3.2.4. Sensitivity analysis

Despite the fact that all parameters affect the model output, the output sensitivity differs from one parameter to another. Sensitivity analysis has been widely applied to reduce model complexity, to determine the significance of model parameters and to identify dominant parameters (Dereli et al., 2010; Silva et al., 2009; Tartakovsky et al., 2008).

The local relative sensitivity analysis method (Dochain and Vanrolleghem, 2001) is employed here in order to calculate sensitivity functions for the dynamic simulations. The numerical calculation of sensitivity functions uses the finite difference approximation (Dochain and Vanrolleghem, 2001). The sensitivities are quantified in terms of the variation of measurable process variables under the perturbation of model parameters in their neighborhood domain (Eq.

3.2). The value of the perturbation factor δ was chosen such that the differences between the resulting sensitivity values of different parameters can be detected.

$$\Gamma_{n,m}(t) = \frac{\partial y_n(t)/y_n(t)}{\partial \theta_m/\theta_m} = \frac{(y_n(t,\ \theta_m + \delta \cdot \theta_m) - y_n(t,\ \theta_m))/y_n(t,\ \theta_m)}{\delta \cdot \theta_m/\theta_m} \quad (3.2)$$

where $\Gamma_{n,m}$ is the dimensionless sensitivity value of the n^{th} process variable with respect to the m^{th} model parameter; y_n (n = 1,. . .,9) denotes the n^{th} process variable (i.e. S_{pro}, S_{ac}, pH, Q_{gas} (gas flow), $S_{gas,ch4}$, $S_{gas,co2}$, S_{so4}, S_{h2s}, and $S_{gas,h2s}$); θ_m is the m^{th} model parameter, m = 1,. . ., 40 (see parameters in Appendix F); and $\theta_m + \delta \cdot \theta_m$ is the perturbated parameter value. The sensitivity values for each process variable to each model parameter for data set D1 (days 0 to 36) and data set D2 (days 37 to 75), were computed as $\sum \Gamma_{n,m}(t)$ (expressed as % in respect to the total $\sum\sum \Gamma_{n,m}(t)$) and arranged in descending order.

3.2.5 Model calibration, parameter uncertainties and validation procedure

Calibration of the more sensitive model parameters is now required. Model calibration was performed on an expert –basis by a trial and error approach, driven by knowledge from the sensitivity analysis and using the parameter ranges reported in the literature as constraints. The iterative procedure reported by (Dereli et al., 2010) was applied.

In order to provide information about the uncertainty of the calibrated parameters, confidence intervals (CI) for the resulting set of parameters were calculated based on the Fisher information matrix (FIM) (Eq. 3.3) (Dochain and Vanrolleghem, 2001).

$$FIM = \sum_{i=1}^{t} \left(\frac{\partial y_n}{\partial \theta_m}(t)\right)^T \sum^{-1} \cdot \left(\frac{\partial y_n}{\partial \theta_m}(t)\right) \quad (3.3)$$

Where, $\partial y_n / \partial \theta_m(t)$ are the absolute sensitivity values and $\sum^{-1}$ is calculated as the inverse of the covariance matrix of the measurement error (Dochain and Vanrolleghem, 2001). Subsequently, the covariance matrix (COV) can be approximated by the inverse of the FIM matrix ($COV = FIM^{-1}$) and the standard deviations (σ) for the parameters (θ_m) can be obtained by using Eq. (3.4) (Dochain and Vanrolleghem, 2001).

$$\sigma(\theta_m) = \sqrt{COV_{m,m}} \quad (3.4)$$

Confidence intervals for the parameters (Eq. 3.5) were calculated for a confidence level of 95% (α=0.05) and the t-value was obtained from the Student-t distribution.

$$\theta_m \pm t_{\alpha,df} \cdot \sigma(\theta_m) \quad (3.5)$$

Once a set of estimated parameters has been obtained, it is necessary to question the predictive quality of the resulting model through validation (Donoso-Bravo et al., 2011). Direct and cross validation are usually considered as steps of the model validation procedure (Donoso-Bravo et al., 2011). Therefore, the data was divided into two subsets as recommended by Donoso-Bravo et al. (2011): (1) data used during model calibration (data set D1) for direct validation, and (2) unseen data (data set D2) for cross validation. The accuracy of the predictions for direct and cross validation were determined by using the mean absolute relative error and they were classified as high (±10%) or medium (10% - 30%) accurate quantitative prediction (Batstone and Keller, 2003).

3.3. Results and discussion

3.3.1. Sensitivity analysis

Steady state simulations using the ADM1 benchmark parameter values (Rosen and Jeppsson, 2006) and values given by Fedorovich et al. (2003) for sulfate reduction showed discrepancies greater than 50% between the experimental results and the model predictions.

To further improve the dynamic predictions, a sensitivity analysis was performed under dynamic conditions in order to determine the most important parameters to be used in the dynamic calibration. The resulting local sensitivity values ($\sum \Gamma_{n,m} / \sum\sum \Gamma_{n,m}$, expressed as %) for each process variable (S_{pro}, S_{ac}, pH, Q_{gas}, $S_{gas,ch4}$, $S_{gas,co2}$, S_{so4}, S_{h2s}, and $S_{gas,h2s}$) are shown in Figure 3.1. The perturbation factor δ was set as 1% for all the calculations as in (Tartakovsky et al., 2008). It is noteworthy that negative values indicated a decrease of the process variable when the parameter was perturbed.

Figure 3.1 allows the identification of the most sensitive model parameters for each process variable. For example, the process variable S_{pro} is highly sensitive to parameters $k_{m,hSRB}$, $K_{S,hSRB}$ and Y_{su} (see nomenclature of the parameters in Appendix F), whereas S_{ac} is highly sensitive to $k_{m,ac}$ and Y_{ac}. The fact that some model parameters affected several process variables at the same time (e.g. the model parameter Y_{su} affected the process variables S_{pro}, pH, $S_{gas,ch4}$ and $S_{gas,co2}$) was also useful for model calibration. Additionally, it was observed from the sensitivity analysis that the effect of the model parameters from days 0 to 36 (data set D1) varied in comparison to those from days 37 to 75 (data set D2) (Figure 3.1). In that sense, an increased sensitivity towards

$k_{m,hSRB}$ on S_{pro} was observed near the end of the experiments (data set D2) because of the increase of influent sulfates (see experimental conditions in Chapter 2), which made the sulfate reduction process predominant leading to a higher sensitivity (with respect to data set D1).

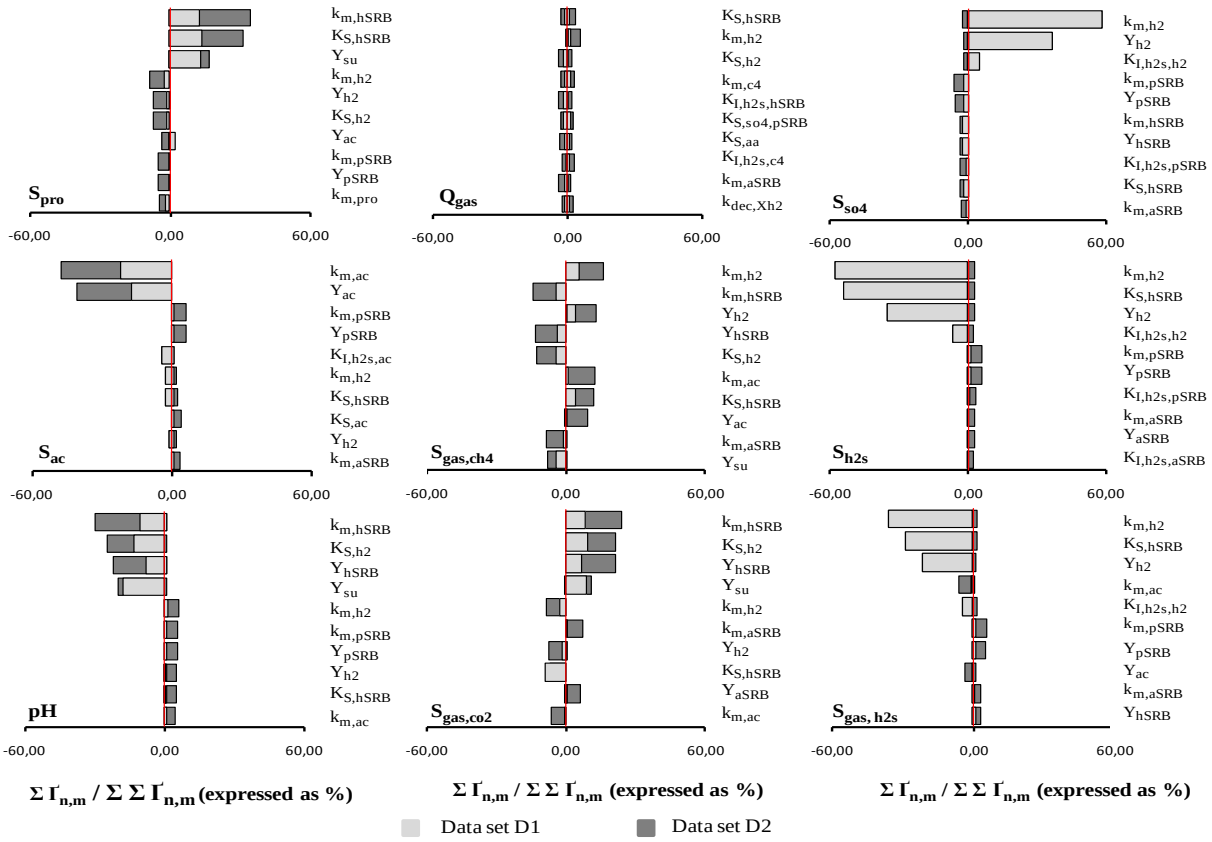

Figure 3.1. Most sensitive model parameters arranged in descending order, for the process variables S_{pro}, S_{ac}, pH, Q_{gas}, $S_{gas,ch4}$, $S_{gas,co2}$, S_{so4}, S_{h2s}, and $S_{gas,h2s}$

Therefore, the sensitivity analysis enabled ranking the effect of the model parameters on each process variable, which yields information useful for model calibration.

3.3.2 Model calibration

The model was calibrated using 36 days of dynamic data obtained in Chapter 2 (data set D1). During these days, the organic loading rate (OLR) of the upflow anaerobic sludge bed (UASB) reactor was gradually increased from 7.66 to 12.00 kg COD m^{-3} d^{-1} and later reduced to 7.9 kg COD m^{-3} d^{-1}. At the same time, the sulfate loading rate (SLR) was increased from 0.36 to 0.76 kg

SO_4^{2-} m^{-3} d^{-1} at a constant hydraulic retention time of 4.86 days, resulting in an increase of the SO_4^{2-}/COD ratio from 0.05 to 0.10 (see Chapter 2) (Barrera et al., 2014).

Initial values of the model state variables were taken from steady state simulations at the operating conditions of E-1 and the dynamic input variables were calculated from the influent characterization of cane-molasses vinasse (Table 3.4), as illustrated in Eq. 3.1.

An iterative method (Dereli et al., 2010) was applied for the calibration of the most sensitive parameters by fitting the model to the experimental results for the process variables S_{so4}, S_{h2s}, $S_{h2s,free}$, $S_{gas,h2s}$, Q_{gas}, $S_{gas,ch4}$, $S_{gas,co2}$, S_{pro}, S_{ac}, eff_COD (effluent COD) and pH. Although a larger number of ADM1 parameters were sensitive to the process variables (Figure 3.1), only $k_{m,pro}$, $k_{m,ac}$, $k_{m,h2}$, and Y_{h2} were used for calibration, as the sensitivity analysis revealed them to be among the most sensitive model parameters (Figure 3.1). In this way, the number of calibrated ADM1 parameters was kept to a strict minimum. In addition, all sulfate reduction parameters (70% among the most sensitive parameters of Figure 3.1) were calibrated. The estimated parameter values providing the best fit (based on the mean absolute relative error) between model predictions and experimental results are reported in column 7 (Calibration this work) of Appendix F. All other parameters were adopted from Rosen and Jeppsson (2006).

During calibration, the values obtained for $k_{m,pro}$, $k_{m,ac}$, and $k_{m,h2}$ were in agreement with values used to calibrate the anaerobic digestion of cane-molasses (Romli et al., 1995) (Column 5, Appendix F). The fact that parameter values used for calibration in (Romli et al., 1995) were used for calibration in this work, was likely because of the similar characteristics of both substrates (cane-molasses and cane-molasses vinasse, respectively), which favored the uptake rate of propionate, acetate and hydrogen leading to required modification (in respect to ADM1 parameter values) of $k_{m,pro}$, $k_{m,ac}$, and $k_{m,h2}$ during the calibration in this work (Appendix F).

Concerning the calibration of the sulfate reduction parameters, the yield coefficients, the Monod maximum specific uptake rates and the half saturation coefficients were found in the range of values found in Chapter 1 (Barrera et al., 2013). However, the 50% inhibitory concentrations of free H_2S (Appendix F) were lower than the values used to calibrate the sulfate reduction processes (Barrera et al., 2013), but similar to experimental values reported as inhibitory (150 mg S L^{-1} (0.0047 kmol m^{-3})) for methanogens and SRB (except for propionate degraders, which is 70 mg S L^{-1} (0.0022 kmol m^{-3})) (Rinzema and Lettinga, 1988). These values agreed well with

the experimental observations (Chapter 2) (Barrera et al., 2014) used for calibration in this work and therefore they can be considered a better approximation for the real phenomena.

In contrast, fitting of $K_{S,so4,pSRB}$, $K_{S,so4,aSRB}$, and $K_{S,so4,hSRB}$ was required to predict S_{so4} as these parameters solely impact this process variable (results not shown). Values 10 times higher than those from Chapter 1 (Barrera et al., 2013) were retrieved for $K_{S,so4,pSRB}$, $K_{S,so4,aSRB}$, and $K_{S,so4,hSRB}$. This observation was attributed to the use (by previous modelers) of experimental observations based on organic deficient substrates (SO_4^{2-}/COD ratios ≥ 1.5) (Alphenaar et al., 1993; Omil et al., 1997a; Omil et al., 1996) to fit models (Fedorovich et al., 2003; Kalyuzhnyi et al., 1998), by increasing the maximum specific uptake rate and decreasing the half saturation coefficient of SRB. The half saturation coefficient for hSRB ($K_{S,hSRB}$) agreed well with values reported (Batstone et al., 2006) and was 86% of the half saturation coefficient of hydrogenotrophic methanogenic archea (hMA), showing that hSRB can outcompete hMA for hydrogen (Omil et al., 1997a; Rinzema and Lettinga, 1988).

3.3.3 Parameter uncertainty estimation

The confidence intervals (CI) for the calibrated parameters are shown in Appendix F. They were found to be below 20% in all cases which yields a satisfactory confidence in the determined set of parameters (confidence level 95%). The correlation between the calibrated parameters was also calculated based on the covariance matrix (COV), rendering the following results:

- Strong correlation (≥ 0.7) between the parameter pairs [$k_{m,aSRB}$, Y_{aSRB}]; [$k_{m,pro}$, $K_{I,h2s,pro}$]; and [$k_{m,ac}$, $K_{I,h2s,ac}$].
- Moderate correlation (0.4 - 0.7) between the parameter pairs [Y_{h2}, Y_{hSRB}]; [$k_{m,pSRB}$, Y_{pSRB}]; [$k_{m,hSRB}$, $K_{S,hSRB}$]; [$K_{S,so4,aSRB}$, $K_{S,so4,hSRB}$]; [$K_{S,so4,hSRB}$, $K_{I,h2s,h2}$]; [$K_{S,so4,pSRB}$, $K_{I,h2s,aSRB}$]; [$K_{S,so4,pSRB}$, $K_{I,h2s,hSRB}$]; and [$k_{m,hSRB}$, $K_{I,h2s,hSRB}$].

3.3.4 Direct validation

The deviation between model predictions and experimental observations was used for direct validation. The results after calibration are shown in Figure 3.2. It can be seen that the process variables (except for S_{pro}) were predicted quite well after the model calibration (Figure 3.2A - H), exhibiting a mean absolute relative error below 10% (1% to 7.7%), which is considered as a high accuracy quantitative prediction (Batstone and Keller, 2003). However, deviations between

model predictions and experimental values for S_{pro} (Figure 3.2G) led to a mean absolute relative error higher than 30%, which can be considered as a qualitative prediction that can demonstrate the overall qualitative response of the system (Batstone and Keller, 2003).

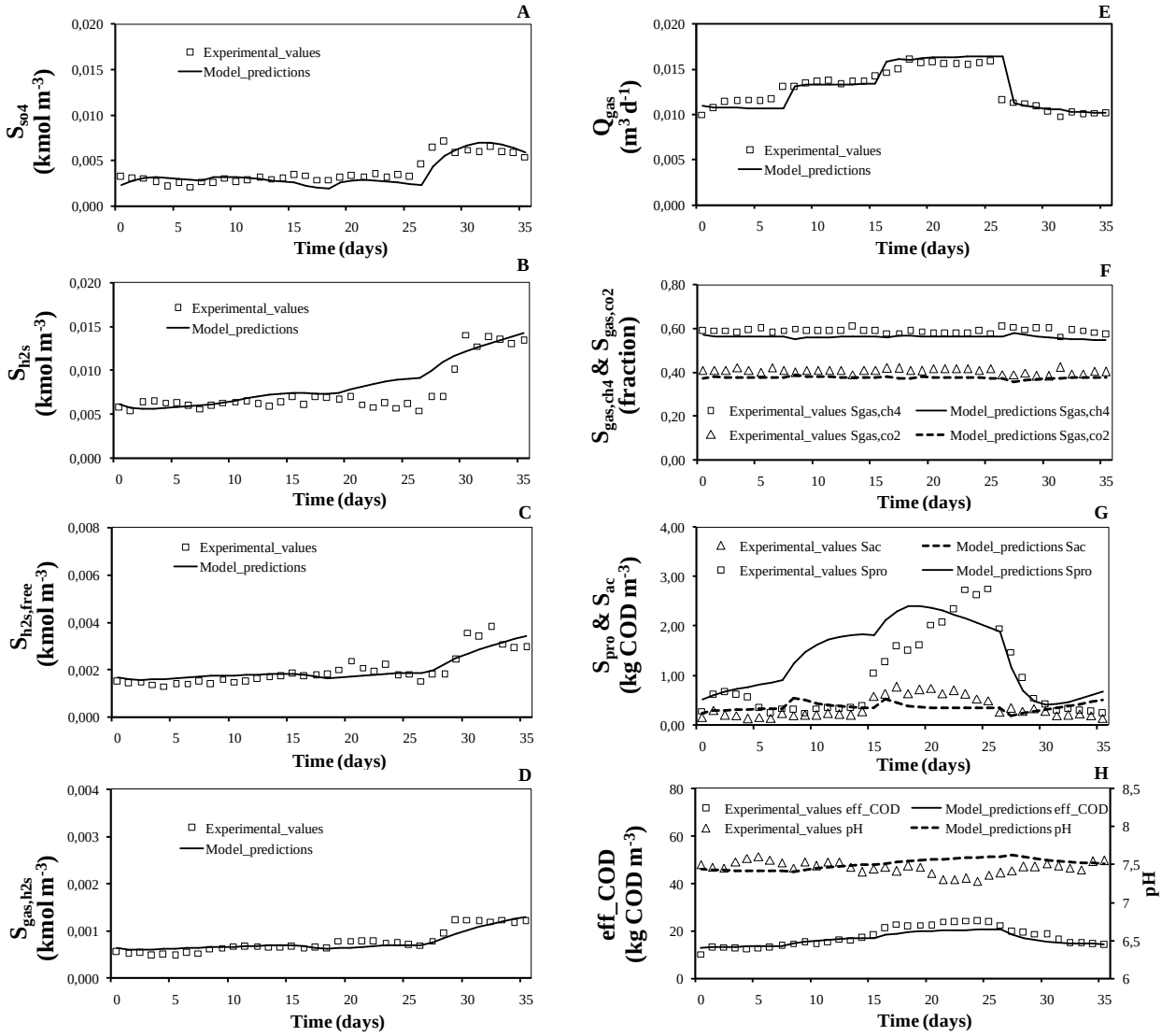

Figure 3.2. Comparison between experimental values and model predictions after the model calibration: (A) S_{so4}, (B) S_{h2s}, (C) $S_{h2s,free}$, (D) $S_{gas,h2s}$, (E) Q_{gas}, (F) $S_{gas,ch4}$ & $S_{gas,co2}$, (G) S_{pro} & S_{ac}, and (H) eff_COD & pH

The increase of the OLR and the influent COD concentration in a UASB reactor fed with vinasse caused an increase of the propionic acid concentration (Harada et al., 1996). However, in the experimental values used for calibration in this work, S_{pro} remained constant (see experimental

values in Chapter 2, Figure 2.2C) when the OLR was increased on day 8 (Barrera et al., 2014). This was likely because sludge in the UASB reactor assimilated the increase of the OLR by degrading the excess of propionate. Despite the fact that the model could not predict this observation (Figure 3.2G), the over prediction observed for S_{pro} during days 8 to 15 when the OLR increased was in agreement with the phenomenon described by Harada et al. (1996). Moreover, the under prediction of S_{pro} during days 23 to 25 can be attributed to the slight under prediction of $S_{h2s,free}$ (constant at the concentration of 0.0018 kmol m^{-3}) that reduces the inhibitory effect of sulfide on propionate degrading bacteria during the simulation (Figure 3.2C). Additionally, the over prediction of S_{h2s} during days 21 to 27 (Figure 3.2B) can be attributed to hydrogen sulfide loss during the experiments used for calibration as the sulfur recovery in the reactor outlet streams decreases from 100% to 90% (see Chapter 2, Figure 2.5) (Barrera et al., 2014).

3.3.5 Cross validation

A cross validation study was performed to assess the quality and applicability of the calibrated model. The model outputs were compared with data set D2 (days 37-75) under the operating conditions E-5, E-6, E-7, E-8 and E-9 (see Chapter 2) without changing the previously optimized parameter set. During these periods, the OLR and SLR of the UASB reactor were in the range of 7.72 to 10.69 kg COD m^{-3} d^{-1} and 0.76 to 1.57 kg SO_4^{2-} m^{-3} d^{-1}, respectively (see Chapter 2) (Barrera et al., 2014). SO_4^{2-}/COD ratios of 0.10, 0.15 and 0.20 were applied in the periods covering the validation study unlike the periods used for the calibration study.

Figure 3.3 (B, C, F, G & H) presents the comparison of model predictions and experimental values for the process variables during the validation study. As it can be seen, S_{h2s}, $S_{h2s,free}$, $S_{gas,ch4}$, $S_{gas,co2}$, S_{ac}, and pH were well predicted by the model showing a mean absolute relative error below 10% (1% to 10%), which is considered as a highly accurate quantitative prediction (±10%) (Batstone and Keller, 2003). A medium accurate quantitative prediction (10% - 30%) was achieved for S_{pro}, S_{so4}, $S_{gas,h2s}$, Q_{gas}, and eff_COD (Figure 3.3A, E, G & H), as the mean absolute relative error ranged from 12% to 26% (Batstone and Keller, 2003).

The underestimation observed for S_{so4} during the days 51 to 62 and 73 to 75 (Figure 3.3A), was in agreement with the lower $S_{h2s,free}$ predicted during these days (Figure 3.3C), which reduced the inhibitory effect of $S_{h2s,free}$ on SRB during the simulation. The excess consumption of sulfate was

accumulated in the gas phase since higher $S_{gas,h2s}$ and Q_{gas} were predicted during these periods (Figure 3.3D & E). This was likely due to the assumption of a constant gas-liquid transfer coefficient (200 d^{-1}) for H_2S even when the biogas production rate, and consequently its stripping effect, decreased after day 60 in the model predictions (Figure 3.3E). The over and under predictions of $S_{h2s,free}$ from days 40 to 45 and 48 to 55, respectively (Figure 3.3C), were attributed to slight deviations (±3.1%) in the pH prediction (Figure 3.3H).

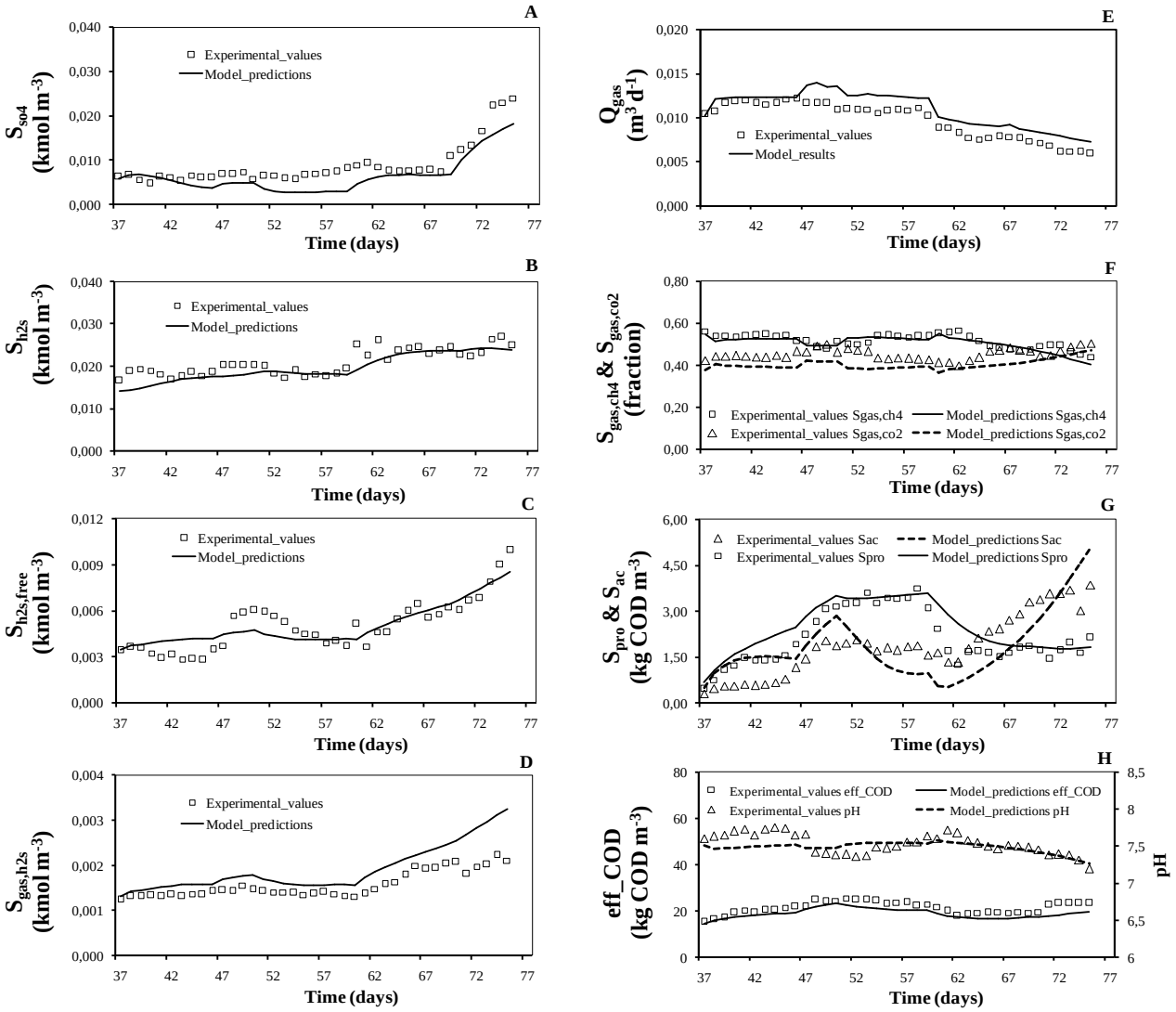

Figure 3.3. Validation of model predictions with experimental values: (A) S_{so4}, (B) S_{h2s}, (C) $S_{h2s,free}$, (D) $S_{gas,h2s}$, (E) Q_{gas}, (F) $S_{gas,ch4}$ & $S_{gas,co2}$, (G) S_{pro} & S_{ac}, and (H) eff_COD & pH

During the validation period the model was also able to predict the reactor failure (for methanogenesis and sulfidogenesis) from days 70 to 75. Methanogenesis failure in the model predictions was evidenced by a pH decrease due to S_{ac} increase, which led to a decrease of Q_{gas} and $S_{gas,ch4}$ (Figure 3.3E, F, G & H). At the same time, sulfidogenesis failure in the model prediction was evidenced by the increase of S_{so4} while S_{h2s} remained constant, showing that the increase in the SLR resulted in accumulation of sulfates in the effluent rather than conversion to hydrogen sulfide (Figure 3.3A & B). In addition, the model predicted an $S_{h2s,free}$ increase as a result of a pH decrease showing a severe sulfide inhibition during these days (Figure 3.3C & H).

3.4 Conclusions

An extension of ADM1 with sulfate reduction was proposed, calibrated and validated for the description of anaerobic digestion of cane-molasses vinasse (very high strength and sulfate rich wastewater). Based on the results of a sensitivity analysis, only four parameters of the original ADM1 ($k_{m,pro}$, $k_{m,ac}$, $k_{m,h2}$ and Y_{h2}) and all the sulfate reduction parameters were fitted during calibration. Despite the fact that some deviations were observed between model predictions and experimental values, it was shown that the process variables S_{so4}, S_{h2s}, $S_{h2s,free}$, $S_{gas,h2s}$, Q_{gas}, $S_{gas,ch4}$, $S_{gas,co2}$, S_{pro}, S_{ac}, eff_COD, and pH were predicted reasonably well during model validation. The model showed high (±10%) to medium (10% - 30%) accurate quantitative predictions with a mean absolute relative error ranging from 1 - 26%. Moreover, the model was able to predict failure of methanogenesis and sulfidogenesis when the sulfate loading rate increased. Therefore, the kinetic parameters and the model structure proposed in this work can be considered as valuable to describe the sulfate reduction process in the anaerobic digestion of cane-molasses vinasse, by predicting the sulfur compounds in the gas and liquid phases, increasing the applicability of ADM1 to specific industrial wastewaters (vinasse).

CHAPTER 4

Impacts of anaerobic digestion power plants as alternative for lagooning Cuban vinasse: Life Cycle Assessment and exergy analysis

The treatment of vinasse in lagoons causes methane emissions during the anaerobic decomposition of the organic matter. The recovery of this methane to produce biogas, replacing fossil fuels and reducing greenhouse gas emission could bring environmental benefits. The aim of this Chapter was to evaluate the impacts of anaerobic digestion power plants as alternative for lagooning Cuban vinasse by means of Life Cycle Assessment (LCA) and exergy analysis (EA). The LCA showed that the anaerobic digestion power plants improve the environmental profile for the endpoint impact categories "ecosystem quality", "human health" and "natural resources". The highest environmental benefit (reducing 60% the total score) and exergy efficiency (43%) for the anaerobic digestion power plants were observed when the subprocesses biogas production from raw vinasse, sulfide removal by biooxidation with air oxygen addition and energy generation in spark ignition engines were used. The inclusion of boiler steam-turbines as energy generation subprocess instead of spark ignition engines showed the second relevant results in the LCA and EA. Since boiler steam-turbines are typically installed in the sugar factories, this alternative can be attractive for the Cuban context. In that case, the treatment of 1072 ton of vinasse (exergy content of 740.6 GJ_{ex}) can produce 143 GJ_{ex} as electricity and heat, 179 GJ_{ex} as sludge (65% dry matter, w/w), 22.4 GJ_{ex} as fertirrigation water and 0.38 GJ_{ex} as sulfur in the filter cake. This way, 44% of the exergy contained in vinasse is converted to electricity, heat and sludge, which makes Cuban vinasse a potential renewable resource. Therefore, the emission of 1.3 million cubic meters of vinasse ($1.34*10^6$ ton/year) reported by the Cuban Ministry of the Cane Sugar Industry can replace 402590 GJ_{ex} (electricity, heat and sludge) per year and reduce the negative environmental impacts for the studied categories.

Redrafted from: Ernesto L. Barrera, Elena Rosa, Henri Spanjers, Osvaldo Romero, Steven De Meester, Jo Dewulf. Impacts of anaerobic digestion power plants as alternative for lagooning Cuban vinasse: Life Cycle Assessment and exergy analysis. Manuscript submitted to Applied Energy.

4.1 Introduction

Vinasse is the liquid wastewater obtained after distillation of sugar-cane molasses in ethanol factories. Most distillery wastewaters are highly polluted and considered to be medium–high strength wastewaters (Ince et al., 2005). Vinasses are dark brown color liquids of acid nature that leave the ethanol distillation tower at high temperature (>50°C) and have a chemical oxygen demand (COD) typically above 60 kg m^{-3} (Barrera et al., 2013). The production of 1.3 million cubic meters of vinasse was reported by the Cuban Ministry of the Cane Sugar Industry in 2009 (Barrera et al., 2013). In Cuba, most of the cane-molasses vinasses (≈99%) are treated in lagoons where methane, carbon dioxide and hydrogen sulfide emissions have been reported as a result of uncontrolled anaerobic decomposition of the organic matter (Safley and Westerman, 1988; Toprak, 1995). As methane is an important greenhouse gas that has a global warming potential of 34 CO_2-equivalents over a 100 year time horizon (IPCC, 2013), the principal environmental damage reported for lagooning is the methane emission (Chen et al., 2013). Typically, the liquid effluent of the lagoons has been used for fertirrigation of the sugar cane plantations while the sludge recovery for fertilization has been less frequent due to the absence of a proper recovery system in the lagoons.

However, vinasse is very suitable for anaerobic digestion, producing biogas (≈60% methane) being a versatile gas fuel that can replace fossil fuels in power and heat generation plants. The energetic value of biogas and its potential to save fossil carbon emissions (Budzianowski, 2011) together with the additional digestate production and COD removal are the principal benefits of anaerobic digestion (Contreras et al., 2009; Nandy et al., 2002). The only biogas production process in Cuba treating vinasse (800 m^3 of vinasse per day) has been designed to treat diluted vinasse (20 kg COD m^{-3}). As sugar and ethanol factories are integrated in Cuba (Figure 1.1, Chapter 1), vinasse is diluted by using sugar wastewater (SWW) during the sugar factory working days (100 days). Typically distilleries operated 300 days, thus vinasse is diluted by using tap water and effluent from the Upflow Anaerobic Sludge Bed reactor (UASB) the remaining 200 d (see section 1.2, Chapter 1). Moreover, this biogas production process in Cuba requires the addition of chemicals for neutralization, while the thermal energy contained in vinasse is released into the environment. In contrast, raw vinasse (COD ≥ 38 kg COD m^{-3}) can be neutralized and diluted with the liquid effluent of the biogas production process only (as in Chapter 2) (Barrera et al., 2014; Nandy et al., 2002), saving the use of chemicals for neutralization and tap water for dilution and

recovering the thermal energy contained in vinasse. This biogas production process requires more electricity for the recycling pump.

Because vinasse is a sulfate-rich substrate (Barrera et al., 2013), anaerobic digestion leads to high H_2S concentrations in biogas ranging from 14 000 to 55 000 ppm_v (Barrera et al., 2014). The removal of H_2S is a prerequisite for the utilization of biogas to avoid corrosion of the energy conversion systems. Elemental sulfur that can be used as fertilizer may be produced during the sulfide removal process and separated by means of filters in a filter cake. Absorption into ferric chelate solution, absorption into aqueous ferric sulfate solution and biooxidation with air oxygen addition have been suggested to remove H_2S from biogas obtained during the anaerobic digestion of vinasse (Barrera et al., 2013). These sulfide removal technologies differ from each other in the amount of chemicals and energy (electricity and heat) demanded for operation as well as in the amount of sulfur produced in the filter cake.

On the other hand, combined heat and power engines (CHP) are typically used to convert biogas into energy (electricity and heat). The H_2S limitations in the fueled biogas vary from one to another CHP application, i.e. spark ignition engines and gas turbines allow H_2S levels between 100-250 ppm_v, while boiler-steam turbines allow levels up to 1000 ppm_v (Weiland, 2010; Wellinger and Linberg, 2000). These differences cause variations in the energy required and the sulfur produced (in the filter cake) during the sulfide removal process as well as in the SO_x emissions during the combustion of hydrogen sulfide in the CHP engine. Therefore, variations in the mass and energy flows of biogas production, sulfide removal and energy generation subprocesses produce variations in the mass and energy flows of the whole anaerobic digestion power plant. The inclusion of anaerobic digestion power plant as a first treatment step creates a new scenario with respect to the lagooning of Cuban vinasse that should be evaluated from the sustainability point of view.

In order to quantify the environmental sustainability of alternative products, processes or services, the methodology of Life Cycle Assessment (LCA) is commonly used (Casas et al., 2011; Contreras et al., 2009; De Meester et al., 2012; Gil et al., 2013). LCA is a powerful tool to identify the different environmental aspects and the potential environmental impact of a product or service throughout its life cycle from raw materials to production, use, collection and end-of-life treatment including any recycling and disposal (European-Commission, 2010a).

The exergy concept can be also applied because exergy quantifies the ability to cause change and it is not fully conserved, in contrast to energy, which allows it to expose the inefficiency of processes (Dewulf et al., 2008). During the exergy analysis, exergy consumption as well as exergy efficiency of the different subprocesses (process level) and of the entire production system (gate-to-gate) can be determined.

Some works have been addressed to assess the environmental impacts of the biogas production in different scenarios (Afrane and Ntiamoah, 2011; Aye and Widjaya, 2006; Contreras et al., 2009; Rocha et al., 2010) in a life cycle perspective, considering the process as a whole (black box) and leaving out the study of the type of technology that can be used at each subprocess in the anaerobic digestion power plant (e.g. biogas production from diluted or from raw vinasse and energy generation in spark ignition engines or in boiler-steam turbines). Although the environmental sustainability of anaerobic digestion as a biomass valorization technology has been assessed based on exergy analysis as well (De Meester et al., 2012), little research has been done to assess the impacts of anaerobic digestion power plants as alternative for lagooning Cuban vinasse.

Therefore, the aim of this Chapter was to assess the impacts of anaerobic digestion power plants as alternative for lagooning Cuban vinasse, by making a comparative study from a life cycle perspective (LCA) and by determining the process inefficiencies by means of exergy analysis (EA).

4.2 Materials and methods

In this section the methods applied to assess the impacts of anaerobic digestion power plants as alternative for lagooning Cuban vinasse are explained. The LCA tool was used according to the ISO 14040/44 guidelines (ISO14040; ISO14044) and the ILCD handbook (European-Commission, 2010a).

4.2.1 Goal and scope definition

The goal and scope of this work is to assess the environmental impacts of anaerobic digestion power plants as alternative for lagooning Cuban vinasse by considering two main scenarios. The functional unit, system boundaries, scenarios description, allocations principles and main assumptions are described in detail below.

4.2.1.1 Functional unit and system boundaries

In Cuba sugar factories and distilleries are always integrated, so, the SWW are usually treated together with vinasse in lagoons or in the anaerobic digestion plant. For that reason, SWW were included in the functional unit of this study. Therefore, the treatment of 1072 ton of vinasse and 398 ton of SWW were considered as the functional unit in the present work, being produced 37 MWh of electricity, 83 MWh of heat, 2431 ton of ferti-irrigation water, 12.6 ton of organic carbon and 0.75 ton of sulfur in the filter cake in all the alternatives.

Two main scenarios were considered for the treatment of vinasse and SWW. The first (scenario 1) is composed of three subprocesses (Figure 4.1): lagooning for the treatment of vinasse and SWW, fertirrigation pumping of the liquid effluent of the lagoons and sludge drying of the sludge obtained from the lagoons. The second (scenario 2) is the treatment of vinasse and SWW in an anaerobic digestion power plant (including three subprocesses: biogas production, sulfide removal and energy generation), followed by the subprocesses considered for scenario 1 ("subprocesses of scenario 1") (Figure 4.1). Therefore, scenario 2 considered besides an anaerobic digestion power plant, the treatment of the liquid effluent of the biogas production in the lagoons (post-treatment lagoons), the fertirrigation pumping (of the liquid effluent of the lagoons) and the drying of the sludge (sludges from the biogas production and from the lagoons).

Figure 4.1 shows the gaseous emissions from the lagoons, the combustion gasses from the energy generation and the chemical wastes from sulfide removal emitted to the ecosphere. Oxygen in air and land used are the resources taken from the ecosphere while energy, vinasse, SWW, ferric compound, calcium oxide and tap water are the resources taken from the technosphere. The products of both scenarios are wastewater for fertirrigation, digestate, electricity, heat and sulfur. Traditional supply chain (TSC) are the common suppliers of products (e.g. electricity produced from fuel oil in centralized power plants or chemical fertilizer factories that supply sulfur as $(NH_4)_2SO_4$), they take resources from the technosphere to produce the required products for the market.

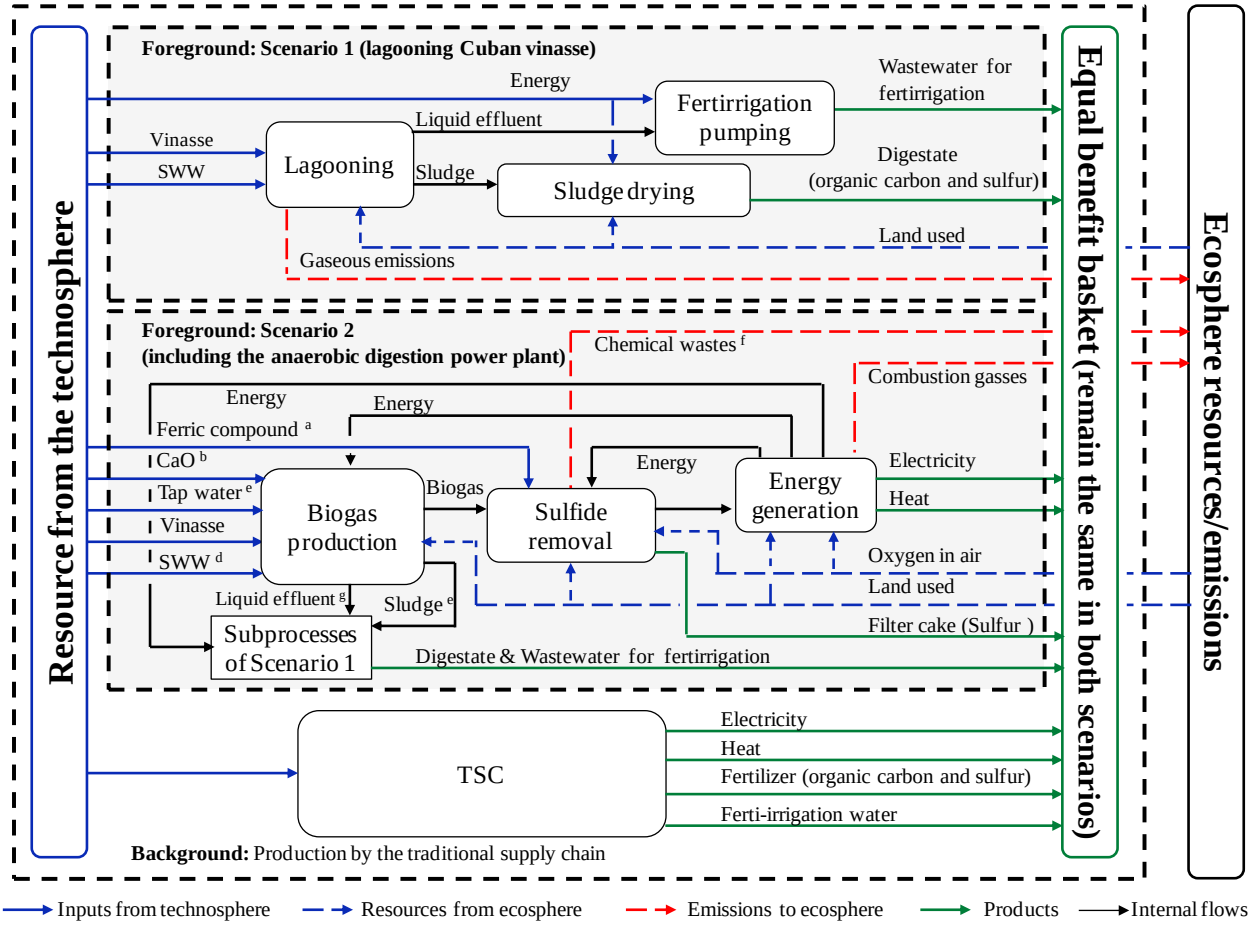

[a] Ferric compounds are consumed from the technosphere when absorption processes are used to remove sulfide. [b] CaO is consumed from the technosphere only when neutralization is required. [c] Tap water is consumed from the technosphere only when dilution of vinasse is required. [d] SWW is sent directly to the subprocesses of scenario 1 when vinasse is not diluted. [e] Sludge is sent to the subprocess of scenario 1 for drying only. [f] Chemical wastes (Fe III EDTA or $Fe_2(SO_4)_3$) are emitted to the ecosphere when absorption processes are used to remove sulfides. [g] Liquid effluent is sent to the subprocesses of scenario 1 for lagooning.

Figure 4.1. System boundaries and scenarios. Scenario 1: traditional treatment of vinasse and SWW in lagoons. Scenario 2: treatment of vinasse and SWW in the anaerobic digestion power plant, followed by the three subprocesses of scenario 1

To make a fair comparison between the two scenarios an equal basket of benefits is constructed, which implies that TSC always need to complete the market demand and fulfill an equal basket of benefits. For example, when vinasse is treated in scenario 1, the benefits are fertirrigation and digestate only, while scenario 2 produces energy (electricity and heat) additionally (Figure 4.1). Then, comparing an equal basket will imply that the TSC should produce electricity and heat in scenario 1 to achieve the equal basket of benefits as for scenario 2. The same was implicit for all the alternatives and products.

4.2.1.2 Scenarios description

Scenario 1: lagooning Cuban vinasse

The current treatment of Cuban vinasse was divided in three subprocesses: lagooning, sludge drying and fertirrigation pumping. Their characteristics are described below:

Lagooning: vinasse is sent to the lagoons at 80ºC and 48 kg COD m^{-3} together with the SWW (25ºC and 9 kg COD m^{-3}). In this subprocess several lagoons were considered. The COD removal efficiency of each lagoon was between 40 and 70% (Toprak, 1995), rendering a total COD removal of 90% for all the alternatives. As a result, methane, carbon dioxide and hydrogen sulfide are emitted to the ecosphere while the liquid effluent and sludge are sent to fertirrigation pumping and sludge drying subprocesses, respectively (Figure 4.1).

Sludge drying: Solar drying has been considered an environmentally friendly alternative to dry sludge (Rehl and Müller, 2011). As in Rehl and Muller (2011), an average evaporation rate of 2 ton water per m^2 drying area per year, as well as an electrical consumption of 200 kWh per ton of removed water to mix and aerate the digestate down to a water content of 35% were considered. The sulfur content of the lagoon sludge substitutes chemical fertilizers (avoided products), such as $(NH_4)_2SO_4$, while its organic carbon content is also applied to the soil for fertilization.

Fertirrigation pumping: The fertirrigation water is used to substitute river water (avoided product). Typically two pumps are installed close to the lagoons. Flow capacity and power consumption of the pumps were 107 m^3 and 152 kWh per hour respectively (data taken from Melanio Hernandez sugar factory in Sancti Spiritus, Cuba).

Scenario 2: including anaerobic digestion power plant

The anaerobic digestion power plant was divided in three subprocesses: biogas production (BP), sulfide removal (SR), and energy generation (EG). For these subprocesses respectively two, three and three different technologies can be used, obtaining a total amount of eighteen alternatives of anaerobic digestion power plants (See Table 4.1). The characteristics of each type of technology for each subprocess are described below:

Biogas production from diluted vinasse (BP-1): BP-1 reflects the unique Cuban experience in the biogas production from vinasse (Heriberto Duquesne biogas plant in Santa Clara, Cuba). In this biogas production, the anaerobic digestion of the liquid substrates occurs in an Upflow Anaerobic Sludge Bed (UASB) reactor after dilution and neutralization. That is:

vinasse is first diluted to 20 kg COD m^{-3} using SWW, effluent from the UASB reactor (maximum of 30% of the total effluent) or tap water. The liquid mixture is neutralized to a pH of 6.5 by adding 3.7 kg of calcium oxide (85%) per m^3 of vinasse before it is sent by centrifugal pumps to a pre-hydrolysis and settling tank.

After the pre-hydrolysis and settling tank, the liquid mixture is pumped into the UASB reactor where the anaerobic digestion occurs under mesophilic conditions (35 ± 1ºC). The liquid effluent of the UASB reactor is sent to the lagoons and the sludge is dried (both in the subprocesses of scenario 1) to produce digestate (65% dry matter, w/w), while the biogas is sent to the hydrogen sulfide removal unit. During this biogas production process the heat contained in vinasse (80ºC) is released into the environment.

Table 4.1. Description of the eighteen alternatives of anaerobic digestion power plants considered for scenario 2

Alternatives*	Biogas production	Sulfide removal	Energy generation
A-1	BP-1: *Diluted vinasse*	SR-1: *absorption into ferric chelates*	EG-1: *Spark-ignition engines*
A-2			EG-2: *Combustion gas turbines*
A-3			EG-3: *Boiler-Steam turbines*
A-4	BP-2: *Raw vinasse*	SR-1: *absorption into ferric chelates*	EG-1: *Spark-ignition engines*
A-5			EG-2: *Combustion gas turbines*
A-6			EG-3: *Boiler-Steam turbines*
A-7	BP-1: *Diluted vinasse*	SR-2: *absorption into ferric sulfates*	EG-1: *Spark-ignition engines*
A-8			EG-2: *Combustion gas turbines*
A-9			EG-3: *Boiler-Steam turbines*
A-10	BP-2: *Raw vinasse*	SR-2: *absorption into ferric sulfates*	EG-1: *Spark-ignition engines*
A-11			EG-2: *Combustion gas turbines*
A-12			EG-3: *Boiler-Steam turbines*
A-13	BP-1: *Diluted vinasse*	SR-3: *biooxidation with air oxygen*	EG-1: *Spark-ignition engines*
A-14			EG-2: *Combustion gas turbines*
A-15			EG-3: *Boiler-Steam turbines*
A-16	BP-2: *Raw vinasse*	SR-3: *biooxidation with air oxygen*	EG-1: *Spark-ignition engines*
A-17			EG-2: *Combustion gas turbines*
A-18			EG-3: *Boiler-Steam turbines*

* including the subprocesses of scenario 1 to treat the liquid effluent and the sludge obtained from the biogas production.

Biogas production from raw vinasse (BP-2): BP-2 has been used for the anaerobic digestion of very high strength and sulfate rich vinasses in full and lab scale studies (Barrera et al., 2014; Nandy et al., 2002). An appreciable amount of alkalinity is generated within the reactor and the utilization of this alkalinity (due to its buffering capacity for neutralization of

the influent) eliminates the necessity of neutralization and dilution of the raw vinasse using chemicals and tap water, respectively (Nandy et al., 2002). In addition, the energy content of vinasse can be used to reduce the heating demand of the reactor. Therefore, in this alternative raw vinasse is pumped to the UASB reactor and the reactor effluent is recycled (recirculation factor effluent/influent ≈ 15) while the SWW is sent straight to the lagoons. Additional energy is required for pumping of the recycled flow. As for BP-1, the liquid effluent of the UASB reactor is sent to the lagoons and the sludge is dried (both in the subprocesses of scenario 1) to produce digestate (65% dry matter, w/w), while the biogas is sent to the hydrogen sulfide removal process. Mesophilic conditions (35 ± 1ºC) were also considered for BP-2.

Sulfide removal by absorption into ferric chelates of EDTA (SR-1): In the sulfide removal by absorption into ferric chelates of EDTA (ethylenediaminetetraacetic acid), physical absorption with mass transfer and chemical reactions occur. The absorber solution contains the iron complex $Fe^{3+}L^{n-}$ (L is the organic ligand and n its charge, equal to 3 for EDTA), which oxidizes the hydrogen sulfide to elemental sulfur, reducing $Fe^{3+}L^{n-}$ to $Fe^{2+}L^{n-}$ in a first reactor, and later the iron complex ($Fe^{3+}L^{n-}$) is regenerated in a second reactor with the addition of air (Barrera et al., 2013). Degradation of $Fe^{2+}L^{n-}$ occurs in the second reactor producing mainly iminodiacetic acid (IDA) which is a chemical waste of this process (Chen et al., 1995). Then, electricity is required for pumping the ferric solutions and for blowing the air oxygen. The sulfur is usually separated by means of filters, obtaining a filter cake (65% dry matter, w/w) that can be used to substitute chemical fertilizers (avoided products), such as $(NH_4)_2SO_4$. The treated biogas is sent to the energy generation step.

Sulfide removal by absorption into ferric sulfate solutions (SR-2): This process includes the chemical absorption of hydrogen sulfide with aqueous ferric solutions ($Fe_2(SO_4)_3$) in a first reactor, followed by a biochemical oxidation of the formed iron ferrous compounds using *Thiobacillus ferrooxidans* under aerobic conditions in a second reactor (Barrera et al., 2013). Therefore, electricity is also required for pumping the ferric solutions and for blowing the air oxygen, while heat is needed to keep temperature at 45ºC in both reactors. Considerations for the filter cake and clean biogas were the same as for SR-1.

Biooxidation with air oxygen addition (SR-3): In this process, H_2S is first absorbed (physical absorption only) into a liquid stream (water or wastewater free of sulfides) and later biodegraded by Chemotrophic bacteria (*Thiobacillus sp.*) in an aerated reactor.

Considerations for the filter cake and clean biogas were the same as for SR-1 and SR-2. One pump and one blower are required for the operation.

Spark-ignition engines (EG-1): Spark-ignition engines are almost exclusively used for CHP applications fueled solely by biogas. For this type of technology, electrical and thermal efficiencies of 39 and 38% (based on the lower heating value (LHV)), respectively, can be achieved for a power capacity of 2.8 MW (Wiser et al., 2010). Biogas with 59 to 60% of methane is fed to EG-1 having a LHV of 19.38 MJ/m^3 (Wiser et al., 2010). The water jacket and the exhaust gases of the engine are used to produce hot water (100 °C) and the final temperature of the exhaust gases was assumed to be 150 °C to avoid corrosion of exhaust system components (Wiser et al., 2010). The level of H_2S required is 100 ppm_v, needing an efficient sulfide removal process. Stoichiometric amount of oxygen is added for the combustion of methane and hydrogen sulfide, resulting in the emission of mainly CO_2 and SO_2.

Combustion gas turbines (EG-2): This type of technology has successfully utilized biogas to simultaneously generate electric power and usable heat energy (Wiser et al., 2010). The electrical and thermal efficiencies are 29 and 44% (based on the LHV), respectively, for gas turbines of 5.6 MW (Wiser et al., 2010). Similar to EG-1, biogas with 59 to 60% of methane is fed to EG-2, having the same LHV (19.38 MJ/m^3) (Wiser et al., 2010). Exhaust gases (480 °C) are produced from the combustion chamber (U.S-EPA., 2008) and they can be used for heat recovery until 150 °C to avoid corrosion of the exhaust system components (U.S-EPA., 2008; Wiser et al., 2010). The level of H_2S required is also 100 ppm_v while stoichiometry oxygen is added for the combustion of methane and hydrogen sulfide, resulting in the emission of CO_2 and SO_2 as well.

Boiler-steam turbines (EG-3): Boiler-steam turbines offer a wide range of fuel flexibility using a variety of fuel sources in the associated boiler (U.S-EPA., 2008). The electrical and thermal efficiencies are 7.3 and 84.2% (based on the LHV), respectively, for steam turbines of 0.5 $MW_{electric}$ (U.S-EPA., 2008). Similar to EG-1 and EG-2, biogas with 59 to 60% of methane is fed to EG-3, having a LHV of 19.38 MJ/m^3 (Wiser et al., 2010). Saturated steam escapes from the steam turbine at the temperature of 150 ºC. Exhaust gases (480 °C) are also obtained from the boiler (U.S-EPA., 2008) and they can be used for heat recovery until 150 °C to avoid corrosion of the exhaust system components (U.S-EPA., 2008; Wiser et al., 2010). The level of H_2S required is 1000 ppm_v, therefore lower efficiencies in the sulfide

removal processes are needed. Stoichiometry oxygen is added for the combustion of methane and hydrogen sulfide, resulting in the emission of CO_2 and SO_2 as for EG-1 and EG-2.

4.2.1.3 Allocation principles and main assumptions

In scenario 2, the energy demand (electricity and heat) of the subprocesses is supplied from the anaerobic digestion power plant when this is sufficient; otherwise it is supplemented from the TSC.

In Cuba, sugar factories and distilleries operate during 100 and 300 days, respectively. It means that SWW can be used for dilution during one third of the distillery working days, whereas tap water must be used for dilution during the remaining two thirds of the distillery working days. This way, the water supplied to the UASB in BP-1 is assumed to be composed of 33.3% SWW and 66.6% tap water daily. Similarly, the steam consumed at the distillery is steam produced from the combustion of bagasse in the sugar factories during 100 days and steam produced from the combustion of fuel oil in the distillery during the remaining 200 days. Therefore, the steam produced in the anaerobic digestion power plant saves steam from bagasse (33.3%) and steam from fuel (66.6%) daily. It was assumed that saving steam from bagasse implies that more bagasse can be combusted in the sugar factory to produce electricity, saving electricity from the Cuban grid.

The Cuban electricity mix is obtained from fuel oil that is used in centralized and decentralized thermal power plants (81.66%), combined cycles with gas turbine using liquefied petroleum gas (13.04%), cogeneration systems using bagasse (4.63%), and renewable technologies (0.67%) (ONE, 2010).

The main assumptions for this study are as follows:

- All calculations are based on 1 day of operation to depict the everyday performance for the different alternatives.
- The effluent COD concentration (eff_COD, g COD m^{-3}) in the lagoons was calculated using Eqs. (4.1) and (4.2) (Toprak, 1995; Wu and Chen, 2011), where, inf_COD is the influent COD concentration (inf_COD, g COD m^{-3}), Θ_h is the mean hydraulic retention time (d) and k_T is the first-order COD removal rate coefficient (d^{-1}) at the lagoon liquid temperature T_{lag} (°C). The COD removal rate coefficient (k_{20}) at 20°C (d^{-1}) was corrected using the temperature correction factor (τ) and T_{lag}. Values of 0.221

d^{-1} and 1.117 (dimensionless) were used for k_{20} and τ respectively (Toprak, 1995; Wu and Chen, 2011).

$$eff\_COD = inf\_COD/(1 + k_T \cdot \Theta_h) \quad (4.1)$$

$$k_T = k_{20} \cdot \tau^{(T_{lag}-20)} \quad (4.2)$$

- The methane gaseous emissions were calculated from the multiplication of the methane production rate, R_{CH4} ($L \cdot m^{-2}\ d^{-1}$, see empirical Eq. (4.3)) (Toprak, 1995) and the occupied surface of the lagoons, where $COD_{removed}$ is the removed COD (kg COD d^{-1}) and T_{air} is the averaged ambient air temperature (°C).

$$R_{CH4} = 0.456 \cdot (COD_{removed})^{0.243} \cdot T_{air}^{\ 0.856} \quad (4.3)$$

- From the composition of the lagoon biogas reported in (Safley and Westerman, 1988), the methane and carbon dioxide contents were 70% and 20% for the gaseous emissions from the lagoons, respectively. The remaining 10% was assumed to be composed of water vapor mainly.
- The organic loading rate (OLR) of the lagoons was 0.25 kg COD $m^{-3}\ d^{-1}$ for all the alternatives (Toprak, 1995). In addition, the depth and the effluent COD concentration were fixed to calculate the land used.
- The sludge production in the lagoons was determined by mass balance calculations. The COD content of biomass was assumed to be 1.222 kg COD/kg biomass (Kalyuzhnyi and Fedorovich, 1998) and the water content of the sludge (before drying) 80% (w/w). The carbon content of the biomass was assumed to be 0.0313 kmol C kg COD biomass (Batstone et al., 2002).
- Organic carbon was taken from ecoinvent 2.2 as "Carbon, in organic matter, in soil" and it was assumed to be consumed in the alternatives. For example, the alternative with the highest organic carbon production does not consume/extract organic carbon from the soil.
- Potassium, phosphorous and nitrogen were not considered as chemical fertilizers (avoided products) because they were assumed to be constant between the alternatives.
- Sulfur content of the filter cake varied as a result of the H_2S level required for the energy generation technologies, whereas the organic carbon content varied in function of the biogas production rate and the methane emission in the lagoons.

- The production of electricity, heat, fertirrigation water, organic carbon (sludge) and sulfur was constant for both scenarios (equal basket of products). Therefore, TSC supplemented these productions when needed.
- In the biogas production technologies (BP-1 and BP-2), the COD and sulfate removal efficiencies (66.7% and 87%, respectively), the biogas composition (CH_4=58.5%, CO_2=40%, and H_2S=1.5%), the organic loading rate (9.83 kg COD m^{-3} d^{-1}), the sulfate loading rate (0.45 kg SO_4^{2-} m^{-3} d^{-1}), and the COD and sulfate concentrations of vinasse (48 kg COD m^{-3} and 2.2 kg SO_4^{2-} m^{-3}) were assumed as in Chapter 2 (Barrera et al., 2014) (experimental condition E-2).
- As the gaseous methane, carbon dioxide and hydrogen sulfide are mainly captured in the biogas during the anaerobic digestion process, the emissions to the air at the anaerobic digestion power plant were neglected.

4.2.2 Life cycle inventory (LCI)

Based on the allocations principles and main assumptions previously described in section 4.2.1.3 the LCI was collected. To ensure data reliability and validity, the inputs and outputs of the studied alternatives in the LCI were calculated by using material and energy balances. Mass consistency was checked by menas of total, COD, carbon, and sulfur mass balances whereas the first law of thermodynamics was used to calculate the energy requirements. Infrastructure was excluded from this study. The ecoinvent database 2.2 was used to model datasets in the background system.

4.2.3 Life cycle impact assessment (LCIA)

To account for emissions and resources the RECIPE methodology with endpoint indicators and the hierarchist perspective was used. Therefore, the endpoint impact categories "ecosystem quality", "human health" and "natural resources" were studied. The environmental impacts were quantified in "Points" for the endpoint impact categories and the total score (sum of the endpoint scores). As RECIPE allows for the linking of midpoint and endpoints categories, the contribution of the midpoint impact categories to each endpoint impact category was analyzed. The open source software for the sustainability assessment, OpenLCA version 1.3.1, was used to calculate the environmental impacts.

4.2.4 Exergy analysis (EA): subprocess level and gate-to-gate level

Exergy is the maximal work that a system can deliver in equilibrium with its environment through a reversible process. It gives an indication of the quality and quantity of material and energy flows.

The calculation of the total exergy of a product or process (Ex_{tot}) within this study was based on several components: physical exergy (Ex_{ph}), chemical exergy (Ex_{ch}), electrical and heat exergy (Ex_e) and solar exergy (Ex_S) (Eq. (4.4)). The reference environment applied for this study has been defined by Szargut et al. (1988) with a reference temperature of 298.15 K and a reference pressure of 1 atm.

$$Ex_{tot}=Ex_{ph}+Ex_{ch}+Ex_e+Ex_S \quad (kJ_{ex}) \quad (4.4)$$

4.2.4.1 Physical exergy

For the calculation of the physical exergy of the warm flows (liquids and gases), Eq. (4.5) was used (Szargut, 2005) at constant pressure. In this equation m is the mass (kg), cp the heat capacity (kJ kg^{-1} K^{-1}), T the temperature of the substance (K) and T_0 the reference temperature (K).

$$Ex_{ph}=m\cdot c_p\cdot[(T-T_0)-T_0\cdot \ln(T/T_0)] \quad (kJ_{ex}) \quad (4.5)$$

The physical exergy of the steam or the hot water produced at the energy generation subprocesses was calculated by using (Eq. (4.6)) (Szargut, 2005). In this equation H and S are the enthalpy (kJ) and entropy (kJ/K) of the substance, respectively, at a certain temperature and pressure, whereas H_0 and S_0 are the enthalpy (kJ) and entropy (kJ/K) of the substance, respectively, at the reference conditions (temperature of 298.15 K and pressure of 1 atm).

$$Ex_{ph}=(H-H_0)-T_0\cdot(S-S_0) \quad (kJ_{ex}) \quad (4.6)$$

4.2.4.2 Chemical exergy

To calculate the chemical exergy (kJ mol^{-1}) of components, Tables 1 and 2 of the appendix of Szargut et al. (1988) were available for retrieval of the standard chemical exergy of many organic and inorganic compounds.

The chemical exergy of EDTA was calculated on the basis of the group contribution, as proposed by Shieh and Fan (1982). Table 3 of the appendix of Szargut et al. (1988) listed the standard chemical exergy (kJ mol^{-1}) for most of the common chemical groups.

The chemical exergy of wastewaters, sludges and digestates was calculated based on the COD flow during 1 day (kg COD) for each stream (Eq. (4.7)) (Tai et al., 1986).

$$Ex_{ch} = 13\,600\ \frac{kJ_{ex}}{kg\ COD}\ COD \qquad (kJ_{ex}) \qquad (4.7)$$

4.2.4.3 Electrical exergy

Electricity produced or demanded is a high quality form of energy and therefore the exergy value was equated to its energy value (Wall, 1997).

4.2.4.4 Solar exergy

As land occupation means solar exergy use (Dewulf et al., 2007), the solar exergy was calculated based on the scenarios occupied surface. The average value of $23.2 \cdot 10^3$ kJ_{ex} m^{-2} $year^{-1}$ reported for Cuban conditions was used (Alvarenga et al., 2013).

4.2.4.5 Exergy efficiencies

A simple definition of exergy efficiency (η_{ex}) expresses all exergy input as used exergy, and all exergy output as utilized exergy. For each subprocess at each scenario, an exergy balance was prepared and used to assess the global exergy efficiency η_{ex} of each subprocess (Eq. (4.8)).

$$\eta_{ex} = \frac{\text{Exergy output}(kJ_{ex})}{\text{Exergy input}(kJ_{ex})} \cdot 100\% \qquad (4.8)$$

However, this efficiency does not always provide an adequate characterization of the thermodynamic efficiency of processes. Often, there exists a part of the output exergy that is unused, i.e. an exergy wasted to the environment (Wall, 2010). The difference between exergy output and exergy waste is called the exergy products (Wall, 2010). At the gate-to-gate level, three exergy efficiencies were calculated to account for the influence of the different products.

The exergy efficiency (η_{ex1}) was calculated with Eq. (4.9), considering electricity, heat, fertirrigation water and sludges as the products ("all products").

$$\eta_{ex1} = \frac{\text{Exergy of all products}(kJ_{ex})}{\text{Exergy input}(kJ_{ex})} \cdot 100\% \quad (4.9)$$

The exergy efficiency (η_{ex2}) was calculated with Eq. (4.10), considering the lagoon sludge and its exergy content as a waste. This way, the contribution of lagoon sludge to the exergy efficiency can be assessed by comparing η_{ex2} with η_{ex1}.

$$\eta_{ex2} = \frac{[\text{Exergy of all products} - \text{Exergy lagoon sludge}](kJ_{ex})}{\text{Exergy input}(kJ_{ex})} \cdot 100\% \quad (4.10)$$

Finally, the exergy efficiency (η_{ex3}) was calculated with (Eq. (4.11)) to show the efficiency of the anaerobic digestion power plants considering electricity and heat as the only products.

$$\eta_{ex3} = \frac{\text{Exergy (electricity \& heat)}(kJ_{ex})}{\text{Exergy input}(kJ_{ex})} \cdot 100\% \quad (4.11)$$

4.3 Results and discussion

4.3.1 Analysis of the LCI

The primary data inventory for scenario 2 [A-1 to A-18] and scenario 1 is depicted in Appendix G, showing the amount of the resources taken from the ecosphere and technosphere, the products and the emissions to air, water and soil. These data were used for the assessment of both scenarios.

4.3.2 Life cycle impact assessment (LCIA)

This section discusses the results of the life cycle impact assessment of eighteen alternatives of anaerobic digestion power plants for lagooning Cuban vinasse.

4.3.2.1 Environmental profiles

From a life cycle perspective, Figure 4.2 shows that the anaerobic digestion power plants improve (with respect to scenario 1) the environmental profiles by decreasing 35 to 60% the total score and 25 to 68% the endpoint impact categories "ecosystem quality", "human health" and "natural resources".

The endpoint impact category "ecosystem quality" contributed to more than 52% of the total score, where the midpoint impact category "agricultural land occupation" had the largest contribution (81%). This result was mainly attributed to differences in the required surface area for lagooning when ≈70% of the organic matter is removed at the biogas production subprocess. In addition, the midpoint impact categories "climate change" and "particulate

matter formation" caused 69 and 28%, respectively, of the score for the endpoint impact category "human health" which is mainly caused by the energy generation in the TSC to fulfill an equal basket of benefits. Furthermore, the endpoint impact category "natural resources" was 100% scored by the midpoint impact category "fossil depletion". Cuba indeed relies mainly on fossil fuels for its energy generation and a gain in renewable energy induces a gain in environmental impact. Since the contributions of the midpoint impact categories were discussed above their scores are not shown in Figure 4.2.

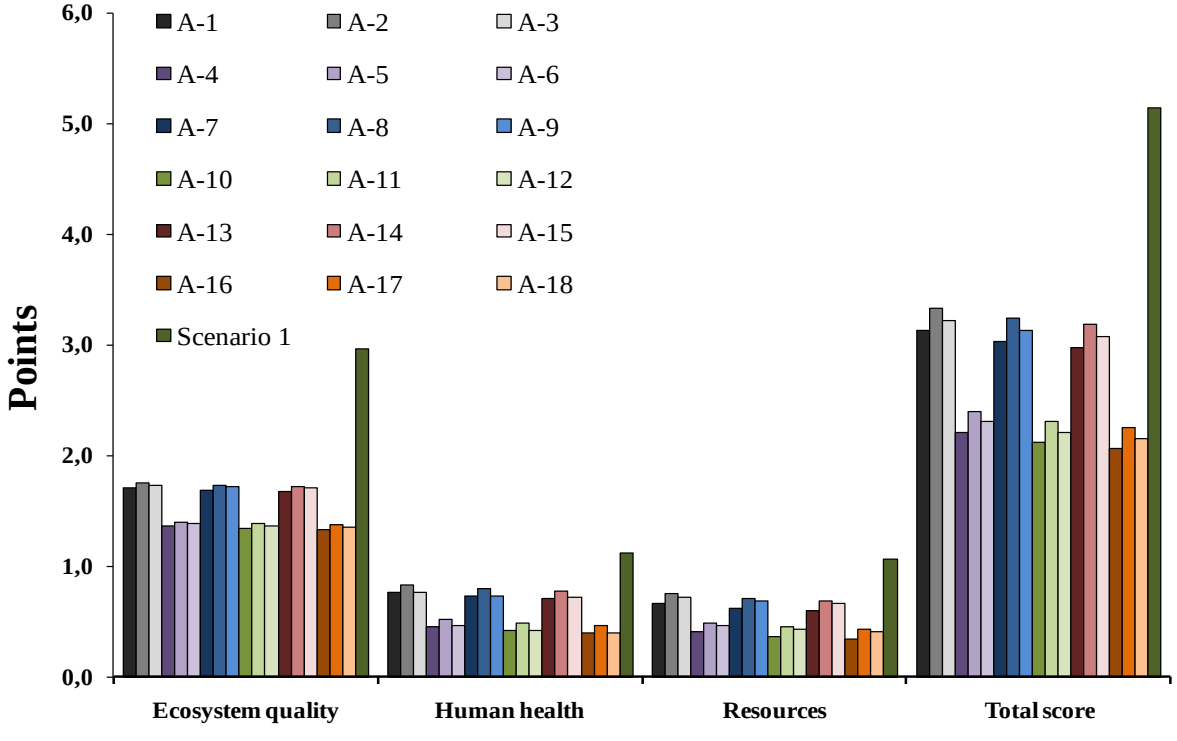

Figure 4.2. Environmental impacts of eighteen alternatives [A-1 to A-18] of anaerobic digestion power plants for lagooning Cuban vinasse (scenario 1) considering the treatment of 1072 ton of vinasse and 398 ton of SWW as the functional unit

The LCA results agree with environmental benefits reported for the anaerobic digestion in the Cuban sugar factories (Contreras et al., 2009). However, Contreras et al. (2009) did not considered the influence of different alternatives of anaerobic digestion power plants. Alternatives [A-1 to A-18] showed differences between their environmental profiles. A remarkable influence of BP-2 (biogas production from raw vinasse) was observed by

comparing [A-4, A-5 & A-6], [A-10, A-11 & A-12] and [A-16, A-17 & A-18] with [A-1, A-2 & A-3], [A-7, A-8 & A-9] and [A-13, A-14 & A-15] respectively, which shows a reduction of the score by 20 to 43% for the studied endpoint impact categories ("ecosystem quality", "human health" and "natural resources") (Figure 4.2). This observation was attributed to several aspects: (1) BP-2 does not need tap water for vinasse dilution, (2) BP-2 does not need chemical compounds (e.g. CaO) for neutralization, and (3) BP-2 saves thermal energy by using the energy content of vinasse (80°C) to keep the UASB reactor under mesophilic conditions (See the inventory in Appendix G). Although the benefits of BP-2 have been previously exposed (Nandy et al., 2002), no reports were found about its environmental impacts from a life cycle perspective.

Differences below 15% were observed among the alternatives using the same biogas production and energy generation subprocess (e.g. when comparing [A-1] with [A-7] and with [A-13], see alternatives description in Table 4.1) for the endpoint categories (Figure 4.2). It suggested that sulfide removal subprocesses influenced the environmental profiles less than biogas production.

Environmental benefits were also observed for the energy generation subprocess EG-1 (spark ignition engines). These differences can be seen by comparing alternatives with the same biogas production and sulfide removal subprocesses (e.g. comparing [A-1] with [A-2] and with [A-3], see alternatives description in Table 4.1) for the endpoint impact categories "ecosystem quality", "human health" and "natural resources". This finding was attributed to the highest electricity production of the spark ignition engines saving the highest amount of electricity from the TSC and contributing to the improvement of the endpoint impact categories "ecosystem quality" and "natural resources". In contrast, the lowest amount of heat is produced in the spark ignition engines, needing the production of more heat from the TSC and affecting the endpoint impact category "human health" due to particulate matter formation (Figure 4.2). For this impact category ("human health"), [A-18] showed the lowest score because of the highest thermal efficiency of the boiler-steam turbines, leading to the lowest heat production from the TSC.

Therefore, the environmental impact assessment from a LCA perspective showed that the anaerobic digestion power plants improve the environmental profile with respect to the lagooning of Cuban vinasse (scenario 1). Based on the single score (Figure 4.2), the highest benefits (reducing 60% the total score) were observed when biogas production from raw

vinasse (BP-2), sulfide removal by biooxidation with air oxygen addition (SR-3) and energy generation in spark ignition engines (EG-1) were used, which corresponds to alternative [A-16]. Although [A-18] showed the second lowest score (Figure 4.2), this alternative can be attractive for the Cuban context considering that boiler-steam turbines are typically installed in the sugar factories.

4.3.3 Exergy analysis (EA)

The exergy efficiencies for scenarios 1 and 2 are shown in Table 4.2, including the exergy efficiency of the process considering all the products (η_{ex1}), the exergy efficiency of the process when the lagoon sludge is considered as a waste (η_{ex2}) and the exergy efficiency of the process considering the electricity and heat as the only products (η_{ex3}).

4.3.3.1 Exergy efficiencies

Table 4.2 shows exergy efficiencies (η_{ex1}) between 30.3 and 43.4% when the exergetic value of all the products (electricity, heat, fertirrigation water, sludge from the UASB reactor, and sludge from the lagoons) was included for scenario 2 [A-1 to A-18]. Although scenario 1 (lagooning) showed the highest exergy efficiency (57.4%), negative environmental impacts for this scenario were already shown in the LCA (Figure 4.2). This result was attributed to under-prediction of methane emissions by the empirical model of Toprak (1995), which led to over-prediction of the COD used for biomass cell growing in the lagoons, being this a limitation of the present study. In addition, it should be remarked that the exergy content of sludge from the lagoons is currently lost in Cuba because lagoons are not provided with a proper sludge recovery system.

In scenario 2 [A-1 to A-18], a 32 to 49% reduction of the exergy efficiency (η_{ex2}) was observed when lagoon sludge was considered as a waste. The exergy efficiency (η_{ex2}) for scenario 1 was 97% lower than η_{ex1}, showing the necessity for a proper sludge recovery system in the current treatment of Cuban vinasse. η_{ex2} for scenario 1 represents the current exergy efficiency (1.5%) of the treatment of vinasse in Cuba.

Table 4.2. Exergy efficiencies of the process considering all the products (η_{ex1}), considering the sludge from the lagoons as a waste (η_{ex2}) and considering the electricity and heat as the only products (η_{ex3}) for scenario 2 [A-1 to A-18] and scenario 1 (lagooning of Cuban vinasse)

Scenarios	η_{ex1}(%) (**all products**)	η_{ex2}(%) (**lagoon sludge as waste**)	η_{ex3}(%) (**electricity & heat**)
A-1	33.8	22.9	18.0
A-2	30.3	19.6	14.6
A-3	31.4	20.6	15.6
A-4	42.7	23.7	19.5
A-5	39.3	20.2	16.0
A-6	41.0	21.9	17.7
A-7	34.0	23.1	18.1
A-8	30.8	19.9	14.9
A-9	31.6	20.7	15.7
A-10	43.0	23.8	19.6
A-11	39.5	20.4	16.1
A-12	41.3	22.1	17.9
A-13	34.2	23.2	18.2
A-14	31.0	20.0	15.0
A-15	31.8	20.8	15.8
A-16	43.4	24.0	19.8
A-17	39.8	20.5	16.3
A-18	41.6	22.2	18.0
Scenario 1	57.4	1.5	0.0

The exergy efficiency (η_{ex3}) represented around 47% with respect to η_{ex1}, showing values between 15 and 20% for scenario 2 [A-1 to A-18]. The highest exergy efficiencies (η_{ex3}) were achieved for alternatives [A-4], [A-10] and [A-16] (19.5, 19.6 and 19.8%, respectively). These alternatives were always based on the subprocesses biogas production from raw vinasses (BP-2) and spark ignition engines (EG-1) (see alternatives in Table 4.1). Therefore these high exergy efficiencies were obtained because of the reduction of exergy inputs and the increase of the exergy outputs in BP-2 and EG-1, respectively: (1) by saving thermal energy when the exergy content of vinasse (80°C) is used to keep the mesophilic conditions of the UASB reactor in BP-2, (2) by avoiding the use of tap water to dilute vinasse in BP-2, (3) by avoiding the use of chemical compounds (CaO) to neutralize vinasse in BP-2, and (4) because of the highest electric efficiency of the spark ignition engines (EG-1). The exergy efficiency η_{ex3} was zero for scenario 1 because there is no energy production in the

lagooning of Cuban vinasse (Table 4.2). A ranking of the alternatives [A-1 to A-18] is provided in the next section for a better understanding of the results.

4.3.4 Ranking of the alternatives [A-1 to A-18]: a comparison by subprocesses

A ranking of the alternatives to support the interpretation of the LCA and EA results is provided in Figure 4.3. The total scores of the LCA and the exergy efficiencies were used to rank the alternatives by subprocesses, expressing the values as: $[\text{points}] - [\eta_{ex1}] - [\eta_{ex2}] - [\eta_{ex3}]$. This way, the lower total score [points] and the higher exergy efficiencies $[\eta_{ex1}] - [\eta_{ex2}] - [\eta_{ex3}]$ indicated the best alternative. For example, by comparing alternatives that differ in the biogas production subprocess only (e.g. [A-1] with [A-4]; or [A-2] with [A-5]), the ones considering BP-2 ([A-4], [A-5], [A-6], [A-10], [A-11], [A-12], [A-16], [A-17] and [A-18]) showed always the best results (see also Table 4.1).

From the alternatives considering BP-2, a comparison was done between the ones differing in the sulfide removal subprocess (e.g. [A-4] with [A-10] and with [A-16]). Although the LCA and EA results of these alternatives were similar, a slight improvement was observed for the ones considering SR-3 (bioxidation with air oxygen addition) (Figure 4.3). Finally, the alternatives considering BP-2 and SR-3 and differing in the energy generation subprocess were compared. Alternatives including EG-1 (spark-ignition engines) rendered the best results (Figure 4.3). The use of boiler-steam turbines (EG-3) as the energy generation subprocess showed the second relevant results [A-18], being also attractive in the Cuban context.

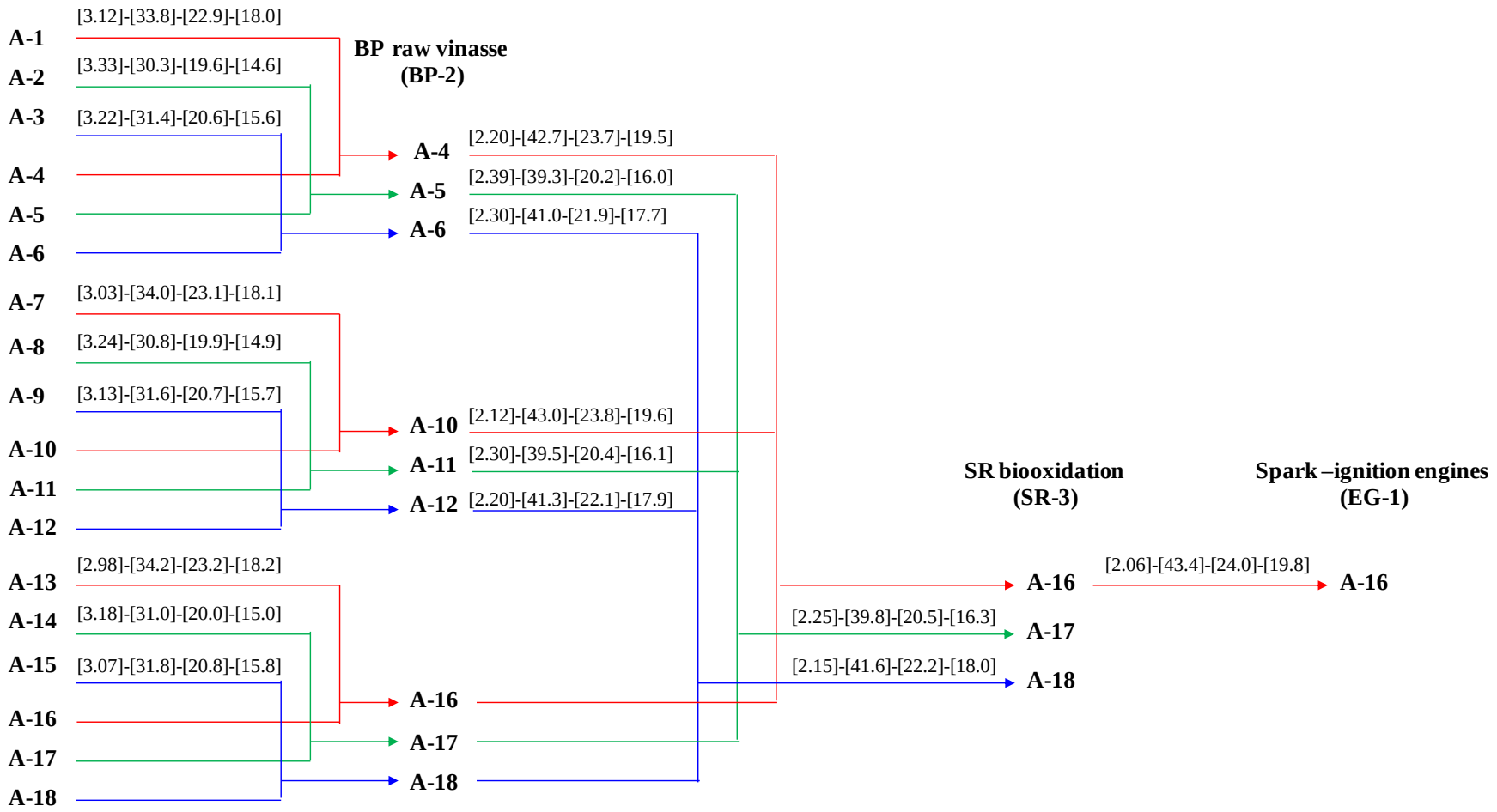

Figure 4.3. Ranking of the alternatives [A-1 to A-18]: a comparison by subprocesses based on LCA and EA results.

The values are expressed as: $[\text{points}] - [\eta_{ex1}] - [\eta_{ex2}] - [\eta_{ex3}]$.

Therefore, combining the effect of the LCA and EA, it can be concluded that the best alternatives include the biogas production from raw vinasse (BP-2), the biooxidation with air oxygen addition (SR-3) and the energy generation in spark ignition engines (EG-1) or boiler-steam turbines (EG-3). These combinations correspond to alternatives [A-16] and [A-18].

4.3.5 Grassmann diagram

Grassmann or exergetic Sankey diagrams are commonly used to depict the exergy analysis results. A Grassmann diagram (Figure 4.4) was constructed to show the exergy flows and irreversibilities of the subprocesses included in one of the best alternatives of scenario 2 [A-18].

The subprocesses sulfide removal, lagooning and sludge drying showed a global exergy efficiency (η_{ex}) above 97% whereas the exergy efficiency of the biogas production and the fertirrigation pumping subprocesses was 85% and 75%, respectively. The highest destruction of the fuel exergy occurred in the boiler-steam turbine system (231GJ_{ex}). This has been attributed to the heat transfer from very high temperature combustion products to the relatively low temperature boiling water and to the combustion process itself (Dewulf et al., 2008). The second highest irreversibility (123.6 GJ_{ex}) was associated with the biogas production subprocess. This result was attributed to the biochemical reactions involved in the anaerobic degradation of the organic matter and the requirements for pumping and heating. Although the irreversibilities in the lagoons (5.8 GJ_{ex}) were only 1.5% of the total irreversibilities (382 GJ_{ex}), more than 85 GJ_{ex} were wasted as methane emissions (non-valorized product), being a potential for process improvement (Figure 4.4).

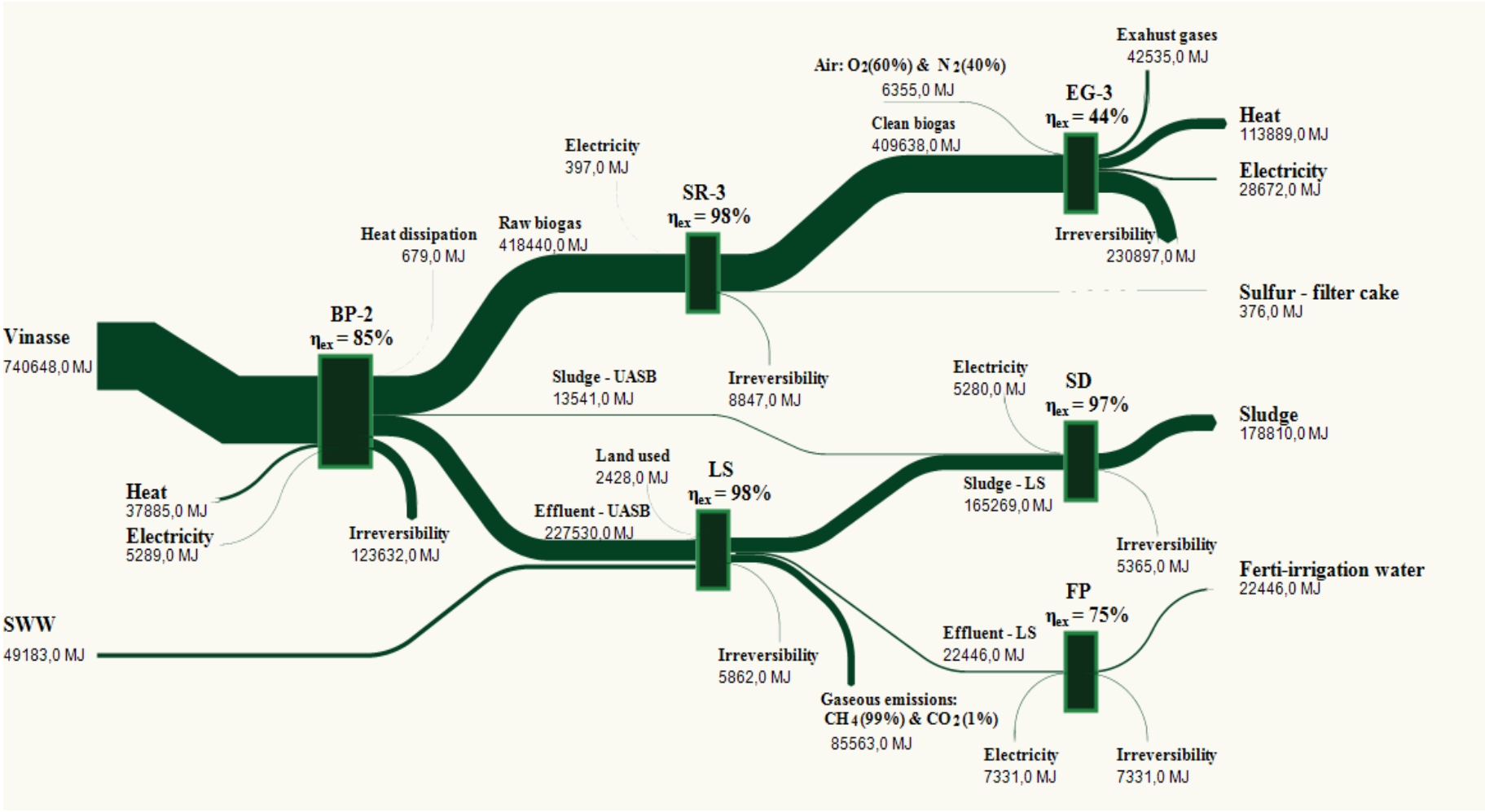

Figure 4.4. Grassmann diagram for alternative [A-18]. BP-2: biogas production from raw vinasse, SR-3: sulfide removal by biooxidation with air oxygen addition, EG-3: energy generation in boiler-steam turbine, LS: lagooning, FP: fertirrigation pumping, SD: sludge drying

Therefore, the treatment of 1072 ton of vinasse (exergy content of 740.6 GJ_{ex}) in alternative [A-18] could produce 143 GJ_{ex} as electricity and heat, 179 GJ_{ex} as sludge (65% dry matter, w/w), 22.4 GJ_{ex} as fertirrigation water and 0.38 GJ_{ex} as sulfur in the filter cake. This way, the exergy contained in vinasse is mainly converted to energy (≈20%) and sludge (24%), making Cuban vinasse a potential renewable resource that can replace 402590 GJ_{ex} (electricity, heat and sludge) per year starting from the 1.3 million cubic meters of vinasse reported by the Cuban Ministry of the Cane Sugar Industry.

4.4 Conclusions

The LCA showed that the anaerobic digestion power plants can improve the environmental profile for the endpoint impact categories "ecosystem quality", "human health" and "natural resources". The highest environmental benefit (reducing 60% the total score) and exergy efficiency (43%) for the anaerobic digestion power plants were observed when the subprocesses biogas production from raw vinasse, sulfide removal by biooxidation with air oxygen addition and energy generation in spark ignition engines were used. The inclusion of boiler steam-turbines as energy generation subprocess instead of spark ignition engines showed the second relevant results in the LCA and EA. Since boiler steam-turbines are typically installed in the sugar factories, this alternative can be attractive for the Cuban context. In that case, the treatment of 1072 ton of vinasse (exergy content of 740.6 GJ_{ex}) in anaerobic digestion power plants could produce 143 GJ_{ex} as electricity and heat, 179 GJ_{ex} as sludge (65% dry matter, w/w), 22.4 GJ_{ex} as fertirrigation water and 0.38 GJ_{ex} as sulfur in the filter cake. This way, 44% of the exergy contained in vinasse is converted to electricity, heat and sludge, which makes Cuban vinasse a potential renewable resource. Therefore, the emission of 1.3 million cubic meters of vinasse ($1.34*10^6$ ton/year) reported by the Cuban Ministry of the Cane Sugar Industry can replace 402590 GJ_{ex} (electricity, heat and sludge) per year and reduce the negative environmental impacts for the studied categories.

CHAPTER 5

General discussion and perspectives

5.1. General discussion

An overview covering the current situation in Cuba, the topics investigated in this research and the further research areas is given in Figure 5.1. Energy is mainly produced from fossil fuels (94.7%) in Cuba, only 5.3% comes from renewable energy sources (ONE, 2010). Recently, the Cuban government announced a strategy for the development and implementation of renewable energy projects, mentioning biogas production from biodegradable wastes as one of the potential technologies to reduce fossil fuels consumption and mitigate environmental pollution (Trade and Investment, 2014).

Vinasse is regarded as a biodegradable waste suitable for anaerobic digestion. The emissions of more than 1.3 million cubic meters of vinasses per year (Cuban Ministry of the Cane Sugar Industry in 2009) as well as their treatment in lagoons, where methane emissions occur as a result of uncontrolled decomposition of organic matter, demonstrate the availability of vinasse to produce biogas in Cuba. However, high levels and variations of the COD and SO_4^{2-} concentrations in vinasse may cause dynamical changes in the sulfate reduction process during its anaerobic treatment, producing sulfur compounds in the gas and liquid phases. These compounds should be predicted to assist the energetic use of the biogas and the process performance. In addition, the sustainability assessment of anaerobic digestion power plants as alternative to lagooning can support decision-makers for the future implementation of this technology in Cuba.

The topics investigated in this research deal with the current situation in Cuba, creating areas for further research (Figure 5.1). Firstly, this research characterizes the sulfate reduction process in the anaerobic digestion of a very high strength and sulfate rich vinasse (Chapter 2). Relevant aspects are discussed below:

Stripping effect of the biogas flow on H_2S_{gas} and inhibition by sulfides: As discussed in Chapter 2, the results show that the increase of inf_COD and inf_SO_4^{2-} at a SO_4^{2-}/COD ratio of 0.05 (< 0.10) do not cause severe inhibition because of the existence of high COD values, which lead to higher biogas production rates and a rapid removal of sulfide as it is formed (H_2S_{gas} increase up to 33%), as stated by Wilkie et al. (2000). These results agree with literature and, therefore, at a SO_4^{2-}/COD ratio of 0.05 sulfide inhibition does not affect the reactor performance whereas the biogas quality is strongly influenced by H_2S_{gas} variations. In contrast, but also in agreement with literature (Wilkie et al., 2000), fluctuations of inf_COD and inf_SO_4^{2-} at SO_4^{2-}/COD ratios ≥ 0.10, cause inhibition by $H_2S_{aq,}$ $[H_2S]_{free}$ and propionic

acid to SRB, methanogens or both, affecting the reactor performance whereas the biogas quality is influenced to a lesser degree by H_2S_{gas} variations.

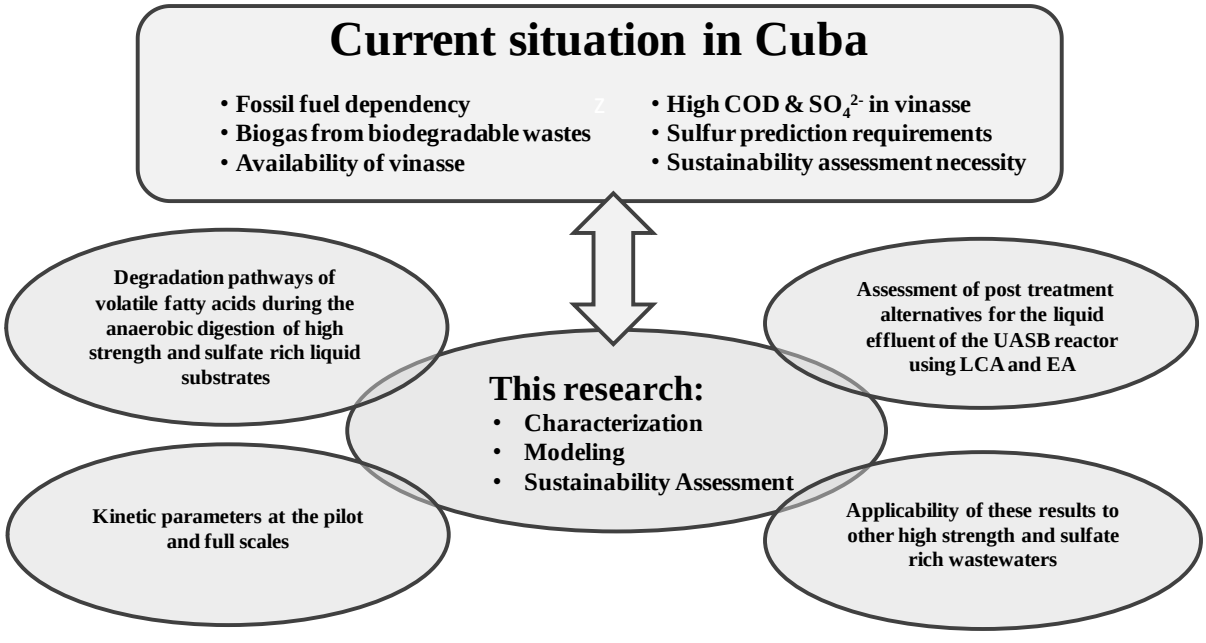

Figure 5.1. Overview of the current situation in Cuba, the topics investigated in this research and the further research areas

Degradation of organic matter by SRB: From the SO_4^{2-}/COD ratio of 0.05 to 0.10, a decrease of inf_COD together with an increase of inf_SO_4^{2-} caused propionic acid degradation (up to 90%), suggesting a strong contribution of pSRB at SO_4^{2-}/COD ratios ≤ 0.10 (see Chapter 2). At a SO_4^{2-}/COD ratio of 0.10, it has been reported that pSRB are poor competitors for hSRB for the available sulfate (Visser, 1995), which means that sulfate is consumed by hSRB rather than by pSRB. Therefore, the results obtained in this research are in contrast to literature. To support the previous observation some differences between sulfate reduction experiments in Visser (1995) and sulfate reduction experiments in this research were grouped in Table 5.1 (see also the aspects discussed in Chapter 2). They are discussed below:

1. The use of synthetic wastewater (S_{bu}, S_{bu}, S_{pro} & S_{ac}) in Visser (1995) makes the whole inf_COD as readily biodegradable COD whereas the use of a real wastewater (vinasse) implies that total COD is divided into (Pasztor et al., 2009):

- Readily biodegradable COD (S_{su}, S_{aa}, S_{fa}, S_{bu}, S_{bu}, S_{pro} & S_{ac})
- Slowly biodegradable COD (X_c, X_{ch}, X_{pr}, X_{li})

- Unbiodegradable COD (S_I & X_I)
- Biomass COD (X_{su}, X_{aa}, $X_{li,}$ X_{c4}, X_{pro}, X_{ac} X_{h2}, X_{pSRB}, $X_{aSRB,}$ & X_{hSRB})

Soluble inert fractions in vinasse represent 26% of the total COD content (See Table 3.4, Chapter 3), which indicates that the SO_4^{2-}/COD ratio of 0.10 (based on the total COD) is equivalent to 0.14 (based on the biodegradable COD only). Therefore, the SO_4^{2-}/COD ratio reported in Visser (1995) is not a fair indicator for complex wastewaters like the very high strength and sulfate rich vinasse used in this research.

Table 5.1. Differences between sulfate reduction experiments in Visser (1995) and in this research

Sulfate reduction in (Visser, 1995)	**Sulfate reduction in this research**
1. Synthetic wastewater used as a substrate to feed the reactor	1. Real and complex wastewater (vinasse)
2. Low strength substrate (5 g COD L^{-1} & 0.5 g SO_4^{2-} L^{-1}) • Low sulfate concentration in the influent and effluent • Low H_2S_{free} concentration in the reactor ($\leq$ 30 mg L^{-1}) • No inhibition of methanogens	2. Very high strength substrate (38-58 g COD L^{-1} & 3.65-5.50 g SO_4^{2-} L^{-1}) • High sulfate concentration in the influent and effluent • High H_2S_{free} concentration in the reactor ($\geq$ 100 mg S L^{-1}) • Inhibition of methanogens
3. Steady state conditions	3. Dynamic conditions

1. Use of a low strength substrate by Visser (1995) leads to low influent and effluent sulfate concentrations (0.5 and 0.1 g SO_4^{2-} L^{-1}, respectively) and low H_2S_{free} concentrations in the reactor bulk ($\leq$ 30 mg S L^{-1}), reducing the inhibitory effect of H_2S_{free} on pDB. Therefore, this allows propionate degradation by pDB in Visser (1995), considering that pDB are inhibited at H_2S_{free} concentrations exceeding 70 mg S L^{-1} (Rinzema and Lettinga, 1988). In contrast, H_2S_{free} concentrations above 100 mg S L^{-1} were observed in this research at a SO_4^{2-}/COD ratio of 0.10 (see Chapter 2), leading to pDB inhibition and propionate degradation by pSRB when sulfate was available. High sulfate concentration of the influent vinasse (3.65-5.50 g SO_4^{2-} L^{-1}) leads to high sulfate concentration in the reactor effluent (0.44 - 0.77 g SO_4^{2-} L^{-1}) and this way sulfate concentrations in the liquid bulk became higher during the anaerobic

digestion of a very high strength and sulfate rich vinasse, increasing the mass transfer of sulfates from the liquid bulk to the granules. Both the availability of sulfates and the inhibition of pDB favored the degradation of propionate by pSRB in this research.

3. In addition, steady state conditions during the experiments of Visser (1995) make differences with the experiments of this research. Fluctuations of inf_SO_4^{2-} and inf_COD in vinasse cause variation in the availability of substrates, leading to variation of the microorganism growth rates and the substrate uptake rates (see Eqs. (5.1) and (5.2) for methanogens and SRB respectively). Based on this Monod type kinetic, a decrease of inf_COD together with an increase of inf_SO_4^{2-} from the SO_4^{2-}/COD ratio of 0.05 to 0.10 (See Chapter 2), decreases the growth rate of methanogens while it increases the growth rate of SRB. This fluctuation is an additional aspect justifying degradation of the available organic acids by SRB at SO_4^{2-}/COD ratios ≥ 0.10.

For methanogens:

$$\rho_{growth,j} = \mu_{max,j} \frac{S_i}{(K_{S,j}+S_i)} \cdot X_i \quad \& \quad \rho_{uptake,j} = k_{m,j} \frac{S_i}{(K_{S,j}+S_i)} \cdot X_i \qquad (5.1)$$

For SRB:

$$\rho_{growth,j} = \mu_{max,j} \frac{S_i}{(K_{S,j}+S_i)} \cdot \frac{S_{SO4}}{(K_{S,SO4j}+S_{SO4})} \cdot X_i \;\&\; \rho_{uptake,j} = k_{m,j} \frac{S_i}{(K_{S,j}+S_i)} \cdot \frac{S_{SO4}}{(K_{S,SO4j}+S_{SO4})} \cdot X_i \qquad (5.2)$$

The latter differences support that organic acid degradation is found during the anaerobic digestion of a very high strength and sulfate rich vinasse at SO_4^{2-}/COD ratios ≤ 0.10, in contrast with literature reports. These aspects offer a further research area to establish degradation pathways of volatile fatty acids during the anaerobic digestion of such vinasses when fluctuations of inf_SO_4^{2-} and inf_COD occur.

This research also models the sulfate reduction process in the anaerobic digestion of a very high strength and sulfate rich vinasse (Chapter 3), dealing with the necessity for the prediction of the sulfur compounds in the gas and liquid phases to assist the energetic use of the biogas and the process performance. Considering the experimental observations, an ADM1 extension was proposed in this research. This included propionate, acetate and hydrogen as a substrate for SRB, in deviation from the extension of Fedorovich et al. (2003) in which valerate and butyrate were also considered (see Chapter 1). Although the inclusion of organic acids in the sulfate degradation pathways for modeling purposes has been considered as complex and useful only for wastewaters with SO_4^{2-}/COD ratios ≥ 0.30

(Batstone, 2006), the experimental observations made in this study lead to a different approach. The model proposed allows for the prediction of the process variables S_{so4}, S_{h2s}, $S_{h2s,free}$, $S_{gas,h2s}$, Q_{gas}, $S_{gas,ch4}$, $S_{gas,co2}$, S_{pro}, S_{ac}, eff_COD, and pH, showing high (±10%) to medium (10% - 30%) accuracy quantitative predictions with a mean absolute relative error between 1% and 26%.

In addition, the parameters "50% inhibitory concentrations of free H_2S" (Appendix F) obtained during the model calibration (Chapter 3) were in agreement with experimental observations available in literature and in this research (Chapter 2), and therefore they can be considered a better approximation to the real phenomena. The values reported for this coefficient can be seen in Table 1.3 (Chapter 1). These values range from 185 to 576 mg S L^{-1} (0.0058 to 0.018 kmol m^{-3}) which are rather far from the 150 mg S L^{-1} (0.0047 kmol m^{-3}) reported as inhibitory for methanogens and SRB (except for propionate degraders, which is 70 mg S L^{-1} (0.0022 kmol m^{-3})) (Rinzema and Lettinga, 1988). This fact can be attributed to the limitation of models for the prediction of total aqueous sulfide (S_{h2s}), free sulfides ($S_{h2s,free}$) and gas phase sulfides ($S_{gas,h2s}$) (Fedorovich et al., 2003; Kalyuzhnyi et al., 1998; Kalyuzhnyi and Fedorovich, 1998; Ristow et al., 2002), leading to overestimation of sulfides and requiring higher parameter values for the "50% inhibitory concentrations of free H_2S". For that reason models including sulfate reduction should be able to predict sulfur compounds in the gas and liquid phases.

Despite of this, some limitations should be considered for the further implementation of the modeling results. A first approach was proposed by Batstone et al. (2005). They found plug flow and completely mixing behaviors for lab and full scale UASB reactors respectively, concluding that the kinetic parameters obtained in the lab scale may require modification in the further implementation at pilot and full scales because of the likely difference in the hydrodynamic conditions (Batstone et al., 2005). Therefore, they exposed that it is perilous to make any performance-based projections from laboratory systems to full scale UASB reactors.

A different approach was proposed by Van Hulle et al. (2014). They demonstrated that using a correct description of the mixing behavior of anaerobic digesters the system performance at a larger scale is better predicted. This way, the kinetic parameters obtained at a lab scale can be used at the full scale without modification. Since the kinetic parameters are properties of the microbial species and they should remain approximately constant while the mixing

conditions from lab to full scale may change, the second approach better describes the real phenomena. Therefore, the mixing conditions in full scale reactors should be properly described when the model approach and the kinetic parameters obtained in this research are to be used.

Finally, this research assesses the sustainability of anaerobic digestion power plants as alternative for lagooning Cuban vinasse by means of LCA and EA to provide knowledge for decision-makers about the potential of vinasse to mitigate the environmental pollution and to produce renewable energy. In addition to anaerobic digestion power plants, other alternatives for vinasse disposal have been assessed in a life cycle perspective, such as: "direct application of vinasse to the soil", "concentration of vinasse and application to the soil", and "concentration of vinasse and combustion" (Rocha et al., 2010). Although these results showed the highest environmental benefits for "concentration of vinasse and application to the soil", benefits for land use and greenhouse gas emissions were obtained for the alternative "anaerobic digestion power plants" (Rocha et al., 2010). Therefore, concentration of the liquid effluent of the UASB reactor to reduce the volume of fertirrigation water is an alternative scenario that can increase the environmental benefits for the treatment of vinasse in the Cuban context. A similar approach was reported in Nandy et al. (2002), using the concentrated effluent for compost production (together with the filter cake obtained from the sugar cane industry) and in this way, a "zero emission scenario" was formed for vinasse treatment. The use of these alternatives in Cuba can result in environmental and technical benefits that can be assessed by using LCA and EA in further researches. Despite of this, there is an agreement in literature that anaerobic digestion power plants are widely accepted as a first treatment step for cane molasses vinasse and they offer benefits for the Cuban context already discussed in Chapter 4.

5.2 Perspectives

In this research, novel and important information is given on the sulfate reduction process in the anaerobic digestion of a very high strength and sulfate rich vinasse, as well as on the sustainability of anaerobic digestion power plants and their impacts on the traditional treatment of Cuban vinasse (lagooning). Starting from these results, new research topics arise for further research; first (already discussed in section 5.1), the applicability of the experimental observations, the modeling and the sustainability assessment results, and

second (discussed in the next section); the potential of anaerobic digestion power plants to be implemented in Cuba for the production of energy and bio-fertilizers. Some suggestions to be discussed in further research are exposed below.

5.2.1 Potential of anaerobic digestion power plants to be implemented in Cuba

Strengths Weaknesses Opportunities Threats (SWOT) profile of anaerobic digestion power plants can provide information about the key internal and external factors to achieve the implementation of this technology in the Cuban context (Table 5.2). The profile helps to formulate strategies that employ the existing strengths, re-address the existing weaknesses, exploit the opportunities and protect against the threats.

Table 5.2. Strengths Weaknesses Opportunities Threats (SWOT) profile for anaerobic digestion power plants

Strength	**Weakness**
Technology design: • Environmental benefits • High exergy efficiency • Fuel flexibility of energy generation systems **Integration with sugar industry** • Facilities for use in-situ of the end products (energy and bio-fertilizers)	**Technology design:** • Control requirements for the biological process • High sulfur content in biogas • High investment cost **Cuban energy market:** • No legislation for the price of renewable energy
Opportunities	**Threats**
• Availability of vinasse • Business expansion • Increasing renewable energy technology • Replacing the fossil fuel power source • Diversification of sugar industry	**Competitive market** • Technologies to produce energy from vinasse (concentration and combustion) • Technologies for sulfur recovery from vinasse • Technological changes to reduce sulfate concentration in vinasse

Strengths: The environmental benefits, the high exergy efficiency, the fuel flexibility of energy generation systems and the facilities for use in-situ of the end products (energy and bio-fertilizers) are the most relevant *strengths* of anaerobic digestion power plants. The environmental benefits and the high exergy efficiency were already exposed in Chapter 4. The fuel flexibility of energy generation systems allows for the use of biogas in spark-ignition engines, combustion gas turbines, and boiler-steam turbines (U.S-EPA., 2008; Wiser et al., 2010). At the same time, these energy generation systems allow for the adaptation of anaerobic digestion power plants to different scenarios, as different electrical and thermal efficiencies can be achieved (U.S-EPA., 2008; Wiser et al., 2010). For example, boiler-steam turbines can be used for scenarios demanding larger amounts of heat (thermal and electrical efficiencies up to 84% and 7%, respectively) whereas spark ignition engines can be used for scenarios demanding more electricity (thermal and electrical efficiencies up to 42% and 49%, respectively).

The facilities for in-situ use of the end products (energy and bio-fertilizers) can reduce losses during the electricity power transmission and distribution, ensuring the heat consumption and attenuating the requirements for bio-fertilizer transportation. Typically, a distillery plant producing 800 hl of alcohol demands 22 ton of saturated steam (P_{abs} = 10 atm) and 500 kWh of electricity (data taken from Melanio Hernandez sugar factory in Sancti Spiritus, Cuba), being a potential consumer for the energy produced at the anaerobic digestion power plant. The bio-fertilizer production, specially the elemental sulfur (750 kg S d^{-1}) in the filter cake (bio-sulfur), is obtained from the biooxidation with air oxygen addition (see Chapter 4). Bio-sulfur has been reported as a growth stimulator increasing up to 50% the yield of plantation in dosages of 15 kg per hectare (Cline et al., 2003). These results place bio-sulfur as an attractive sulfur fertilizer that can be produced in anaerobic digestion power plants treating vinasse and can be used to increase the yield of the sugar cane plantations. Considering a yield of 48 ton per hectare (Contreras et al., 2009), the production of 2300 ton of sugar cane per day could demand 720 kg S per day, which means that most (96%) of the bio-sulfur produced will be consumed during the agricultural activities of this sugar factory.

Opportunities: The Cuban National Program for Renewable Energy Development towards 2030 calls for the increase of up to 24% in the use of renewable resources to produce energy. In this context the sugar energy sector is expected to contribute to 14% of the energy generation. Therefore, considering the availability of vinasse in the Cuban sugar industry, the

anaerobic digestion power plants turns into *opportunities* for business expansion, increasing renewable energy technology, replacing the fossil fuel power source and diversifying the sugar industry.

Weakness: Despite these strengths and opportunities, the control requirements for the biological process to avoid inhibition and reactor failure, the high sulfur content in biogas that requires additional cost for investment and operation to clean biogas as well as the absence of legislation for the price of the renewable energy, should be considered as the main *weakness* of anaerobic digestion power plants.

The experimental results obtained here agree with literature with respect to the inhibition encountered at SO_4^{2-}/COD ratios $\geq$ 0.10 (Rinzema and Lettinga, 1988; Wilkie et al., 2000). Some strategies can be used to overcome this limitation, such as dilution of the wastewater, increase of pH, precipitation of sulfides with iron and stripping of sulfides (Lens et al., 1998). Advantages and disadvantages of these alternatives were detailed in Lens et al. (1998) and could be applied depending on the case studies. In addition, the model proposed predicts the reactor behavior starting from the characteristics of vinasse. Thus, control strategies based on the characteristics of vinasse associated with modeling tools can be used to predict sulfur compounds and to avoid sulfide inhibition problems.

The high sulfur content in biogas requires additional investment and operational costs to clean the biogas compared with the digestion of substrates of low/non sulfate content. However, this *weakness* can be addressed by exploiting the bio-sulfur production (*strength*) during the sulfide removal process. Although sulfide removal alternatives show similar environmental impacts and exergy efficiencies, economic indicators can be useful in the final decision. The investment costs for the sulfide removal process in anaerobic digestion power plants treating vinasse (5000 m^3) have been reported around 4528 $USD/year (Salomon et al., 2011).

Investment and operational costs below 15 $USD per m^3 of biogas and year have been reported for anaerobic digestion power plants treating vinasse, showing payback periods between 1.4 and 3.6 years (Salomon et al., 2011), being an attractive alternative from the economical point of view as well. The existence of boiler-steam turbine units already placed in the sugar and distilleries factories may make the payback period of the investment cost negligible as the energy generation systems represent more than 85% of the investment cost (Salomon et al., 2011).

Since the Cuban funding is not enough for investment in renewable energy projects, foreign capital will be needed and thus, the price of the energy produced will play a key role on the payback periods. Legislation for the renewable energy price is not available in Cuba, but recent declarations (Ministry of the Electric Company) pointed that it will be based on the fossil fuel substitution. Thus, considering the actual price of fuel (93.58 $/barrel, http://www.preciopetroleo.net/) and the specific fuel consumption of Cuban power plants (220 g/kWh, Ministry of the Electric Company), an estimation of around 160 $USD/MWh can be made. In Brazil, a price of 79 $USD/MWh ensured a payback period below 3.6 years for anaerobic digestion power plants treating vinasse (Salomon et al., 2011). Although energy prices versus investment cost should be evaluated to fairly motivate the development of all renewable technologies, the price of 160 $USD/MWh could accelerate the availability of foreign capital for investing in anaerobic digestion power plants treating vinasse in Cuba. Therefore, depending on new legislation the lack of legislation onto renewable energy prices in Cuba should be addressed to provide the foreign capital.

Threats: They are associated to the competitive market to produce energy from vinasse (concentration and combustion), to recover sulfur from vinasse and to reduce sulfate concentration in vinasse. An alternative to produce energy from vinasse is the concentration in evaporators up to 65% (w/w) and the direct combustion in boilers (no other alternatives were found in literature) (Rocha et al., 2010). Since 7 kg of concentrated vinasse requires 1 kg of fuel oil for combustion, this alternative has been reported as unfavorable with respect to anaerobic digestion from the environmental point of view (Rocha et al., 2010). In addition, this alternative has not been widely adopted because of being highly energy intensive (Nandy et al., 2002). An increase of the operation cost is also expected because of the use of fossil fuel in this alternative but no studies onto this issue were found.

Most of the literature reports about sulfur recovery from vinasse are based on anaerobic digestion technologies. An alternative discussed in literature is the internal micro-oxygenation inside anaerobic digesters (van der Zee et al., 2007; Weiland, 2010). This alternative has been widely applied over the world and it allows for the removal of sulfides from the biogas and the recovering of bio-sulfur from the reactor's top. However, reformation of S^0 into H_2S inside the reactor is one of the crucial drawbacks of this method and for that reason external sulfide removal process are recommended (Naegele et al., 2013).

Simultaneous removal of sulfur and nitrogen in anaerobic digesters (Fdz-Polanco et al., 2001) could be considered as an attractive alternative in the near future, although the reaction mechanism is still under research and it has been applied to the lab scale only (Fdz-Polanco et al., 2001). This process allows for the recovery of sulfur in the reactor sludge (S^0) as well as for the production of nitrogen (N_2) in biogas. As nitrogen in the substrate is also required (in addition to sulfur), its applicability depends on the characteristics of vinasse. Nitrogen in most of cane molasses vinasse is considered to be used for microorganism growth cell only during anaerobic digestion (see Chapter 2), which may limit the applicability of this process.

To reduce the high sulfate concentration in vinasse, alternatives at the ethanol factories can be used. Sulfates in vinasse come mainly from the use of sulfuric acid to adjust pH during the fermentation of cane molasses vinasse (see Chapter 1). Nitric and phosphoric acids have been considered as alternatives to reduce/eliminate sulfuric acid additions in distilleries (Rojas-Sariol et al., 2011). The fact that five times larger volumes for nitric and phosphoric acids are needed (to adjust pH to 4.5) together with their higher prices in the market (more than double) leads to consider sulfuric acid as the more attractive alternative (Rojas-Sariol et al., 2011). The high sulfate content in vinasse from different countries (e.g. India, Brazil and Cuba, Table 1.1, Chapter 1) suggests that sulfuric acid is widely used nowadays at ethanol factories, which ensures the applicability of this research.

5.2.2 Further research areas

In short, the further research areas arising from the present research can be summarized into the following aspects:

- *Degradation pathways of volatile fatty acids during the anaerobic digestion of very high strength and sulfate rich liquid substrates*: As the composition of real wastewater is complex this further research area becomes also complex. That is why most of sulfate reduction studies are based on the use of synthetic wastewaters. Specific techniques to monitor online volatile fatty acid and sulfate concentrations inside the reactors could be helpful in the elucidation of these degradation pathways.
- *Mixing conditions at the pilot and full scales*: Since the mixing conditions from lab to full scale may change affecting the predictive capacity of the model, they must be determine for the proper implementation of these results. This way, the model and

kinetic parameters proposed in this research could be used for projection and implementation at the full scale.

- *Assessment of post treatment alternatives for the liquid effluent of the UASB reactor using LCA and EA:* Evaporation and concentration of the liquid effluent of the UASB reactor could be an attractive alternative to reduce the volume of fertirrigation water, reducing transport distance and land used for lagooning. However, additional energy supply and investment cost will be required, and LCA and EA will be useful to support decision makers.
- *Applicability of these results to other very high strength and sulfate rich wastewaters*: although it was not discussed in this Chapter 5, the results obtained for vinasse could be useful to study other very high strength and sulfate rich wastewater. For example, the wastewater from industrial processes such as the production of citric acid, molasses edible oils, paper and chemicals (Erdirencelebi et al., 2007). In these cases, new interaction can arise concerning degradation pathways, microorganism involved and inhibitory compounds.

Overall, it can be concluded that many research fields are still to be discovered and explored. Research in these fields can be helpful in process operation and decision making concerning for the current and future implementation of anaerobic digestion power plants.

SUMMARY

In the present research the sulfate reduction process in the anaerobic digestion of a very high strength and sulfate rich vinasse (characterization and modeling) and the impacts of anaerobic digestion power plants as alterative for lagooning Cuban vinasse have been studied. Firstly, **Chapter 1** reviews the state-of-the-art of the sulfate reduction process in the anaerobic digestion of vinasse, with emphasis on the modeling of sulfate reduction including the process and reaction involved, the kinetics (growth, inhibition and endogenous processes), the acid–base equilibrium and the gas–liquid transfer equations. In addition, the principal approaches to model sulfate reduction were discussed. It is concluded that vinasse is a typical sulfate-rich liquid substrate for anaerobic digestion but the sulfate reduction processes in the anaerobic digestion of vinasses with similar simultaneous high levels of COD and SO_4^{2-} should be studied. In addition, it is shown that the model equations are available in literature but no results have been shown (as an extension of ADM1) to predict the concentrations of total aqueous sulfide (S_{h2s}), free sulfides ($S_{h2s,free}$) and gas phase sulfides ($S_{gas,h2s}$). Therefore, kinetic coefficients to model sulfate reduction in the anaerobic digestion of vinasse have not been reported in literature and this fact is limiting the prediction of the sulfur compound in the gas and liquid phases to assist the energetic use of the biogas and the process performance. Finally, this chapter shows an overview of the currently available environmental sustainability concepts of life cycle assessment and exergy analysis. In **Chapter 2**, the sulfate reduction process in the anaerobic digestion of a very high strength and sulfate rich vinasse is characterized, by giving COD and SO_4^{2-} pulses at different SO_4^{2-}/COD ratios to obtain dynamical responses. A set of dynamic data reliable for calibrating mathematical models, when sulfate reduction in the anaerobic digestion of a very high strength and sulfate rich vinasse is of primary interest, is given in this Chapter 2. The results shows deterioration of the biogas quality at a SO_4^{2-}/COD ratio of 0.05 (when inf_COD and inf_SO_4^{2-} increased), strong contribution of pSRB to the degradation of propionate at SO_4^{2-}/COD ratios $\leq$ 0.10 (in contrast to literature results), inhibition by $H_2S_{aq,}$ $[H_2S]_{free}$ and propionic acid to SRB, methanogens or both at a SO_4^{2-}/COD ratio of 0.10 (deterioration of the anaerobic digestion process) and severe inhibition for methanogens and SRB at a SO_4^{2-}/COD ratio of 0.15 and 0.20 (leading to reactor failure). The results of the mass balance calculations (COD and sulfur) are also shown in this chapter.

In **Chapter 3**, the modeling of the anaerobic digestion of cane-molasses vinasse, extending the Anaerobic Digestion Model No. 1 with sulfate reduction for very high strength and

sulfate rich wastewaters is presented. Results of the sensitivity analysis based on the local relative sensitivity methods are shown. The model predictions were mostly classified as high (±10%) or medium (10% - 30%) accuracy quantitative predictions during model calibration and validation, based on a mean absolute relative error for the process variables: sulfates, total aqueous sulfide, free sulfides, methane, carbon dioxide and sulfide in the gas phase, gas flow, propionic and acetic acids, chemical oxygen demand (COD), and pH. As a result, the model is considered as valid to assist the sulfate reduction process in the anaerobic digestion of cane-molasses vinasse when sulfate and organic loading rates range from 0.36 to 1.57 kg SO_4^{2-} m^{-3} d^{-1} and from 7.66 to 12 kg COD m^{-3} d^{-1}, respectively.

In **Chapter 4**, the impacts of eighteen alternatives of anaerobic digestion power plants for lagooning Cuban vinasse was assessed by using Life Cycle Assessment and exergy analysis. The environmental profiles of anaerobic digestion power plants with respect to the lagooning of Cuban vinasse for the endpoint impact categories "ecosystem quality", "human health" and "natural resources" are shown. The exergy efficiency was used to assess potential process improvement and irreversibilities in the subprocesses that form the anaerobic digestion power plants. The alternatives with the highest benefits for the Life Cycle Assessment and the exergy analysis are discussed. In general, the treatment of 1072 ton of vinasse (exergy content of 740.6 GJ_{ex}) in anaerobic digestion power plants can produce 143 GJ_{ex} as electricity and heat, 179 GJ_{ex} as sludge (65% dry matter, w/w), 22.4 GJ_{ex} as ferti-irrigation water and 0.38 GJ_{ex} as sulfur in the filter cake. This way, 44% of the exergy contained in vinasse is converted to electricity, heat and sludge, becoming vinasse a potential renewable resource that can replace 402590 GJ_{ex} (electricity, heat and sludge) per year in Cuba and reduce the negative environmental impacts for the studied categories. **Chapter** 5 includes the general conclusions and perspectives of this research to support decision-makers in the further implementation of anaerobic digestion power plants for the treatment of vinasses in Cuba.

SAMENVATTING

Deze studie onderzoekt het sulfaatreductieproces bij anaerobe vergisting van een sulfaatrijke vinasse met zeer hoge COD inhoud (karakterisatie en modellering), en de impact van energiecentrales op basis van anaerobe vergisting als een alternatief voor de lagunering van Cubaanse vinasse. **Hoofdstuk 1**, ten eerste, geeft een overzicht van de state-of-the-art van het sulfaatreductieproces bij anaerobe vergisting van vinasse, met nadruk op het modelleren van de sulfaatreductie, inclusief het betrokken proces en reactie, de kinetiek (groei, inhibitie en endogene processen), het zuur-base evenwicht en de gas-vloeistof transfer vergelijkingen. Daarnaast worden de belangrijkste werkwijzen bij het modelleren van sulfaatreductie behandeld. Er wordt besloten dat vinasse een typisch sulfaatrijk en vloeibaar substraat is voor anaerobe vergisting. Het sulfaatreductieproces bij anaerobe vergisting van vinasse, tegelijk met vergelijkbaar hoge gehaltes aan COD en SO_4^{2-}, moet echter verder onderzocht worden. Bovendien wordt aangetoond dat de modelvergelijkingen in de literatuur beschikbaar zijn, maar dat geen resultaten worden weergegeven (als een uitbreiding op ADM1) voor het voorspellen van de concentraties van de totale hoeveelheid sulfide in wateroplossing (S_{h2s}), vrije sulfiden ($S_{h2s,free}$), en sulfiden in de gasfase ($S_{gas,h2s}$). Vandaar worden de kinetische coëfficiënten voor de modellering van sulfaatreductie bij anaerobe vergisting van vinasse niet gerapporteerd in de literatuur. Dit is limiterend bij het voorspellen van het sulfaatgehalte in de gas- en vloeistoffases om de energetische valorisatie van biogas en de procesprestaties te verbeteren. Tenslotte geeft dit hoofdstuk een overzicht weer van de op dit moment beschikbare concepten op vlak van milieu-georiënteerde duurzaamheid, namelijk levenscyclusanalyse en exergieanalyse.

In **Hoofdstuk 2** wordt het sulfaatreductieproces bij anaerobe vergisting van een sulfaatrijke vinasse met zeer hoge COD inhoud gekarakteriseerd. Dit wordt uitgevoerd door het geven van COD en SO_4^{2-} pulsen bij verschillende SO_4^{2-}/COD verhoudingen, zodat een dynamische respons verkregen wordt. In dit hoofdstuk wordt ook een set van dynamische data gegeven, voor het kalibreren van mathematische modellen met als primaire functie de sulfaatreductie bij anaerobe vergisting van een sulfaatrijke vinasse met zeer hoge COD inhoud. De resultaten tonen een verminderde kwaliteit van het biogas bij een SO_4^{2-}/COD verhouding van 0,05 (met een verhoging van inf_COD en inf_ SO_4^{2-}), een hoge bijdrage van pSRB bij de degradatie van propionaat bij SO_4^{2-}/COD verhoudingen $\leq$ 0,10 (in tegenstelling tot de resultaten in de literatuur), inhibitie door H_2S_{aq}, $[H_2S]_{free}$ en propionzuur van SRB, methanogenen of beide, bij een SO_4^{2-}/COD verhouding van 0,10 (achteruitgang van het anaerobe vergistingsproces)

en sterke inhibitie van methanogenen en SRB bij een SO_4^{2-}/COD verhouding van 0,15 en 0,20 (wat leidt tot het falen van de reactor). Ook de resultaten van de massabalansberekeningen (COD en zwavel) worden in dit hoofdstuk weergegeven.

In **Hoofdstuk 3** wordt de modellering van de anaerobe vergisting van vinasse uit rietmolasse weergegeven, waardoor het Anaerobe Vergistingsmodel No. 1 wordt uitgebreid met sulfaatreductie bij sulfaatrijke afvalwaters met een zeer hoge COD inhoud. Ook de resultaten van de sensitiviteitsanalyse, gebaseerd op de lokale relatieve sensitiviteitsmethodes, worden weergegeven. De voorspellingen van het model werden vooral ingedeeld als van hoge (±10%) of gemiddelde (10% - 30%) nauwkeurigheid met betrekking tot kwantitatieve voorspellingen tijdens de kalibratie en validatie van het model. Dit is gebaseerd op een gemiddelde absolute relatieve fout voor de verschillende procesvariabelen: sulfaten, totaal sulfide in wateroplossing, vrije sulfiden, methaan, kooldioxide en sulfiden in de gas fase, gasstroom, propionzuur en azijnzuur, chemische zuurstofvraag (COD), en pH. Het model wordt in staat geacht te helpen bij het beschrijven van het sulfaatreductieproces bij de anaerobe vergisting van vinasse uit rietmolasse, bij een bereik van sulfaat en organische belasting van respectievelijk 0,36 tot 1,57 kg SO_4^{2-} m^{-3} d^{-1} en 7.66 tot 12 kg COD m^{-3} d^{-1},.

In **Hoofdstuk 4** worden achttien alternatieven voor energiecentrales met anaerobe vergisting voor de lagunering van Cubaanse vinasse vergeleken door middel van levenscyclusanalyse en exergieanalyse. De milieuprofielen van energiecentrales met anaerobe vergisting voor de lagunering van Cubaanse vinasse voor de endpoint-categorieën "ecosysteemkwaliteit", "menselijke gezondheid" en "natuurlijke hulpbronnen" worden weergegeven. Exergie-efficiëntie werd gebruikt voor het evalueren van mogelijke procesverbeteringen en irreversibiliteiten in de sub-processen waaruit de energiecentrales met anaerobe vergisting bestaan. De interessantste alternatieven op het vlak van efficiëntie in levenscyclusanalyse en exergieanalyse worden besproken. Over het algemeen kan de behandeling van 1072 ton vinasse (met een exergie inhoud van 740,6 GJ_{ex}) in een energiecentrale met anaerobe vergisting 143 GJ_{ex} als elektriciteit en warmte produceren, 179 GJ_{ex} als slib (met een massafractie aan droge stof van 65%), 22,4 GJ_{ex} als fertigatiewater, en 0,38 GJ_{ex} als zwavel in de filterkoek. Zo wordt 44% van de exergie inhoud van de vinasse omgezet tot elektriciteit, water en slib. Dit toont aan dat vinasse een mogelijke hernieuwbare grondstof is die in Cuba 402590 GJ_{ex} (elektriciteit, warmte en slib) per jaar kan vervangen, en de negatieve milieu-impact voor de bestudeerde impactcategorieën kan verminderen.

Hoofdstuk 5 bevat de algemene conclusies en vooruitzichten van dit onderzoek, met als doel het ondersteunen van beleidsmakers bij de verdere implementatie van energiecentrales met anaerobe vergisting voor het behandelen van vinasse in Cuba.

CURRICULUM VITAE

Personal data

Name: Ernesto Luis Barrera Cardoso

Address: Ranfla No 62, e/ Línea y Céspedes, kilo 12, 60100 Sancti Spiritus, Cuba

Date and place of brith: 20/07/1977, Sancti Spiritus, Cuba

Nationality: Cuban

Phone: +53 54154248

e-mail: ernestol@uniss.edu.cu

Occupation: Chemical Engineering, professor at the university

Department: Study Center of Energy and Industrial Processes. Sancti Spíritus University

Work address: Avenida de los Mártires #360, 60100 Sancti Spíritus, Cuba

Education

- 2006-2007: Master in Energy Efficiency: Cienfuegos University "Carlos Rafael Rodríguez", Cuba.

  Thesis title: Technological alternatives to produce biogas with energetic aims starting from the available wastes in Sancti Spiritus, Cuba
- 1996-2001**:** Chemical Engineering. Central University of Las Villas. Faculty of Chemistry and Pharmacy. Cuba.

  Thesis title: Cogeneration. Alternatives for thermal schemes and the associated emissions

Professional activities

- 2010 - … Doctoral Research in Applied Biological Sciences. Environmental Organic Chemistry and Technology Research Group (EnVOC), Faculty of Bioscience Engineering, Ghent University

  Title: The anaerobic digestion of a very high strength and sulfate-rich vinasse: from experiments to modeling and sustainability assessment

  - Project ZEIN2009PR362: Biogas production from waste from local food, wood and sugar cane industries for increasing self−sufficiency of energy in Sancti Spiritus, Cuba.
- 2007 - … Researcher and professor at the Study Center of Energy and Industrial Processes. Sancti Spíritus University, Cuba.
- 2003-2007: Professor at the Industrial Engineering Department. Sancti Spíritus University.
- 2002-2003: Specialist in quality control. Dairy industry, Sancti Spiritus, Cuba.

- 2001-2002: Engineering in training. Dairy industry, Sancti Spiritus, Cuba.

Teaching and tutoring experience

- 2005 -... Tutor of 8 thesis students
    - 2011-2012: Action planning for the efficient consumption of energy carriers in the Agrarian Enterprise of Sancti Spiritus, Cuba.
    - 2010-2011: Weighting of sustainability indicators to support decision makers in the selection of biogas production alternatives.
    - 2009-2010: Assessment of renewable energy alternatives in the agrarian enterprise "Ramón Ponciano, Sancti Spiritus, Cuba"
    - 2009-2010: Action planning for the efficient consumption of energetic carriers in the dairy industry of Sancti Spiritus, Cuba.
    - 2007-2008: Environmental, economic and technical feasibility of the biodegradable wastes to produce biogas in the sugar cane factory of "Uruguay, Sancti Spiritus, Cuba"
    - 2006-2007: Proposal of technologies to produce renewable energy from biogas
    - 2006-2007: Biogas production as a renewable energy alternative in the farm of "Remberto Abad Alemán"
    - 2005-2006: Stay of the art of the biogas technologies available in Cuba and over world
- 2005-2006: Teaching "Organic Chemistry"
- 2006-2007: Teaching "Statistics"
- 2006-2009: Teaching "Thermodynamics"
- 2009- … Teaching "Technological processes"

Workshops

2013: 13th Anaerobic Digestion Congress. Santiago de Compostela, Spain.

2010: 7th Higher Education Congress. University 2010. Havana, Cuba.

2008: III International Symposium: Society Tourism and Human Development. Sancti Spiritus, Cuba.

2007: XII National workshop of Biogas. Granma, Cuba.

2006: II International Symposium: Society Tourism and Human Development. Sancti Spiritus, Cuba.

2006: 5th Higher Education Congress. University 2006. Havana, Cuba.

2005: II National Workshop of Biogas. Sancti Spíritus, Cuba.

2005: Workshop: "Labor stability and work motivation for graduated young people"

2005: III International Congress of the Agrarian Themes. Sancti Spíritus, Cuba.

2004: 4th Higher Education Congress. University 2004. Havana, Cuba.

Courses

2009: Environmental Life Cycle Assessment. Sancti Spíritus, Cuba.

2009: Biochemistry and Microbiology of the Anaerobic Digestion. Sancti Spíritus, Cuba.

2008: Quantitative Techniques for Reserching. Sancti Spíritus, Cuba.

2007: Environmental Impact Assessment of Projects. Environmental impact assessment methods. University of Córdova, Spain.

2006: Master courses in energy efficiency. Cienfuegos University (UCF), Cuba.

- Advanced Heat Transfer, Applied mathematics, Efficiently management of the energy, Methodology of the Scientific Research, Cleaner productions (PML), Investigation courses II, Renewable Energy Sources, Refrigeration, Combustion and Steam Generation, Flow of Fluids, Efficiently use of the energy for the transportation, Efficiently use of the electrical power I, and Efficiently use of the electrical power II.

2006: English Teaching for Adults Education Degree in Cienfuegos language School "William Shakespeare", Cuba.

2005: Basic English. Sancti Spíritus, Cuba.

2004: Simulation of Processes. Sancti Spiritus University, Cuba.

2003: Training Courses for Nicaraguan developers. Sancti Spíritus, Cuba.

2003: Risk and Critical Points for Control Analysis. Dairy Enterprise. Sancti Spíritus, Cuba.

2002: English studies of the program "INTERCHANCE", level INTRO. 2. Dairy Enterprise. Sancti Spíritus, Cuba.

Participation in projects research

1. Prospective study for the biogas production with energetic aims in Sancti Spíritus.

Supported financially by:

- CITMA (Ministry of Science, Technology and Environment)
- MES (Ministry of Higher Education)

2. Project ZEIN2009PR362: Biogas production from waste from local food, wood and sugar cane industries for increasing self−sufficiency of energy in Sancti Spiritus, Cuba.

- Supported financially by VLIR Program

Scientific publications

- Barrera, E.L., Spanjers, H., Romero, O., Rosa, E. and Dewulf, J., 2014. Characterization of the sulfate reduction process in the anaerobic digestion of a very high strength and sulfate rich vinasse. Chemical Engineering Journal 248, 383–393.
- Barrera, E.L., Spanjers, H., Dewulf, J., Romero, O. and Rosa, E., 2013. The sulfur chain in biogas production from sulfate-rich liquid substrates: a review on dynamic modeling with vinasse as model substrate. Journal of Chemical Technology and Biotechnology 88, 1405–1420.
- Barrera, E.L., Romero, O., López, L. and Chong, L. Adaptación y modificación de la estrategia para la transferencia tecnológica de un proceso químico a la producción de biogas con fines energéticos en escenarios de la industria azucarera (Adaptation and modification of a technological transfer strategy from a chemical process to the biogas production in the sugar cane industry). "Centro Azúcar" Journal. 2009. ISBN. 0253 5757.
- López, L.; Romero, O. and Barrera, E.L. La producción de biogás en la empresa Melanio Hernández: una alternativa energética (The biogas production in Melanio Hernandez enterprise: an energetic alternative). "Centro Azúcar" Journal. 2007. ISBN. 0253 5757.
- Romero, O., Barrera, E.L. y col. Posibilidades de ahorro energético en la entrega de energía al SEN por fábricas de azúcar (Potential for energy saving in the energy delivery to the electricity grid from the sugar factories). "Centro Azúcar Journal", 2005. ISBN. 0253 5757
- Romero, O., Barrera, E.L. y col. Diagnóstico de las emisiones en un proyecto de cogeneración con bagazo (Study of the emissions in a cogeneration project). "Centro Azúcar Journal" 2005 ISBN. 0253 5757.

Conference contributions

- Barrera, E.L., Spanjers, H., Dewulf, J., Romero O., and Rosa E. Evaluation of UASB reactor performance during start-up operation using Cuban vinasse as a sulfate rich liquid substrate. 13th Anaerobic Digestion Congress. Santiago de Compostela, Spain.
- Romero, O., Barrera, E.L. and Obregon, J.J. Experiencias en investigacionese energética de elevada demanda social desde la universidad (Experiences in energetic investigations of high social demand from the university). 7th Higher Education Congress, University 2010.
- Barrera, E.L., Romero, O., Hermidas, F.O. and López, L. El biogás como fuente renovable y alternativa ambiental en una granja del MINAZ en Sancti Spíritus (Biogas as a renewable

energy source and environmental alternative in a farm of the sugar industry in Sancti Spíritus). III Symposium Society, Tourism and Human Development 2008.

- Lopez, L., Contreras, L.M., Romero, O., Rivadeneira, O. and Barrera, E.L. Estimación de la producción de biogás con fines energéticos en la provincia de Sancti Spiritus (Estimation of the biogas production to produce energy in Sancti Spíritus). III International Congress of the Agrarian Themes. 2005. ISBN. 959-250-219-6.
- Romero, O., Barrera, E.L. y col. Generación anual con biomasa cañera como alternativa energética sostenible (Annual generation with cane biomass as a sustainable alternative). III International Congress of the Agrarian Themes 2005. ISBN. 959-250-219-6.

APPENDIXES

Appendix A. This appendix includes the last sections of the article cited below. These sections are related to the modeling of sulfide removal processes. Since they were used for mass balance calculations in Chapter 4 only, they were placed here for a proper balance of Chapter 1.

Last sections of the article:

Barrera, E.L., Spanjers, H., Dewulf, J., Romero, O. and Rosa, E., 2013. The sulfur chain in biogas production from sulfate-rich liquid substrates: a review on dynamic modeling with vinasse as model substrate. Journal of Chemical Technology and Biotechnology 88, 1405–1420.

DYNAMIC MODELING OF SULFIDE REMOVAL PROCESSES

After the modeling of sulfate reduction processes, sulfide removal processes should be modeled to predict the H_2S concentration in the conditioned biogas. Methods to remove hydrogen sulfide from biogas streams may be grouped as: physical absorption, chemical absorption, adsorption, and chemical and biochemical conversion (direct conversion to S^0). Examples of each category and its common reagent were reviewed by Lens and Hulshoff (Lens and Hulshoff Pol, 2000). The selection of what method to use is largely dependent on the amount of hydrogen sulfide to be removed (Lens and Hulshoff Pol, 2000).

If the method to remove hydrogen sulfide changes as a function of the amount of hydrogen sulfide to be removed, the SCBP also changes. For example, in the case of Cuban vinasse the Ministry of the Cane Sugar Industry reported in 2009 the discharge of 1.3 millions of cubic meters of vinasse (Final Report of Sugar Production 2007-2008). From this value the average of vinasse produced by each Cuban distillery was 682 $m^3\ d^{-1}$ (considering 8 distilleries of the Sugar Ministry), and the expected biogas production per biogas plant could range from 16 857 to 18 018 $m^3\ d^{-1}$. If a H_2S composition between 20 000 to 30 000 ppm_V in the biogas is assumed, 0.65 to 1 t d^{-1} of sulfur can be obtained per distillery-biogas plant. The technologies based on direct conversion processes (e.i., Sulferox, Lo-Cat or Shell-Thiopaq) are usually recommended when the range of sulfur load in the fed biogas is between 0.1 and 15 t d^{-1} (Lens and Hulshoff Pol, 2000). Hence, this review on the modeling of the sulfide removal process (based on sulfur conversion and transfer processes) following the SCBP with vinasse as model substrate (Cuban vinasse as an example) will focus on those technologies using as reagent:

- Iron III complexes, based on the process **Sulfide removal by absorption into "Ferric Chelates" solutions** of EDTA (ethylenediaminetetraacetic acid) and HEDTA (hydroxylethylethylenediaminetriacetic acid). Sulferox and Lo-Cat processes.
- Iron III sulfates, based on the process **Sulfide removal by absorption into "Aqueous Ferric" solutions** (using *Thiobacillus ferrooxidants* to regenerate the ferric solution), as an improved method over the **Sulfide removal by absorption into "Ferric Chelates" solutions**.
- Air oxygen, based on the process **Sulfide removal by biooxidation with air oxygen addition** as a biological method to remove hydrogen sulfide from biogas, instead of Shell-Thiopaq.

Sulfide removal by absorption into "Ferric Chelates" solutions: a two stage process

The Sulferox and Lo-Cat processes are based on the oxidation of hydrogen sulfide to elemental sulfur by means of air with the aid of a compound that is easily oxidized by the atmospheric air and easily reduced by H_2S (Lens and Hulshoff Pol, 2000). In the sulfide removal by absorption into ferric chelates solutions of EDTA and HEDTA, physical absorption with mass transfer and chemical reactions occur. The overall scheme of the process is shown in Fig 3, where the absorber solution contains the iron complex $Fe^{3+}L^{n-}$ (L is the organic ligand and n its charge), which oxidizes the hydrogen sulfide to elemental sulfur, reducing $Fe^{3+}L^{n-}$ to $Fe^{2+}L^{n-}$ (reactor 1, absorption of H_2S into ferric chelates solutions). The iron complex ($Fe^{3+}L^{n-}$) is regenerated in the reactor 2 with the addition of air (oxidation of ferrous chelates solutions) and the sulfur is separated by means of filters, settler presses or sulfur smelter (3).

After a careful literature search, it turns out that the main research on this topic was done by the team of Beenackers (Demmink and Beenackers, 1997; Demmink and Beenackers, 1998; Wubs and Beenackers, 1994; Wubs and Beenackers, 1993) The kinetic model of the whole process was studied and reported by Wubs and Beenackers (Wubs and Beenackers, 1994; Wubs and Beenackers, 1993) and later, a new model with the inclusion of mass transfer equation based on the penetration theory and charge balance was developed by Demmink and Beenackers (Demmink and Beenackers, 1997; Demmink and Beenackers, 1998). The reactions involved, mass transfer equations and kinetic equations are discussed below.

Modeling of the absorption of H_2S into "Ferric Chelates" solutions

Reactions involved:

The absorption of H_2S into ferric chelates solutions is the first stage of the process described above for reactor 1 in Fig. 3. The general reaction pathway of the process can be described through the Equations (16) and (17) (Demmink and Beenackers, 1998; Wubs and Beenackers, 1994; Zegers, 1987).

$$H_2S_{(g)} \leftrightarrows H_2S_{(aq)} \quad (16)$$

$$H_2S_{(aq)} + 2Fe^{3+}L^{n-} \leftrightarrows 2Fe^{2+}L^{n-} + 2H^+ + S^0 \quad (17)$$

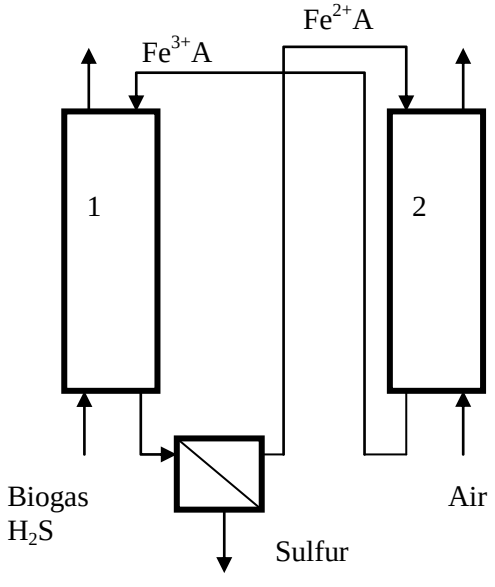

Figure 3. Scheme of the sulfide removal processes by absorption into ferric solutions. 1: Reactor in which hydrogen sulfide is oxidized to elemental sulfur, reducing Fe^{3+} to Fe^{2+}. 2: Reactor in which Fe^{2+} is oxidized with air addition to regenerated Fe^{3+}. 3: Separator of sulfur (filter, settler press or sulfur melter). A, means the ligand (L^{n-}) in the absorption with ferric chelates solutions and sulfates (SO_4^{2-}) in the absorption into aqueous ferric solutions

Wubs and Beenackers (1994) studied a reaction pathway starting from the monohydroxy ferric chelate. However a more complex reaction mechanism was proposed by Demmink and Beenackers (1998). The reaction mechanism is shown in Table 4 (chemical reactions (1-6)), with a common formula to represent both, EDTA if n=4 or HEDTA if n=3. Here, following reactions (1) and (2), an intermediate meta-stable ferric sulfide complex ($Fe^{3+}L^{n-}(SH^-)$) is considered to obtain the end products of Equation (17). At high pH values, similar reactions

ought to occur from hydroxylated species by means of chemical reactions (3) and (4) for EDTA and HEDTA, respectively.

Table 4. Reaction pathway and dissociated species of the absorption of H_2S into ferric chelates solutions

Reaction mechanism	Kinetics	No
$H_2S + Fe^{3+}L^{n-} \underset{k_{-1}}{\overset{k_1}{\rightleftarrows}} Fe^{3+}L^{n-}(SH^-) + H^+$	$-r_A^{(mo)} = k_{1.1} * C_A * C_B^{(mo}$	1
$Fe^{3+}L^{n-}(SH^-) + Fe^{3+}L^{n-} \xrightarrow{k_2} 2Fe^{2+}L^{n-} + H^+ + S$		2
$H_2S + Fe^{3+}L^{n-}(OH^-) \underset{k_{-3}}{\overset{k_3}{\rightleftarrows}} Fe^{3+}L^{n-}(SH^-) + H_2O$	$-r_A^{(m1)} = k_{1.1} * C_A * C_B^{(m1}$	3
$Fe^{3+}L^{n-}(SH^-) + Fe^{3+}L^{n-}(OH^-) \xrightarrow{k_4} 2Fe^{2+}L^{n-} + H_2O + S$		4
$H_2S + Fe^{3+}L^{n-}(OH^-)_2 \underset{k_{-5}}{\overset{k_5}{\rightleftarrows}} Fe^{3+}L^{n-}(SH^-) + OH^- + H_2O$	$-r_A^{(m2)} = k_{1.1} * C_A * C_B^{(m2}$	5
$Fe^{3+}L^{n-}(SH^-) + Fe^{3+}L^{n-}(OH^-)_2 \xrightarrow{k_6} 2Fe^{2+}L^{n-} + OH^- + H_2O +$		6
$Fe^{3+}L^{n-} + H_2O \underset{\leftarrow}{\overset{k_7}{\rightleftarrows}} Fe^{3+}L^{n-}(OH^-) + H^+$	$K_7 = \frac{C^{m1}C_{H+}}{C^{m0}}$	7
$Fe^{3+}L^{n-}(OH^-) + H_2O \underset{\leftarrow}{\overset{k_8}{\rightleftarrows}} Fe^{3+}L^{n-}(OH^-)_2 + H^+$	$K_8 = \frac{C^{m2}C_{H+}}{C^{m1}}$	8
$2Fe^{3+}L^{n-}(OH^-) \underset{\leftarrow}{\overset{k_9}{\rightleftarrows}} (Fe^{3+}L^{n-})_2(O^{2-}) + H_2O$	$K_9 = \frac{C_{(FeL)_2O^{2-}}}{(C^{m1})^2}$	9
$Fe^{3+}L^{n-}(OH^-) + Fe^{3+}L^{n-} \underset{\leftarrow}{\overset{k_{10}}{\rightleftarrows}} (Fe^{3+}L^{n-})_2(O^{2-}) + H^+$	$K_{10} = \frac{C_{H+}C_{(FeL)_2O^{2-}}}{C^{m0}C^{m1}}$	10

Chemical reactions 5 and 6 were also proposed. However, the low concentration of $Fe^{+3}L^{n-}(OH^-)_2$ (m2) dissociated at operational pH range (6 - 9) and the existence of this species only for HEDTA may lead to disregard those reactions to avoid model complexities. In spite of that, its high reactivity and its high reaction rate ($k_{1.1}^{(m2)}$) lead to consider carefully the conditions in each case study (Demmink and Beenackers, 1998; Wubs and Beenackers, 1994). Special attention should be paid to the process pH and its relationship with the dissociated compound. The dissociation reactions of chelates starting from $Fe^{+3}L^{n-}$ (m0) to the more reactive hydroxylated species $Fe^{+3}L^{n-}(OH)$ (m1), and also to $Fe^{+3}L^{n-}(OH^-)_2$ (m2) are also shown in Table 4 (Dissociation equations (7-10)). In the model, the μ-oxi-bridged ferric chelates ($(Fe^{+3}L^{n-})_2(O^{2-})$) form is considered as non-reactive species to H_2S. That is why it may participate in Equation (17) through dissociation, only by the backward dissociation

equations (9) and (10) (Table 4). The equilibrium constants taken from different authors were reported in Table 2 of Demmink and Beenackers (1998).

Mass transfer:

The absorption rate per unit of gas-liquid interface has been used to describe the absorption of one component followed by its chemical reaction (Equation (18)) (Demmink and Beenackers, 1998; Wubs and Beenackers, 1994; Zegers, 1987). It describes the process as a function of an enhancement factor E_A, which is calculated from the reaction regime of the process. As hydrogen sulfide is totally consumed, its concentration in the bulk is commonly assumed to be zero, $C_A = 0$.

$$J_A = k_L E_A \left(C^i_{A,liq} - C_A\right) \quad (18)$$

The process has been studied in low ($p°_A$= 3.5 kPa) and high ($p°_A$=8.95 kPa) hydrogen sulfide partial pressure (Demmink and Beenackers, 1998; Wubs and Beenackers, 1994). Wubs and Beenackers (1994) considered the film model with instantaneous reaction for the high pressure regime. Equation (19) describes its enhancement factor (Zegers, 1987). Here, E_A is only dependent on the mass transfer properties of the species involved and the kinetic parameter is not included due to an instantaneous reaction that takes place in a plane between the gas – liquid interface and the liquid bulk.

$$E_{A\infty} = 1 + \frac{D_B C_B}{b D_A C_A} \quad (19)$$

However, based on Dalton's law, an estimated partial pressure of hydrogen sulfide in the biogas from Cuban vinasse could range from 2.03 to 3.04 kPa, considering hydrogen sulfide concentrations between 20 000 – 30 000 ppm_v and atmospheric pressure in the biogas stream, which is near to the low pressure regime ($p°_A$= 3.5 kPa) in the experiments of Wubs and Beenackers (1994).

For this low pressure regime, the comprehensive model of Demmink and Beenackers (1998) based on penetration theory was tested with the experimental data obtained by Wubs and Beenackers (1994). This model calculated the enhancement factor (E_A) as follows:

$$E_A = \frac{D_A}{k_L C^i_{A,liq} \Theta} \int_0^{\Theta} \left[\left(\frac{\partial C_A}{\partial x}\right)_{x=0,t}\right] dt \quad (20)$$

Equation 20 describes the enhancement factor as a function of the time-dependent concentration gradients $(\partial C_A/\partial x)$. The term $\partial C_A/\partial x$ was written as a dimensionless mass balance equation combined with a charge balance term to determine the relative concentration of each species in the liquid (Demmink and Beenackers, 1997), allowing the modeling of a wide range of operational conditions (pH values and species concentrations). This equation and its sub-equations, as well as the boundary conditions were established by Demmink and Beenackers (1998) as a more accurate approach to describe reactive absorption of hydrogen sulfide with EDTA and HEDTA ferric chelates. Now, kinetic rates to deal with concentration profile of hydrogen sulfide and chelates species in the reactor 1 are required.

Kinetics:

Wubs and Beenackers (1994) demonstrated that kinetics is of first order in both H_2S and iron chelates, based on a plot of H_2S partial pressure for the slow to instantaneous reaction regime (experiments in low pressure regime of H_2S). A detailed review was done finding the same order in most cases (Demmink and Beenackers, 1998), which leads to first order kinetics for the uptake of the species ($-r_A$) (see Table 4). Equilibrium expressions (7), (8), (9) and (10) are shown in Table 4.

The Arrhenius equation was used to correct the kinetic coefficients ($k_{1.1}^{(m0)}$, $k_{1.1}^{(m1)}$ and $k_{1.1}^{(m2)}$) as a function of temperature, being pH independent. Values in the same order of magnitude for $k_{1.1}^{(m1)}$ and $k_{1.1}^{(m2)}$ (values are shown in Table 1 of Demmink and Beenackers (1998)) were reported, whereas $k_{1.1}^{(m0)}$ was considered approximately zero because of the high reactivity observed in the hydroxylated species.

In conclusion, the studies mentioned above (Demmink and Beenackers, 1998; Wubs and Beenackers, 1994) can be used to model the reactive absorption of hydrogen sulfide in chelates and are able to predict the concentration profile of the involved species along the depth from the gas-liquid interface until the liquid bulk.

Modeling of the oxidation of "Ferrous Chelates" solutions

Reactions involved:

In the oxidation of ferrous chelates solutions (Fig 3, reactor 2), $Fe^{2+}L^{n-}$ is oxidized by O_2 in air to regenerate $Fe^{3+}L^{n-}$. The general reaction pathway of the process can be represented by

Equations (21) and (22), with an overall stoichiometry coefficient ($v_B^0 = 2 + v^*$) reported between 3 and 4 ($3 \leq v_B{}^0 \leq 4$) (Wubs and Beenackers, 1993).

$$O_{2(g)} \leftrightarrows O_{2(aq)} \quad (21)$$

$$O_{2(aq)} + (2 + v^*)Fe^{2+}L^{n-} + 2H_2O \leftrightarrows (2 + v^*)Fe^{3+}L^{n-} + OH^- \quad (22)$$

The reaction mechanism proposed by Wubs and Beenackers (1993) to describe Equation (22) is shown in Table 5. When low concentrations of ferrous iron are present, the chemical reaction (12) is rate controlling whereas reaction (13) is negligible. At higher concentrations of the ferrous iron the chemical reaction (13) becomes more important and will finally override reaction (12), thus changing the reaction order in $Fe^{2+}L^{n-}$ from 1 to 2 (Demmink and Beenackers, 1997). Demmink and Beenackers (1997) pointed that in the chemical reaction (15), $v^* = 2$ ($v_B^0 = 4$) can be assumed if there is no degradation of organic compound (OC). Chemical reaction (15) is very fast and is never rate determining; only when ligand degradation exists, a more detailed knowledge of this reaction is required (Demmink and Beenackers, 1997). To avoid model complexities ligand degradation can be disregarded.

In addition, $Fe^{3+}L^{n-}$ is formed during the oxidation of ferrous compounds and the dissociation equations (7 - 10) of Table 4, must be included (Demmink and Beenackers, 1997; Wubs and Beenackers, 1993).

Table 5. Reaction mechanism proposed by Wubs and Beenackers (1993) for the oxidation of ferrous chelates solutions

Reactions mechanism	**No**
$Fe^{2+}L^{n-} + O_2 \underset{k_{-11}}{\overset{k_{11}}{\rightleftarrows}} Fe^{2+}O_2L^{n-}$	11
$Fe^{2+}O_2L^{n-} \underset{k_{-12}}{\overset{k_{12}}{\rightleftarrows}} Fe^{3+}L^{n-} + O_2^-$	12
$Fe^{2+}L^{n-} + Fe^{2+}O_2L^{n-} + H_2O \xrightarrow{k_{13}} 2Fe^{3+}L^{n-} + H_2O_2 + 2OH^-$	13
$Fe^{2+}L^{n-} + O_2^- + 2H_2O \xrightarrow{k_{14}} Fe^{3+}L^{n-} + H_2O_2 + 2OH^-$	14
$v^*Fe^{2+}L^{n-} + H_2O_2 + (2 - v^*)OC \underset{\text{fast}}{\overset{k_{15}}{\longrightarrow}} v^*Fe^{3+}L^{n-} + (2 - v^*)DP + 2OH^-$	15

OC: organic compound; DP: degraded product; v^*: stoichiometry defined in the chemical reaction (15)

Demmink and Beenackers (1997) concluded that the reaction mechanism of Table 5 seems to be the only reaction scheme available in literature that is capable of explaining the observed reaction order at both low and high $C_{Fe\ II}$ for ferrous EDTA and HEDTA. This is relevant because high concentrations of ferrous iron are found in industrial applications (0.1 – 10 kmol m^{-3}).

Mass transfer:

Analogous to the mass transfer rate of hydrogen sulfide in reactor 1, the mass transfer rate of oxygen in ferrous compounds (reactor 2) can be described as in Equation (18). This process has been experimentally studied to determine the reaction order from hypothetical reaction regime by means of enhancement factor and Hatta number calculation (Wubs and Beenackers, 1993). The concentration profile of each species along de reactor can be described as in Demmink and Beenackers (1997) for the oxidation of ferrous nitriloacetic acid with oxygen. The equations of Demmink and Beenackers (1997) are based on the dimensionless mass balance equation combined with a charge balance term described by Demmink and Beenackers (1998) with E_A calculated by using Equation (20).

Kinetics:

The reaction order in Equation (22) was always found first order in oxygen and first to second order for ferrous chelate when its concentration was increased (Wubs and Beenackers, 1993).

The uncertainty in ferrous chelate concentration after the removal of hydrogen sulfide in reactor 1 suggests the use of Equation (23), which can adopt different forms as a function of the concentration of the ferrous compound. For that reason, the overall kinetics expressed by means of Equation (23) (for reaction mechanism of Table 5) was proposed to analyze each particular case (Wubs and Beenackers, 1993).

$$-r_B = (2 + v_B^*) \cdot k_{11} \frac{1+\frac{k_{12}/k_{13}C_B}{1+k_{-12}C_p/k_{14}C_B}}{1+k_{-11}/k_{13}C_B+\frac{k_{12}/k_{13}C_B}{1+k_{-12}C_p/k_{14}C_B}} C_A C_B \qquad (23)$$

For example, if a high concentration of ferrous chelates C_B is found (valid in most of the industrial applications), $k_{-11}/k_{13}C_B << 1$ and Equation (23) could be simplified to Equation

(24). Some other cases and possible combinations in the reaction rate are also shown in Wubs and Beenackers (1993).

$$-r_B = (2 + v_B^*) \cdot k_{11} C_A C_B \qquad (24)$$

In short, the kinetic model was able to predict the behavior of both reactants and products. However, mass transfer rate equations based on the enhancement factor for the oxidation of ferrous chelates solutions must be added analogous to Demmink and Beenackers (1997).

Sulfide removal by absorption into "Aqueous Ferric" solutions: a two stage process

The sulfide removal by absorption into aqueous ferric solutions is included in the present article because it is a novel process for H_2S gas treatment with the advantages (comparing with the absorption into ferric chelates solutions) of mild pressure and temperature conditions (typical for biotechnological processes), lower costs and closed-loop operation without input of chemicals or output of wastes (Pagella and De Faveri, 2000). In addition, the reaction between hydrogen sulfide and ferric sulfate is reported as very rapid and goes to completion (Mesa et al., 2004), and there are no solvent degradation problems (Ebrahimi et al., 2003).

A model for the sulfide removal by absorption into aqueous ferric solutions was developed by Pagella and De Faveri (2000), including the chemical absorption of hydrogen sulfide with aqueous ferric solution (commonly iron III sulfate) as a first step followed by a biochemical oxidation of the formed iron ferrous compounds using *Thiobacillus ferrooxidans* in aerobic conditions. The general scheme is also described in the two reactor columns of Fig 3.

Modeling of the absorption of H_2S into "Aqueous Ferric" solutions

Reactions involved:

The reaction pathway for the chemical absorption of H_2S into aqueous ferric solutions has been reported several times as described in Equation (25) (Abatzoglou and Boivin, 2009; Ebrahimi et al., 2003; Mesa et al., 2004; Pagella and De Faveri, 2000).

$$H_2S + 2Fe^{3+} \leftrightarrows 2Fe^{2+} + 2H^+ + S^0 \qquad (25)$$

The dissociation equations to supply Fe^{3+} concentrations must be considered as a starting point to achieve an accurate reaction scheme for the model (Table 6). The concentration of the dissociated species in the solution has been found pH-dependent. $FeOH^{2+}$ is the most prevalent ion when the solution pH is between 1.4 and 1.8 (Pagella and De Faveri, 2000).

However, concentrations of $Fe_2(OH)_2^{4+}$ and $Fe_3(OH)_4^{5+}$ have been found in the same order of magnitude (Ebrahimi et al., 2003). Hence, it indicates that the reaction may be developed from these most probable species rather than from iron III sulfate.

Table 6. Dissociation equations for the chemical equilibrium of aqueous iron sulfate $Fe_2(SO_4)_3$

Dissociated species	No	References
$Fe^{3+} + OH^- \leftrightarrows FeOH^{2+}$	1	
$Fe^{3+} + 2OH^- \leftrightarrows Fe(OH)^{2+}$	2	
$Fe^{3+} + 3OH^- \leftrightarrows Fe(OH)_3$	3	
$2Fe^{3+} + 4OH^- \leftrightarrows Fe_2(OH)_4^{2+}$	4	(Pagella and De Faveri, 2000)
$3Fe^{3+} + 4OH^- \leftrightarrows Fe_3(OH)_4^{5+}$	5	(Ebrahimi et al., 2003)
$Fe^{3+} + HSO_4^- \leftrightarrows FeHSO_4^{2+}$	6	
$H^+ + SO_4^{2-} \leftrightarrows HSO_4^-$	7	
$H^+ + OH^- \leftrightarrows H_2O$	8	
$2Fe^{3+} + 2OH^- \leftrightarrows Fe_2(OH)_2^{4+}$	9	
$Fe^{3+} + SO_4^{2-} \leftrightarrows Fe(SO_4)^+$	10	(Ebrahimi et al., 2003)
$Fe^{3+} + 2SO_4^{2-} \leftrightarrows Fe(SO_4)_2^-$	11	
$Fe^{3+} + 2HSO_4^- \leftrightarrows Fe(HSO_4)^+$	12	

Mass transfer:

In general, the absorption rate of a component A from the gas to the liquid phase is described by Equation (18). The concentration of hydrogen sulfide in bulk has been considered to be zero and the expression for the enhancement factor (Equation (26)) in the chemical absorption is often written as a function of the Hatta number (Equation (27)), for a fast chemical reaction (Ebrahimi et al., 2003; Pagella and De Faveri, 2000; Zegers, 1987).

$$E_A = \sqrt{1 + {H_a}^2} \quad (26)$$

$$H_a = \frac{\sqrt{D_A k_{1.1} C_B}}{k_L} \quad (27)$$

From these values the regime of the reaction is usually characterized by a chemically enhanced mass transfer or not, when E_A or Ha are over 1 or 0.1, respectively. After that, the combination between Equations (18) and (26) describes the chemical absorption profile of hydrogen sulfide in the aqueous ferric solution as a function of the reactant initial concentrations.

Kinetics:

Pagella and De Faveri (2000) considered iron monohydrate species as key reactant with first order kinetics for both reactants in the reaction represented by Equation (25). Ebrahimi *et al.* (2003) studied the kinetics of this reaction, considering that some other dissociated species (mentioned before) were also able to react with hydrogen sulfide. For that reason, total iron concentration was used in the kinetic model, although it was stated that further research had to be done to account for the different kinds of iron dissociated species. Hence, the kinetics equation was proposed as a first order reaction for both reactants in the chemical absorption of hydrogen sulfide (Equation (28)).

$$-r_A = k_{1.1} C_A C_{B,Total} \quad (28)$$

Ebrahimi *et al.* (2003) used a constant rate $k_{1.1,}$ obtained by adjustment with temperature based in the Arrhenius's equation, showing values between 10 and 110 $m^3\,kmol^{-1}\,s^{-1}$ for the range of 30 – 70 °C, whereas Pagella and De Faveri (2000) reported a constant value of 4100 $m^3\,kmol^{-1}\,s^{-1}$ at 30 °C. The strong differences between the above results are probably due to the assumption of different reactant species in each model. That is, to obtain the same reaction conversion in Equation (28), the reaction rate coefficient $k_{1.1}$ in Pagella and De Faveri (2000) must be higher than the kinetic constant $k_{1.1}$ in Ebrahimi *et al.*, (2003) because the first considered only one of the reactant species ($FeOH^{2+}$) whereas the second also considered $Fe_2(OH)_2^{4+}$ and $Fe_3(OH)_4^{5+}$ species. Therefore, the kinetic constant range proposed by Ebrahimi *et al.*, (2003) is more representative to describe the real phenomena in which $FeOH^{2+}$, $Fe_2(OH)_2^{4+}$ and $Fe_3(OH)_4^{5+}$ are considered as reactant species.

Modeling of the biooxidation of "Aqueous Ferrous" solutions

The biooxidation of aqueous ferrous solutions is commonly applied after the absorption of hydrogen sulfide into aqueous ferric solutions. *Thiobacillus ferrooxidans* is an example of a chemoautotrophic aerobic microorganism that can oxidize Fe^{2+} to regenerate Fe^{3+}. This bacterial group can grow in acid conditions with pH values in the range of 1-6 (Optimum pH=2), preferring a mesophilic condition (Abatzoglou and Boivin, 2009).

Reactions involved:

The general reaction has been considered several times as is described in Equation (29) (Abatzoglou and Boivin, 2009; Ebrahimi et al., 2003; Mesa et al., 2004; Pagella and De Faveri, 2000).

$$0.5O_2 + 2Fe^{2+} + 2H^+ \leftrightarrows 2Fe^{3+} + H_2O \quad (29)$$

No dissociation reactions of the species in Equation (29) have been reported; despite of this, Fe^{3+} could follow the equilibrium depicted in Table 6. The overall performance of the process depends on the bacteria effectiveness to oxidize the ferrous iron solution, for that reason the kinetics of this biochemical process must be modeled. Although authors have confirmed that kinetics limitation in the biooxidation of aqueous ferrous solution could be caused by physical phenomena and mass transfer processes (Mesa et al., 2004), these aspects were not included in models.

Kinetics:

The kinetic model was only reported by Pagella and De Faveri (2000). They predicted the oxidation of ferrous compounds (Fe^{2+}) by *Thiobacillus ferrooxidans* and proposed a simplified Monod type equation for cellular growth (Equation (30)), enabling the calculation of substrates uptake by dividing Equation (30) by the bacterial yield coefficient on the substrate (Equation (31)).

$$\rho_{growth} = \mu_{max} \frac{[Fe^{2+}]}{K_S^*(1+[Fe^{2+}]/K_{P2})+[Fe^{2+}]} X_{ferro} \quad (30)$$

$$\rho_{uptake} = \rho_{growth}(1/Y) \quad (31)$$

The maximum specific growth rate (μ_{max}) can be determined as a function of pH and temperature during the process performance by Equations (32) and (33). From these

equations, the maximum specific growth rate changes with pH and temperature, hence affecting the oxidation rate of Fe^{2+} in Equation (31). Based on Equation (32) where pH_0= 2.2, the optimum value of the pH is around 2, which agrees with Abatzoglou and Boivin (2009).

$$\mu_{max} = \mu_0 \cdot \exp(-k_0(pH - pH_0)^2) \quad (32)$$

$$\mu_{max} = 0.047 \cdot 1.035^{(T-20)} \quad T < 50\ ^oC \quad (33)$$

Although the kinetic equations reported are useful to describe the microorganism growth and the production – consumption of the involved species, further information will be needed to include the endogenous process and the inhibition factors of the involved species on the microbial groups.

Sulfide removal by biooxidation with air oxygen addition: a single stage process

Biooxidation of hydrogen sulfide with air oxygen was included in the present review instead of Shell Thiopaq process, because Shell Thiopaq was developed to treat natural gas based on biological oxidation technologies to remove H_2S from biogas streams (Lens and Hulshoff Pol, 2000).

Modeling of the biooxidation of H_2S with air oxygen addition

The biooxidation of hydrogen sulfide, also called biological air treatment, may use either biofilters or biotrickling filters. Many systems have been developed ranging from biofilters to true biotrickling filters and most of them lie somewhere in between (Devinny and Ramesh, 2005).

An established methodology calls for chemotropic bacterial species for hydrogen sulfide removal (Abatzoglou and Boivin, 2009). Chemotrophic bacteria (Thiobacillus sp.) are widely used for the conversion of H_2S by biological processes and have the ability to grow under various environmental stress conditions (e.g., oxygen deficiency, acid conditions) (Syed et al., 2006).

Biodegradation of H_2S by chemotrophs can occur in aerobic conditions with O_2 as an electron acceptor or in anaerobic conditions with alternative electron acceptors (e.g., nitrate), depending on the type of bacteria (Syed et al., 2006). However, the great majority of reactors utilize aerobic respiration (Devinny and Ramesh, 2005). This process consists in

the addition of air oxygen and nutrients in continuous (biotrickling filters) or discontinuous supply (biofilters) (Fig 4).

Reactions involved

In aerobic conditions, Thiobacillus sp. evoke a redox-reaction which produces S^0 under limited oxygen conditions (Equation (34)) and conversely an excess of oxygen will lead to SO_4^{2-} generation and thus acidification, as shows Equation (35) (Abatzoglou and Boivin, 2009; Syed et al., 2006).

$$HS^- + 0.5O_2 \rightarrow S^0 + OH^- \quad (34)$$

$$HS^- + 2O_2 \rightarrow SO_4^{2-} + H^+ \quad (35)$$

This bacterial group biodegrades hydrogen sulfide by using inorganic carbon (CO_2) as a carbon source, and chemical energy is obtained from the oxidation of reduced inorganic compounds, such as H_2S (Abatzoglou and Boivin, 2009; Syed et al., 2006).

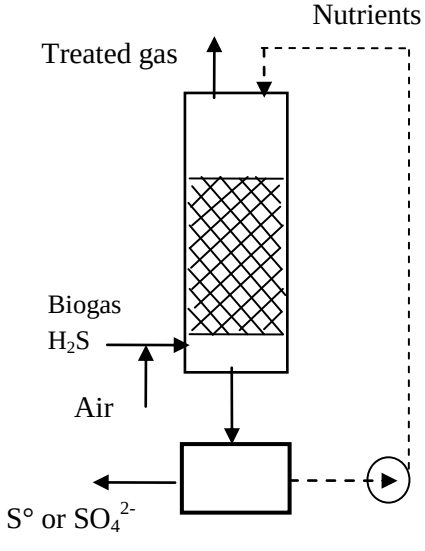

Figure 4. Scheme of biooxidation of H_2S with air oxygen addition

Discontinuous arrows (- - - ►) means flow of nutrients (intermittent in biofilters or continuous in biotrickling filters).

Highlights of the Devinny and Ramesh's phenomenological review

A phenomenological review on the modeling of biofilters (biofilters and biotrickling filters) was carried out by Devinny and Ramesh (2005). In the article the general aspects of the mass transfer and kinetics rates are described. The authors made uniform variables and grouped the

topics by the phenomena, that is, thickness of the flowing water layer, advective transport of the contaminant, phase transfer, diffusion within the biofilm, adsorption on the solid phase, biomass growth and biodegradation, biofilm growth, evaporation and surface morphology of the packing and biofilm.

In order to avoid redundancies and reduce complexity, the equations to model the biooxidation of H_2S with air oxygen reviewed by Devinny and Ramesh (2005) are not exposed in the present review and only their main considerations and conclusions are described as follows:

- **Thickness of the flowing water layer** was calculated as a function of the water flow, physical properties and reactor characteristics (surface area of the packing and height of the column).
- **Advective transport of the contaminant** (e.g., H_2S) can be determined by considering only longitudinal dispersion of the contaminant in the gas flow. It is a function of the dispersion coefficient and contaminant concentrations at the axial dimension. Radial dispersion is considered important only for biofilters operating at high (empty bed detention times of a few seconds) flow rates, which is in most cases negligible.
- **Phase transfer** in biotrickling filters (with hydrogen sulfide as a contaminant) can be assumed to be limited by diffusion resistance in the laminar layer of the gas at the surface (It is most likely to occur where contaminant solubility is high and biodegradation is rapid). In that case, it is calculated as a function of: contaminant concentrations in the gas phase, Henry's coefficient, contaminant concentrations in the biofilm and mass transfer coefficient from gas to the biofilm. Transfers between the phases in the biofilter was controlled by diffusion resistance in the surface of the biofilm, and calculated as a function of the diffusion coefficient of the contaminant and its concentration in the coordinate perpendicular to the biofilm surface.
- **Diffusion within the biofilm** was calculated, by using Fick's Law, as a function of the molecular diffusion coefficient of the contaminant in the biofilm. Diffusion coefficients in the biofilm can be calculated from the diffusion coefficients of the contaminants in water and the bacterial density in a biofilm.
- **Adsorption on the solid phase** (packing material) was calculated proportional to the contaminant concentration or by using non-equilibrium adsorption. Adsorption into

the packing material can be considered negligible in the modeling of biofilters because some biofilm compounds may compete with the contaminant for adsorption sites, reducing its adsorption. Then, the adsorptive capacity of the packing material is an inactive reservoir that has no influence on treatment efficiency.

- **Biomass growth and biodegradation** were modeled, using Monod kinetics, as a function of the concentration of contaminants and microorganisms, and Monod coefficients (K_S and μ_{max}). Nutrient limitation, inhibitor compounds, temperature dependences, biofilm water content and pH inhibition have been included in the biodegradation rate equations to appropriately describe the phenomena. Often the appropriate values of K_S and μ_{max} are uncertain, because they are strongly dependent on the conditions under which they are determined.
- **Biofilm growth** was calculated by means of an integration function that represents the net growth of the biofilm throughout the depth. The growth of the biofilm was determined by an integral (along the depth of the biofilm) which depends on biomass death rate, inactive and total biomass concentration in the biofilm, yield coefficient of bacteria, contaminant concentration in the biofilm and Monod coefficients for contaminant (K_S and μ_{max}).
- **Evaporation** was locally predicted as instantaneous evaporation rate. It is calculated as an empirical function of the maximum evaporation rates, which depend on the air velocities, temperature and relative humidity. It is also a function of the degree in which the biofilm water content exceeds the water content that would be in equilibrium with the gas phase and on the critical water content at which a surface free water phase just disappears.
- **Surface morphology of the packing and biofilm** is accepted as a flat surface model. Results from models that had considered irregular biofilm growth are not better than those that assume a flat layer. However, Silva *et al*. (2010) modeled the variation of active biomass along the biotrickling filter fed with different H_2S loading rates. The model of Silva *et al*. was able to predict variations in biomass concentration along spatial distribution of the biofilm and the gas variation in the axial distribution of the column finding better fitting than when a constant biofilm model was used. Nevertheless, the model was validated for H_2S inlet concentrations between 10 and

221 ppm_v, which is extremely low compared with the expected concentration in biogas obtained from vinasse (up to 30 000 ppm_v).

Although the available models were able to describe the process for research purposes, some limitations have been found. They lay in the determination of appropriate diffusion constants of the contaminant, the knowledge of Monod and maximum growth rate coefficients for actual conditions in biofilters and the modeling of the irregular biofilm growth for the expected hydrogen sulfide concentrations in vinasse biogas (effect of variable biomass). That is why Devinny and Ramesh (2005) considered that a simple model able to predict the behavior of biofilters has not been developed yet. For that reason, biofilter modeling remains primarily a research tool.

Symbols for Appendix A

b	Stoichiometry of the rate limiting reaction step	-
C	Concentration	$kmol \cdot m^{-3}$
D	Diffusion coefficient	$m^2 s^{-1}$
E	Chemical enhancement factor	-
$[Fe^{2+}]$	Ferrous ion concentration	$kg \cdot m^{-3}$
$[Fe^{3+}]$	Ferric ion concentration	$kg \cdot m^{-3}$
Ha	Hatta number	-
J	Specific absorption rate	$kmol \cdot m^{-2} \cdot s^{-1}$
k_0	Coefficient of a model used to correct μ_{max} in Equation (32)	-
$k_{1,1}$	Reaction rate coefficient defined for Equations (1-6), Table 4 and Equation (28)	$m^3 \cdot kmol^{-1} \cdot s^{-1}$
k_L	Liquid-side mass-transfer coefficient	$m \cdot s^{-1}$
$K_{7\text{-}10}$	Equilibrium constants of Table 4	
	• Equilibrium Equation 7 and 8	$kmol \cdot m^{-3}$
	• Equilibrium Equation 9	$m^3 \cdot kmol^{-1}$
	• Equilibrium Equation 10	-
K_{p2}	Competitive product inhibition coefficient in Equation (30)	$kg \cdot m^{-3}$
K_S^*	Half saturation value in absence of inhibitor in Equation (30)	$kg \cdot m^{-3}$
L^{n-}	Organic ligand	-
pH_0	pH of the maximum growth rate of *Thiobacillus ferrooxidans*	-
r	Reaction rate	$kmol \cdot m^{-3} \cdot s^{-1}$
T	Temperature	°C
t	Time	s
x	Distance from gas-liquid interface	m
Y	Yield of biomass on the substrate	$kg\ VSS \cdot kg\ COD\_S_i^{-1}$
Greek letter		
ρ_{uptake}	Kinetic rate of substrate uptake	$kg\ COD\_S_i \cdot m^{-3} \cdot d^{-1}$
ρ_{growth}	Kinetic rate of bacterial growth	$kg\ VSS \cdot m^{-3} \cdot d^{-1}$
μ_{max}	Maximum specific growth rate of microorganisms	d^{-1}
μ_0	Maximum value μ_{max} as a function of pH in Equation (32)	d^{-1}

ν^*	Stoichiometry defined in the chemical reaction 15, Table 5	-
$\nu_B{}^0$	Overall stoichiometry coefficient	-
Θ	Average contact time	s

Subscript

i	Pertaining to substrates or species
A	Pertaining to gas-phase reactant
B	Pertaining to the ferric or ferrous reactant
liq	Liquid phase
0	Initial value of the parameter
P	Pertaining to products
ferro	Pertaining to the bacterial group of *Thiobacillus ferrooxidans*
∞	Instantaneous reaction

Superscript

i	Interface
m0	Pertaining to monomeric species $Fe^{3+}\ L^{n-}$
m1	Pertaining to monomeric species $Fe^{3+}\ L^{n-}\ OH$
m2	Pertaining to monomeric species $Fe^{3+}\ L^{n-}\ (OH)_2$

Appendix B. Dynamic data set on COD, carbon and sulfur content during the experiments (days 1 to 75)

This appendix includes the experimental data set ("numbers") on COD, carbon and sulfur obtained in Chapter 2.

	Influent vinasse			**Effluent of the UASB reactor**															
	COD	Carbon	Sulfur	COD				Carbon									Sulfur			
Days	Vinasse	Vinasse	Vinasse	$COD\_CH_{4\ gas}$	$COD\_\Delta SO_4^{2-}$	eff_COD	Total COD	CH_4	CO_2	HCO_3^-	HVa	HBu	HPr	HAc	Soluble inert	Total Carbon	$eff\_SO_4^{2-}$	H_2S_{aq}	$S\_H_2S_{gas}$	Total Sulfur
	g COD/d	g C/d	mg S/d	g COD/d	g COD/d	g COD/d	g COD/d	g C/d	g C/d	g C/d	g C/d	g C/d	g C/d	g C/d	g C/d	g C/d	mg S/d	mg S/d	mg S/d	mg S/d
1	25.00	9.88	383.7	15.74	0.63	6.73	23.10	2.95	2.11	0.36	0.000	0.009	0.065	0.042	2.45	7.98	68	121.0	184.4	373.9
2	26.45	9.34	406.0	15.73	0.67	9.04	25.45	2.95	2.28	0.38	0.003	0.019	0.140	0.079	2.59	8.43	69	119.7	174.8	363.4
3	28.23	9.88	433.4	16.73	0.72	9.83	27.28	3.13	2.41	0.43	0.001	0.010	0.152	0.054	2.76	8.96	74	151.6	189.6	415.2
4	27.70	10.55	425.3	16.56	0.72	9.16	26.45	3.10	2.49	0.42	0.002	0.010	0.141	0.051	2.71	8.93	63	150.2	173.5	386.9
5	27.36	10.35	420.0	17.12	0.74	8.95	26.80	3.20	2.47	0.43	0.000	0.010	0.129	0.034	2.68	8.95	51	145.4	179.6	375.9
6	27.74	10.22	425.8	17.15	0.73	9.36	27.24	3.21	2.37	0.47	0.000	0.010	0.079	0.041	2.71	8.90	60	146.7	171.4	378.2
7	27.55	10.37	422.9	16.84	0.75	9.35	26.93	3.15	2.54	0.44	0.000	0.009	0.054	0.037	2.70	8.93	50	137.8	196.3	383.5
8	34.94	13.05	533.9	19.10	0.94	10.02	30.06	3.58	2.76	0.45	0.000	0.009	0.078	0.063	3.42	10.35	64	131.0	214.7	409.3
9	33.36	13.10	509.7	19.41	0.90	10.16	30.48	3.63	2.69	0.43	0.000	0.010	0.071	0.052	3.26	10.15	58	132.1	252.3	442.2
10	33.55	12.51	512.6	19.67	0.89	10.63	31.18	3.68	2.84	0.45	0.000	0.004	0.056	0.053	3.28	10.36	70	141.2	267.7	478.8
11	34.90	12.58	533.1	19.96	0.94	10.67	31.58	3.74	2.88	0.47	0.000	0.009	0.077	0.053	3.41	10.64	62	149.0	288.1	499.2
12	34.51	13.09	527.3	20.05	0.92	11.08	32.04	3.75	2.90	0.47	0.000	0.010	0.079	0.063	3.38	10.65	67	149.6	286.8	503.0
13	34.75	12.94	530.9	19.32	0.92	12.00	32.24	3.62	2.82	0.51	0.001	0.011	0.076	0.057	3.40	10.50	73	142.6	279.6	495.1
14	34.51	13.03	527.3	20.45	0.92	11.59	32.95	3.83	2.74	0.51	0.000	0.011	0.080	0.054	3.38	10.59	69	135.2	276.7	481.2
15	34.66	12.94	529.5	19.99	0.92	12.24	33.15	3.74	2.88	0.51	0.000	0.013	0.088	0.073	3.39	10.70	71	147.3	282.1	500.1
16	42.05	15.67	565.5	20.74	0.97	13.22	34.93	3.88	3.00	0.50	0.016	0.022	0.239	0.155	4.11	11.92	80	162.4	294.7	537.1
17	41.47	15.73	557.7	21.06	0.96	15.07	37.09	3.94	3.17	0.49	0.030	0.031	0.292	0.169	4.06	12.19	77	139.4	292.1	509.0
18	42.46	15.52	571.0	21.53	1.01	16.66	39.19	4.03	3.24	0.47	0.047	0.044	0.367	0.206	4.15	12.56	68	162.5	302.3	533.2
19	41.64	15.88	634.2	23.53	1.13	15.75	40.41	4.40	3.39	0.46	0.041	0.032	0.347	0.172	4.07	12.93	67	158.0	314.2	539.1
20	40.72	15.58	620.1	22.85	1.10	15.76	39.71	4.28	3.30	0.46	0.044	0.039	0.372	0.193	3.98	12.66	71	150.2	384.3	605.5
21	42.28	15.23	644.0	22.59	1.13	16.26	39.98	4.23	3.40	0.47	0.047	0.041	0.469	0.200	4.14	12.99	78	163.3	387.1	628.1
22	41.59	15.82	633.4	22.31	1.12	17.14	40.58	4.18	3.36	0.48	0.064	0.042	0.480	0.170	4.07	12.84	72	140.5	379.2	592.2
23	42.46	15.56	646.6	22.32	1.13	17.42	40.87	4.18	3.37	0.48	0.079	0.056	0.540	0.188	4.15	13.04	84	136.2	375.9	595.7
24	42.34	15.88	644.8	22.24	1.14	17.74	41.13	4.16	3.35	0.49	0.048	0.021	0.634	0.168	4.14	13.01	73	146.7	363.4	583.3
25	42.86	15.84	652.8	22.93	1.14	17.84	41.91	4.29	3.31	0.50	0.040	0.015	0.606	0.141	4.19	13.09	81	135.2	362.5	578.8
26	41.99	16.04	639.5	22.81	1.13	17.16	41.10	4.27	3.43	0.46	0.045	0.017	0.637	0.132	4.11	13.10	75	142.6	348.8	566.7
27	27.78	10.28	889.4	17.48	1.56	16.40	35.44	3.27	2.32	0.52	0.028	0.013	0.452	0.070	2.72	9.40	108	126.5	250.1	484.5
28	27.55	10.38	882.1	17.15	1.47	14.28	32.90	3.21	2.28	0.49	0.027	0.011	0.340	0.091	2.70	9.14	149	162.4	279.7	591.5
29	27.40	10.30	877.2	16.61	1.42	13.83	31.87	3.11	2.30	0.51	0.017	0.007	0.218	0.075	2.68	8.92	165	161.5	334.9	661.2
30	27.51	10.24	880.9	16.34	1.49	13.53	31.36	3.06	2.17	0.54	0.011	0.006	0.127	0.090	2.69	8.70	136	233.1	420.2	789.2

Appendix B. (*continued*)

Days	Influent vinasse			Effluent of the UASB reactor															
	COD	Carbon	Sulfur	COD				Carbon									Sulfur		
	Vinasse	Vinasse	Vinasse	$COD\_CH_{4\ gas}$	$COD\_\Delta SO_4^{2-}$	eff_COD	Total COD	CH_4	CO_2	HCO_3^-	HVa	HBu	HPr	HAc	Soluble inert	Total Carbon	$eff\_SO_4^{2-}$	H_2S_{aq}	$S\_H_2S_{gas}$	Total Sulfur
	g COD/d	g C/d	mg S/d	g COD/d	g COD/d	g COD/d	g COD/d	g C/d	g C/d	g C/d	g C/d	g C/d	g C/d	g C/d	g C/d	g C/d	mg S/d	mg S/d	mg S/d	mg S/d
31	27.93	10.28	894.3	15.45	1.50	13.61	30.56	2.89	2.05	0.55	0.005	0.002	0.096	0.075	2.73	8.41	146	330.8	400.0	876.2
32	27.55	10.44	882.1	13.66	1.49	11.83	26.98	2.56	2.14	0.51	0.002	0.000	0.069	0.050	2.70	8.02	138	295.8	370.7	805.0
33	27.59	10.30	883.3	15.03	1.46	10.71	27.20	2.81	2.08	0.51	0.003	0.001	0.074	0.054	2.70	8.23	152	320.9	383.1	856.5
34	27.63	10.31	884.5	14.74	1.49	10.73	26.95	2.76	2.04	0.50	0.003	0.000	0.067	0.059	2.70	8.13	139	314.8	387.7	841.8
35	27.66	10.32	885.7	14.75	1.50	10.55	26.80	2.76	2.13	0.51	0.000	0.000	0.063	0.052	2.71	8.22	137	302.8	374.6	814.1
36	27.74	10.34	888.2	14.42	1.52	10.31	26.25	2.70	2.17	0.51	0.000	0.000	0.055	0.035	2.71	8.19	127	313.2	382.3	822.1
37	33.31	13.14	1064.1	14.56	1.85	10.59	26.99	2.73	2.28	0.49	0.001	0.001	0.109	0.083	3.26	8.95	140	369.2	402.6	912.0
38	34.37	12.49	1097.9	14.41	1.89	11.77	28.07	2.70	2.45	0.51	0.000	0.003	0.177	0.128	3.36	9.32	153	431.0	442.5	1026.2
39	35.14	12.89	1122.4	15.77	1.98	12.50	30.26	2.95	2.68	0.54	0.005	0.006	0.250	0.154	3.44	10.02	132	453.1	482.9	1068.0
40	34.56	13.18	1104.0	15.87	1.99	13.97	31.83	2.97	2.74	0.52	0.006	0.009	0.287	0.153	3.38	10.07	110	437.8	494.4	1041.9
41	34.99	12.96	1117.8	16.14	1.94	14.70	32.78	3.02	2.76	0.55	0.020	0.016	0.341	0.168	3.42	10.30	149	423.5	496.0	1068.3
42	34.80	13.12	1111.7	15.74	1.93	14.04	31.72	2.95	2.65	0.55	0.025	0.017	0.325	0.154	3.40	10.07	145	389.3	494.9	1029.2
43	35.18	13.05	1123.9	15.89	1.99	14.94	32.82	2.97	2.61	0.56	0.023	0.018	0.320	0.166	3.44	10.11	127	415.6	479.2	1021.4
44	34.90	13.19	1114.7	15.38	1.92	14.84	32.14	2.88	2.70	0.54	0.031	0.020	0.328	0.184	3.41	10.10	154	434.0	491.8	1079.5
45	34.18	13.09	1091.7	15.85	1.90	15.21	32.96	2.97	2.74	0.55	0.028	0.025	0.365	0.212	3.34	10.23	140	405.1	495.4	1040.3
46	39.27	14.95	1309.0	15.48	2.34	15.67	33.49	2.90	2.93	0.55	0.037	0.046	0.447	0.314	4.05	11.27	140	426.3	539.4	1105.9
47	39.11	14.99	1303.5	15.54	2.29	15.64	33.47	2.91	2.80	0.54	0.041	0.039	0.516	0.391	4.03	11.27	158	462.2	549.2	1169.7
48	39.16	14.93	1305.3	14.14	2.29	17.64	34.08	2.65	2.97	0.53	0.040	0.048	0.615	0.501	4.04	11.38	158	462.1	524.5	1144.9
49	38.72	14.95	1290.7	13.85	2.25	16.97	33.07	2.59	3.01	0.52	0.043	0.059	0.712	0.554	3.99	11.49	167	458.3	567.0	1192.2
50	34.70	12.67	1132.7	14.01	2.00	17.58	33.59	2.62	2.61	0.49	0.048	0.052	0.733	0.506	3.39	10.45	135	467.8	498.8	1101.6
51	35.04	13.01	1143.7	13.62	1.98	18.53	34.13	2.55	2.73	0.48	0.033	0.047	0.751	0.532	3.43	10.55	153	470.1	493.7	1117.2
52	35.28	13.14	1151.5	13.59	1.99	18.35	33.93	2.54	2.66	0.47	0.023	0.053	0.755	0.558	3.45	10.51	156	432.2	478.5	1066.5
53	34.80	13.23	1135.8	13.86	2.00	18.02	33.87	2.59	2.63	0.46	0.028	0.065	0.838	0.527	3.40	10.55	138	402.4	481.4	1022.0
54	34.51	13.05	1126.4	14.15	1.99	17.54	33.68	2.65	2.38	0.47	0.024	0.072	0.760	0.464	3.38	10.19	133	437.9	458.1	1029.5
55	34.56	12.94	1128.0	14.59	1.95	16.62	33.16	2.73	2.41	0.50	0.029	0.040	0.799	0.488	3.38	10.37	154	403.9	454.3	1012.0
56	34.18	12.96	1115.5	14.46	1.91	16.79	33.15	2.71	2.45	0.50	0.024	0.039	0.792	0.465	3.34	10.31	159	414.4	468.6	1041.7
57	34.80	12.82	1135.8	14.39	1.94	17.24	33.57	2.69	2.43	0.52	0.025	0.057	0.796	0.500	3.40	10.42	164	409.6	481.3	1055.3
58	35.33	13.05	1153.1	14.91	1.95	16.44	33.30	2.79	2.47	0.53	0.036	0.067	0.869	0.507	3.46	10.73	176	431.3	473.5	1080.7
59	27.40	10.45	1357.9	13.77	2.33	16.43	32.53	2.58	2.26	0.51	0.034	0.055	0.717	0.426	2.68	9.26	192	450.6	425.4	1067.8
60	26.79	10.24	1327.8	12.17	2.25	15.32	29.74	2.28	1.90	0.51	0.025	0.057	0.565	0.445	2.62	8.40	202	566.1	362.1	1129.8
61	26.33	10.01	1305.2	12.28	2.19	13.80	28.27	2.30	1.91	0.50	0.015	0.046	0.392	0.365	2.58	8.11	209	499.0	380.6	1088.9

Appendix B. (*continued*)

Days	Influent vinasse			Effluent of the UASB reactor															
	COD	Carbon	Sulfur	COD				Carbon								Sulfur			
	Vinasse	Vinasse	Vinasse	$COD\_CH_{4\ gas}$	$COD\_\Delta SO_4^{2-}$	eff_COD	Total COD	CH_4	CO_2	HCO_3^-	HVa	HBu	HPr	HAc	Soluble inert	Total Carbon	$eff\_SO_4^{2-}$	H_2S_{aq}	$S\_H_2S_{gas}$	Total Sulfur
	g COD/d	g C/d	mg S/d	g COD/d	g COD/d	g COD/d	g COD/d	g C/d	g C/d	g C/d	g C/d	g C/d	g C/d	g C/d	g C/d	g C/d	mg S/d	mg S/d	mg S/d	mg S/d
62	27.32	9.84	1354.1	12.37	2.31	12.82	27.50	2.32	1.71	0.52	0.007	0.012	0.292	0.360	2.67	7.89	197	602.5	406.0	1205.3
63	23.71	10.21	1175.2	10.27	2.04	11.62	23.93	1.92	1.69	0.43	0.013	0.049	0.385	0.486	2.32	7.30	154	431.8	380.8	966.9
64	26.14	8.86	1295.7	9.70	2.26	13.16	25.12	1.82	1.71	0.46	0.009	0.023	0.394	0.575	2.56	7.54	164	522.9	383.5	1070.8
65	27.82	9.77	1378.6	9.41	2.39	14.21	26.02	1.76	1.87	0.49	0.002	0.035	0.381	0.634	2.72	7.89	182	572.4	432.7	1187.1
66	28.31	10.39	1403.1	9.53	2.44	14.47	26.45	1.78	1.94	0.48	0.009	0.046	0.346	0.654	2.77	8.02	182	585.6	493.0	1260.1
67	28.58	10.58	1416.3	9.26	2.45	14.37	26.08	1.73	1.96	0.49	0.010	0.053	0.384	0.732	2.80	8.16	190	554.2	473.1	1216.8
68	27.66	10.68	1371.1	9.03	2.40	14.17	25.60	1.69	1.87	0.47	0.008	0.064	0.420	0.785	2.71	8.01	170	551.1	467.6	1188.3
69	28.77	10.34	1892.5	8.72	3.26	14.45	26.42	1.63	1.78	0.49	0.013	0.102	0.435	0.892	2.82	8.16	264	594.2	468.0	1326.4
70	28.31	10.75	1862.5	8.79	3.14	14.54	26.47	1.65	1.64	0.49	0.008	0.080	0.399	0.913	2.77	7.95	293	540.9	466.2	1300.1
71	28.12	10.58	1850.0	8.48	3.07	16.68	28.23	1.59	1.59	0.50	0.005	0.075	0.337	0.964	2.75	7.81	313	527.6	390.8	1231.7
72	27.89	10.51	1835.0	7.58	2.89	17.24	27.71	1.42	1.48	0.45	0.013	0.100	0.401	0.967	2.73	7.57	391	543.9	380.2	1315.5
73	27.70	10.42	1822.5	7.25	2.60	17.05	26.89	1.36	1.57	0.44	0.006	0.121	0.458	1.001	2.71	7.66	522	617.5	392.8	1532.7
74	27.17	10.35	1787.5	6.89	2.52	16.67	26.08	1.29	1.59	0.42	0.008	0.132	0.385	0.816	2.66	7.30	527	617.0	428.6	1572.4
75	27.47	10.15	1807.5	6.45	2.51	16.95	25.90	1.21	1.54	0.43	0.014	0.217	0.496	1.046	2.69	7.64	554	578.4	388.8	1521.5

Appendix C. Simulink architecture for steady state and dynamic simulation using ordinary differential equations (ODE)

This appendix explains the simulink architecture used to model sulfate reduction in the anaerobic digestion of a very high strength and sulfate rich vinasse as an extension of ADM1.

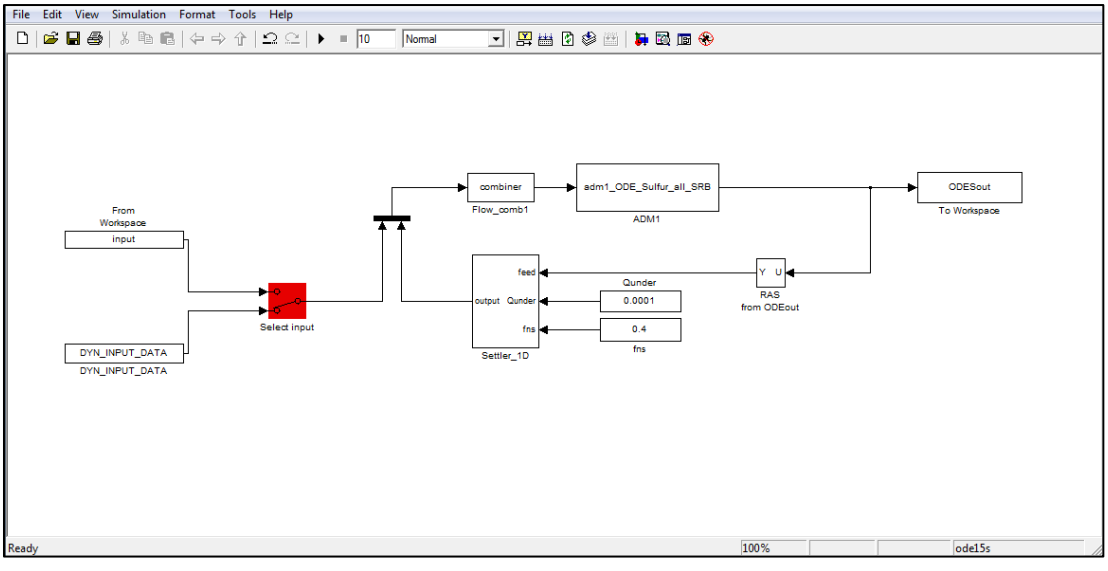

Figure C.1. Simulink architecture for steady state and dynamic simulation using ordinary differential equations (ODE)

In the schematic of Figure C.1 the following blocks can be found:

- The input blocks "input" and "DYN_INPUT_DATA" are used to run the steady state or the dynamics simulations respectively. They are connected with a "select input" block.
- The block "combiner" combines the soluble and particulate concentration of the recycling flow coming from the settler point with the soluble and particulate concentration of the influent vinasse to obtain a single stream (see the c-codes in Appendix D-2).
- The block "adm1_ODE_Sulfur_all_SRB" includes the ADM1 implementation with the addition of sulfate reduction equations (c-code Appendix D-1).
- The block "ODESout" write to the workspace the output matrix containing the soluble and particulate concentration of the reactor effluent.
- The block "RAS" select the soluble and particulate component (from ODESout) needed for the settler point implementation within the block "Settler_1D".

Appendix C. (*continued*)

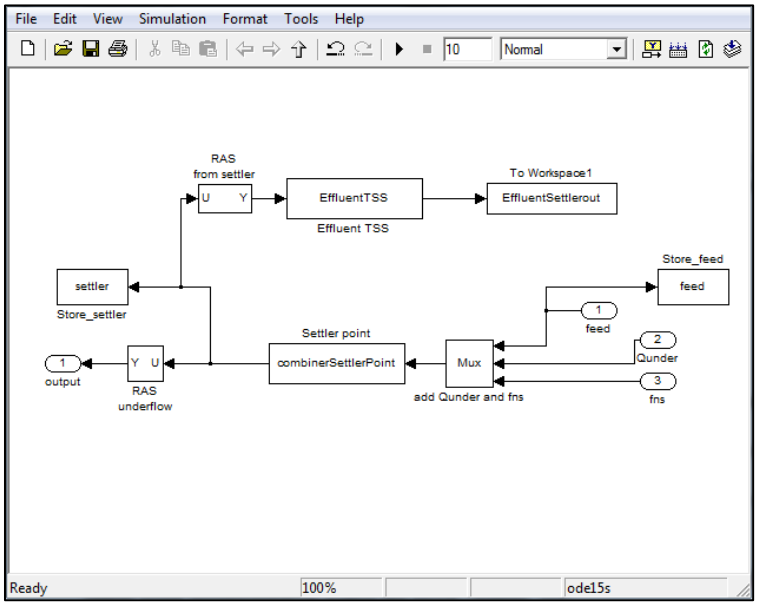

Figure C.2. Simulink architecture to model a settler point (Settler_1D)

The block Settler_1D contains a sub-model (Simulink architecture, Figure C.2) for the settler point implementation. A briefly description of the blocks included for this sub-model can be found below:

- The block "Store_feed" saves the soluble and particulate components fed to the settler point from the block "RAS".
- The block "Mux" adds the values of the recycling flow (Qunder) and the fraction of non-seatable solids (fns).
- The blocks combinerSttlerPoint contanis the c-codes for the settler point (see the c-code in Appendix D-3).
- The output (1) contains the concentrations of the soluble and particulate components recycled to the reactor bottom (underflow from the settler point).
- The block "Store_settler" storages the concentration of the soluble and particulate components leaving the settler point.
- The block "EffluentTSS" contanis c-code to calculate the total suspended solid concentration in the reactor effluent (see the c-codes in Appendix D-4).
- The block "EffluentSettlerout" storages the soluble and particulate components and the total suspended solid concentration in the outlet of the settler point.

Appendix D-1. C-code for the ADM1 (ODE implementation) extension for sulfate reduction of a very high strength and sulfate rich vinasse

```
/*
 * adm1_ODE_Sulfur_all_SRB.c is a C-file S-function for IAWQ AD Model No.
1.
 * In addition to the ADM1, 3 sulfate reduction processes are added to
model the anaerobic digestion of vinasse.
 *
 * Copyright for the Original ADM1 (2006):
 * Dr Christian Rosen, Dr Darko Vrecko and Dr Ulf Jeppsson
 * Dept. Industrial Electrical Engineering and Automation (IEA)
 * Lund University, Sweden
 * http://www.iea.lth.se/
 */
 #define S_FUNCTION_NAME adm1_ODES
 #include "simstruc.h"
 #include <math.h>
 #define XINIT   ssGetArg(S,0)
 #define PAR     ssGetArg(S,1)
 #define V       ssGetArg(S,2)
 /*
 * mdlInitializeSizes - initialize the sizes array
 */
static void mdlInitializeSizes(SimStruct *S)
{
    ssSetNumContStates(    S, 50);  /* number of continuous states
*/
    ssSetNumDiscStates(    S, 0);   /* number of discrete states
*/
    ssSetNumInputs(        S, 38);  /* number of inputs
*/
    ssSetNumOutputs(       S, 102); /* number of outputs
*/
    ssSetDirectFeedThrough(S, 1);   /* direct feedthrough flag
*/
    ssSetNumSampleTimes(   S, 1);   /* number of sample times
*/
    ssSetNumSFcnParams(    S, 3);   /* number of input arguments
*/
    ssSetNumRWork(         S, 0);   /* number of real work vector elements
*/
    ssSetNumIWork(         S, 0);   /* number of integer work vector
elements*/
    ssSetNumPWork(         S, 0);   /* number of pointer work vector
elements*/
}

/*
 * mdlInitializeSampleTimes - initialize the sample times array
 */
static void mdlInitializeSampleTimes(SimStruct *S)
{
    ssSetSampleTime(S, 0, CONTINUOUS_SAMPLE_TIME);
    ssSetOffsetTime(S, 0, 0.0);
}

/*
```

```
 * mdlInitializeConditions - initialize the states
 */
static void mdlInitializeConditions(double *x0, SimStruct *S)
{
int i;

for (i = 0; i < 50; i++) {
   x0[i] = mxGetPr(XINIT)[i];
}
}


/*
 * mdlOutputs - compute the outputs
 */
static void mdlOutputs(double *y, double *x, double *u, SimStruct *S, int
tid)
{
  double R, T_base, T_op, P_atm, p_gas_h2o, P_gas, k_P, q_gas, V_liq,
procT8, procT9, procT10, p_gas_h2, p_gas_ch4, p_gas_co2;
  double kLa, K_H_h2_base, K_H_ch4_base, K_H_co2_base, phi, S_H_ion,
pK_w_base, K_H_h2o_base, K_H_h2, K_H_ch4, K_H_co2, K_w, factor;
  double K_H_h2s_base, K_H_h2s, p_gas_h2s, procT9a; /* added for sulfate
reduction */
  int i;

  R = mxGetPr(PAR)[77];
  T_base = mxGetPr(PAR)[78];
  T_op = mxGetPr(PAR)[79];
  P_atm = mxGetPr(PAR)[93];
  p_gas_h2o = mxGetPr(PAR)[94];
  V_liq = mxGetPr(V)[0];
  kLa = mxGetPr(PAR)[95];
  K_H_h2_base = mxGetPr(PAR)[98];
  K_H_ch4_base = mxGetPr(PAR)[97];
  K_H_h2s_base = mxGetPr(PAR)[150];
  K_H_co2_base = mxGetPr(PAR)[96];
  K_H_h2o_base = mxGetPr(PAR)[95];
  pK_w_base = mxGetPr(PAR)[80];
  k_P = mxGetPr(PAR)[99];

  factor = (1.0/T_base - 1.0/T_op)/(100.0*R);
  K_H_h2 = K_H_h2_base*exp(-4180.0*factor);     /* T adjustment for K_H_h2
*/
  K_H_ch4 = K_H_ch4_base*exp(-14240.0*factor);  /* T adjustment for
K_H_ch4 */
  K_H_h2s = K_H_h2s_base*exp(-2100.0*factor); /* T adjustment for K_H_h2s
De Bruyn et al., 1995 (added for sulfate reduction) */
  K_H_co2 = K_H_co2_base*exp(-19410.0*factor);  /* T adjustment for
K_H_co2 */
  K_w = pow(10,-pK_w_base)*exp(55900.0*factor); /* T adjustment for K_w */
  p_gas_h2o = K_H_h2o_base*exp(5290.0*(1.0/T_base - 1.0/T_op));  /* T
adjustement for water vapour saturation pressure */

  for (i = 0; i < 26; i++) {
      y[i] = x[i];
  }

  y[26] = u[26];   /* flow */
```

```
  y[27] = T_op - 273.15;      /* Temp = 35 degC */

  p_gas_h2 = x[32]*R*T_op/16.0;
  p_gas_ch4 = x[33]*R*T_op/64.0;
  p_gas_co2 = x[34]*R*T_op;
  p_gas_h2s = x[42]*R*T_op; /* added for sulfate reduction */
  P_gas = p_gas_h2 + p_gas_ch4 + p_gas_co2 + p_gas_h2o + p_gas_h2s;
  q_gas = k_P*(P_gas - P_atm);
  if (q_gas < 0)
    q_gas = 0.0;

  procT8 = kLa*(x[7] - 16.0*K_H_h2*p_gas_h2);
  procT9 = kLa*(x[8] - 64.0*K_H_ch4*p_gas_ch4);
  procT9a = kLa*((x[38] - x[43]) - K_H_h2s*p_gas_h2s);
  procT10 = kLa*((x[9] - x[30]) - K_H_co2*p_gas_co2);


  phi = x[24]+(x[10]-x[31])-x[30]-x[29]/64.0-x[28]/112.0-x[27]/160.0-
x[26]/208.0-x[25]-x[43]-2*x[37]+x[44]; /* */
  S_H_ion = -phi*0.5+0.5*sqrt(phi*phi+4.0*K_w);

  y[28] = -log10(S_H_ion);     /* pH */
  y[29] = S_H_ion;             /* SH+ */
  y[30] = x[26];               /* Sva- */
  y[31] = x[27];               /* Sbu- */
  y[32] = x[28];               /* Spro- */
  y[33] = x[29];               /* Sac- */
  y[34] = x[30];               /* Shco3- */
  y[35] = x[9] - x[30];        /* SCO2 */
  y[36] = x[31];               /* Snh3 */
  y[37] = x[10] - x[31];       /* SNH4+ */
  y[38] = x[32];               /* Sgas,h2 */
  y[39] = x[33];               /* Sgas,ch4 */
  y[40] = x[34];               /* Sgas,co2 */
  y[41] = p_gas_h2;
  y[42] = p_gas_ch4;
  y[43] = p_gas_co2;
  y[44] = P_gas;        /* total head space pressure from H2, CH4, CO2 and
H2O */
  y[45] = q_gas * P_gas/P_atm; /* The output gas flow is recalculated to
atmospheric pressure (normalization) */
  y[46] = x[37];   /* S_so4 Total (added for sulfate reduction) */
  y[47] = x[38];   /* S_h2s (added for sulfate reduction) */
  y[48] = x[39];   /* X_pSRB (added for sulfate reduction) */
  y[49] = x[40];   /* X_aSRB (added for sulfate reduction) */
  y[50] = x[41];   /* X_hSRB (added for sulfate reduction) */
  y[51] = x[42];   /* S_gas_h2s (added for sulfate reduction) */
  y[52] = p_gas_h2s; /* added for sulfate reduction*/
  y[53] = x[43];     /* Shs- (added for sulfate reduction)*/
  y[54] = x[44];     /* Shso4- (added for sulfate reduction)*/
  y[55] = x[37]-x[44]; /* S_(so4)2- anions (added for sulfate reduction)*/
  y[56] = x[38]-x[43];   /* Free hydrogen sulfide (added for sulfate
reduction)*/
  y[57] = x[45];   /* Dummy state 1, soluble */
  y[58] = x[46];   /* Dummy state 2, soluble */
  y[59] = x[47];   /* Dummy state 1, particulate */
  y[60] = x[48];   /* Dummy state 2, particulate */
  y[61] = x[49];   /* Dummy state 3, particulate */
```

```
}
/*
 * mdlUpdate - perform action at major integration time step
 */
static void mdlUpdate(double *x, double *u, SimStruct *S, int tid)
{
}
/*
 * mdlDerivatives - compute the derivatives
 */
static void mdlDerivatives(double *dx, double *x, double *u, SimStruct *S,
int tid)
{

double f_sI_xc, f_xI_xc, f_ch_xc, f_pr_xc, f_li_xc, N_xc, N_I, N_aa, C_xc,
C_sI, C_ch;
double C_pr, C_li, C_xI, C_su, C_aa, f_fa_li, C_fa, f_h2_su, f_bu_su,
f_pro_su, f_ac_su;
double N_bac, C_bu, C_pro, C_ac, C_bac, Y_su, f_h2_aa, f_va_aa, f_bu_aa,
f_pro_aa, f_ac_aa;
double C_va, Y_aa, Y_fa, Y_c4, Y_pro, C_ch4, Y_ac, Y_h2;
double k_dis, k_hyd_ch, k_hyd_pr, k_hyd_li, K_S_IN, k_m_su, K_S_su,
pH_UL_aa, pH_LL_aa;
double k_m_aa, K_S_aa, k_m_fa, K_S_fa, K_Ih2_fa, k_m_c4, K_S_c4, K_Ih2_c4,
k_m_pro, K_S_pro;
double K_Ih2_pro, k_m_ac, K_S_ac, K_I_nh3, pH_UL_ac, pH_LL_ac, k_m_h2,
K_S_h2, pH_UL_h2, pH_LL_h2;
double k_dec_Xsu, k_dec_Xaa, k_dec_Xfa, k_dec_Xc4, k_dec_Xpro, k_dec_Xac,
k_dec_Xh2;
double R, T_base, T_op, pK_w_base, pK_a_va_base, pK_a_bu_base,
pK_a_pro_base, pK_a_ac_base, pK_a_co2_base, pK_a_IN_base;
double K_w, K_a_va, K_a_bu, K_a_pro, K_a_ac, K_a_co2, K_a_IN, K_H_co2,
K_H_ch4, K_H_h2;
double K_A_Bva, K_A_Bbu, K_A_Bpro, K_A_Bac, K_A_Bco2, K_A_BIN;
double P_atm, p_gas_h2o, P_gas, k_P, kLa, K_H_h2o_base, K_H_co2_base,
K_H_ch4_base, K_H_h2_base, factor;
double V_liq, V_gas;
double eps, pH_op, phi, S_H_ion;
double proc1, proc2, proc3, proc4, proc5, proc6, proc7, proc8, proc9,
proc10, proc11, proc12, proc13;
double proc14, proc15, proc16, proc17, proc18, proc19, procA4, procA5,
procA6, procA7, procA10, procA11;
double procT8, procT9, procT10;
double I_pH_aa, I_pH_ac, I_pH_h2, I_IN_lim, I_h2_fa, I_h2_c4, I_h2_pro,
I_nh3;
double reac1, reac2, reac3, reac4, reac5, reac6, reac7, reac8, reac9,
reac10, reac11, reac12, reac13;
double reac14, reac15, reac16, reac17, reac18, reac19, reac20, reac21,
reac22, reac23, reac24;
double stoich1, stoich2, stoich3, stoich4, stoich5, stoich6, stoich7,
stoich8, stoich9, stoich10, stoich11, stoich12, stoich13;
double xtemp[51], inhib[6];
double p_gas_h2, p_gas_ch4, p_gas_co2, q_gas;
double pHLim_aa, pHLim_ac, pHLim_h2, a_aa, a_ac, a_h2, n_aa, n_ac, n_h2;

/* Parameters added for sulfate reduction */
double f_ac_bu, f_h2_bu, f_ac_pro, f_h2_pro, f_ch4_ac, f_ch4_h2,
f_so4_hSRB;
double Y_hSRB, k_m_hSRB, K_S_hSRB, K_S_so4_hSRB, K_I_h2s_c4, K_I_h2s_pro;
```

```
double K_I_h2s_ac, K_I_h2s_h2, K_I_h2s_hSRB, pH_UL_hSRB;
double pH_LL_hSRB, k_dec_XhSRB, pK_a_so4_base, pK_a_h2s_base, k_A_so4,
k_A_h2s, K_H_h2s_base;
double K_a_h2s, K_a_so4, K_H_h2s, p_gas_h2s, I_pH_hSRB, pHLim_hSRB,
n_hSRB, I_h2s_c4, I_h2s_pro, I_h2s_ac, I_h2s_h2, I_h2s_hSRB;
double proc12a, proc19a, procA12, procA13, procT9a;
double stoich12a;
double reac8a, reac9a, reac23a;
double pH, SRT;
double Y_pSRB, Y_aSRB;
double f_so4_pSRB, f_so4_aSRB;
double k_m_pSRB, k_m_aSRB, K_S_pSRB, K_S_aSRB, K_S_so4_pSRB, K_S_so4_aSRB,
K_I_h2s_pSRB, K_I_h2s_aSRB;
double pH_UL_pSRB, pH_LL_pSRB, pH_UL_aSRB, pH_LL_aSRB, k_dec_XpSRB,
k_dec_XaSRB, pHLim_pSRB, n_pSRB, pHLim_aSRB, n_aSRB;
double I_pH_pSRB, I_pH_aSRB, I_h2s_pSRB, I_h2s_aSRB;
double proc10a, proc11a, proc17a, proc18a, stoich10a, stoich11a, reac21a,
reac22a;

int i;

eps = 0.000001;

f_sI_xc = mxGetPr(PAR)[0];
f_xI_xc = mxGetPr(PAR)[1];
f_ch_xc = mxGetPr(PAR)[2];
f_pr_xc = mxGetPr(PAR)[3];
f_li_xc = mxGetPr(PAR)[4];
N_xc = mxGetPr(PAR)[5];
N_I = mxGetPr(PAR)[6];
N_aa = mxGetPr(PAR)[7];
C_xc = mxGetPr(PAR)[8];
C_sI = mxGetPr(PAR)[9];
C_ch = mxGetPr(PAR)[10];
C_pr = mxGetPr(PAR)[11];
C_li = mxGetPr(PAR)[12];
C_xI = mxGetPr(PAR)[13];
C_su = mxGetPr(PAR)[14];
C_aa = mxGetPr(PAR)[15];
f_fa_li = mxGetPr(PAR)[16];
C_fa = mxGetPr(PAR)[17];
f_h2_su = mxGetPr(PAR)[18];
f_bu_su = mxGetPr(PAR)[19];
f_pro_su = mxGetPr(PAR)[20];
f_ac_su = mxGetPr(PAR)[21];
N_bac = mxGetPr(PAR)[22];
C_bu = mxGetPr(PAR)[23];
C_pro = mxGetPr(PAR)[24];
C_ac = mxGetPr(PAR)[25];
C_bac = mxGetPr(PAR)[26];
Y_su = mxGetPr(PAR)[27];
f_h2_aa = mxGetPr(PAR)[28];
f_va_aa = mxGetPr(PAR)[29];
f_bu_aa = mxGetPr(PAR)[30];
f_pro_aa = mxGetPr(PAR)[31];
f_ac_aa = mxGetPr(PAR)[32];
C_va = mxGetPr(PAR)[33];
Y_aa = mxGetPr(PAR)[34];
Y_fa = mxGetPr(PAR)[35];
```

```
Y_c4 = mxGetPr(PAR)[36];
Y_pro = mxGetPr(PAR)[37];
C_ch4 = mxGetPr(PAR)[38];
Y_ac = mxGetPr(PAR)[39];
Y_h2 = mxGetPr(PAR)[40];
k_dis = mxGetPr(PAR)[41];
k_hyd_ch = mxGetPr(PAR)[42];
k_hyd_pr = mxGetPr(PAR)[43];
k_hyd_li = mxGetPr(PAR)[44];
K_S_IN = mxGetPr(PAR)[45];
k_m_su = mxGetPr(PAR)[46];
K_S_su = mxGetPr(PAR)[47];
pH_UL_aa = mxGetPr(PAR)[48];
pH_LL_aa = mxGetPr(PAR)[49];
k_m_aa = mxGetPr(PAR)[50];
K_S_aa = mxGetPr(PAR)[51];
k_m_fa = mxGetPr(PAR)[52];
K_S_fa = mxGetPr(PAR)[53];
K_Ih2_fa = mxGetPr(PAR)[54];
k_m_c4 = mxGetPr(PAR)[55];
K_S_c4 = mxGetPr(PAR)[56];
K_Ih2_c4 = mxGetPr(PAR)[57];
k_m_pro = mxGetPr(PAR)[58];
K_S_pro = mxGetPr(PAR)[59];
K_Ih2_pro = mxGetPr(PAR)[60];
k_m_ac = mxGetPr(PAR)[61];
K_S_ac = mxGetPr(PAR)[62];
K_I_nh3 = mxGetPr(PAR)[63];
pH_UL_ac = mxGetPr(PAR)[64];
pH_LL_ac = mxGetPr(PAR)[65];
k_m_h2 = mxGetPr(PAR)[66];
K_S_h2 = mxGetPr(PAR)[67];
pH_UL_h2 = mxGetPr(PAR)[68];
pH_LL_h2 = mxGetPr(PAR)[69];
k_dec_Xsu = mxGetPr(PAR)[70];
k_dec_Xaa = mxGetPr(PAR)[71];
k_dec_Xfa = mxGetPr(PAR)[72];
k_dec_Xc4 = mxGetPr(PAR)[73];
k_dec_Xpro = mxGetPr(PAR)[74];
k_dec_Xac = mxGetPr(PAR)[75];
k_dec_Xh2 = mxGetPr(PAR)[76];
R = mxGetPr(PAR)[77];
T_base = mxGetPr(PAR)[78];
T_op = mxGetPr(PAR)[79];
pK_w_base = mxGetPr(PAR)[80];
pK_a_va_base = mxGetPr(PAR)[81];
pK_a_bu_base = mxGetPr(PAR)[82];
pK_a_pro_base = mxGetPr(PAR)[83];
pK_a_ac_base = mxGetPr(PAR)[84];
pK_a_co2_base = mxGetPr(PAR)[85];
pK_a_IN_base = mxGetPr(PAR)[86];
K_A_Bva = mxGetPr(PAR)[87];
K_A_Bbu = mxGetPr(PAR)[88];
K_A_Bpro = mxGetPr(PAR)[89];
K_A_Bac = mxGetPr(PAR)[90];
K_A_Bco2 = mxGetPr(PAR)[91];
K_A_BIN = mxGetPr(PAR)[92];
P_atm = mxGetPr(PAR)[93];
kLa = mxGetPr(PAR)[94];
```

```
K_H_h2o_base = mxGetPr(PAR)[95];
K_H_co2_base = mxGetPr(PAR)[96];
K_H_ch4_base = mxGetPr(PAR)[97];
K_H_h2_base = mxGetPr(PAR)[98];
k_P = mxGetPr(PAR)[99];
/* ADDED FOR SULFATE REDUCTION */
f_ac_bu = mxGetPr(PAR)[100];
f_h2_bu = mxGetPr(PAR)[101];
f_ac_pro = mxGetPr(PAR)[102];
f_h2_pro = mxGetPr(PAR)[103];
f_so4_pSRB = mxGetPr(PAR)[104];
f_so4_aSRB = mxGetPr(PAR)[105];
f_so4_hSRB = mxGetPr(PAR)[106];
Y_pSRB = mxGetPr(PAR)[107];
Y_aSRB = mxGetPr(PAR)[108];
Y_hSRB = mxGetPr(PAR)[109];
k_m_pSRB = mxGetPr(PAR)[110];
k_m_aSRB = mxGetPr(PAR)[111];
k_m_hSRB = mxGetPr(PAR)[112];
K_S_pSRB = mxGetPr(PAR)[113];
K_S_aSRB = mxGetPr(PAR)[114];
K_S_hSRB = mxGetPr(PAR)[115];
K_S_so4_pSRB = mxGetPr(PAR)[116];
K_S_so4_aSRB = mxGetPr(PAR)[117];
K_S_so4_hSRB = mxGetPr(PAR)[118];
K_I_h2s_c4 = mxGetPr(PAR)[119];
K_I_h2s_pro = mxGetPr(PAR)[120];
K_I_h2s_ac = mxGetPr(PAR)[121];
K_I_h2s_h2 = mxGetPr(PAR)[122];
K_I_h2s_pSRB = mxGetPr(PAR)[123];
K_I_h2s_aSRB = mxGetPr(PAR)[124];
K_I_h2s_hSRB = mxGetPr(PAR)[125];
pH_UL_pSRB = mxGetPr(PAR)[126];
pH_LL_pSRB = mxGetPr(PAR)[127];
pH_UL_aSRB = mxGetPr(PAR)[128];
pH_LL_aSRB = mxGetPr(PAR)[129];
pH_UL_hSRB = mxGetPr(PAR)[130];
pH_LL_hSRB = mxGetPr(PAR)[131];
k_dec_XpSRB = mxGetPr(PAR)[132];
k_dec_XaSRB = mxGetPr(PAR)[133];
k_dec_XhSRB = mxGetPr(PAR)[134];
pK_a_so4_base = mxGetPr(PAR)[135];
pK_a_h2s_base = mxGetPr(PAR)[136];
k_A_so4 = mxGetPr(PAR)[137];
k_A_h2s = mxGetPr(PAR)[138];
K_H_h2s_base = mxGetPr(PAR)[139];
SRT = mxGetPr(PAR)[140];

V_liq = mxGetPr(V)[0];
V_gas = mxGetPr(V)[1];

for (i = 0; i < 50; i++) {
   if (x[i] < 0)
     xtemp[i] = 0;
   else
     xtemp[i] = x[i];
}

factor = (1.0/T_base - 1.0/T_op)/(100.0*R);
```

```
K_w = pow(10,-pK_w_base)*exp(55900.0*factor); /* T adjustment for K_w */
K_a_va = pow(10,-pK_a_va_base);
K_a_bu = pow(10,-pK_a_bu_base);
K_a_pro = pow(10,-pK_a_pro_base);
K_a_ac = pow(10,-pK_a_ac_base);
K_a_co2 = pow(10,-pK_a_co2_base)*exp(7646.0*factor); /* T adjustment for
K_a_co2 */
K_a_IN = pow(10,-pK_a_IN_base)*exp(51965.0*factor); /*T adjustment for
K_a_IN */
K_a_h2s = pow(10,-pK_a_h2s_base);
K_a_so4 = pow(10,-pK_a_so4_base);
K_H_h2  = K_H_h2_base*exp(-4180.0*factor);    /* T adjustment for K_H_h2
*/
K_H_ch4 = K_H_ch4_base*exp(-14240.0*factor);  /* T adjustment for K_H_ch4
*/
K_H_co2 = K_H_co2_base*exp(-19410.0*factor);  /* T adjustment for K_H_co2
*/
K_H_h2s = K_H_h2s_base*exp(-2100.0*factor);   /* T adjustment for K_H_h2s
De Bruyn et al., 1995 (added for sulfate reduction)*/
p_gas_h2o = K_H_h2o_base*exp(5290.0*(1.0/T_base - 1.0/T_op));  /* T
adjustement for water vapour saturation pressure */
phi = xtemp[24]+(xtemp[10]-xtemp[31])-xtemp[30]-xtemp[29]/64.0-
xtemp[28]/112.0-xtemp[27]/160.0-xtemp[26]/208.0-xtemp[25]-xtemp[43]-
2*xtemp[37]+xtemp[44]; /* */
S_H_ion = -phi*0.5+0.5*sqrt(phi*phi+4.0*K_w); /* SH+ */
pH_op = -log10(S_H_ion); /* pH */
p_gas_h2 = xtemp[32]*R*T_op/16.0;
p_gas_ch4 = xtemp[33]*R*T_op/64.0;
p_gas_h2s = xtemp[42]*R*T_op; /* added for sulfate reduction */
p_gas_co2 = xtemp[34]*R*T_op;
P_gas = p_gas_h2 + p_gas_ch4 + p_gas_h2s + p_gas_co2 + p_gas_h2o;
/* Hill function on SH+ used within BSM2, ADM1 Workshop, Copenhagen 2005.
*/
pHLim_aa = pow(10,(-(pH_UL_aa + pH_LL_aa)/2.0));
pHLim_ac = pow(10,(-(pH_UL_ac + pH_LL_ac)/2.0));
pHLim_h2 = pow(10,(-(pH_UL_h2 + pH_LL_h2)/2.0));
n_aa = 3.0/(pH_UL_aa-pH_LL_aa);
n_ac = 3.0/(pH_UL_ac-pH_LL_ac);
n_h2 = 3.0/(pH_UL_h2-pH_LL_h2);
I_pH_aa = pow(pHLim_aa,n_aa)/(pow(S_H_ion,n_aa)+pow(pHLim_aa ,n_aa));
I_pH_ac = pow(pHLim_ac,n_ac)/(pow(S_H_ion,n_ac)+pow(pHLim_ac ,n_ac));
I_pH_h2 = pow(pHLim_h2,n_h2)/(pow(S_H_ion,n_h2)+pow(pHLim_h2 ,n_h2));

/* Hill function on SH+ used within BSM2, ADM1 Workshop, Copenhagen 2005.
(for pH inhibition of sulfate reducing bacteria)*/
pHLim_pSRB = pow(10,(-(pH_UL_pSRB + pH_LL_pSRB)/2.0));
n_pSRB = 3.0/(pH_UL_pSRB-pH_LL_pSRB);
I_pH_pSRB = pow(pHLim_pSRB,n_pSRB)/(pow(S_H_ion,n_pSRB)+pow(pHLim_pSRB
,n_pSRB));

pHLim_aSRB = pow(10,(-(pH_UL_aSRB + pH_LL_aSRB)/2.0));
n_aSRB = 3.0/(pH_UL_aSRB-pH_LL_aSRB);
I_pH_aSRB = pow(pHLim_aSRB,n_aSRB)/(pow(S_H_ion,n_aSRB)+pow(pHLim_aSRB
,n_aSRB));

pHLim_hSRB = pow(10,(-(pH_UL_hSRB + pH_LL_hSRB)/2.0));
n_hSRB = 3.0/(pH_UL_hSRB-pH_LL_hSRB);
I_pH_hSRB = pow(pHLim_hSRB,n_hSRB)/(pow(S_H_ion,n_hSRB)+pow(pHLim_hSRB
,n_hSRB));
```

```
I_IN_lim = 1.0/(1.0+K_S_IN/xtemp[10]);
I_h2_fa = 1.0/(1.0+xtemp[7]/K_Ih2_fa);
I_h2_c4 = 1.0/(1.0+xtemp[7]/K_Ih2_c4);
I_h2_pro = 1.0/(1.0+xtemp[7]/K_Ih2_pro);
I_nh3 = 1.0/(1.0+xtemp[31]/K_I_nh3);

/* A non-competitive inhibition function for h2s free, Knobel and Lewis,
2002 */
I_h2s_c4  = 1/(1+(xtemp[38]-xtemp[43])/K_I_h2s_c4);
I_h2s_pro = 1/(1+(xtemp[38]-xtemp[43])/K_I_h2s_pro);
I_h2s_ac  = 1/(1+(xtemp[38]-xtemp[43])/K_I_h2s_ac);
I_h2s_h2  = 1/(1+(xtemp[38]-xtemp[43])/K_I_h2s_h2);

I_h2s_pSRB = 1/(1+(xtemp[38]-xtemp[43])/K_I_h2s_pSRB);
I_h2s_aSRB = 1/(1+(xtemp[38]-xtemp[43])/K_I_h2s_aSRB);
I_h2s_hSRB = 1/(1+(xtemp[38]-xtemp[43])/K_I_h2s_hSRB);

inhib[0] = I_pH_aa*I_IN_lim;
inhib[1] = inhib[0]*I_h2_fa;
inhib[2] = inhib[0]*I_h2_c4;
inhib[3] = inhib[0]*I_h2_pro;
inhib[4] = I_pH_ac*I_IN_lim*I_nh3;
inhib[5] = I_pH_h2*I_IN_lim;

proc1 = k_dis*xtemp[12]; /* Disintegration rate of particulate matter  Xc
*/
proc2 = k_hyd_ch*xtemp[13]; /* Hydrolisis rate of carbohydrates  Xch */
proc3 = k_hyd_pr*xtemp[14]; /* Hydrolisis rate of proteins  Xpr */
proc4 = k_hyd_li*xtemp[15]; /* Hydrolisis rate of lipids  Xli */
proc5 = (k_m_su*xtemp[0]/(K_S_su+xtemp[0]))*xtemp[16]*inhib[0]; /* uptake
rate of S_su Acidogenic organism are not inhibited by H2S*/
proc6 = (k_m_aa*xtemp[1]/(K_S_aa+xtemp[1]))*xtemp[17]*inhib[0]; /* uptake
rate of S_aa Acidogenic organism are not inhibited by H2S*/
proc7 = (k_m_fa*xtemp[2]/(K_S_fa+xtemp[2]))*xtemp[18]*inhib[1]; /* uptake
rate of S_fa Acidogenic organism are not inhibited by H2S*/
proc8 =
(k_m_c4*xtemp[3]/(K_S_c4+xtemp[3]))*xtemp[19]*(xtemp[3]/(xtemp[3]+xtemp[4]
+eps))*inhib[2]*I_h2s_c4; /* uptake rate of S_va included INHIBITION of
h2s for C4 in general */
proc9 =
(k_m_c4*xtemp[4]/(K_S_c4+xtemp[4]))*xtemp[19]*(xtemp[4]/(xtemp[3]+xtemp[4]
+eps))*inhib[2]*I_h2s_c4; /* uptake rate of S_bu, including sulfide
INHIBITION for sulfate reduction implementation*/
proc10 =
(k_m_pro*xtemp[5]/(K_S_pro+xtemp[5]))*xtemp[20]*inhib[3]*I_h2s_pro; /*
uptake rate of S_pro, including sulfide INHIBITION for sulfate reduction
implementation*/
proc10a =
(k_m_pSRB*xtemp[5]/(K_S_pSRB+xtemp[5]))*(xtemp[37]/(K_S_so4_pSRB+xtemp[37]
))*xtemp[39]*I_pH_pSRB*I_h2s_pSRB*f_so4_pSRB; /* uptake rate of S_pro by
pSRB, added for sulfate reduction */
proc11 = (k_m_ac*xtemp[6]/(K_S_ac+xtemp[6]))*xtemp[21]*inhib[4]*I_h2s_ac;
/* uptake rate of S_ac, including sulfide INHIBITION for sulfate reduction
implementation*/
proc11a =
(k_m_aSRB*xtemp[6]/(K_S_aSRB+xtemp[6]))*(xtemp[37]/(K_S_so4_aSRB+xtemp[37]
))*xtemp[40]*I_pH_aSRB*I_h2s_aSRB*f_so4_aSRB; /* uptake rate of S_ac by
aSRB, added for sulfate reduction */
```

```
proc12 = (k_m_h2*xtemp[7]/(K_S_h2+xtemp[7]))*xtemp[22]*inhib[5]*I_h2s_h2;
/* uptake rate of S_h2, including sulfide INHIBITION for sulfate reduction
implementation*/
proc12a =
xtemp[41]*(k_m_hSRB*xtemp[7]/(K_S_hSRB+xtemp[7]))*(xtemp[37]/(K_S_so4_hSRB
+xtemp[37]))*I_pH_hSRB*I_h2s_hSRB*f_so4_hSRB; /* uptake rate of S_h2 by
hSRB, added for sulfate reduction */
proc13 = k_dec_Xsu*xtemp[16]; /* death rate of X_su(sugar degraders) */
proc14 = k_dec_Xaa*xtemp[17]; /* death rate of X_aa(aminoacids degraders)
*/
proc15 = k_dec_Xfa*xtemp[18]; /* death rate of X_fa(fatty acids degraders)
*/
proc16 = k_dec_Xc4*xtemp[19]; /* death rate of X_C4(butyric and valeric
degraders) */
proc17 = k_dec_Xpro*xtemp[20]; /* death rate of X_pro (propionic
degraders)*/
proc17a = k_dec_XpSRB*xtemp[39]; /* death rate of X_pSRB, added for
sulfate reduction */
proc18 = k_dec_Xac*xtemp[21]; /* death rate of X_ac(acetic degraders) */
proc18a = k_dec_XaSRB*xtemp[40]; /* death rate of X_aSRB, added for
sulfate reduction */
proc19 = k_dec_Xh2*xtemp[22]; /* death of X_h2(hydrogens degraders) */
proc19a = k_dec_XhSRB*xtemp[41];/*death of X_hSRB, added for sulfate
reduction */
procA4 = K_A_Bva*(xtemp[26]*(K_a_va+S_H_ion)-K_a_va*xtemp[3]); /* valerate
acid-base rate */
procA5 = K_A_Bbu*(xtemp[27]*(K_a_bu+S_H_ion)-K_a_bu*xtemp[4]); /* butyrate
acid-base rate */
procA6 = K_A_Bpro*(xtemp[28]*(K_a_pro+S_H_ion)-K_a_pro*xtemp[5]); /*
propionate acid-base rate  */
procA7 = K_A_Bac*(xtemp[29]*(K_a_ac+S_H_ion)-K_a_ac*xtemp[6]); /* acetate
acid-base rate */
procA10 = K_A_Bco2*(xtemp[30]*(K_a_co2+S_H_ion)-K_a_co2*xtemp[9]); /*
inorganic carbon acid-base rate */
procA11 = K_A_BIN*(xtemp[31]*(K_a_IN+S_H_ion)-K_a_IN*xtemp[10]); /*
inorganic nitrogen acid-base rate */
procA12 = k_A_h2s*(xtemp[43]*(K_a_h2s+S_H_ion)-K_a_h2s*xtemp[38]); /* h2s
acid-base rate, added for sulfate reduction */
procA13 = k_A_so4*(xtemp[37]*S_H_ion-xtemp[44]*(K_a_so4+S_H_ion)); /*
hso4- acid-base rate, added for sulfate reduction */
procT8 = kLa*(xtemp[7]-16.0*K_H_h2*p_gas_h2);
procT9 = kLa*(xtemp[8]-64.0*K_H_ch4*p_gas_ch4);
procT9a = kLa*((xtemp[38]-xtemp[43])-K_H_h2s*p_gas_h2s); /* added for
sulfate reduction */
procT10 = kLa*((xtemp[9]-xtemp[30])-K_H_co2*p_gas_co2);

stoich1 = -
C_xc+f_sI_xc*C_sI+f_ch_xc*C_ch+f_pr_xc*C_pr+f_li_xc*C_li+f_xI_xc*C_xI; /*
particulate matter */
stoich2 = -C_ch+C_su; /* carbohydrates */
stoich3 = -C_pr+C_aa; /* proteins */
stoich4 = -C_li+(1.0-f_fa_li)*C_su+f_fa_li*C_fa; /* lipids */
stoich5 = -C_su+(1.0-
Y_su)*(f_bu_su*C_bu+f_pro_su*C_pro+f_ac_su*C_ac)+Y_su*C_bac; /*
monosaccharides */
stoich6 = -C_aa+(1.0-
Y_aa)*(f_va_aa*C_va+f_bu_aa*C_bu+f_pro_aa*C_pro+f_ac_aa*C_ac)+Y_aa*C_bac;
/* amoinoacids */
stoich7 = -C_fa+(1.0-Y_fa)*0.7*C_ac+Y_fa*C_bac; /* LCFA */
```

```
stoich8 = -C_va+(1.0-Y_c4)*0.54*C_pro+(1.0-Y_c4)*0.31*C_ac+Y_c4*C_bac; /*
valeric acid */
stoich9 = -C_bu+(1.0-Y_c4)*0.8*C_ac+Y_c4*C_bac; /* butyric acid */
stoich10 = -C_pro+(1.0-Y_pro)*0.57*C_ac+Y_pro*C_bac; /* propionic acid */
stoich10a = -C_pro+(1.0-Y_pSRB)*0.57*C_ac+Y_pSRB*C_bac; /* added for
sulfate reduction */
stoich11 = -C_ac+(1.0-Y_ac)*C_ch4+Y_ac*C_bac; /* acetic acid */
stoich11a = -C_ac+Y_aSRB*C_bac; /* added for sulfate reduction */
stoich12 = (1.0-Y_h2)*C_ch4+Y_h2*C_bac; /* hydrogen */
stoich12a = Y_hSRB*C_bac; /* added for sulfate reduction */
stoich13 = -C_bac+C_xc;

reac1 = proc2+(1.0-f_fa_li)*proc4-proc5;  /* uptake of monosaccharides */
reac2 = proc3-proc6; /* uptake of aminoacids */
reac3 = f_fa_li*proc4-proc7; /* uptake of LCFA */
reac4 = (1.0-Y_aa)*f_va_aa*proc6-proc8; /* uptake of valeric */
reac5 = (1.0-Y_su)*f_bu_su*proc5+(1.0-Y_aa)*f_bu_aa*proc6-proc9; /* uptake
of butiric acid */
reac6 = (1.0-Y_su)*f_pro_su*proc5+(1.0-Y_aa)*f_pro_aa*proc6+(1.0-
Y_c4)*0.54*proc8-proc10-proc10a; /* uptake of propionic modified to add
sulfate reduction*/
reac7 = (1.0-Y_su)*f_ac_su*proc5+(1.0-Y_aa)*f_ac_aa*proc6+(1.0-
Y_fa)*0.7*proc7+(1.0-Y_c4)*0.31*proc8+(1.0-Y_c4)*0.8*proc9+(1.0-
Y_pro)*0.57*proc10-proc11+(1.0-Y_pSRB)*0.57*proc10a-proc11a; /* uptake of
acetic acid modified to add sulfate reduction */
reac8 = (1.0-Y_su)*f_h2_su*proc5+(1.0-Y_aa)*f_h2_aa*proc6+(1.0-
Y_fa)*0.3*proc7+(1.0-Y_c4)*0.15*proc8+(1.0-Y_c4)*0.2*proc9+(1.0-
Y_pro)*0.43*proc10-proc12-proc12a-procT8; /* uptake of hydrogen modified
to add sulfate reduction*/
reac8a = -(1.0-Y_hSRB)*proc12a/64-(1.0-Y_pSRB)*0.43*proc10a/64-(1.0-
Y_aSRB)*proc11a/64; /* uptake of sulfates, added for sulfate reduction*/
reac9 = (1.0-Y_ac)*proc11+(1.0-Y_h2)*proc12-procT9;  /* uptake of methane
*/
reac9a = (1.0-Y_pSRB)*0.43*proc10a/64+(1.0-Y_aSRB)*proc11a/64+(1.0-
Y_hSRB)*proc12a/64-procT9a;  /*  /* uptake H2S, added for sulfate
reduction*/
reac10 = -stoich1*proc1-stoich2*proc2-stoich3*proc3-stoich4*proc4-
stoich5*proc5-stoich6*proc6-stoich7*proc7-stoich8*proc8-stoich9*proc9-
stoich10*proc10-stoich10a*proc10a-stoich11*proc11-stoich11a*proc11a-
stoich12*proc12-stoich12a*proc12a-stoich13*proc13-stoich13*proc14-
stoich13*proc15-stoich13*proc16-stoich13*proc17-stoich13*proc17a-
stoich13*proc18-stoich13*proc18a-stoich13*proc19-stoich13*proc19a-procT10;
/*uptake inorganic carbon modified to add sulfate reduction*/
reac11 = (N_xc-f_xI_xc*N_I-f_sI_xc*N_I-f_pr_xc*N_aa)*proc1-
Y_su*N_bac*proc5+(N_aa-Y_aa*N_bac)*proc6-Y_fa*N_bac*proc7-
Y_c4*N_bac*proc8-Y_c4*N_bac*proc9-Y_pro*N_bac*proc10-Y_pSRB*N_bac*proc10a-
Y_ac*N_bac*proc11-Y_aSRB*N_bac*proc11a-Y_h2*N_bac*proc12-
Y_hSRB*N_bac*proc12a+(N_bac-
N_xc)*(proc13+proc14+proc15+proc16+proc17+proc17a+proc18+proc18a+proc19+pr
oc19a); /* uptake of inorganic nitrogen modified to add sulfate
reduction*/
reac12 = f_sI_xc*proc1; /* uptake of soluble inerts */
reac13 = -
proc1+proc13+proc14+proc15+proc16+proc17+proc17a+proc18+proc18a+proc19+pro
c19a; /* uptake of pariculate matter, modified to add sulfate reduction */
reac14 = f_ch_xc*proc1-proc2; /* uptake of carbohydrates */
reac15 = f_pr_xc*proc1-proc3; /* uptake of proteins */
reac16 = f_li_xc*proc1-proc4; /* uptake of lipids */
reac17 = Y_su*proc5-proc13; /* uptake of X_su */
```

```
reac18 = Y_aa*proc6-proc14; /* uptake of X_aa */
reac19 = Y_fa*proc7-proc15; /* uptake of X_li */
reac20 = Y_c4*proc8+Y_c4*proc9-proc16; /* uptake of X_c4 */
reac21 = Y_pro*proc10-proc17; /* uptake of X_pro */
reac21a = Y_pSRB*proc10a-proc17a; /* uptake of X_pSRB, added for sulfate
reduction */
reac22 = Y_ac*proc11-proc18; /* uptake of X_ac */
reac22a = Y_aSRB*proc11a-proc18a; /* uptake of X_aSRB, added for sulfate
reduction */
reac23 = Y_h2*proc12-proc19; /* uptake of X_h2 */
reac23a = Y_hSRB*proc12a-proc19a; /* uptake of X_hSRB, added for sulfate
reduction */
reac24 = f_xI_xc*proc1; /* uptake of X_I */

 q_gas = k_P*(P_gas-P_atm);
if (q_gas < 0)
   q_gas = 0.0;

dx[0] = 1.0/V_liq*(u[26]*(u[0]-x[0]))+reac1; /* Ssu */
dx[1] = 1.0/V_liq*(u[26]*(u[1]-x[1]))+reac2; /* Saa */
dx[2] = 1.0/V_liq*(u[26]*(u[2]-x[2]))+reac3; /* Sfa */
dx[3] = 1.0/V_liq*(u[26]*(u[3]-x[3]))+reac4; /* Sva */
dx[4] = 1.0/V_liq*(u[26]*(u[4]-x[4]))+reac5; /* Sbu */
dx[5] = 1.0/V_liq*(u[26]*(u[5]-x[5]))+reac6; /* Spro */
dx[6] = 1.0/V_liq*(u[26]*(u[6]-x[6]))+reac7; /* Sac */
dx[7] = 1.0/V_liq*(u[26]*(u[7]-x[7]))+reac8; /* Sh2 */
dx[8] = 1.0/V_liq*(u[26]*(u[8]-x[8]))+reac9; /* Sch4 */
dx[9] = 1.0/V_liq*(u[26]*(u[9]-x[9]))+reac10;    /* SIC */
dx[10] = 1.0/V_liq*(u[26]*(u[10]-x[10]))+reac11; /* SIN */
dx[11] = 1.0/V_liq*(u[26]*(u[11]-x[11]))+reac12; /* SI */

dx[12] = 1.0/V_liq*(u[26]*(u[12]-x[12]))+reac13; /*(u[12]*u[26]/V_liq)-
(x[12]/(SRT+(V_liq/u[26])))+reac13; /* Xxc */
dx[13] = 1.0/V_liq*(u[26]*(u[13]-x[13]))+reac14; /*
Xch...(u[13]*u[26]/V_liq)-(x[13]/(SRT+(V_liq/u[26]))) */
dx[14] = 1.0/V_liq*(u[26]*(u[14]-x[14]))+reac15; /* Xpr
...(u[14]*u[26]/V_liq)-(x[14]/(SRT+(V_liq/u[26])))*/
dx[15] = 1.0/V_liq*(u[26]*(u[15]-x[15]))+reac16; /*
Xli...(u[15]*u[26]/V_liq)-(x[15]/(SRT+(V_liq/u[26]))) */
dx[16] = (u[16]*u[26]/V_liq)-(x[16]/(SRT+(V_liq/u[26])))+reac17; /* Xsu
...*/
dx[17] = (u[17]*u[26]/V_liq)-(x[17]/(SRT+(V_liq/u[26])))+reac18; /* Xaa */
dx[18] = (u[18]*u[26]/V_liq)-(x[18]/(SRT+(V_liq/u[26])))+reac19; /* Xfa */
dx[19] = (u[19]*u[26]/V_liq)-(x[19]/(SRT+(V_liq/u[26])))+reac20; /* Xc4 */
dx[20] = (u[20]*u[26]/V_liq)-(x[20]/(SRT+(V_liq/u[26])))+reac21; /* Xpro
*/
dx[21] = (u[21]*u[26]/V_liq)-(x[21]/(SRT+(V_liq/u[26])))+reac22; /* Xac */
dx[22] = (u[22]*u[26]/V_liq)-(x[22]/(SRT+(V_liq/u[26])))+reac23; /* Xh2 */
dx[23] = 1.0/V_liq*(u[26]*(u[23]-x[23]))+reac24; /* XxI
...(u[23]*u[26]/V_liq)-(x[23]/(SRT+(V_liq/u[26])))*/
dx[24] = 1.0/V_liq*(u[26]*(u[24]-x[24])); /* Scat+ */
dx[25] = 1.0/V_liq*(u[26]*(u[25]-x[25])); /* San- */
dx[26] = -procA4;  /* Sva- */
dx[27] = -procA5;  /* Sbu- */
dx[28] = -procA6;  /* Spro- */
dx[29] = -procA7;  /* Sac- */
dx[30] = -procA10; /* SHCO3- */
dx[31] = -procA11; /* SNH3 */
```

```
dx[32] = -xtemp[32]*q_gas/V_gas+procT8*V_liq/V_gas;
dx[33] = -xtemp[33]*q_gas/V_gas+procT9*V_liq/V_gas;
dx[34] = -xtemp[34]*q_gas/V_gas+procT10*V_liq/V_gas;

dx[35] = 0; /* Flow */

dx[36] = 0; /* Temp */

/* ADDED for sulfate reduction */
dx[37] = 1.0/V_liq*(u[26]*(u[28]-x[37]))+reac8a;   /* S_(so4)total, added
for sulfate reduction*/
dx[38] = 1.0/V_liq*(u[26]*(u[29]-x[38]))+reac9a;   /* S_h2s, added for
sulfate reduction */
dx[39] = (u[30]*u[26]/V_liq)-(x[39]/(SRT+(V_liq/u[26])))+reac21a; /*
X_pSRB, added for sulfate reduction */
dx[40] = (u[31]*u[26]/V_liq)-(x[40]/(SRT+(V_liq/u[26])))+reac22a;   /*
X_aSRB, added for sulfate reduction */
dx[41] = (u[32]*u[26]/V_liq)-(x[41]/(SRT+(V_liq/u[26])))+reac23a;   /*
X_hSRB, added for sulfate reduction */
dx[42] = -xtemp[42]*q_gas/V_gas+procT9a*V_liq/V_gas; /* S_h2s in biogas,
added for sulfate reduction */
dx[43] = -procA12; /* acid - base rate of Shs-, added for sulfate
reduction */
dx[44] = procA13; /* acid - base rate for Shso4-, added for sulfate
reduction */

/* Dummy states */
dx[45] = 0;
dx[46] = 0;
dx[47] = 0;
dx[48] = 0;
dx[49] = 0;
}

/*
 * mdlTerminate - called when the simulation is terminated.
 */
static void mdlTerminate(SimStruct *S)
{
}

#ifdef  MATLAB_MEX_FILE    /* Is this file being compiled as a MEX-file?
*/
#include "simulink.c"      /* MEX-file interface mechanism */
#else
#include "cg_sfun.h"       /* Code generation registration function */
#endif
```

Appendix D-2. C-code to combine the streams of the recycled sludge and the influent vinasse to model the higher retention time of the sludge in the UASB reactor

```
/*
 * combiner.c calculates the concentrations when adding two flow
 * streams together. It was used to combine the stream of the recycled
sludge and the influent vinasse to model the higher retention time of the
sludge in the UASB reactor

* Copyright: Ulf Jeppsson, IEA, Lund University, Lund, Sweden
 */

#define S_FUNCTION_NAME combiner
#include "simstruc.h"

/*
 * mdlInitializeSizes - initialize the sizes array
 */
static void mdlInitializeSizes(SimStruct *S)
{
    ssSetNumContStates(    S, 0);   /* number of continuous states    */
    ssSetNumDiscStates(    S, 0);   /* number of discrete states       */
    ssSetNumInputs(        S, 71);   /* number of inputs               */
    ssSetNumOutputs(       S, 38);   /* number of outputs        */
    ssSetDirectFeedThrough(S, 1);   /* direct feedthrough flag         */
    ssSetNumSampleTimes(   S, 1);   /* number of sample times          */
    ssSetNumSFcnParams(    S, 0);   /* number of input arguments       */
    ssSetNumRWork(         S, 0); /* number of real work vector elements*/
    ssSetNumIWork(         S, 0);/* number of integer work vector
elements*/
    ssSetNumPWork(         S, 0);   /* number of pointer work vector
elements*/
}

/*
 * mdlInitializeSampleTimes - initialize the sample times array
 */
static void mdlInitializeSampleTimes(SimStruct *S)
{
    ssSetSampleTime(S, 0, CONTINUOUS_SAMPLE_TIME);
    ssSetOffsetTime(S, 0, 0.0);
}

/*
 * mdlInitializeConditions - initialize the states
 */
static void mdlInitializeConditions(double *x0, SimStruct *S)
{
}
/*
 * mdlOutputs - compute the outputs
 */
 static void mdlOutputs(double *y, double *x, double *u, SimStruct *S, int
tid)
{
  if ((u[26] > 0) || (u[64] > 0)) {
    y[0]=(u[0]*u[26] + u[38]*u[64])/(u[26]+u[64]);
    y[1]=(u[1]*u[26] + u[39]*u[64])/(u[26]+u[64]);
```

```
  y[2]=(u[2]*u[26] + u[40]*u[64])/(u[26]+u[64]);
  y[3]=(u[3]*u[26] + u[41]*u[64])/(u[26]+u[64]);
  y[4]=(u[4]*u[26] + u[42]*u[64])/(u[26]+u[64]);
  y[5]=(u[5]*u[26] + u[43]*u[64])/(u[26]+u[64]);
  y[6]=(u[6]*u[26] + u[44]*u[64])/(u[26]+u[64]);
  y[7]=(u[7]*u[26] + u[45]*u[64])/(u[26]+u[64]);
  y[8]=(u[8]*u[26] + u[46]*u[64])/(u[26]+u[64]);
  y[9]=(u[9]*u[26] + u[47]*u[64])/(u[26]+u[64]);
  y[10]=(u[10]*u[26] + u[48]*u[64])/(u[26]+u[64]);
  y[11]=(u[11]*u[26] + u[49]*u[64])/(u[26]+u[64]);
  y[12]=(u[12]*u[26] + u[50]*u[64])/(u[26]+u[64]);
  y[13]=(u[13]*u[26] + u[51]*u[64])/(u[26]+u[64]);
  y[14]=(u[14]*u[26] + u[52]*u[64])/(u[26]+u[64]);
  y[15]=(u[15]*u[26] + u[53]*u[64])/(u[26]+u[64]);
  y[16]=(u[16]*u[26] + u[54]*u[64])/(u[26]+u[64]);
  y[17]=(u[17]*u[26] + u[55]*u[64])/(u[26]+u[64]);
  y[18]=(u[18]*u[26] + u[56]*u[64])/(u[26]+u[64]);
  y[19]=(u[19]*u[26] + u[57]*u[64])/(u[26]+u[64]);
  y[20]=(u[20]*u[26] + u[58]*u[64])/(u[26]+u[64]);
  y[21]=(u[21]*u[26] + u[59]*u[64])/(u[26]+u[64]);
  y[22]=(u[22]*u[26] + u[60]*u[64])/(u[26]+u[64]);
  y[23]=(u[23]*u[26] + u[61]*u[64])/(u[26]+u[64]);
  y[24]=(u[24]*u[26] + u[62]*u[64])/(u[26]+u[64]);
  y[25]=(u[25]*u[26] + u[63]*u[64])/(u[26]+u[64]);
  y[26]=u[26] + u[64];
  y[27]=u[27];
  y[28]=(u[28]*u[26] + u[66]*u[64])/(u[26]+u[64]);
  y[29]=(u[29]*u[26] + u[67]*u[64])/(u[26]+u[64]);
  y[30]=(u[30]*u[26] + u[68]*u[64])/(u[26]+u[64]);
  y[31]=(u[31]*u[26] + u[69]*u[64])/(u[26]+u[64]);
  y[32]=(u[32]*u[26] + u[70]*u[64])/(u[26]+u[64]);
  y[33]= 0;
  y[34]= 0;
  y[35]= 0;
  y[36]= 0;
  y[37]= 0;

}
else {
  y[0]= 0;
  y[1]= 0;
  y[2]= 0;
  y[3]= 0;
  y[4]= 0;
  y[5]= 0;
  y[6]= 0;
  y[7]= 0;
  y[8]= 0;
  y[9]= 0;
  y[10]= 0;
  y[11]= 0;
  y[12]= 0;
  y[13]= 0;
  y[14]= 0;
  y[15]= 0;
  y[16]= 0;
  y[17]= 0;
  y[18]= 0;
  y[19]= 0;
```

```
    y[20]= 0;
    y[21]= 0;
    y[22]= 0;
    y[23]= 0;
    y[24]= 0;
    y[25]= 0;
    y[26]= 0;
    y[27]= 0;
    y[28]= 0;
    y[29]= 0;
    y[30]= 0;
    y[31]= 0;
    y[32]= 0;
    y[33]= 0;
    y[34]= 0;
    y[35]= 0;
    y[36]= 0;
    y[37]= 0;

  }
}

/*
 * mdlUpdate - perform action at major integration time step
 */
static void mdlUpdate(double *x, double *u, SimStruct *S, int tid)
{
}
/*
 * mdlDerivatives - compute the derivatives
 */
static void mdlDerivatives(double *dx, double *x, double *u, SimStruct *S,
int tid)
{
}

/*
 * mdlTerminate - called when the simulation is terminated.
 */
static void mdlTerminate(SimStruct *S)
{
}

#ifdef  MATLAB_MEX_FILE    /* Is this file being compiled as a MEX-file?
*/
#include "simulink.c"      /* MEX-file interface mechanism */
#else
#include "cg_sfun.h"       /* Code generation registration function */
#endif
```

Appendix D-3. C-code for the implementation of a settler point which allows for the recycling of the solids from the effluent to the reactor bottom, modeling the higher retention time of the sludge in the UASB reactor

```
/*
 * combinerSettlerPoint.c is a c-file modified from:
 *
 * Copyright: Ulf Jeppsson, IEA, Lund University, Lund, Sweden
 */ combinerSettlerPoint.c recycles the solids from the liquid effluent of
the reactor to the reactor bottom.
 *
#define S_FUNCTION_NAME combiner
#include "simstruc.h"
/*
 * mdlInitializeSizes - initialize the sizes array
 */
static void mdlInitializeSizes(SimStruct *S)
{
    ssSetNumContStates(    S, 0);   /* number of continuous states      */
    ssSetNumDiscStates(    S, 0);   /* number of discrete states        */
    ssSetNumInputs(        S, 35);   /* number of inputs                */
    ssSetNumOutputs(       S, 66);   /* number of outputs               */
    ssSetDirectFeedThrough(S, 1);   /* direct feedthrough flag          */
    ssSetNumSampleTimes(   S, 1);   /* number of sample times           */
    ssSetNumSFcnParams(    S, 0);   /* number of input arguments        */
    ssSetNumRWork(         S, 0); /* number of real work vector elements*/
    ssSetNumIWork(         S, 0); /* number of integer work vector
elements*/
    ssSetNumPWork(         S, 0);   /* number of pointer work vector
elements*/
}

/*
 * mdlInitializeSampleTimes - initialize the sample times array
 */
static void mdlInitializeSampleTimes(SimStruct *S)
{
    ssSetSampleTime(S, 0, CONTINUOUS_SAMPLE_TIME);
    ssSetOffsetTime(S, 0, 0.0);
}
/*
 * mdlInitializeConditions - initialize the states
 */
static void mdlInitializeConditions(double *x0, SimStruct *S)
{
}
/*
 * mdlOutputs - compute the outputs
 */
static void mdlOutputs(double *y, double *x, double *u, SimStruct *S, int
tid)
{
  int i;

/* Soluble compunds UNDER_FLOW */
for (i = 0; i < 12; i++) {
      y[i] = u[i];
```

```
  }
for (i = 24; i < 26; i++) {
       y[i] = u[i];
  }
y[26]=u[33]; /* Q_under sludge recycled flow*/
 y[27]=u[27]; /* Temperature */
for (i = 28; i < 30; i++) {
      y[i] = u[i];
  }
/* Particulate componets under_FLOW */
for (i = 12; i < 24; i++) {
     y[i] = u[26]*u[i]*(1-(u[34]*(u[26]-u[33])/u[26]))/u[33];
  }
for (i = 30; i < 33; i++) {
     y[i] = u[26]*u[i]*((1-u[34]*(u[26]-u[33])/u[26]))/u[33];
  }
/* Soluble compunds OUT_FLOW */
for (i = 0; i < 12; i++) {
      y[i+33] = u[i];  /* expressed as kgCOD/m3*/
  }
for (i = 24; i < 26; i++) {
       y[i+33] = u[i]; /* expressed as kmol/m3*/
  }
y[59]=u[26]-u[33];  /* Q_out flow out of the reactor*/
y[60]=u[27];        /* Temperature*/
for (i = 28; i < 30; i++) {
      y[i+33] = u[i]; /* expressed as kmol/m3*/
  }
/* Particulate componets OUT_FLOW */
for (i = 12; i < 24; i++) {
         y[i+33] = u[i]*u[34]; /*expressed as kgCOD/m3*/
  }
for (i = 30; i < 33; i++) {
        y[i+33] = u[i]*u[34]; /* expressed as kgCOD/m3*/
  }
}
/*
 * mdlUpdate - perform action at major integration time step
 */
static void mdlUpdate(double *x, double *u, SimStruct *S, int tid)
{
}
/*
 * mdlDerivatives - compute the derivatives
 */
static void mdlDerivatives(double *dx, double *x, double *u, SimStruct *S,
int tid)
{
}
* mdlTerminate - called when the simulation is terminated.
 */
static void mdlTerminate(SimStruct *S)
{
}
#ifdef  MATLAB_MEX_FILE   /* Is this file being compiled as a MEX-file? */
#include "simulink.c"      /* MEX-file interface mechanism */
#else
#include "cg_sfun.h"       /* Code generation registration function */
#endif
```

Appendix D-4. C-code to determine the total suspended solid concentration in the reactor effluent

```
/*
 * EffluentTSS.c is a c-file modified from:
 * Copyright: Ulf Jeppsson, IEA, Lund University, Lund, Sweden
 */ EffluentTSS.c contanis c-code to calculate the total suspended solid
concentration in the reactor effluent*/

#define S_FUNCTION_NAME combiner
#include "simstruc.h"
/*
 * mdlInitializeSizes - initialize the sizes array
 */
static void mdlInitializeSizes(SimStruct *S)
{
    ssSetNumContStates(    S, 0);/* number of continuous states         */
    ssSetNumDiscStates(    S, 0);/* number of discrete states           */
    ssSetNumInputs(        S, 33);/* number of inputs                   */
    ssSetNumOutputs(       S, 35);/* number of outputs                  */
    ssSetDirectFeedThrough(S, 1); /* direct feedthrough flag             */
    ssSetNumSampleTimes(   S, 1); /* number of sample times              */
    ssSetNumSFcnParams(    S, 0); /* number of input arguments           */
    ssSetNumRWork(         S, 0);/* number of real work vector elements */
    ssSetNumIWork(         S, 0);/* number of integer work vector
elements*/
    ssSetNumPWork(         S, 0);   /* number of pointer work vector
elements*/
}

/*
 * mdlInitializeSampleTimes - initialize the sample times array
 */
static void mdlInitializeSampleTimes(SimStruct *S)
{
    ssSetSampleTime(S, 0, CONTINUOUS_SAMPLE_TIME);
    ssSetOffsetTime(S, 0, 0.0);
}
/*
 * mdlInitializeConditions - initialize the states
 */
static void mdlInitializeConditions(double *x0, SimStruct *S)
{
}
/*
 * mdlOutputs - compute the outputs
 */
static void mdlOutputs(double *y, double *x, double *u, SimStruct *S, int
tid)
{
  if ((u[26] > 0) || (u[64] > 0)) {
    y[0]=u[0];
    y[1]=u[1];
    y[2]=u[2];
    y[3]=u[3];
    y[4]=u[4];
    y[5]=u[5];
    y[6]=u[6];
```

```
    y[7]=u[7];
    y[8]=u[8];
    y[9]=u[9];
    y[10]=u[10];
    y[11]=u[11];
    y[12]=u[12];
    y[13]=u[13];
    y[14]=u[14];
    y[15]=u[15];
    y[16]=u[16];
    y[17]=u[17];
    y[18]=u[18];
    y[19]=u[19];
    y[20]=u[20];
    y[21]=u[21];
    y[22]=u[22];
    y[23]=u[23];
    y[24]=u[24];
    y[25]=u[25];
    y[26]=u[26];
    y[27]=u[27];
    y[28]=u[28];
    y[29]=u[29];
    y[30]=u[30];
    y[31]=u[31];
    y[32]=u[32];
    y[33]=
0.75*(u[12]+u[13]+u[14]+u[15]+u[16]+u[17]+u[18]+u[19]+u[20]+u[21]+u[22]+u[
23]+u[30]+u[31]+u[32]); /*gTSS/L*/
    y[34]=
u[12]+u[13]+u[14]+u[15]+u[16]+u[17]+u[18]+u[19]+u[20]+u[21]+u[22]+u[23]+u[
30]+u[31]+u[32]; /*gTSS-COD/L*/;
  }
}
/*
 * mdlUpdate - perform action at major integration time step
 */
static void mdlUpdate(double *x, double *u, SimStruct *S, int tid)
{
}
/*
 * mdlDerivatives - compute the derivatives
 */
static void mdlDerivatives(double *dx, double *x, double *u, SimStruct *S,
int tid)
{
}
/*
 * mdlTerminate - called when the simulation is terminated.
 */
static void mdlTerminate(SimStruct *S)
{
}
#ifdef  MATLAB_MEX_FILE    /* Is this file being compiled as a MEX-file?
*/
#include "simulink.c"      /* MEX-file interface mechanism */
#else
#include "cg_sfun.h"       /* Code generation registration function */
#endif
```

Appendix E. Input values for soluble and particulate components used for the dynamic simulations

This appendix depicts the ADM1 input values used during the dynamic simulations. The nomenclature is used according to the original ADM1 report (Batstone et al., 2002).

Table E.1. Dynamic input used in the model (E-1 values were used for steady state simulation)

Exp	Days	S_{su}	S_{aa}	S_{fa}	S_{va}	S_{bu}	S_{pro}	S_{ac}	S_{h2}	S_{ch4}	S_{IC}	S_{IN}	S_I	X_{xc}	X_{ch}	X_{pr}	X_{li}
E-1	0-7	19.67	3.4	0.05	0	0.0082	0.0014	0.793	1.00e-08	0.00018	0	0.00018	10.33	0	4.03	0.05	0.08
E-2	8 - 15	24.84	4.29	0.06	0	0.0104	0.0018	1.001	1.26e-08	0.00023	0	0.00023	12.50	0	5.09	0.07	0.11
E-3	16 -26	30.01	5.18	0.08	0	0.0125	0.0022	1.210	1.53e-08	0.00027	0	0.00027	15.76	0	6.15	0.08	0.13
E-4	27 - 36	19.67	3.40	0.05	0	0.0082	0.0014	0.793	1.00e-08	0.00018	0	0.00018	10.33	0	4.03	0.05	0.08
E-5	37 - 45	24.84	4.29	0.06	0	0.0104	0.0018	1.001	1.26e-08	0.00023	0	0.00023	13.04	0	5.09	0.07	0.11
E-6	46 - 49	28.98	5.00	0.07	0	0.0121	0.0021	1.168	1.47e-08	0.00027	0	0.00026	14.58	0	5.94	0.08	0.12
E-7	50 - 58	24.84	4.29	0.06	0	0.0104	0.0018	1.001	1.26e-08	0.00023	0	0.00023	13.04	0	5.09	0.07	0.11
E-8	59 - 68	19.67	3.40	0.05	0	0.0082	0.0014	0.793	1.00e-08	0.00018	0	0.00018	10.33	0	4.03	0.05	0.08
E-9	69 - 75	19.67	3.40	0.05	0	0.0082	0.0014	0.7930	1.00e-08	0.00018	0	0.00018	10.33	0	4.03	0.05	0.08

Table E.1. (*continued*)

Exp	Days	X_{su}	X_{aa}	X_{fa}	X_{c4}	X_{pro}	X_{ac}	X_{h2}	X_I	S_{cat}	S_{an}	Q_{gas}	T	S_{so42-}	S_{h2s}	X_{pSRB}	X_{aSRB}	X_{hSRB}
E-1	0-7	0	0.0100	0.0100	0.0100	0.0100	0.0100	0.0100	0	0.200	0.042	0.00072	35	0.0182	0	0	0	0
E-2	8 - 15	0	0.0129	0.0129	0.0129	0.0129	0.0129	0.0129	0	0.258	0.054	0.00072	35	0.0229	0	0	0	0
E-3	16 -26	0	0.0156	0.0156	0.0156	0.0156	0.0156	0.0156	0	0.312	0.065	0.00072	35	0.0277	0	0	0	0
E-4	27 - 36	0	0.0100	0.0100	0.0100	0.0100	0.0100	0.0100	0	0.239	0.042	0.00072	35	0.0380	0	0	0	0
E-5	37 - 45	0	0.0129	0.0129	0.0129	0.0129	0.0129	0.0129	0	0.302	0.054	0.00072	35	0.0479	0	0	0	0
E-6	46 - 49	0	0.0151	0.0151	0.0151	0.0151	0.0151	0.0151	0	0.352	0.062	0.00072	35	0.0573	0	0	0	0
E-7	50 - 58	0	0.0129	0.0129	0.0129	0.0129	0.0129	0.0129	0	0.302	0.054	0.00072	35	0.0479	0	0	0	0
E-8	59 - 68	0	0.0100	0.0100	0.0100	0.0100	0.0100	0.0100	0	0.281	0.042	0.00072	35	0.0589	0	0	0	0
E-9	69 - 75	0	0.0100	0.0100	0.0100	0.0100	0.0100	0.0100	0	0.319	0.042	0.00072	35	0.0781	0	0	0	0

Appendix F. Stoichiometric and kinetic parameters selected for sensitivity analysis. Values reported in literature and calibrated for this work.

This appendix shows the paremeter (including names, nomenclature and units) values reported in literature and calibrated for this work (with the confidence intervals)

Parameter	Names	Units	Benchmark values (1)	Cane-molasses (2)	Sulfate reduction (3)	Calibration this work	CI (95%)
Y_{su}	Yield of sugar degraders (X_{su})	kg COD_X_{su} kg COD_S_{su}^{-1}	0.100			0.100	
Y_{aa}	Yield of amino acids degraders (X_{aa})	kg COD_X_{aa} kg COD_S_{aa}^{-1}	0.080			0.080	
Y_{fa}	Yield of LCFA degraders (X_{fa})	kg COD_X_{fa} kg COD_S_{fa}^{-1}	0.060			0.060	
Y_{c4}	Yield of valerate and butyrate degraders (X_{c4})	kg COD_X_{c4} kg COD_$S_{va\ \&\ bu}^{-1}$	0.060			0.060	
Y_{pro}	Yield of propionate degraders (X_{pro})	kg COD_X_{pro} kg COD_S_{pro}^{-1}	0.040			0.040	
Y_{ac}	Yield of acetate degraders (X_{ac})	kg COD_X_{ac} kg COD_S_{ac}^{-1}	0.050			0.050	
Y_{h2}	Yield of hydrogen degraders (X_{h2})	kg COD_X_{h2} kg COD_S_{h2}^{-1}	0.060			0.070	±0.0042
Y_{pSRB}	Yield of pSRB (X_{pSRB})	kg COD_X_{pSRB} kg COD_S_{pro}^{-1}	0.0329[a]		0.027 - 0.035	0.035	±0.0040
Y_{aSRB}	Yield of aSRB (X_{aSRB})	kg COD_X_{aSRB} kg COD_S_{ac}^{-1}	0.0342[a]		0.033 - 0.041	0.041	±0.0060
Y_{hSRB}	Yield of hSRB (X_{hSRB})	kg COD_X_{hSRB} kg COD_S_{h2}^{-1}	0.0366[a]		0.037 - 0.077	0.051	±0.0047
$k_{m,su}$	Monod maximum specific uptake rate of sugars by X_{su}	kg COD_S_{su} kg COD_X_{su}^{-1} d^{-1}	30			30	
$k_{m,fa}$	Monod maximum specific uptake rate of LCFA by X_{aa}	kg COD_S_{fa} kg COD_X_{fa}^{-1} d^{-1}	6			6	
$k_{m,c4}$	Monod maximum specific uptake rate of HVa & HBu by X_{c4}	kg COD_$S_{va\ \&\ bu}$ kg COD_X_{c4}^{-1} d^{-1}	20			20	
$k_{m,pro}$	Monod maximum specific uptake rate of HPr by X_{pro}	kg COD_S_{pro} kg COD_X_{pro}^{-1} d^{-1}	13	15		16	±1.21
$k_{m,ac}$	Monod maximum specific uptake rate of HAc by X_{ac}	kg COD_S_{ac} kg COD_X_{ac}^{-1} d^{-1}	8	9.4		12	±0.73
$k_{m,h2}$	Monod maximum specific uptake rate of H_2 by X_{h2}	kg COD_S_{h2} kg COD_X_{h2}^{-1} d^{-1}	35	43		43	±4.26
$k_{m,pSRB}$	Monod maximum specific uptake rate of HPr by pSRB	kg COD_S_{pro} kg COD_X_{pSRB}^{-1} d^{-1}	12.6[a]		9.60 - 23.1	23	±2.35
$k_{m,aSRB}$	Monod maximum specific uptake rate of HAc by aSRB	kg COD_S_{ac} kg COD_X_{aSRB}^{-1} d^{-1}	7.1[a]		4.19 - 18.5	18.5	±2.32
$k_{m,hSRB}$	Monod maximum specific uptake rate of H_2 by hSRB	kg COD_S_{h2} kg COD_X_{hSRB}^{-1} d^{-1}	26.7[a]		26.7 - 64.9	63	±7.81
$k_{dec,Xac}$	First order decay rate for X_{ac}	d^{-1}	0.020			0.020	

(1) Rosen and Jeppsson (2006); (2) Romli et al. (1995); (2) Barrera et al. (2013); [a] Fedorovich et al. (2003); [b] Batstone et al. (2006); CI: confidence interval

Appendix F. (*continued*)

Parameter	Names	Units	Benchmark values (1)	Cane-molasses (2)	Sulfate reduction (3)	Calibration this work	CI (95%)
$k_{dec,Xh2}$	First order decay rate for X_{h2}	d^{-1}	0.020			0.020	
$K_{S,su}$	Half saturation coefficient for the uptake of sugars by X_{su}	kg COD_S_{su} m^{-3}	0.500			0.500	
$K_{S,aa}$	Half saturation coefficient for the uptake of amino acids by X_{aa}	kg COD_S_{aa} m^{-3}	0.300			0.300	
$K_{S,c4}$	Half saturation coefficient for the uptake of HVa & HBu by X_{c4}	kg COD_S_{fa} m^{-3}	0.200			0.200	
$K_{S,pro}$	Half saturation coefficient for the uptake of HPr by X_{pro}	kg COD_S_{pro} m^{-3}	0.100			0.100	
$K_{S,ac}$	Half saturation coefficient for the uptake of HAc by X_{ac}	kg COD_S_{ac} m^{-3}	0.150			0.150	
$K_{S,h2}$	Half saturation coefficient for the uptake of H_2 by X_{h2}	kg COD_S_{h2} m^{-3}	7.0e-6			7.0e-6	
$K_{S,pSRB}$	Half saturation coefficient for the uptake of HPr by pSRB	kg COD_S_{pro} m^{-3}	0.110[a]		0.015 - 0.295	0.110	±0.010
$K_{S,aSRB}$	Half saturation coefficient for the uptake of HAc by aSRB	kg COD_S_{ac} m^{-3}	0.220[a]		0.024 - 0.220	0.120	±0.015
$K_{S,hSRB}$	Half saturation coefficient for the uptake of H_2 by hSRB	kg COD_S_{h2} m^{-3}	0.000100[a]		4.0e-6[b] – 1.0e-4	6e-06	±6.2e-7
$K_{S,so4,pSRB}$	Half saturation coefficient for the uptake of SO_4^{2-} by pSRB	kmol m^{-3}	0.000200[a]		7.7e-5 – 2.0e-4	0.00200	±0.00039
$K_{S,so4,aSRB}$	Half saturation coefficient for the uptake of SO_4^{2-} by aSRB	kmol m^{-3}	0.000100[a]		1.0e-4 – 2.9e-4	0.00100	±0.00023
$K_{S,so4,hSRB}$	Half saturation coefficient for the uptake of SO_4^{2-} by hSRB	kmol m^{-3}	0.000104[a]		9.0e-6 – 1.0e-4	0.00105	±0.00017
$K_{I,h2s,c4}$	50% inhibitory concentration of free H_2S for X_{c4}	kmol m^{-3}	0.00750[a]		0.0075[a]	0.00440	±0.00065
$K_{I,h2s,pro}$	50% inhibitory concentration of free H_2S for X_{pro}	kmol m^{-3}	0.00750[a]		0.0075[a]	0.00280	±0.00048
$K_{I,h2s,ac}$	50% inhibitory concentration of free H_2S for X_{ac}	kmol m^{-3}	0.00720[a]		0.0072[a]	0.00440	±0.00053
$K_{I,h2s,h2}$	50% inhibitory concentration of free H_2S for X_{h2}	kmol m^{-3}	0.00630[a]		0.0063[a]	0.00440	±0.00075
$K_{I,h2s,pSRB}$	50% inhibitory concentration of free H_2S for pSRB	kmol m^{-3}	0.00813[a]		0.0058 – 0.0089	0.00480	±0.00086
$K_{I,h2s,aSRB}$	50% inhibitory concentration of free H_2S for aSRB	kmol m^{-3}	0.00780[a]		0.0051 – 0.018	0.00470	±0.00028
$K_{I,h2s,hSRB}$	50% inhibitory concentration of free H_2S for hSRB	kmol m^{-3}	0.00780[a]		0.0078 – 0.017	0.00470	±0.00083

(1) Rosen and Jeppsson (2006); (2) Romli et al. (1995); (3) Barrera et al. (2013); [a] Fedorovich et al. (2003); [b] Batstone et al. (2006); CI: confidence interval

Appendix G. Life cycle inventory (LCI) for scenarios 1 and 2

This appendix shows the inputs and outpus from/to the technosphere and the ecosphere for the scenarios considered in Chapter 4

	Units	A-1	A-2	A-3	A-4	A-5	A-6	A-7	A-8	A-9	A-10
Inputs from the technosphere											
Influent vinasse (48 kg COD/m3)	ton	1072	1072	1072	1072	1072	1072	1072	1072	1072	1072
Water (30 º C)	ton	995	995	995	0.00	0.00	0.00	995	995	995	0
CaO (85%)	ton	3.84	3.84	3.84	0.00	0.00	0.00	3.84	3.84	3.84	0.00
SWW	ton	398	398	398	398	398	398	398	398	398	398
Chemicals (Fe III EDTA or $Fe_2(SO_4)_3$)	ton	0.281	0.281	0.258	0.255	0.255	0.240	0.0068	0.0068	0.0064	0.0063
Inputs from the ecosphere											
Oxygen in air	ton	145	145	145	135	135	135	145	145	145	135
Land used	m^2	46642	46642	46642	40076	40076	40076	46642	46642	46643	40076
Inputs of energy											
Electricity	MWh	16.96	16.96	16.89	7.60	7.60	7.54	16.26	16.26	16.19	6.91
Heat	MWh	33.88	33.88	33.88	8.71	8.71	8.71	34.10	34.10	34.02	8.92
Outputs to the technosphere: Products											
Electricity	MWh	45.29	33.50	8.58	42.07	31.11	7.96	45.29	33.50	8.58	42.07
Heat	MWh	44.06	51.42	98.91	40.93	47.76	91.86	44.06	51.42	98.91	40.93
Ferti-irrigation water	ton	2431	2431	2431	1429	1429	1429	2431	2431	2431	1429
Sulfur as fertilizer	ton	0.75	0.75	0.72	0.75	0.75	0.73	0.75	0.75	0.72	0.75
Organic carbon as fertilizer	ton	4.04	4.04	4.04	5.50	5.50	5.50	4.04	4.04	4.04	5.50
Outputs to the ecosphere: emissions to soil											
Chemicals (Iminodiacetic acid (IDA) as EDTA)	ton	0.23	0.23	0.22	0.22	0.22	0.20	0.00	0.00	0.00	0,00
Chemicals (Fe III EDTA or $Fe_2(SO_4)_3$)	ton	0.0065	0.0065	0.0061	0.0060	0.0060	0.0057	0.0068	0.0068	0.0064	0.0063
Outputs to the ecosphere: emissions to air											
Sulfur as SO_2	ton	0.0058	0.0058	0.0586	0.0052	0.0052	0.0522	0.0058	0.0058	0.0586	0.0052
Methane	ton	1.79	1.79	1.79	1.64	1.64	1.64	1.79	1.79	1.79	1.64
Carbon dioxide	ton	39.60	39.60	39.60	36.76	36.76	36.76	39.60	39.60	39.60	36.76
Hydrogen sulfide	ton	0.00	0.00	0.00	0.00	0.00	0.00	0.00	0.00	0.00	0.00

Appendix G. (*continued*)

	Units	A-11	A-12	A-13	A-14	A-15	A-16	A-17	A-18	Scenario 1
Inputs from the technosphere										
Influent vinasse (48 kg COD m^{-3})	ton	1072	1072	1072	1072	1072	1072	1072	1072	1072
Water	ton	0	0	995	995	995	0	0	0	0
CaO (85%)	ton	0.00	0.00	3.84	3.84	3.84	0.00	0.00	0.00	0.00
SWW	ton	398	398	398	398	398	398	398	398	398
Chemicals (Fe III EDTA or $Fe_2(SO_4)_3$)	ton	0.0063	0.0059	0.000	0.000	0.000	0.000	0.000	0.000	0.00
Inputs from the ecosphere										
Oxygen in air	ton	135	135	145	145	145	135	135	135	0
Land used	m^2	40076	40076	46637	46637	46637	40071	40071	40071	83899
Inputs of energy										
Electricity	MWh	6.91	6.86	14.45	14.45	14.43	5.10	5.10	5.08	5.06
Heat	MWh	8.92	8.87	33.88	33.88	33.88	8.71	8.71	8.71	0.00
Outputs to the technosphere: products										
Electricity	MWh	31.11	7.96	45.29	33.50	8.58	42.07	31.11	7.96	0.00
Heat	MWh	47.76	91.86	44.06	51.42	98.91	40.93	47.76	91.86	0.00
Ferti-irrigation water	ton	1429	1429	2431	2431	2431	1429	1429	1429	1393
Sulfur as fertilizer	ton	0.75	0.73	0.75	0.75	0.72	0.75	0.75	0.73	0.43
Organic carbon as fertilizer	ton	5.50	5.50	4.04	4.04	4.04	5.50	5.50	5.50	12.56
Outputs to the ecosphere: emissions to soil										
Chemicals (Iminodiacetic acid (IDA) as EDTA)	ton	0.00	0.00	0.00	0.00	0.00	0.00	0.00	0.00	0.00
Chemicals (Fe III EDTA or $Fe_2(SO_4)_3$)	ton	0.0063	0.0059	0.0000	0.0000	0.0000	0.000	0.000	0.000	0.00
Outputs to the ecosphere: emissions to air										
Sulfur as SO_2	ton	0.0052	0.0522	0.0058	0.0058	0.0585	0.0052	0.0052	0.0522	0.00
Methane	ton	1.64	1.64	1.79	1.79	1.79	1.64	1.64	1.64	4.80
Carbon dioxide	ton	36.76	36.77	39.60	39.60	39.61	36.76	36.76	36.77	3.43
Hydrogen sulfide	ton	0.00	0.00	0.00	0.00	0.00	0.00	0.00	0.00	0.46

REFERENCES

Abatzoglou, N., Boivin, S. 2009. A review of biogas purification processes. *Biofuels Bioproducts and Biorefining*, **3**(1), 42-71.

Afrane, G., Ntiamoah, A. 2011. Comparative Life Cycle Assessment of Charcoal, Biogas, and Liquefied Petroleum Gas as Cooking Fuels in Ghana. *Journal of Industrial Ecology*, **15**(4), 539-549.

Aiyuk, S., Amoako, J., Raskin, L., Van Haandel, A., Verstraete, W. 2004. Removal of carbon and nutrients from domestic wastewater using a low investment, integrated treatment concept. *Water Research*(38), 3031–3042.

Alphenaar, P., Visser, A., Lettinga, G. 1993. The effect of liquid upward velocity and hydraulic retention time on granulation in UASB reactors treating wastewater with a high sulphate content. *Bioresource Technology*, **43**(3), 249-258.

Alvarenga, R.A.F., Dewulf, J., Langenhove, H.V., Huijbregts, M.A.J. 2013. Exergy-based accounting for land as a natural resource in life cycle assessment. *International Journal of Life Cycle Assessment*, **18**, 939-947.

Annachhatre, A.P., Suktrakoolvait, S. 2001. Biological Sulfate Reduction Using Molasses as a Carbon Source. *Water Environment Research*, **73**(1), 118-126.

Aye, L., Widjaya, E.R. 2006. Environmental and economic analyses of waste disposal options for traditional markets in Indonesia. *Waste Management*, **26**, 1180–1191.

Azapagic, A. 1999. Life cycle assessment and its application to process selection, design and optimisation. *Chemical Engineering Journal*, **73**, 1-21.

Banerjee, S., Biswas, G.K. 2004. Studies on biomethanation of distillery wastes and its mathematical analysis. *Chemical Engineering Journal*, **102**(2), 193-201.

Barrera, E.L., Spanjers, H., Dewulf, J., Romero, O., Rosa, E. 2013. The sulfur chain in biogas production from sulfate-rich liquid substrates: a review on dynamic modeling with vinasse as model substrate. *Journal of Chemical Technology and Biotechnology*, **88**, 1405–1420.

Barrera, E.L., Spanjers, H., Romero, O., Rosa, E., Dewulf, J. 2014. Characterization of the sulfate reduction process in the anaerobic digestion of a very high strength and sulfate rich vinasse. *Chemical Engineering Journal*, **248**, 383–393.

Batstone, D. 2006. Mathematical Modelling of Anaerobic Reactors Treating Domestic Wastewater: Rational Criteria for Model Use. *Reviews in Environmental Science and Biotechnology*, **5**(1), 57-71.

Batstone, D.J. 2013. Modelling and control in anaerobic digestion: achievements and challenges. *13th World Congress on Anaerobic Digestion*, 25-28th June, 2013, Santiago de Compostela. Spain.

Batstone, D.J., Hernandez, J.L.A., Schmidt, J.E. 2005. Hydraulics of laboratory and full-scale upflow anaerobic sludge blanket (UASB) reactors. *Biotechnology and Bioengineering*, **91**(3), 387-391.

Batstone, D.J., Keller, J. 2003. Industrial applications of the IWA anaerobic digestion model No. 1 (ADM1). *Water Science and Technology*, **47**(12), 199-206.

Batstone, D.J., Keller, J., Angelidaki, I., Kalyuzhnyi, S.V., Pavlostathis, S.G., Rozzi, A., Sanders, W.T.M., Siegrist, H., Vavilin, V.A. 2002. *The IWA Anaerobic Digestion Model No 1, Scientific and Technical Report No. 13*. IWA Publishing, London.

Batstone, D.J., Keller, J., Steyer, J.P. 2006. A review of ADM1 extensions, applications, and analysis: 2002-2005. *Water Science and Technology*, **54**(4), 1-10.

Batstone, D.J., Pind, P.F., Angelidaki, I. 2003. Kinetics of thermophilic, anaerobic oxidation of straight and branched chain butyrate and valerate. *Biotechnology and Bioengineering*, **84**(2), 195-204.

Bremner, J.M., Keeney, R.D. 1965. Steam distillation methods for determination of ammonium, nitrate and nitrite. *Analytica Chimica Acta*, **32**, 485-495.

Budzianowski, W.M. 2011. Can 'negative net CO_2 emissions' from decarbonised biogas-to-electricity contribute to solving Poland's carbon capture and sequestration dilemmas? *Energy*, **36**, 6318-6325.

Casas, Y. 2012. Introduction of advanced technology (Solid Oxide Fuel Cell) in the sugar cane industry: technical and sustainability analysis. Doctoral thesis in Applied Biological Sciences. Gent University. Belgium.

Casas, Y., Dewulf, J., Arteaga-Pérez, L., Morales, M., Langenhove, H., Rosa, E. 2011. Integration of Solid Oxide Fuel Cell in a sugareethanol factory: analysis of the efficiency and the environmental profile of the products. *Journal of Cleaner Production*, **19**, 1395 -1404.

Chen, D., Martell, A., McManus, D. 1995. Studies on the mechanism of chelate degradation in iron-based, liquid redox H,S removal processes. *Canadian Journal of Chemistry*, **73**, 264-274.

Chen, H., Zhu, Q., Peng, C., Wu, N., Wang, Y., Fang, X., Jiang, H., Xiang, W., Chang, J., Deng, X., Yu, G. 2013. Methane emissions from rice paddies natural wetlands, and lakes in China: synthesis and new estimate. *Global Change Biology*, **19**, 19–32.

Chen, Y., Cheng, J.J., Creamer, K.S. 2008. Inhibition of anaerobic digestion process: A review. *Bioresource Technology*, **99**, 4044–4064.

Clesceri, L.S., Greenberg, A.E., Eaton, A.D. 1999. *The Standard Methods for the Examination of Water and Wastewater*. 20 ed., American Public Health Association, Washington, DC.

Cline, C., Hoksberg, A., Abry, R., Janssen, A. 2003. Biological process for H_2S removal from gas streams the Shell-Paques/THIOPAQ^{TM} gas desulfurization process, Paper for the LRGCC, 23 –26 February 2003, Norman (Oklahoma), USA.

Constantino, G.C., Higa, M. 2011. Thermal analysis in cogeneration plant using biogas in sugar cane industry. *21st Brazilian Congress of Mechanical Engineering*, Natal, RN, Brazil.

Contreras, A.M. 2007. Metodologia para el analisis de ciclo de vida combinado con el analisis exergetico en la industria azucarera cubana. Doctoral thesis. Las Villas Central University, Villa Clara. Cuba.

Contreras, A.M., Domínguez, R., Van Langenhove, H., Herrero, S., Gil, P., Ledón, C., Dewulf, J. 2013. Exergetic analysis in cane sugar production in combination with Life Cycle Assessment. *Journal of Cleaner Production*, **59**, 43-50.

Contreras, A.M., Rosa, E., Perez, M., Langenhove, H.V., Dewulf, J. 2009. Comparative Life Cycle Assessment of four alternatives for using by-products of cane sugar production. *Journal of Cleaner Production*, **17**, 772–779.

De Meester, S., Demeyer, J., Velghe, F., Peene, A., Van Langenhove, H., Dewulf, J. 2012. The environmental sustainability of anaerobic digestion as a biomass valorization technology. *Bioresource Technology*, **121**, 396–403.

Demirel, B., Yenigün, O. 2002. The effects of change in volatile fatty acid (VFA) composition on methanogenic upflow filter reactor (UFAF) performance. *Environmental Technology*, **Oct 23**(10), 1179-1187.

Demmink, J.F., Beenackers, A. 1997. Oxidation of ferrous nitrilotriacetic acid with oxygen: A model for oxygen mass transfer parallel to reaction kinetics. *Industrial and Engineering Chemistry Reserach*, **36**(6), 1989-2005.

Demmink, J.F., Beenackers, A.A.C.M. 1998. Gas Desulfurization with Ferric Chelates of EDTA and HEDTA: New Model for the Oxidative Absorption of Hydrogen Sulfide. *Industrial and Engineering Chemistry Research*, **37**(4), 1444-1453.

Dereli, R.K., Ersahin, M.E., Ozgun, H., Ozturk, I., Aydin, A.F. 2010. Applicability of Anaerobic Digestion Model No. 1 (ADM1) for a specific industrial wastewater: Opium alkaloid effluents. *Chemical Engineering Journal*, **165**(1), 89-94.

Devinny, S.J., Ramesh, J. 2005. A phenomenological review of biofilter models. *Chemical Engineering Journal*, **113**(2-3), 187-196.

Dewulf, J., Bosch, M.E., Demeester, B., Vandervors, T.G., Vanlangenhove, H., Hellweg, G.S., Huijbregts, M.A.J. 2007. Cumulative Exergy Extraction from the Natural Environment (CEENE): a comprehensive Life Cycle Impact Assessment method for resource accounting. *Enrironmental Science and Technology*, **41**(24), 8477–8483.

Dewulf, J., Langenhove, H.V., Muys, B., Bruers, S., Bakshi, B.R., Grubb, G.F., Paulus, D.M., Sciubba, E. 2008. Exergy: Its Potential and Limitations in Environmental Science and Technology. *Environmental Science and Technology*, **42**(7), 2221-2232.

Dochain, D., Vanrolleghem, P.A. 2001. *Dynamical Modelling and Estimation in Wastewater Treatment Processes*. IWA Publishing, London, UK.

Donoso-Bravo, A., Mailier, J., Martin, C., Rodríguez, J., Aceves-Lara, C.A., Wouwer, A.V. 2011. Model selection, identification and validation in anaerobic digestion: A review. *Water Research*, **45**(17), 5347-5364.

Driessen, W., Tielbaard, M.H., Vereijken, T. 1994. Experience on anaerobic treatment of distillery effluent with the UASB process. *Water Science and Technology*, **30**(12), 193-201.

Ebrahimi, S., Kleerebezem, R., van Loosdrecht, M.C.M., Heijnen, J.J. 2003. Kinetics of the reactive absorption of hydrogen sulfide into aqueous ferric sulfate solutions. *Chemical Engineering Science*, **58**(2), 417-427.

Egan, H., Kirk, R., Sawyer, R. 1981. Pearson's Chemical Analysis of Foods. 8th edition. Churchill Livingstone, Edingburgh. *Deutsche Lebensmittel-Rundschau*, **3**(69), 20-115.

Erdirencelebi, D., Ozturk, I., Cokgor, E.U. 2007. System Performance in UASB Reactors Receiving Increasing Levels of Sulfate. *Clean Journal*, **35**(3), 275–281.

Espinosa, A., Rosas, L., Ilangovan, K., Noyola, A. 1995. Effect of trace metals on the anaerobic degradation of volatile fatty acids in molasses stillage. *Water Science and Technology*, **32**(12), 121-129.

European-Commission. 2010a. Joint Research Centre. Institute for Environment and Sustainability. International Reference Life Cycle Data System (ILCD) Handbook – general guide for life cycle assessment – detailed guidance, first ed. Publications Office of the European Union, Luxembourg.

European-Commission. 2010b. Joint Reserach Centre. Institute for Environmental and Sustainbility. ILCD Handbook: Analysis of existing Environmental Impact Assessment methodologies for use in Life Cycle Assessment.

Fdz-Polanco, F., Fdz-Polanco, M., Fernandez, N., Urueña, M.A., Garcia, P.A., Villaverde, S. 2001. New process for simultaneous removal of nitrogen and sulphur under anaerobic conditions. *Water Research*, **35**(4), 1111-1114.

Fedorovich, V., Lens, P., Kalyuzhnyi, S. 2003. Extension of Anaerobic Digestion Model No. 1 with Processes of Sulfate Reduction. *Applied Biochemestry and Biotechnology*, **109**, 33-45.

Fezzani, B., Cheikh, R.B. 2008. Implementation of IWA anaerobic digestion model No. 1 (ADM1) for simulating the thermophilic anaerobic co-digestion of olive mill wastewater with olive mill solid waste in a semi-continuous tubular digester. *Chemical Engineering Journal*, **141**(1–3), 75-88.

Fuentes, M., Scenna, N.J., Aguirre, P.A., Mussati, M.C. 2008. Application of two anaerobic digestion models to biofilm systems. *Biochemical Engineering Journal*, **38**(2), 259-269.

Gil, M., Moya, A., Domínguez, E. 2013. Life cycle assessment of the cogeneration processes in the Cuban sugar industry. *Journal of Cleaner Production*, **41**, 222-231.

Goedkoop, M., Heijungs, R., Huijbregts, M., Schryver, A.D., Struijs, J., Zelm, R.v. 2008. ReCiPe. A life cycle impact assessment method which comprises harmonised category indicators at the midpoint and the endpoint level. First edition. Report I: Characterisation.

Guinee, J.B., Gorree, M., Heijungs, R., Huppes, G., Kleijn, R., Udode Haes, H.A., Vander Voet, E., Wrisberg, M.N. 2002. Life cycle assessment. An Operational Guide to ISO Standards. **vol. 1, 2, 3**.

Harada, H., Uemura, S., Chen, A.-C., Jayadevan, J. 1996. Anaerobic treatment of a recalcitrant distillery wastewater by a thermophilic UASB reactor. *Bioresource Technology*, **55**(3), 215-221.

Harada, H., Uemura, S., Momonoi, K. 1994. Interaction between sulfate-reducing bacteria and methane-producing bacteria in UASB reactors fed with low strength wastes containing different levels of sulfate. *Water Research*, **28**(2), 355-367.

Hinken, L., Patón Gassó, M., Weichgrebe, D., Rosenwinkel, K.H. 2013. Implementation of sulphate reduction and sulphide inhibition in ADM1 for modelling of a pilot plant treating bioethanol wastewater. *13th World Congress on Anaerobic Digestion*, Santiago de Compostela. Spain.

Ince, O., Kolukirik, M., Oz, N.A., Ince, B.K. 2005. Comparative evaluation of full-scale UASB reactors treating alcohol distillery wastewaters in terms of performance and methanogenic activity. *Journal of Chemical Technology and Biotechnology* **80**, 138–144

IPCC. 2013. The Physical Science Basis. Contribution of Working Group I to the Fifth Assessment Report of the Intergovernamental Panel on Climate Change. Cambridge University Press, Cambridge, United Kingdom and New York, NY, USA.

Isa, Z., Grusenmeyer, S., Verstraete, W. 1986. Sulfate Reduction Relative to Methane Production in High-Rate Anaerobic Digestion: Technical Aspects. *Applied and Environmental Microbiology*, **51**(3), 572-579.

ISO14040. Environmental management — Life cycle assessment — Principles and framework. Second edition, Switzerland, 2006, Vol. ISO 14040:2006(E).

ISO14044. Environmental management — Life cycleassessment — Requirements and guidelines. First edition, Switzerland, 2006, Vol. ISO 14044:2006(E).

Kalyuzhnyi, S., Fedorovich, V., Lens, P., Hulshoff Pol, L., Lettinga, G. 1998. Mathematical modelling as a tool to study population dynamics between sulfate reducing and methanogenic bacteria. *Biodegradation*, **9**(3), 187-199.

Kalyuzhnyi, S.V., Fedorovich, V.V. 1998. Mathematical modelling of competition between sulphate reduction and methanogenesis in anaerobic reactors. *Bioresource Technology*, **65**(3), 227-242.

Kaparaju, P., Serrano, M., Angelidaki, I. 2010. Optimization of biogas production from wheat straw stillage in UASB reactor. *Applied Energy*, **87**(12), 3779-3783.

Knobel, A.N., Lewis, A.E. 2002. A mathematical model of a high sulphate wastewater anaerobic treatment system. *Water Research*, **36**(1), 257-265.

Kotas, T.J. 1995. *The exergy method of thermal plant analysis, Florida: Krieger Publishing Company*, reprint ed. Krieger, Malabar, FL.

Lauwers, J., Appels, L., Thompson, I.P., Degrève, J., Impe, J.F.V., Dewil, R. 2013. Mathematical modelling of anaerobic digestion of biomass and waste: Power and limitations. *Progress in Energy and Combustion Science*, (39), 383-402.

Lens, P., Hulshoff Pol, L.W. 2000. *Environmental Technologies to treat sulfur pollution*. IWA Publishing, London.

Lens, P.N.L., Visser, A., Janssen, A.J.H., Pol, L.W.H., Lettinga, G. 1998. Biotechnological Treatment of Sulfate-Rich Wastewaters. *Critical Reviews in Environmental Science and Technology*, **28**(1), 41-88.

Mesa, M.M., Andrades, J.A., Macías, M., Cantero, D. 2004. Biological oxidation of ferrous iron: study of bioreactor efficiency. *Journal of Chemical Technology and Biotechnology*, **79**(2), 163-170.

Naegele, H.-J., Lindner, J., Merkle, W., Lemmer, A., Jungbluth, T., Bogenrieder, C. 2013. Effects of temperature, pH and O_2 on the removal of hydrogen sulfide from biogas by external biological desulfurization in a full scale fixed-bed trickling bioreactor (FBTB). *International Journal of Agriculture and Biology*, **6**(169), 69 - 81.

Nandy, T., Shastry, S., Kaul, S.N. 2002. Wastewater management in a cane molasses distillery involving bioresource recovery. *Journal of Environmental Management*, **65**(1), 25-38.

Nzila, C., Dewulf, J., Spanjers, H., Tuigong, D., Kiriamiti, H., van Langenhove, H. 2012. Multi criteria sustainability assessment of biogas production in Kenya. *Applied Energy*, **93**(0), 496-506.

Obaya, M.C., Valdés, E., Pérez, O.L.L., Carmouse, M.M., Bonachea, O.P., Llanes, S.D., Rojas, O.V. 2004. Tratamiento combinado de las vinazas de destilería y residuales azucareros en reactores UASB. *Tecnología del agua*, **249/Junio** 78-85.

Omil, F., Lens, P., Hulshoff Pol, L.W., Lettinga, G. 1997a. Characterization of biomass from a sulfidogenic, volatile fatty acid-degrading granular sludge reactor. *Enzyme and Microbial Technology*, **20**, 229–236.

Omil, F., Lens, P., Hulshoff Pol, L.W., Lettinga, G. 1996. Effect of Upward Velocity and Sulphide Concentration on Volatile Fatty Acid Degradation in a Sulphidogenic Granular Sludge Reactor. *Process Biochemestry*, **31**, 699–710.

Omil, F., Oude Elferink, S.J.W.H., Lens, P., Hulshoff Pol, L.W., Lettinga, G. 1997b. Effect of the inoculation with Desulforhabdus amnigenus and pH or O_2 shocks on the competition between sulphate reducing and methanogenic bacteria in an acetate fed UASB reactor. *Bioresource Technology*, **60**(2), 113-122.

ONE. 2010. Oficina Nacional de Estadística de Cuba, Available at: http://www.one.cu [Accessed on 5th March, 2011].

Pagella, C., De Faveri, D.M. 2000. H_2S gas treatment by iron bioprocess. *Chemical Engineering Science*, **55**(12), 2185-2194.

Pant, D., Adholeya, A. 2007. Biological approaches for treatment of distillery wastewater: A review. *Bioresource Technology*, **98**(12), 2321-2334.

Parkin, G.F., Lynch, N.A., Kuo, W.-C., Keuren, E.L.V., Bhattacharya, S.K. 1990. Interaction between Sulfate Reducers and Methanogens Fed Acetate and Propionate. *Research Journal of the Water Pollution Control Federation*, **62**(6), 780-788.

Parkin, G.F., Owen, W.E. 1986. Fundamentals of Anaerobic Digestion of Wastewater Sludges. *Journal of Environmental Engineering*, **112**(5), 867-920.

Parnaudeau, V., Condom, N., Oliver, R., Cazevieille, P., Recous, S. 2008. Vinasse organic matter quality and mineralization potential, as influenced by raw material, fermentation and concentration processes. *Bioresource Technology*, **99**(6), 1553-1562.

Pasztor, I., Thury, P., Pulai, J. 2009. Chemical oxygen demand fractions of municipal wastewater for modelling of wastewater treatment. *International Journal of Environmental Science and Technology*, **6**(1), 51-56.

Poinapen, J., Ekama, G.A. 2010. Biological sulphate reduction with primary sewage sludge in an upflow anaerobic sludge bed reactor - Part 6: Development of a kinetic model for BSR. *Water S.A.*, **36**(3), 203-213.

Poinapen, J., Ekama, G.A., Wentzel, M.C. 2009a. Biological sulphate reduction with primary sewage sludge in an upflow anaerobic sludge bed (UASB) reactor - Part 2: Modification of simple wet chemistry analytical procedures to achieve COD and S mass balances. *Water S.A.*, **35**(5), 535-542.

Poinapen, J., Ekama, G.A., Wentzel, M.C. 2009b. Biological sulphate reduction with primary sewage sludge in an upflow anaerobic sludge bed (UASB) reactor - Part 3: Performance at 20 degrees C and 35 degrees C. *Water S.A.*, **35**(5), 543-552.

Poinapen, J., Wentzel, M.C., Ekama, G.A. 2009c. Biological sulphate reduction with primary sewage sludge in an upflow anaerobic sludge bed (UASB) reactor - Part 1: Feasibility study. *Water S.A.*, **35**(5), 525-534.

Prosuite. 2013. Handbook on a novel methodology for the sutainability impact asessment of new technologies.

Rehl, T., Müller, J. 2011. Life cycle assessment of biogas digestate processing technologies. *Resources, Conservation and Recycling*, 92-104.

Rieger, L., Gillot, S., Langergraber, G., Shaw, A. 2012. *Good Modelling Practice: Guidelines for Use of Activated Sludge Models*. IWA Publishing.

Riera, F.S., Cordoba, P., Sineriz, F. 1985. Use of the UASB reactor for the anaerobic treatment of stillage from sugar-cane molasses. *Biotechnology and Bioengineering*, **27**(12), 1710-1716.

Rinzema, A., Lettinga, G. 1988. in: *Anaerobic treatment of sulfate-containing waste water*, (Ed.) D.L. Wise, Biotreatment Systems, vol. III, CRC Press Inc. Boca Raton, USA, pp. 65-109.

Ristow, N.E., Whittington-Jones, K., Corbett, C., Rose, P., Hansford, G.S. 2002. Modelling of a recycling sludge bed reactor using AQUASIM. *Water S.A.*, **28**(1), 111-120.

Rocha, M.H., Lora, E.E.S., VenturinI, O.J., Escobar, J.C.P., Santos, J.J.C.S., Moura, A.G. 2010. Use of the life cycle assessment (LCA) for comparison of the environmental performance of four alternatives for the treatment and disposal of bioethanol stillage. *International Sugar Journal*, **112**(1343), 611 - 622.

Rojas-Sariol, L., Lorenzo-Acosta, Y., Domenech-López, F. 2011. Estudio del consumo de ácidos en el ajuste de pH en diferentes medios de fermentación alcohólica. *ICIDCA. Sobre los Derivados de la Caña de Azúcar*, **45**(2), 57 - 62.

Romero Romero, O. 2005. Metodología para incrementar el aporte de electricidad con bagazo y alternativa de combustible para generar fuera de zafra. Doctoral thesis. Las Villas Central University, Villa Clara. Cuba.

Romli, M., Keller, J., Lee, P.J., Greenfield, P.F. 1995. Model prediction and verification of a two stage high-rate anaerobic wastewater treatment system subject to shock loads. *Process Safety Environmental Protection*, (73), 151-154.

Rosen, C., Jeppsson, U. 2006. Aspects on ADM1 implementation within the BSM2 framework. Department of Industrial Electrical Engineering and Automation (IEA), Lund University. Lund, Sweden. Technical report.

Rosen, M.A., Dincer, I., Kanoglu, M. 2008. Role of exergy in increasing efficiency and sustainability and reducing environmental impact. *Energy Policy*, **36**, 128–137.

Safley, L.M., Westerman, P.W. 1988. Biogas production from anaerobic lagoons. *Biological Wastes*, **23**(3), 181-193.

Salomon, K.R., Silva, E.E. 2009. Estimate of the electric energy generating potential for different sources of biogas in Brazil. *Biomass Bioenergy*, **33**(9), 1101-1107.

Salomon, K.R., Silva Lora, E.E., Rocha, M.H., Almazán del Olmo, O. 2011. Cost calculations for biogas from vinasse biodigestion and its energy utilization. *Sugar Industry*, **136**(4), 217 - 223.

Shieh, J.H., Fan, L.T. 1982. Energy and exergy estimating using the group contribution method. ACS symposium Series 235, [351-371].

Silva, F., Nadais, H., Prates, A., Arroja, L., Capela, I. 2009. Modelling of anaerobic treatment of evaporator condensate (EC) from a sulphite pulp mill using the IWA anaerobic digestion model no. 1 (ADM1). *Chemical Engineering Journal*, **148**, 319-326.

Silva, J., Morales, M., Cáceres, M., Martín, R.S., Gentina, J.C., Aroca, G. 2010. Effect of the biomass in the modelling and simulation of the biofiltration of hydrogen sulphide: simulation and experimental validation. *Journal of Chemical Technology and Biotechnology*, **85**(10), 1374-1379.

Syed, M., Soreanu, G., Falletta, P., Béland, M. 2006. Removal of hydrogen sulfide from gas streams using biological processes - A review. *Canadian Biosystems Engineering*, **48**, 2.1-2.14.

Szargut, J. 2005. Exergy Method: Technical and Ecological Applications. WIT press.

Szargut, J., Morris, D.R., Steward, F.R. 1988. Exergy Analysis of Thermal, Chemical and Metallurgical Processes. Hemisphere Publishing Corporation, Berlin.

Tai, S., Matsushige, K., Goda, T. 1986. Chemical exergy of organic matter in wastewater. *International Journal of Environmental Studies*, **27**, 301-315.

Tartakovsky, B., Mu, S.J., Zeng, Y., Lou, S.J., Guiot, S.R., Wu, P. 2008. Anaerobic digestion model No. 1-based distributed parameter model of an anaerobic reactor: II. Model validation. *Bioresource Technology*, **99**(9), 3676-3684.

Thaveesri, J., Liessens, B., Verstraete, W. 1995. Granular sludge growth under different reactor liquid surface tensions in lab-scale upflow anaerobic sludge blanket reactors treating wastewater from sugar-beet processing. *Applied Microbiology and Biotechnology*, **43**, 1122–1127.

Toprak, H.k. 1995. Temperature and organic loading dependency of methane and carbon dioxide emission rates of a full-scale anaerobic waste stabilization pond. *Water Research*, **29**(4), 1111-1119.

Trade and Investment, U.K. 2014. Renewable Energy in Cuba, Available at: https://www.gov.uk/government/uploads/system/uploads/attachment_data/file/345400/Renewable_Energy_in_Cuba.pdf, [Accessed on 1st Septembe, 2014].

U.S-EPA. 2008. Catalag of CHP technologies. Combined Heat and Power Partnership, Available at: http://www.epa.gov/chp/documents/catalog_chptech_full.pdf [Accessed on 14th May, 2014].

van der Zee, F.P., Villaverde, S., García, P.A., Fdz.-Polanco, F. 2007. Sulfide removal by moderate oxygenation of anaerobic sludge environments. *Bioresource Technology*, **98**(3), 518-524.

Van Hulle, S.W.H., Vesvikar, M., Poutiainen, H., Nopens, I. 2014. Importance of scale and hydrodynamics for modeling anaerobic digester performance. *Chemical Engineering Journal*, **255**, 71-77.

Visser, A. 1995. The anaerobic treatment of sulfate containing wastewater, Doctoral thesis, Wageningen Agricultural University, Wageningen, The Netherlands.

Visser, A., Hulshoff Pol, L.W., Lettinga, G. 1996. Competition of methanogenic and sulfidogenic bacteria. *Water Science and Technology*, **33**(3), 99-110.

Wall, G. 1997. Exergy – A Useful Concept Within Resource Accounting. Institute of Theoretical Physics, Chalmers University of Technology and University of Göteborg.

Wall, G. 1990. Exergy conversion in the Japanese society. *Energy*, **15**, 435-444.

Wall, G. 2010. On Exergy and Sustainable Development in Environmental Engineering. *The Open Environmental Engineering Journal*, **3**, 21-32.

Wang, Y., Zhang, Y., Wang, J., Meng, L. 2009. Effects of volatile fatty acid concentrations on methane yield and methanogenic bacteria. *Biomass Bioenergy*, (33), 848 – 853.

Weiland, P. 2010. Biogas production: current state and perspectives. *Applied Microbiology and Biotechnology*, **85**(4), 849-860.

Wellinger, A., Linberg, A. 2000. Biogas Upgrading and Utilization - IEA Bioenergy Task 24. International Energy Association, Paris, France, Available at: http://wellowgate.co.uk/biogas/Scrubbing.pdf [Accessed on 25th June, 2014].

Wiegant, W.M., de Man, A.W.A. 1986. Granulation of biomass in thermophilic upflow anaerobic sludgeblanket reactors treating acidified wastewaters. *Biotechnology and Bioengineering*, **28**, 718-727.

Wilkie, A.C., Riedesel, K.J., Owens, J.M. 2000. Stillage characterization and anaerobic treatment of ethanol stillage from conventional and cellulosic feedstocks. *Biomass Bioenergy*, **19**, 63-102.

Wiser, J., Schettler, J., Willis, J. 2010. Evaluation of Combined Heat and Power Technologies for Wastewater Facilities, Available at: http://www.cwwga.org/documentlibrary/121_EvaluationCHPTechnologiespreliminary%5B1%5D.pdf [Accessed on 25th June, 2014].

Wu, B., Chen, Z. 2011. An integrated physical and biological model for anaerobic lagoons. *Bioresource Technology*, **102**(8), 5032-5038.

Wubs, H.J., Beenackers, A. 1994. Kinetics of H_2S absorption into aqueous ferric solutions of EDTA and HEDTA. *American Institute of Chemical Engineers Journal*, **40**(3), 433-444.

Wubs, H.J., Beenackers, A. 1993. Kinetics of the oxidation of ferrous chelates of EDTA and HEDTA in aqueous-solution. *Industrial and Engineering Chemistry Research*, **32**(11), 2580-2594.

Zegers, F. 1987. Arranque y operación de sistemas de flujo ascendente con manto de lodo. *Manual del curso. Parte I. Tratamiento anaerobico de las vinazas*.

Zub, S., Kurissoo, T., Menert, A., Blonskaja, V. 2008. Combined biological treatment of high-sulphate wastewater from yeast production. *Water Environmental Journal*, **22**(4), 274-286.